

Climate change projections and impacts for Tairāwhiti and Hawke's Bay

*Prepared for Envirolink, Gisborne District Council and Hawke's Bay
Regional Council*

November 2020

Prepared by:

John-Mark Woolley (climate change data analysis; report writing)
Chris Eager (sea level data analysis; report writing)
Javad Jozaei (data analysis; report writing)
Vijay Paul (GIS analysis and mapping - climate projections)
Ryan Paulik (inundation exposure modelling)
Petra Pearce (data analysis; report writing; exposure assessment)
Abha Sood (RCM projections; RCM bias corrections and downscaling)
Stephen Stuart (RCM projections)
Alex Vincent (report writing – sea-level rise)
Sanjay Wadhwa (GIS analysis and mapping – river flows)
Christian Zammit (river flow data analysis; report writing)



For any information regarding this report please contact:

Petra Pearce
Manager - Climate, Atmosphere and Hazards
Climate and Environmental Applications
+64-9-375 2052
petra.pearce@niwa.co.nz

National Institute of Water & Atmospheric Research Ltd
Private Bag 99940
Viaduct Harbour
Auckland 1010

Phone +64 9 375 2050

NIWA CLIENT REPORT No: 2020298AK
Report date: November 2020
NIWA Project: ELF20104 / GDC20101

Quality Assurance Statement		
	Reviewed by:	Dr Daithi Stone Climate Scientist – NIWA Wellington
	Formatting checked by:	Petra Pearce
	Approved for release by:	Dr Andrew Tait Chief Scientist – Climate, Atmosphere and Hazards NIWA Wellington

© All rights reserved. This publication may not be reproduced or copied in any form without the permission of the copyright owner(s). Such permission is only to be given in accordance with the terms of the client's contract with NIWA. This copyright extends to all forms of copying and any storage of material in any kind of information retrieval system.

Whilst NIWA has used all reasonable endeavours to ensure that the information contained in this document is accurate, NIWA does not give any express or implied warranty as to the completeness of the information contained herein, or that it will be suitable for any purpose(s) other than those specifically contemplated during the Project or agreed by NIWA and the Client.

Contents

Executive summary	14
1 Introduction	18
1.1 Global and New Zealand climate change.....	21
1.2 Year to year climate variability and climate change.....	23
2 Methodology.....	26
2.1 Climate modelling.....	26
2.2 Maps and tabulated climate projections.....	30
2.3 Hydrological modelling	31
2.4 Sea-level rise data analysis	33
2.5 Inundation exposure modelling.....	34
2.6 Limitations	36
3 Current and future climate of Tairāwhiti/Hawke's Bay.....	38
4 Temperature	38
4.1 Mean temperature	38
4.2 Minimum temperature.....	54
4.3 Frosts.....	69
4.4 Heatwaves	74
5 Rainfall.....	79
5.1 Rainfall totals	79
5.2 Extreme, rare rainfall events	94
5.3 Maximum 1-day rainfall.....	115
5.4 Maximum 5-day rainfall.....	122
5.5 Snow	129
6 Drought.....	130
6.1 Potential evapotranspiration deficit.....	130
6.2 Extreme potential evapotranspiration deficit (>300 mm).....	136
6.3 Soil moisture deficit	141
7 Impacts on river flows.....	157
7.1 Mean annual discharge.....	157

7.2	Mean annual low flow	158
7.3	High flows	161
7.4	Mean Annual Flood.....	163
8	Sea-level rise and coastal erosion	166
8.1	Datums and mean sea level.....	166
8.2	Impacts of sea-level rise	168
8.3	Historic trend in SLR focused on Gisborne and Hawke's Bay	169
8.4	Projections for New Zealand sea-level rise.....	173
8.5	Tides and the effect of rising sea level	177
8.6	Storm-tide elevations and effect of SLR	181
8.7	Generic impacts of climate change on coastal erosion	186
9	Exposure analysis – coastal and fluvial inundation	189
9.1	Coastal inundation exposure	190
9.2	Fluvial exposure	191
10	Impacts of climate change on key sectors	192
10.1	Forestry 192	
10.2	Horticulture.....	194
10.3	Agriculture	197
10.4	Tourism 198	
10.5	Ecosystem health.....	199
10.6	Human health	208
10.7	Infrastructure and the built environment	211
11	Summary and conclusions.....	212
11.1	Recommendations for future work	218
12	Acknowledgements	220
13	Glossary of abbreviations and terms	220
Appendix A	Coastal and fluvial inundation exposure	223
14	References.....	240

Tables

Table 2-1:	Projected change in global mean surface air temperature for the mid- and late-21st century relative to the reference period of 1986-2005 for different RCPs.	29
Table 2-2:	Approximate years (nearest 5 years) when specific SLR increments would be reached for wider NZ.	35
Table 5-1:	Modelled historical and projected rainfall depths (mm) for Waikura Valley for different event durations with a 50-year return period (ARI)	96
Table 5-2:	Modelled historical and projected rainfall depths (mm) for Waikura Valley for different event durations with a 100-year return period (ARI)	96
Table 5-3:	Modelled historical and projected rainfall depths (mm) for East Cape at Lighthouse for different event durations with a 50-year return period (ARI)	96
Table 5-4:	Modelled historical and projected rainfall depths (mm) for East Cape at Lighthouse for different event durations with a 100-year return period (ARI)	97
Table 5-5:	Modelled historical and projected rainfall depths (mm) for Ruatoria Telemetry Station at Barry Ave for different event durations with a 50-year return period (ARI)	97
Table 5-6:	Modelled historical and projected rainfall depths (mm) for Ruatoria Telemetry Station at Barry Ave for different event durations with a 100-year return period (ARI)	97
Table 5-7:	Modelled historical and projected rainfall depths (mm) for Puketoro Telemetry Station for different event durations with a 50-year return period (ARI)	98
Table 5-8:	Modelled historical and projected rainfall depths (mm) for Puketoro Telemetry Station for different event durations with a 100-year return period (ARI)	98
Table 5-9:	Modelled historical and projected rainfall depths (mm) for Te Puia for different event durations with a 50-year return period (ARI)	98
Table 5-10:	Modelled historical and projected rainfall depths (mm) for Te Puia for different event durations with a 100-year return period (ARI)	99
Table 5-11:	Modelled historical and projected rainfall depths (mm) for Te Rata Telemetry Station for different event durations with a 50-year return period (ARI)	99
Table 5-12:	Modelled historical and projected rainfall depths (mm) for Te Rata Telemetry Station for different event durations with a 100-year return period (ARI)	99
Table 5-13:	Modelled historical and projected rainfall depths (mm) for Tutamoe Station Telemetry Station for different event durations with a 50-year return period (ARI)	100
Table 5-14:	Modelled historical and projected rainfall depths (mm) for Tutamoe Station Telemetry Station for different event durations with a 100-year return period (ARI)	100
Table 5-15:	Modelled historical and projected rainfall depths (mm) for Hikuwai River at Willowflat for different event durations with a 50-year return period (ARI)	100
Table 5-16:	Modelled historical and projected rainfall depths (mm) for Hikuwai River at Willowflat for different event durations with a 100-year return period (ARI)	101
Table 5-17:	Modelled historical and projected rainfall depths (mm) for Matawai Telemetry Station for different event durations with a 50-year return period (ARI)	101
Table 5-18:	Modelled historical and projected rainfall depths (mm) for Matawai Telemetry Station for different event durations with a 100-year return period (ARI)	101

Table 5-19:	Modelled historical and projected rainfall depths (mm) for Panikau Rd – Reed Rd for different event durations with a 50-year return period (ARI)	102
Table 5-20:	Modelled historical and projected rainfall depths (mm) for Panikau Rd – Reed Rd for different event durations with a 100-year return period (ARI)	102
Table 5-21:	Modelled historical and projected rainfall depths (mm) for Waipaoa River at Kanakanaia for different event durations with a 50-year return period (ARI)	102
Table 5-22:	Modelled historical and projected rainfall depths (mm) for Waipaoa River at Kanakanaia for different event durations with a 100-year return period (ARI)	103
Table 5-23:	Modelled historical and projected rainfall depths (mm) for Wharekopae School for different event durations with a 50-year return period (ARI)	103
Table 5-24:	Modelled historical and projected rainfall depths (mm) for Wharekopae School for different event durations with a 100-year return period (ARI)	103
Table 5-25:	Modelled historical and projected rainfall depths (mm) for Caesar Rd No. 1 Bore for different event durations with a 50-year return period (ARI)	104
Table 5-26:	Modelled historical and projected rainfall depths (mm) for Caesar Rd No. 1 Bore for different event durations with a 100-year return period (ARI)	104
Table 5-27:	Modelled historical and projected rainfall depths (mm) for Cameron Rd No. 1 Bore for different event durations with a 50-year return period (ARI)	104
Table 5-28:	Modelled historical and projected rainfall depths (mm) for Cameron Rd No. 1 Bore for different event durations with a 100-year return period (ARI)	105
Table 5-29:	Modelled historical and projected rainfall depths (mm) for Te Arai River at Pykes Weir for different event durations with a 50-year return period (ARI)	105
Table 5-30:	Modelled historical and projected rainfall depths (mm) for Te Arai River at Pykes Weir for different event durations with a 100-year return period (ARI)	105
Table 5-31:	Modelled historical and projected rainfall depths (mm) for Mangapoike at Reservoir for different event durations with a 50-year return period (ARI)	106
Table 5-32:	Modelled historical and projected rainfall depths (mm) for Mangapoike at Reservoir for different event durations with a 100-year return period (ARI)	106
Table 5-33:	Modelled historical and projected rainfall depths (mm) for Waikaretaheke River at Terapatiki for different event durations with a 50-year return period (ARI)	107
Table 5-34:	Modelled historical and projected rainfall depths (mm) for Waikaretaheke River at Terapatiki for different event durations with a 100-year return period (ARI)	108
Table 5-35:	Modelled historical and projected rainfall depths (mm) for Wairoa River at Marumaru for different event durations with a 50-year return period (ARI)	108
Table 5-36:	Modelled historical and projected rainfall depths (mm) for Wairoa River at Marumaru for different event durations with a 100-year return period (ARI)	108
Table 5-37:	Modelled historical and projected rainfall depths (mm) for Taharua Climate for different event durations with a 50-year return period (ARI)	109
Table 5-38:	Modelled historical and projected rainfall depths (mm) for Taharua Climate for different event durations with a 100-year return period (ARI)	109
Table 5-39:	Modelled historical and projected rainfall depths (mm) for Ngahere for different event durations with a 50-year return period (ARI)	109

Table 5-40:	Modelled historical and projected rainfall depths (mm) for Ngahere for different event durations with a 100-year return period (ARI)	110
Table 5-41:	Modelled historical and projected rainfall depths (mm) for Glengarry for different event durations with a 50-year return period (ARI)	110
Table 5-42:	Modelled historical and projected rainfall depths (mm) for Glengarry for different event durations with a 100-year return period (ARI)	110
Table 5-43:	Modelled historical and projected rainfall depths (mm) for Kohatanui for different event durations with a 50-year return period (ARI)	111
Table 5-44:	Modelled historical and projected rainfall depths (mm) for Kohatanui for different event durations with a 100-year return period (ARI)	111
Table 5-45:	Modelled historical and projected rainfall depths (mm) for Keirunga for different event durations with a 50-year return period (ARI)	111
Table 5-46:	Modelled historical and projected rainfall depths (mm) for Keirunga for different event durations with a 100-year return period (ARI)	112
Table 5-47:	Modelled historical and projected rainfall depths (mm) for Glenwood for different event durations with a 50-year return period (ARI)	112
Table 5-48:	Modelled historical and projected rainfall depths (mm) for Glenwood for different event durations with a 100-year return period (ARI)	112
Table 5-49:	Modelled historical and projected rainfall depths (mm) for Tukipo River at SH 50 for different event durations with a 50-year return period (ARI)	113
Table 5-50:	Modelled historical and projected rainfall depths (mm) for Tukipo River at SH 50 for different event durations with a 100-year return period (ARI)	113
Table 5-51:	Modelled historical and projected rainfall depths (mm) for Tukituki River at Tapairu Road for different event durations with a 50-year return period (ARI)	113
Table 5-52:	Modelled historical and projected rainfall depths (mm) for Tukituki River at Tapairu Road for different event durations with a 100-year return period (ARI)	114
Table 5-53:	Modelled historical and projected rainfall depths (mm) for Mangaorapa for different event durations with a 50-year return period (ARI)	114
Table 5-54:	Modelled historical and projected rainfall depths (mm) for Mangaorapa for different event durations with a 100-year return period (ARI)	114
Table 5-55:	Modelled annual maximum daily rainfall (mm) for selected sites in Tairāwhiti.	120
Table 5-56:	Modelled annual maximum daily rainfall (mm) for selected sites in Hawke's Bay.	121
Table 5-57:	Modelled annual maximum 5-day rainfall (mm) for selected sites in Tairāwhiti.	128
Table 5-58:	Modelled annual maximum 5-day rainfall (mm) for selected sites in Hawke's Bay.	129
Table 8-1:	Mean sea level and datum offsets at Gisborne and Napier.	166
Table 8-2:	Approximate years, from possible earliest to latest, when specific sea-level rise increments (metres above 1986–2005 baseline) could be reached for various projection scenarios of SLR for the wider New Zealand region.	174
Table 8-3:	Tidal levels at Gisborne and Napier.	177
Table 8-4:	High-tide values from 100 year tidal predictions for both Gisborne and Napier.	177

Table 8-5:	Extreme sea-level estimates.	185
Table 10-1:	Overall impacts of climate change on the main horticultural crops in NZ.	195
Table A-1:	Exposure of land and reserves in Gisborne District to a 1% annual exceedance probability (AEP) storm tide event and different increments of sea-level rise.	229
Table A-2:	Exposure of transport infrastructure in Gisborne District to a 1% annual exceedance probability (AEP) storm tide event and different increments of sea-level rise.	230
Table A-3:	Exposure of buildings and population in Gisborne District to a 1% annual exceedance probability (AEP) storm tide event and different increments of sea-level rise.	230
Table A-4:	Exposure of land and regional parks in Hawke's Bay Region to a 1% annual exceedance probability (AEP) storm tide event and different increments of sea-level rise.	230
Table A-5:	Exposure of transport infrastructure in Hawke's Bay Region (ordered by territorial authority) to a 1% annual exceedance probability (AEP) storm tide event and different increments of sea-level rise.	231
Table A-6:	Exposure of buildings and population in Hawke's Bay Region (ordered by territorial authority) to a 1% annual exceedance probability (AEP) storm tide event and different increments of sea-level rise.	232
Table A-7:	Exposure of land and reserves in Gisborne District to the flood hazard area.	235
Table A-8:	Exposure of transport infrastructure in Gisborne District to the flood hazard area.	235
Table A-9:	Exposure of buildings and population in Gisborne District to the flood hazard area.	235
Table A-10:	Exposure of land and regional parks in Hawke's Bay Region to the flood hazard area.	236
Table A-11:	Exposure of transport infrastructure in Hawke's Bay Region (ordered by territorial authority) to the flood hazard area.	237
Table A-12:	Exposure of buildings and population in Hawke's Bay Region (ordered by territorial authority) to the flood hazard area.	239

Figures

Figure 1-1:	Tairāwhiti regional boundary.	19
Figure 1-2:	Hawke's Bay regional boundary.	20
Figure 1-3:	New Zealand national temperature series, 1909-2019.	22
Figure 1-4:	Average summer percentage of normal rainfall during El Niño (left) and La Niña (right).	24
Figure 1-5:	New Zealand air temperature - historical record (black) and future projections for four RCPs and six downscaled climate models, illustrating future year-to-year variability.	26
Figure 2-1:	Schematic diagram showing the dynamical downscaling approach.	27
Figure 2-2:	CMIP5 multi-model simulated time series from 1950-2100 for change in global annual mean surface temperature relative to 1986-2005.	29

Figure 2-3:	Map showing the resolution and spatial coverage of modelled historic and future climate data (grey-black pixels) in the Tairāwhiti and Hawke's Bay regions.	31
Figure 4-1:	Modelled annual mean temperature for Tairāwhiti, average over 1986-2005.	40
Figure 4-2:	Modelled annual mean temperature for Hawke's Bay region, average over 1986-2005 .	41
Figure 4-3:	Modelled seasonal mean temperature for Tairāwhiti, average over 1986-2005 .	42
Figure 4-4:	Modelled seasonal mean temperature for Hawke's Bay region, average over 1986-2005 .	43
Figure 4-5:	Projected annual mean temperature changes for Tairāwhiti by 2040 and 2090 under RCP4.5 and RCP8.5.	44
Figure 4-6:	Projected annual mean temperature changes for Hawke's Bay by 2040 and 2090 under RCP4.5 and RCP8.5.	45
Figure 4-7:	Projected seasonal mean temperature changes for Tairāwhiti by 2040 under RCP4.5.	46
Figure 4-8:	Projected seasonal mean temperature changes for the Hawke's Bay region by 2040 under RCP4.5.	47
Figure 4-9:	Projected seasonal mean temperature changes for Tairāwhiti by 2090 under RCP4.5.	48
Figure 4-10:	Projected seasonal mean temperature changes for the Hawke's Bay region by 2090 under RCP4.5.	49
Figure 4-11:	Projected seasonal mean temperature changes for Tairāwhiti by 2040 under RCP8.5.	50
Figure 4-12:	Projected seasonal mean temperature changes for the Hawke's Bay region by 2040 under RCP8.5.	51
Figure 4-13:	Projected seasonal mean temperature changes for Tairāwhiti by 2090 under RCP8.5.	52
Figure 4-14:	Projected seasonal mean temperature changes for the Hawke's Bay region by 2090 under RCP8.5.	53
Figure 4-15:	Modelled annual mean minimum temperature for Tairāwhiti, average over 1986-2005.	55
Figure 4-16:	Modelled annual mean minimum temperature for Hawke's Bay region, average over 1986-2005.	56
Figure 4-17:	Modelled seasonal mean minimum temperature for Tairāwhiti, average over 1986-2005.	57
Figure 4-18:	Modelled seasonal mean minimum temperature for Hawke's Bay region, average over 1986-2005.	58
Figure 4-19:	Projected annual mean minimum temperature changes for Tairāwhiti by 2040 and 2090 under RCP4.5 and RCP8.5.	59
Figure 4-20:	Projected annual mean minimum temperature changes for Hawke's Bay by 2040 and 2090 under RCP4.5 and RCP8.5.	60
Figure 4-21:	Projected seasonal mean minimum temperature changes for Tairāwhiti by 2040 under RCP4.5.	61
Figure 4-22:	Projected seasonal mean minimum temperature changes for the Hawke's Bay region by 2040 under RCP4.5.	62

Figure 4-23:	Projected seasonal mean minimum temperature changes for Tairāwhiti by 2090 under RCP4.5.	63
Figure 4-24:	Projected seasonal mean minimum temperature changes for the Hawke's Bay region by 2090 under RCP4.5.	64
Figure 4-25:	Projected seasonal mean minimum temperature changes for Tairāwhiti by 2040 under RCP8.5.	65
Figure 4-26:	Projected seasonal mean minimum temperature changes for the Hawke's Bay region by 2040 under RCP8.5.	66
Figure 4-27:	Projected seasonal mean minimum temperature changes for Tairāwhiti by 2090 under RCP8.5.	67
Figure 4-28:	Projected seasonal mean minimum temperature changes for the Hawke's Bay region by 2090 under RCP8.5.	68
Figure 4-29:	Modelled annual number of frost days (daily minimum temperature <0°C) for Tairāwhiti, average over 1986-2005.	70
Figure 4-30:	Modelled annual number of frost days (daily minimum temperature <0°C) for Hawke's Bay region, average over 1986-2005 .	71
Figure 4-31:	Projected annual number of frost days (daily minimum temperature <0°C) changes for Tairāwhiti by 2040 and 2090 under RCP4.5 and RCP8.5.	72
Figure 4-32:	Projected annual number of frost days (daily minimum temperature <0°C) changes for Hawke's Bay by 2040 and 2090 under RCP4.5 and RCP8.5.	73
Figure 4-33:	Modelled annual number of heatwave days (≥ three consecutive days with maximum temperatures > 25°C) for Tairāwhiti, average over 1986-2005.	75
Figure 4-34:	Modelled annual number of heatwave days (≥ three consecutive days with maximum temperatures > 25°C) for Hawke's Bay region, average over 1986-2005 .	76
Figure 4-35:	Projected annual number of heatwave days (≥ three consecutive days with maximum temperatures > 25°C) changes for Tairāwhiti by 2040 and 2090 under RCP4.5 and RCP8.5.	77
Figure 4-36:	Projected annual number of heatwave days (≥ three consecutive days with maximum temperatures > 25°C) changes for Hawke's Bay by 2040 and 2090 under RCP4.5 and RCP8.5.	78
Figure 5-1:	Modelled annual rainfall (mm) for Tairāwhiti, average over 1986-2005.	80
Figure 5-2:	Modelled annual rainfall (mm) for Hawke's Bay, average over 1986-2005.	81
Figure 5-3:	Modelled seasonal rainfall (mm) for Tairāwhiti, average over 1986-2005.	82
Figure 5-4:	Modelled seasonal rainfall (mm) for Hawke's Bay, average over 1986-2005.	83
Figure 5-5:	Projected annual rainfall changes (%) for Tairāwhiti.	84
Figure 5-6:	Projected annual rainfall changes (%) for Hawke's Bay.	85
Figure 5-7:	Projected seasonal rainfall changes (%) for Tairāwhiti by 2040 for RCP4.5.	86
Figure 5-8:	Projected seasonal rainfall changes (%) for Hawke's Bay by 2040 for RCP4.5.	87
Figure 5-9:	Projected seasonal rainfall changes (%) for Tairāwhiti by 2090 for RCP4.5.	88
Figure 5-10:	Projected seasonal rainfall changes (%) for Hawke's Bay by 2090 for RCP4.5.	89
Figure 5-11:	Projected seasonal rainfall changes (%) for Tairāwhiti by 2040 for RCP8.5.	90
Figure 5-12:	Projected seasonal rainfall changes (%) for Hawke's Bay by 2040 for RCP8.5.	91
Figure 5-13:	Projected seasonal rainfall changes (%) for Tairāwhiti by 2090 for RCP8.5.	92
Figure 5-14:	Projected seasonal rainfall changes (%) for Hawke's Bay by 2090 for RCP8.5.	93

Figure 5-15:	Selected sites in the Tairāwhiti region for location specific rainfall intensity projections.	95
Figure 5-16:	Selected sites in the Hawke's Bay region for location specific rainfall intensity projections.	107
Figure 5-17:	Modelled annual maximum daily rainfall (Rx1day) for Tairāwhiti, average over 1986-2005.	116
Figure 5-18:	Modelled annual maximum daily rainfall (Rx1day) for Hawke's Bay region, average over 1986-2005 .	117
Figure 5-19:	Projected annual maximum daily rainfall (Rx1day) changes for Tairāwhiti by 2040 and 2090 under RCP4.5 and RCP8.5.	118
Figure 5-20:	Projected annual maximum daily rainfall (Rx1day) changes for Hawke's Bay by 2040 and 2090 under RCP4.5 and RCP8.5.	119
Figure 5-21:	Modelled annual maximum 5-day rainfall (Rx5day) for Tairāwhiti, average over 1986-2005.	123
Figure 5-22:	Modelled annual maximum 5-day rainfall (Rx5day) for Hawke's Bay region, average over 1986-2005 .	124
Figure 5-23:	Projected annual maximum 5-day rainfall (Rx5day) changes for Tairāwhiti by 2040 and 2090 under RCP4.5 and RCP8.5.	125
Figure 5-24:	Projected annual maximum 5-day rainfall (Rx5day) changes for Hawke's Bay by 2040 and 2090 under RCP4.5 and RCP8.5.	126
Figure 5-25:	Projected annual maximum 5-day rainfall (Rx5day) changes for New Zealand by 2090 under RCP8.5.	127
Figure 6-1:	Modelled annual potential evapotranspiration deficit accumulation (mm) for Tairāwhiti, average over 1986-2005.	131
Figure 6-2:	Modelled annual potential evapotranspiration deficit accumulation (mm) for Hawke's Bay region, average over 1986-2005 .	132
Figure 6-3:	Projected annual potential evapotranspiration deficit accumulation (mm) changes for Tairāwhiti by 2040 and 2090 under RCP4.5 and RCP8.5.	133
Figure 6-4:	Projected annual potential evapotranspiration deficit accumulation (mm) changes for Hawke's Bay by 2040 and 2090 under RCP4.5 and RCP8.5.	134
Figure 6-5:	Projected annual potential evapotranspiration deficit accumulation (mm) changes for New Zealand by 2090 under RCP8.5.	135
Figure 6-6:	Modelled probability of Potential Evapotranspiration Deficit exceeding 300 mm in any year for Tairāwhiti, average over 1986-2005.	137
Figure 6-7:	Modelled probability of Potential Evapotranspiration Deficit exceeding 300 mm in any year for Hawke's Bay region, average over 1986-2005 .	138
Figure 6-8:	Projected probability of annual Potential Evapotranspiration Deficit exceeding 300 mm for Tairāwhiti by 2040 and 2090 under RCP4.5 and RCP8.5.	139
Figure 6-9:	Projected annual potential evapotranspiration deficit accumulation (mm) changes for Hawke's Bay by 2040 and 2090 under RCP4.5 and RCP8.5.	140
Figure 6-10:	Modelled annual number of days of soil moisture deficit for Tairāwhiti, average over 1986-2005.	142
Figure 6-11:	Modelled annual number of days of soil moisture deficit for Hawke's Bay region, average over 1986-2005 .	143
Figure 6-12:	Modelled seasonal number of days of soil moisture deficit for Tairāwhiti, average over 1986-2005 .	144

Figure 6-13:	Modelled seasonal number of days of soil moisture deficit for Hawke's Bay region, average over 1986-2005 .	145
Figure 6-14:	Projected change in the number of annual soil moisture deficit days for Tairāwhiti by 2040 and 2090 under RCP4.5 and RCP8.5.	146
Figure 6-15:	Projected change in the number of annual soil moisture deficit days for Hawke's Bay by 2040 and 2090 under RCP4.5 and RCP8.5.	147
Figure 6-16:	Projected change in the number of seasonal soil moisture deficit days for Tairāwhiti by 2040 under RCP4.5.	148
Figure 6-17:	Projected change in the number of seasonal soil moisture deficit days for the Hawke's Bay Region by 2040 under RCP4.5.	149
Figure 6-18:	Projected change in the number of seasonal soil moisture deficit days for Tairāwhiti by 2090 under RCP4.5.	150
Figure 6-19:	Projected change in the number of seasonal soil moisture deficit days for the Hawke's Bay Region by 2090 under RCP4.5.	151
Figure 6-20:	Projected change in the number of seasonal soil moisture deficit days for Tairāwhiti by 2040 under RCP8.5.	152
Figure 6-21:	Projected change in the number of seasonal soil moisture deficit days for the Hawke's Bay Region by 2040 under RCP8.5.	153
Figure 6-22:	Projected change in the number of seasonal soil moisture deficit days for Tairāwhiti by 2090 under RCP8.5.	154
Figure 6-23:	Projected change in the number of seasonal soil moisture deficit days for the Hawke's Bay Region by 2090 under RCP8.5.	155
Figure 6-24:	Projected change in annual soil moisture deficit days by 2090 under RCP8.5.	156
Figure 7-1:	Percent changes in multi-model median of the mean discharge across Tairāwhiti for mid (top) and late-century (bottom).	157
Figure 7-2:	Percent changes in multi-model median of the mean discharge across Hawke's Bay region for mid (top) and late-century (bottom).	158
Figure 7-3:	Percent changes in multi-model median of the mean annual low flow (MALF) across Tairāwhiti for mid (top) and late-century (bottom).	159
Figure 7-4:	Percent changes in multi-model median of the mean annual low flow (MALF) across Hawke's Bay region for mid (top) and late-century (bottom).	160
Figure 7-5:	Percent changes in multi-model median of the Q5% across Tairāwhiti for mid (top) and late-century (bottom).	161
Figure 7-6:	Percent changes in multi-model median of the Q5% across Hawke's Bay region for mid (top) and late-century (bottom).	162
Figure 7-7:	Percent changes in multi-model median of the mean annual flood (MAF across Tairāwhiti for mid (top) and late-century (bottom).	164
Figure 7-8:	Percent changes in multi-model median of the mean annual flood (MAF) across Hawke's Bay region for mid (top) and late-century (bottom).	165
Figure 8-1:	Mean sea level and datum offsets at Gisborne and Napier.	167
Figure 8-2:	Annual MSL at the Port of Gisborne.	167
Figure 8-3:	Annual MSL at the Port of Napier.	168
Figure 8-4:	Relative SLR rates up to and including 2019 (excluding Whangarei), determined from longer sea-level gauge records at the four main ports (Auckland, Wellington, Lyttelton, Dunedin) and shorter records from the remaining sites.	170

Figure 8-5:	Map of regional trend in SLR from 1993 to 1 September 2020 based on satellite altimetry missions.	171
Figure 8-6:	Average vertical land movement for near-coastal continuous GPS Sites across the North Island, New Zealand.	172
Figure 8-7:	Four scenarios of New Zealand-wide regional SLR projections, with extensions to 2150.	175
Figure 8-8:	Change in annual MSL for Gisborne from 2011–2019.	175
Figure 8-9:	Change in annual MSL for Napier from 1990–2019.	176
Figure 8-10:	Change in annual MSL for Gisborne and Napier from 1990–2019.	176
Figure 8-11:	High-tide exceedance curve for all predicted high tides at Gisborne (excluding effects of weather, climate and SLR).	179
Figure 8-12:	High-tide exceedance curve for all predicted high tides at Napier (excluding effects of weather, climate and SLR).	180
Figure 8-13:	Components that contribute to storm-tide and wave overtopping.	181
Figure 8-14:	Seasonal cycle in monthly sea level at the Port of Gisborne averaged over the period 2009-2019.	182
Figure 8-15:	Seasonal cycle in monthly sea level at the Port of Napier averaged over the period 1989-2019.	183
Figure 8-16:	Extreme sea level at Gisborne.	184
Figure 8-17:	Extreme sea level at Napier.	184
Figure 8-18:	New Zealand coastal sensitivity index for future coastal erosion from climate change.	186
Figure 10-1:	Erosion beside a sea wall in Whitianga. Photo: R. Bell, NIWA.	203
Figure 10-2:	Regional variation of the projected change in SST for the End-Century (2081-2100) compared with present-day (1976-2005) under RCP8.5 (Law et al., 2016).	204
Figure 10-3:	Ecoclimatic Index scores for the Queensland fruitfly, <i>Bactrocera tryoni</i> , for three periods 1980-1999, 2030-2049, and 2080-2099.	206
Figure A-1:	Map of New Zealand showing regional boundaries and coastline coverage represented by LiDAR and satellite Digital Elevation Models (DEMs).	224
Figure A-2:	1% AEP storm tide + sea-level rise elevations exposure for Tairāwhiti.	225
Figure A-3:	1% AEP storm tide + sea-level rise elevations exposure near Tolaga Bay, Tairāwhiti.	226
Figure A-4:	1% AEP storm tide + sea-level rise elevations exposure near Poverty Bay, Tairāwhiti.	226
Figure A-5:	1% AEP storm tide + sea-level rise elevations exposure for Hawke's Bay Region.	227
Figure A-6:	1% AEP storm tide + sea-level rise elevations exposure near Napier, Hawke's Bay Region.	228
Figure A-7:	1% AEP storm tide + sea-level rise elevations exposure near Wairoa, Hawke's Bay Region.	228
Figure A-8:	1% AEP storm tide + sea-level rise elevations exposure just northwest of Mahia (township), Hawke's Bay Region.	229
Figure A-9:	Flood Hazard Area for Tairāwhiti.	233
Figure A-10:	Flood Hazard Area for the Hawke's Bay Region.	234

Executive summary

The climate of Tairāwhiti and Hawke's Bay is changing, and these changes will continue for the foreseeable future. It is internationally accepted that human greenhouse gas emissions are the dominant cause of recent global climate change, and that further changes will result from increasing concentrations of greenhouse gases in the atmosphere. The rate of future climate change depends on how fast atmospheric greenhouse gas concentrations increase.

Envirolink, Gisborne District Council and Hawke's Bay Regional Council commissioned NIWA to undertake a review of climate change projections and impacts for the Tairāwhiti and Hawke's Bay regions. This report addresses expected changes for 11 different climate variables out to 2100 and draws heavily on climate model simulations from the Intergovernmental Panel on Climate Change (IPCC) Fifth Assessment Report. The following bullet points outline some key findings of this report:

- The projected temperature changes for the two regions increase with time and greenhouse gas concentration pathway. Future annual average warming spans a wide range: 0.5-1.0°C by 2040, and 1.0-1.5°C (medium concentration pathway) or 2.0-3.0°C (high concentration pathway) by 2090.
- Similarly, annual average minimum temperatures are expected to increase for most locations in both regions by 0.5-1.0°C by 2040. By 2090, minimum temperatures at most locations are projected to increase by 0.5-1.0°C (medium concentration pathway) or 1.5-2.5°C (high concentration pathway).
- The average number of frost days is expected to decrease with time and greenhouse gas concentrations. The largest decreases are projected for high elevation locations in the west, where 5-20 fewer frost days are projected by 2040, and 10-30 fewer days by 2090 (10-50 fewer days under high concentrations). Smaller decreases are generally projected for coastal locations because fewer frosts currently occur in these locations.
- The average number of heatwave days per year is projected to increase with time and greenhouse gas concentrations, particularly for eastern and coastal locations. By 2090, and under high greenhouse gas concentrations, the majority of both regions is projected to receive 20-60 additional heatwave days per year. Increases are generally not as large for higher elevation locations further inland.
- Projected changes in rainfall show variability across the two regions. By 2040 under both medium and high greenhouse gas concentration pathways, annual rainfall is expected to decrease by a small amount for the majority of both regions, generally in the 0-5% range. By 2090, larger and more extensive decreases to annual rainfall are projected, decreasing by up to 10% under the medium concentration pathway, and up to 15% under high concentrations. Spring is generally projected to experience the greatest and most extensive drying, while winter rainfall is generally projected to increase on the western side of the mountain ranges (despite a drying signal for the eastern majority of both regions for most winter projections presented in this report).
- Extreme, rare rainfall events are projected to become more severe in the future. Short duration rainfall events have the largest relative increases compared with longer duration rainfall events. For the selected locations analysed in this report, rainfall

depths for 1-in-50-year and 1-in-100-year events are projected to increase across the greenhouse gas concentration scenarios and future time periods.

- The annual maximum 1-day rainfall total is generally projected to increase or decrease by 0-5 mm across the two regions by 2040 under the medium greenhouse gas concentration pathway. Under high greenhouse gas concentrations and further into the future, larger and more widespread increases are projected. By 2090 under high greenhouse gas concentrations, the entirety of both regions is projected to experience increases to the annual maximum 1-day rainfall total, with large increases projected for northern Tairāwhiti and over or just west of the mountain ranges that separate the two regions from Bay of Plenty.
- Projected changes to the annual maximum 5-day rainfall total vary across Tairāwhiti. Large increases are projected for locations over and west of the Raukumara Range, except for the 2040 period under the medium greenhouse gas concentration pathway where there is less of a clear signal. Decreasing totals are generally projected for several eastern and inland parts of Tairāwhiti, and by 2090 under high greenhouse gas concentrations, this portion of the region is among the few parts of New Zealand projected to see decreases of more than 5 mm to the annual maximum 5-day rainfall total. Projected changes are also variable across the Hawke's Bay Region however most locations are projected to see increasing totals under high greenhouse gas concentrations.
- Drought potential is projected to increase across both regions, with annual accumulated Potential Evapotranspiration Deficit (PED) totals increasing with time and increasing greenhouse gas concentrations. Areas east of the mountain ranges are projected to observe the largest increases to PED accumulation, and eastern Tairāwhiti is projected to experience some of the largest increases in the country by 2090. The probability of PED exceeding 300 mm in a given year is also projected to increase significantly for most eastern and coastal locations in both regions. Additionally, large portions of both regions are projected to experience some of the largest increases to the annual number of days of soil moisture deficit compared to other parts of the country.

The effects of climate change on hydrological characteristics were examined by driving NIWA's national hydrological model with downscaled Global Climate Model outputs from 1971-2099 under different greenhouse gas concentration scenarios. The changing climate over this century is projected to lead to the following hydrological effects:

- Annual average discharge is expected to decrease across greenhouse gas concentration scenarios and future time periods.
- Mean annual low flows (MALF) are also expected to decrease across greenhouse gas concentration scenarios and future periods for most catchments. However, under the medium greenhouse gas concentration pathway, a number of catchments are expected to see an increase in MALF, as summer rainfall is expected to slightly increase for those catchments.
- High flows (expressed as Q5% flow) are generally expected to see larger decreases by mid-century (2036-2056) under the medium greenhouse gas concentration pathway

when compared to the high concentration scenario. Increases to high flows are also expected for some catchments by the mid-century time period, with larger increases expected under high greenhouse gas concentrations (particularly in Hawke's Bay). The largest decreases to high flows are modelled for the high greenhouse gas concentration pathway by the end of the century (2086-2099). It is noted that the climate models underpinning this analysis are not able to correctly reproduce ex-tropical cyclone tracks and other large storms, the intensity (rain and wind rates) of which is generally projected to increase with more warming. Further research and modelling is therefore required to understand future changes to high flows.

- Changes in the Mean Annual Flood (MAF) are expected to be spatially diverse across time and greenhouse gas concentration scenarios. By the end of the century, under high concentrations, MAF is expected to increase by up to 50% for around half of the Hawke's Bay region's rivers and a smaller proportion of rivers across Tairāwhiti.

One of the major and most certain (and so foreseeable) consequences of increasing concentrations of atmospheric greenhouse gases and associated warming is the rising sea level. Rising sea level in past decades has already affected human activities and infrastructure in coastal areas in New Zealand, with a higher base mean sea level contributing to increased vulnerability to storms and tsunamis.

- Rising sea level has already been observed within the Tairāwhiti and Hawke's Bay regions. Absolute sea-level rise (SLR), calculated from satellite altimetry, shows the region is trending at an increase of around 4 mm/year (trend for 1993-present), which is close to the New Zealand-wide average of 4.4 mm/year (calculated up to the end of 2015). Similarly, local measurements of relative sea-level rise (RSLR) calculated from sea-level gauges are estimated as 2.15 and 1.40 mm/year at the Port of Gisborne and Napier since the establishment of the local vertical datums in 1926 and 1962, respectively.
- As sea levels rise, so will the probability of current high-water marks being exceeded, while the average recurrence interval of rare storm-tide event will become smaller. A 0.4 m SLR (estimated to be reached by 2090 under medium greenhouse gas concentrations, and 2060 under high concentrations) would mean that any coastal location currently affected by the present-day mean high water spring (MHWS-10 level), which is exceeded by only 10% of all high tides (tide only), will be exceeded by 100% of all high tides by 2060 (under high concentrations). A present-day rare storm-tide event (0.2% annual exceedance probability (AEP) with a 500-year average recurrence interval (ARI)), would become, for example, a 20% AEP (5-year event) after a RSLR of around 0.16 m.
- In the present-day the risk caused by the hazard of coastal erosion is generally *very low* to *low*, but recreation and rural residential land will become increasingly vulnerable for future erosion scenarios, reaching *very high* economic losses and *low to very high* (extremely case dependent) social/cultural losses by 2120. While the estimated sensitivity to coastal erosion from climate change in the Tairāwhiti/Hawke's Bay region varies from location to location along the coast, due to the complex nature of coastal shoreline change, it is rated from *Moderate* to *Very High*. The widths of the mapped areas susceptible to coastal erosion are shown to be generally increasing (to estimated

widths of 60 to 180 m by 2115) and must be taken into consideration for the current and future planning of coastal use.

The following points summarise ongoing and potential future impacts of a changing climate on different sectors and environments in Tairāwhiti and Hawke's Bay.

- Increasing temperatures due to human-induced climate change will likely impact primary sector activities through increasing the incidence of pests and diseases. Cattle become more stressed during heatwaves (which are projected to increase under a warming climate), which may affect milk production in the dairy sector to a greater degree than at present. Increasing temperatures affect the rate of plant growth, which may affect the quality and quantity of harvested fruit and vegetable crops, as well as the productivity of forestry and pasture. Human health will also be affected by a changing climate due to the increasing prevalence of hot conditions and heatwaves. Warmer temperatures in the future may increase the length of the tourism season and provide opportunities for new crops to be grown.
- A warmer atmosphere in the future is expected to result in increases to rainfall intensity. Increased rainfall intensity is associated with more slips, floods, and erosion, and hence damage to infrastructure (e.g. roads, water supply), the forestry sector, and agricultural land productivity. Loss of infrastructure connectivity is a risk for the tourism sector. Increased rainfall intensity increases the risk of reduced quality of fruit and vegetables, as well as causing soil saturation issues for horticulture and agriculture.
- Future reductions in rainfall and increases in drought severity may cause fire risk to increase in the Tairāwhiti and Hawke's Bay regions, affecting forestry, the natural environment, and the tourism sector. Future reductions to water availability from decreasing rainfall as well as lower river flows may affect the available water take for irrigation and urban supply, and also affect freshwater ecosystems.
- Ongoing sea-level rise caused by climate change is likely to increase exposure of infrastructure and primary sector activities to extreme coastal flooding, as well as cause habitat loss at the coastal margins where ecosystems are not able to move further inland (coastal squeeze). Exposure is likely to increase over time in response to higher sea levels.
- Warming oceans will induce pressures on the distribution and abundance of marine species, and ocean acidification will affect species with carbonate shells (e.g. paua, oysters).
- Increased concentrations of carbon dioxide should increase forest, pasture, crop, and horticulture productivity, if not limited by water availability.

1 Introduction

Climate change is already affecting New Zealand and the Tairāwhiti-Hawke's Bay regions with downstream effects on our natural environment, the economy, and communities. In the coming decades, climate change is highly likely to increasingly pose challenges to New Zealanders' way of life.

Envirolink, Gisborne District Council and Hawke's Bay Regional Council commissioned the National Institute of Water and Atmospheric Research (NIWA) to undertake a review of climate change projections and impacts for the Tairāwhiti-Hawke's Bay regions (regional extents shown in Figure 1-1 and Figure 1-2). This work follows the publication of the Intergovernmental Panel on Climate Change (IPCC) Fifth Assessment Report in 2013 and 2014, and the New Zealand climate change projections report published by the Ministry for the Environment (updated 2018) (Ministry for the Environment, 2018). The contents of this technical report include analysis of climate projections for the Tairāwhiti and Hawke's Bay regions in greater detail than the national-scale analysis. Regional-scale climate projection maps have been provided for 10 different climate variables, and GIS data files have been provided to the Councils.

This technical report describes changes which may occur over the 21st century to the climate of the Tairāwhiti and Hawke's Bay regions. Consideration about future change incorporates knowledge of both natural variations in the climate and changes that may result from increasing global concentrations of greenhouse gases that are contributed to by human activities. Climatic variables discussed in this report include temperature, rainfall, potential evapotranspiration deficit (a measure of drought potential), and soil moisture. Projections for sea-level rise and river flows are also discussed. Commentary on climate change impacts and implications for some of the different environments and sectors of Tairāwhiti and Hawke's Bay are provided, including biosecurity, horticulture, agriculture, forestry, and health.

Some of the information that underpins portions of this report resulted from academic studies based on the latest assessments of the Intergovernmental Panel on Climate Change (IPCC, 2013, IPCC, 2014c, IPCC, 2014a, IPCC, 2014b). Details specific to Tairāwhiti and Hawke's Bay were based on data for New Zealand that were generated by NIWA from downscaling of global climate model simulations. This effort utilised several IPCC representative concentration pathways (RCPs) for the future and this was achieved through NIWA's Regional Climate Modelling Programme. The climate change information presented in this report is consistent with recently-updated national-scale climate change guidance produced for the Ministry for the Environment (2018), and sea-level rise information is consistent with the coastal hazards guidance manual published by Ministry for the Environment (2017).

The remainder of this chapter includes a brief introduction of global and New Zealand climate change, based on the IPCC Fifth Assessment Report. It includes an introduction to the climate change scenarios used in this report, and the methodology that explains the modelling approach for the climate change projections that are presented for the Tairāwhiti and Hawke's Bay regions.

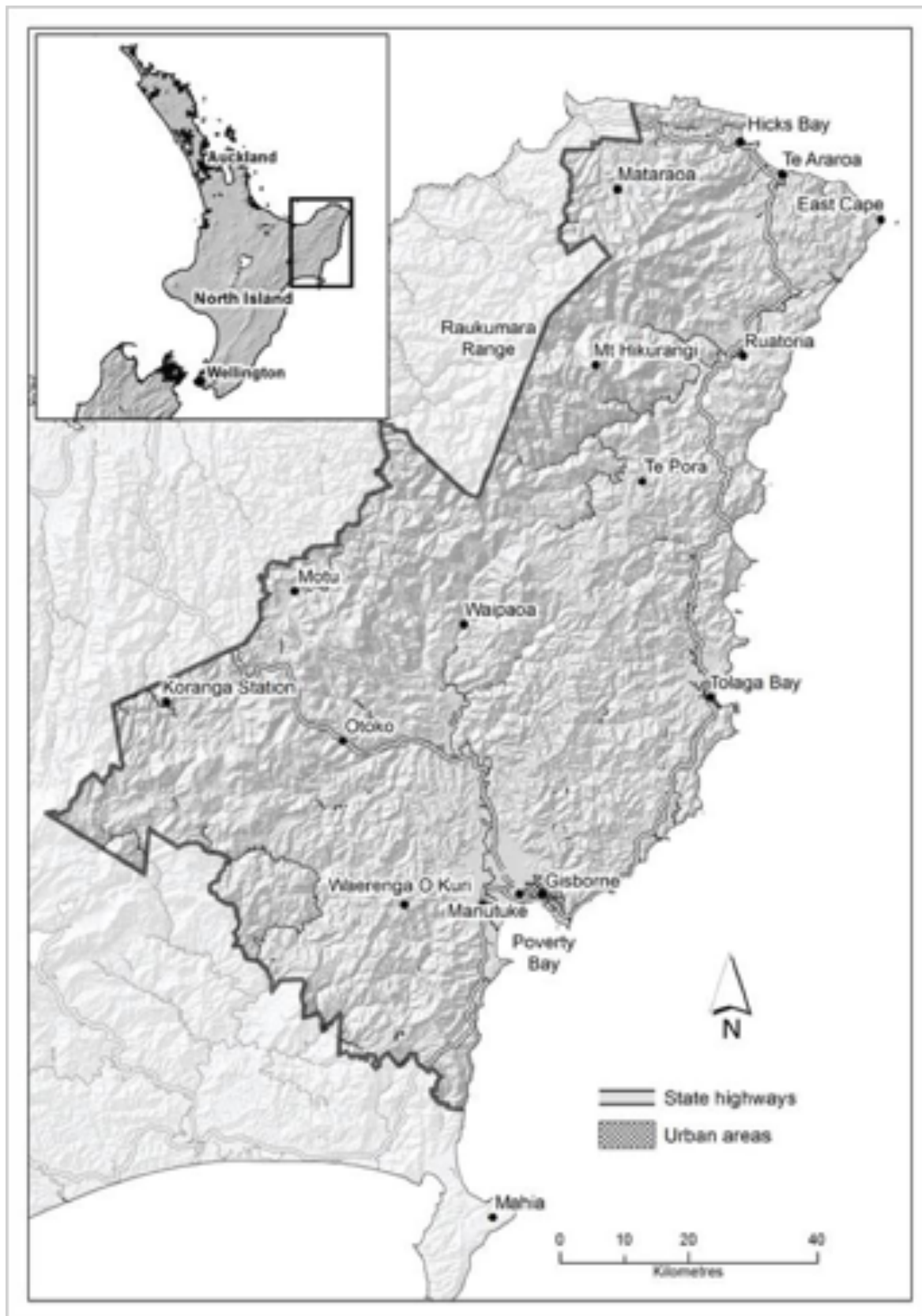


Figure 1-1: Tairāwhiti regional boundary. Sourced from Chappell (2016).

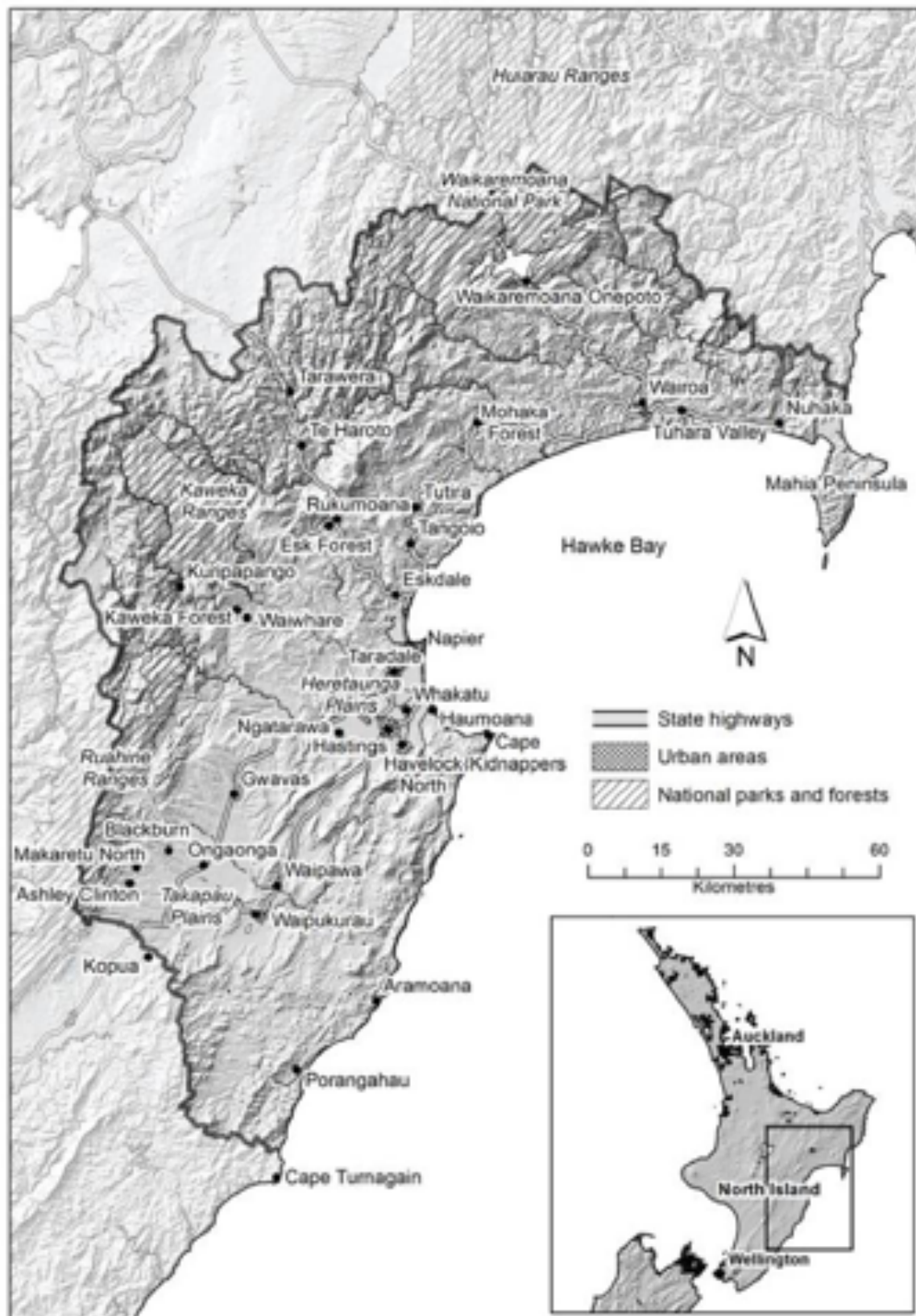


Figure 1-2: Hawke's Bay regional boundary. Sourced from Chappell (2013).

1.1 Global and New Zealand climate change

Key messages

- The global climate system is warming and many of the recently observed climate changes are unprecedented.
- Global mean sea level has risen over the past century at a rate of about 1.7 mm/year and has very likely accelerated to 3.2 mm/year since 1993.
- Human activities (and associated greenhouse gas emissions) are estimated to have caused approximately 1.0°C of global warming above pre-industrial levels.
- Estimated human-induced global warming is currently increasing at 0.2°C per decade due to past and ongoing emissions.
- Continued increases in greenhouse gas emissions will cause further warming and impacts on all parts of the global climate system.

Warming of the global climate system is unequivocal, and since the 1950s, many of the observed climate changes are unprecedented over short and long timescales (decades to millennia) (IPCC, 2013). These changes include warming of the atmosphere and ocean, diminishing of ice and snow, sea-level rise, and increases in the concentration of greenhouse gases in the atmosphere. Climate change is already influencing the intensity and frequency of many extreme weather and climate events globally. Shifts in average temperatures will result in proportionally large increases in the occurrence of extreme temperatures. The Earth's atmosphere has warmed by 0.85°C on average over the period 1880-2012. The rate of sea-level rise since the mid-19th century has been larger than the mean rate of change during the previous two millennia. Over the period 1901-2010, global mean sea level rose by 0.19 m.

The atmospheric concentrations of carbon dioxide have increased to levels unprecedented in at least the last 3 million years (Willeit et al., 2019). Carbon dioxide concentrations have increased by at least 40% since pre-industrial times, primarily from fossil fuel emissions and secondarily from net land use change emissions (IPCC, 2013). In May 2019, the carbon dioxide concentration of the atmosphere reached 415 parts per million. The ocean has absorbed about 30% of the emitted anthropogenic carbon dioxide, causing ocean acidification. Due to the influence of increasing carbon dioxide and other greenhouse gases on the global climate system, it is extremely likely that human influence has been the dominant cause of the observed warming since the mid-20th century (IPCC, 2013, IPCC, 2018).

Published information about the expected impacts of climate change on New Zealand is summarised and assessed in the Australasia chapter of the IPCC Working Group II assessment report (Reisinger et al., 2014) as well as a report published by the Royal Society of New Zealand (Royal Society of New Zealand, 2016). Key findings from these publications include:

The regional climate is changing. The Australasia region continues to demonstrate long-term trends toward higher surface air and sea surface temperatures, more hot extremes and fewer cold extremes, and changed rainfall patterns. Over the past 50 years, increasing greenhouse gas concentrations have contributed to rising average temperatures in New Zealand. Changing

precipitation patterns have resulted in increases in rainfall for the south and west of the South Island and west of the North Island and decreases in the northeast of the South Island and the east and north of the North Island. Some heavy rainfall events already carry the fingerprint of a changed climate, in that they have become more intense due to higher temperatures allowing the atmosphere to carry more moisture (Dean et al., 2013). Cold extremes have become rarer and hot extremes have become more common.

The region has exhibited warming to the present and is virtually certain to continue to do so. New Zealand's mean annual temperature has increased, on average, by 1.02°C ($\pm 0.25^{\circ}\text{C}$) per century since 1909 (Figure 1-3).

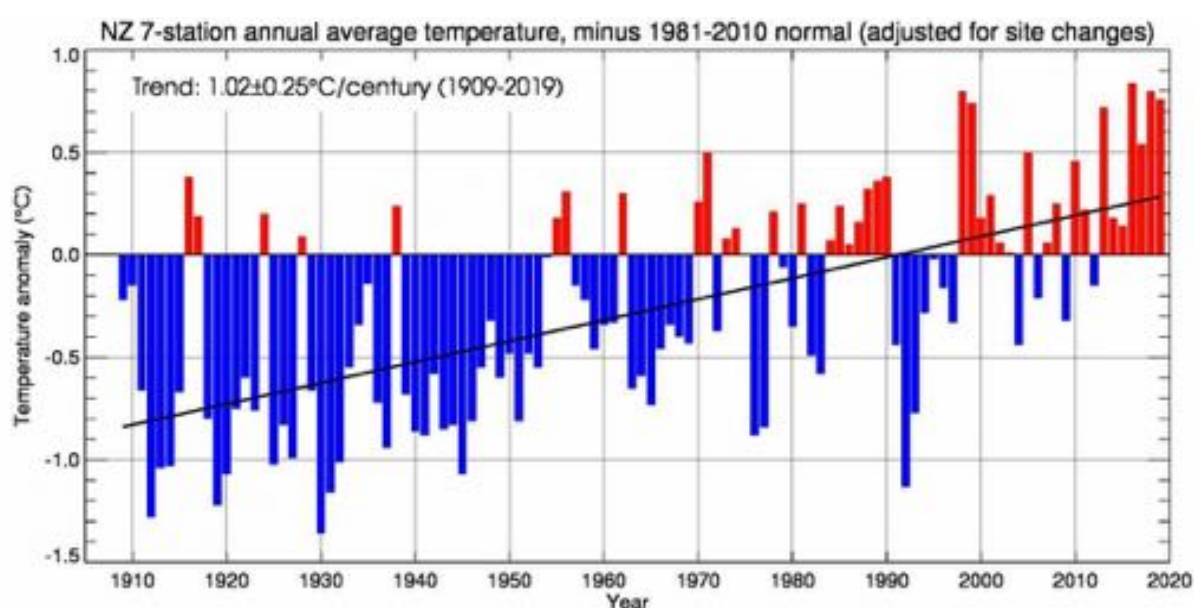


Figure 1-3: New Zealand national temperature series, 1909-2019. More information about the New Zealand seven-station temperature series can be found at <https://www.niwa.co.nz/our-science/climate/information-and-resources/nz-temp-record/seven-station-series-temperature-data>

Warming is projected to continue through the 21st century along with other changes in climate.

Warming is expected to be associated with rising snow lines, more frequent hot extremes, less frequent cold extremes, and increasing extreme rainfall related to flood risk or droughts in many locations. Annual average rainfall is expected to decrease in the northeast of the South Island and north and east of the North Island, and to increase in other parts of New Zealand. Fire hazard is projected to increase in many parts of New Zealand. Regional sea-level rise will very likely exceed the historical rate, consistent with global mean trends.

Impacts and vulnerability: Without adaptation, further climate-related changes are projected to have substantial impacts on water resources, coastal ecosystems, infrastructure, health, agriculture, and biodiversity. However, uncertainty in projected rainfall changes and other climate-related changes remains large for many parts of New Zealand, which creates significant challenges for adaptation.

Additional information about recent New Zealand climate change can be found in Ministry for the Environment (2018).

1.2 Year to year climate variability and climate change

Key messages

- Natural variability is an important consideration in addition to the underlying climate change signal.
- El Niño-Southern Oscillation is the most dominant mode of inter-annual climate variability and it impacts New Zealand primarily through changing wind, temperature and rainfall patterns.
- The Interdecadal Pacific Oscillation affects New Zealand through drier conditions in the east and wetter conditions in the west during the positive phase. The opposite occurs in the negative phase.
- The Southern Annular Mode affects New Zealand through higher temperatures and settled weather during the positive phase and lower temperatures and unsettled weather during the negative phase.
- Natural variability will continue to affect the year-to-year climate of New Zealand into the future.

Much of the material in this report focuses on the projected impact on the climate of the Tairāwhiti and Hawke's Bay regions over the coming century due to increases in global anthropogenic greenhouse gas concentrations. However, natural variations will also continue to occur. Much of the variation in New Zealand's climate is random and lasts for only a short period, but longer term, quasi-cyclic variations in climate can be attributed to different factors. Three large-scale oscillations that influence climate in New Zealand are the El Niño-Southern Oscillation, the Interdecadal Pacific Oscillation, and the Southern Annular Mode (Ministry for the Environment, 2008). Those involved in (or planning for) climate-sensitive activities in the Tairāwhiti and Hawke's Bay regions will need to cope with the sum of both anthropogenic change and natural variability.

1.2.1 The effect of El Niño and La Niña

El Niño-Southern Oscillation (ENSO) is a natural mode of climate variability that has wide-ranging impacts around the Pacific Basin (Ministry for the Environment, 2008). ENSO involves a movement of warm ocean water from one side of the equatorial Pacific to the other, changing atmospheric circulation patterns in the tropics and subtropics, with corresponding shifts for rainfall across the Pacific.

During the El Niño phase of ENSO, easterly trade winds weaken and warm water 'spills' eastward across the equatorial Pacific, accompanied by higher rainfall than normal in the central-east Pacific. The La Niña phase produces opposite effects and is typified by an intensification of easterly trade winds, retention of warm ocean waters over the western Pacific. El Niño events occur on average 3 to 7 years apart, typically becoming established in November and persisting through to March.

During El Niño events, the weakened trade winds cause New Zealand to experience a stronger than normal south-westerly airflow. This generally brings lower seasonal temperatures to the country and drier than normal conditions to the north and east of New Zealand, including the Tairāwhiti and Hawke's Bay regions (Salinger and Mullan, 1999) (Figure 1-4). During La Niña conditions, the strengthened trade winds cause New Zealand to experience more north-easterly airflow than

normal, higher-than-normal temperatures (especially during summer), and wetter conditions in the north and east of the North Island, including the Tairāwhiti and Hawke's Bay regions (Figure 1-4).

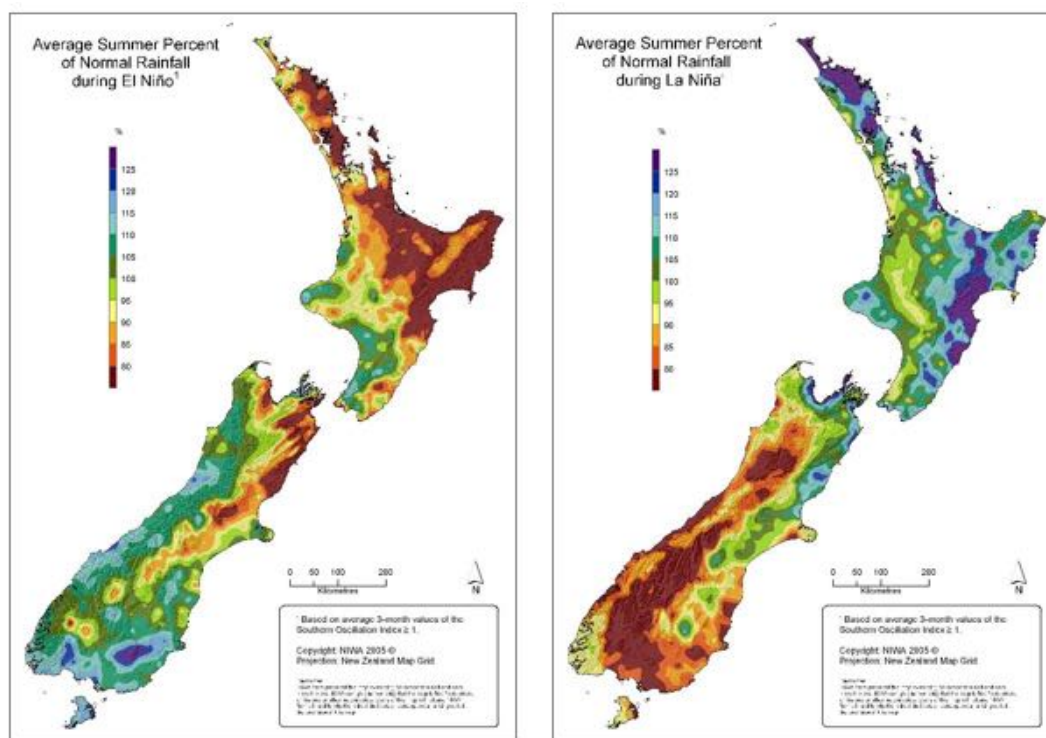


Figure 1-4: Average summer percentage of normal rainfall during El Niño (left) and La Niña (right). El Niño composite uses the following summers: 1963/64, 1965/66, 1968/69, 1969/70, 1972/73, 1976/77, 1977/78, 1982/83, 1986/87, 1987/88, 1991/92, 1994/95, 1997/98, 2002/03. La Niña composite uses the following summers: 1964/65, 1970/71, 1973/74, 1975/76, 1983/84, 1984/85, 1988/89, 1995/96, 1998/99, 1999/2000, 2000/01. This figure was last updated in 2005. © NIWA.

According to IPCC (2013), ENSO is highly likely to remain the dominant mode of natural climate variability in the 21st century, and that rainfall variability relating to ENSO is likely to increase. However, there is uncertainty about future changes to the amplitude and spatial pattern of ENSO.

1.2.2 The effect of the Interdecadal Pacific Oscillation

The Interdecadal Pacific Oscillation (IPO) is a large-scale, long-period oscillation that influences climate variability over the Pacific Basin including New Zealand (Salinger et al., 2001). The IPO operates at a multi-decadal scale, with phases lasting around 20 to 30 years. During the positive phase of the IPO, sea surface temperatures around New Zealand tend to be lower, and westerly winds stronger, resulting in drier conditions for eastern areas of both North and South Islands (including Tairāwhiti and Hawke's Bay). The opposite occurs in the negative phase. The IPO can modify New Zealand's connection to ENSO, and it also positively reinforces the impacts of El Niño (during IPO+ phases) and La Niña (during IPO- phases).

1.2.3 The effect of the Southern Annular Mode

The Southern Annular Mode (SAM) represents the variability of circumpolar atmospheric jets that encircle the Southern Hemisphere that extend out to the latitudes of New Zealand. The SAM is often coupled with ENSO, and both phenomena affect New Zealand's climate in terms of westerly wind strength and storm occurrence (Renwick and Thompson, 2006). In its positive phase, the SAM is associated with relatively light winds and more settled weather over New Zealand, with stronger westerly winds further south towards Antarctica. In contrast, the negative phase of the SAM is associated with unsettled weather and stronger westerly winds over New Zealand, whereas wind and storms decrease towards Antarctica.

The phase and strength of the SAM is influenced by the size of the ozone hole, giving rise to positive trends in the past during spring and summer. In the future other drivers are likely to have an impact on SAM behaviour, for example changing temperature gradients between the equator and the high southern latitudes would have an impact on westerly wind strength in the mid-high latitudes.

1.2.4 The influence of natural variability on climate change projections

It is important to consider human-induced climate change in the context of natural climate variability. An example of this for temperature is shown in Figure 1-5. The solid black line on the left-hand side represents the annual average temperature for New Zealand based on the average of a number of climate simulations forced by historic greenhouse gas concentrations. All the other line plots and shading refer to the modelled air temperature averaged over the New Zealand region from individual simulations. Post-2005, the coloured line plots show the annual temperature changes for the New Zealand region under four different scenarios of future greenhouse gas concentrations, with the heavier lines showing the six-model average temperature projections for each concentration scenario, and the lighter lines showing the results for each of the six downscaled climate models for both historical and future periods.

For the future 2006-2100 period, the models show very little warming trend after about 2030 under the low greenhouse gas concentration ("RCP2.6", blue shading) scenario, whereas the models 'take off' to be anywhere between +2.0°C and +3.5°C by 2100 under the high concentration ("RCP8.5", red shading) scenario.

Figure 1-5 should not be interpreted as a set of specific predictions for individual years. However, it illustrates that although we expect a long term overall continuing upward trend in temperatures (other than for the RCP2.6 scenario), there will still be some relatively cool years. For this particular example, a year which is unusually warm under our present climate could become the norm by about 2050, and an "unusually warm" year in 30-50 years' time (under the higher concentration scenarios) is likely to be warmer than anything we currently experience. The strength of future anthropogenic trends in other climate variables will be smaller in relation to their large year-to-year variability, with the notable exception of sea-level rise.

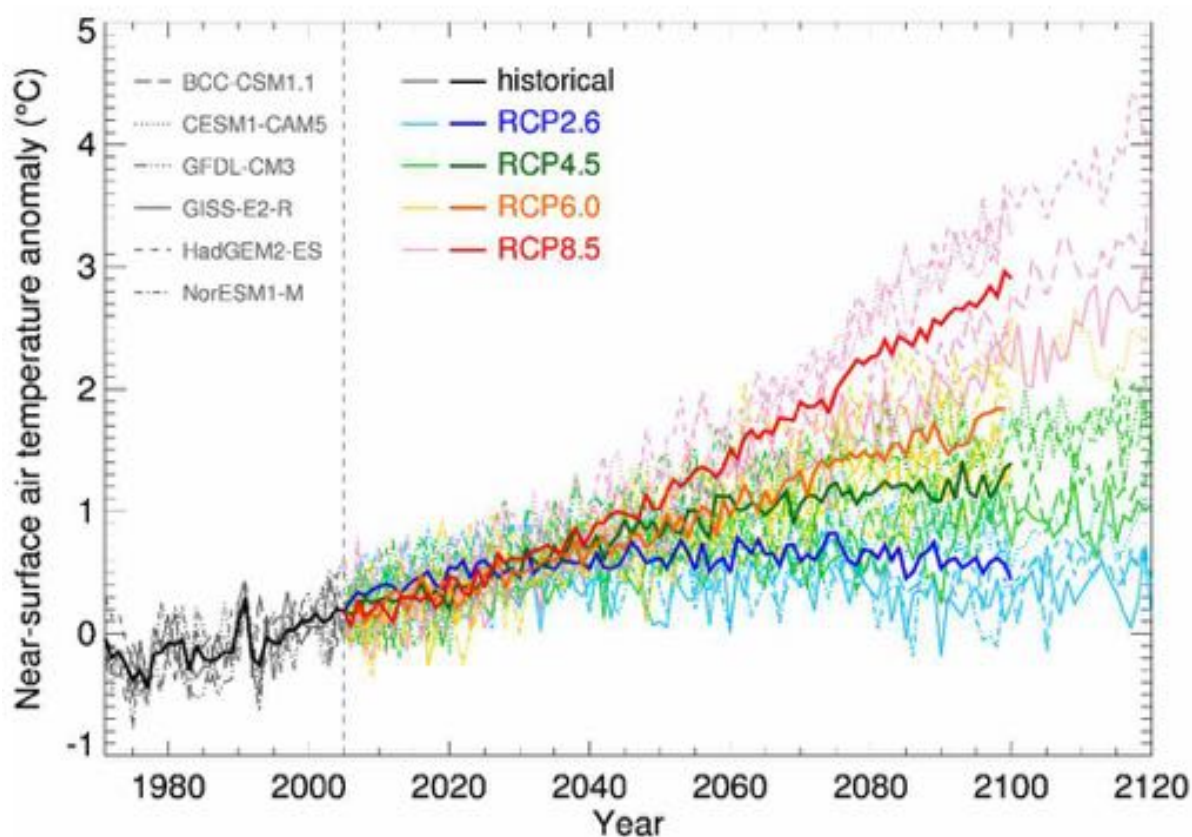


Figure 1-5: New Zealand air temperature - historical record (black) and future projections for four RCPs and six downscaled climate models, illustrating future year-to-year variability. (See text for full explanation). From Ministry for the Environment (2018).

2 Methodology

2.1 Climate modelling

NIWA has used global climate model simulations from the IPCC Fifth Assessment to generate climate change projections for New Zealand using both dynamical (regional climate modelling, RCM) and statistical downscaling procedures. These are described in more detail in a climate guidance manual prepared for the Ministry for the Environment (2018), but a short explanation for the dynamical procedure is provided below. All climate variables and indices presented in this report are based on the dynamical downscaling approach.

Coupled global atmosphere-ocean general circulation models (GCMs) are used to generate climate change projections for prescribed future greenhouse gas concentration scenarios, and results from these models are available through the Fifth Coupled Model Inter-comparison Project (CMIP5) archive (Taylor et al., 2012). Simulations from six GCMs were selected by NIWA for dynamical modelling, and the bias corrected sea surface temperatures (SSTs) from these six CMIP5 models were used to drive a global atmosphere-only GCM, which in turn drives a higher resolution regional climate model (RCM) for the New Zealand domain. These CMIP5 models were chosen because they produced the most consistent results when compared to historical climate and circulation patterns in the New Zealand and Southwest Pacific region. Additional selection criteria for the parent global

models was that they were the least similar to each other as they were expected to span the likely range of model differences. The dynamical downscaling procedure involves forcing a higher-resolution regional climate model (RCM) with data from a coarser global model (GCM) at the lateral boundaries to obtain finer scale detail over a limited area.

The six GCMs chosen for the sea surface temperatures were BCC-CSM1.1, CESM1-CAM5, GFDL-CM3, GISS-E2-R, HadGEM2-ES and NorESM1-M. The NIWA downscaling (GCM then RCM) produced simulations that contain daily climate variables, including precipitation and surface temperature, from 1971 through to 2100. The native resolution of the regional climate model is approximately 30 km (0.27 degree). However, climate models are known to have considerable biases due to inadequate representation of some critical features (clouds, precipitation). The daily precipitation projections, as well as daily maximum and minimum temperatures, were bias corrected so that the probability distributions from the RCM matched those from the Virtual Climate Station Network (VCSN) data on the model resolution when the RCM is driven by the observed large scale circulation across New Zealand (known as 're-analysis' data, REAN) (Sood, 2015). When the RCM is driven from the free-running GCM, forced by CMIP5 SSTs, additional biases occur due to biases in the large-scale circulation in the global model without data assimilation. Therefore, the climate variables from RCM nested in the free running GCM forced by historic greenhouse gas concentrations (RCPpast) are expected to have larger biases than where the lateral boundaries of the RCM are forced by reanalysis (REAN) data derived from observations.

The RCM output is then downscaled using interpolation and physically based models from ~30 km to a ~5 km grid at a daily time-step. The ~5 km grid corresponds to the VCSN grid¹. Figure 2-1 shows a schematic for the dynamical downscaling method used in this report.

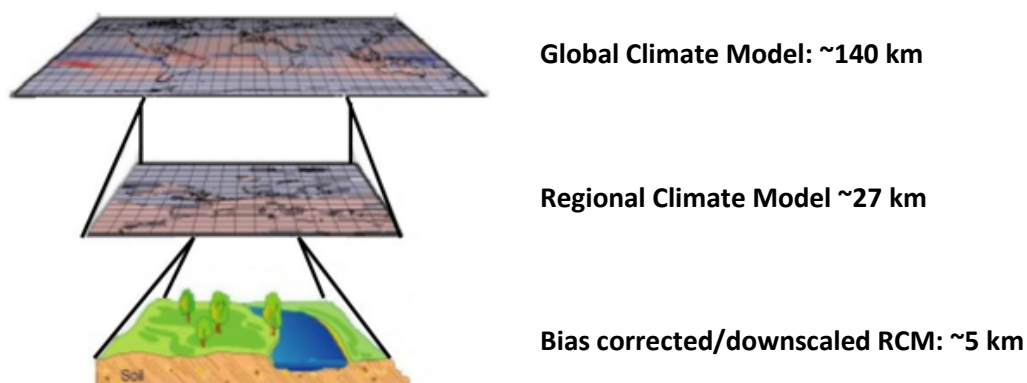


Figure 2-1: Schematic diagram showing the dynamical downscaling approach.

The change in the mean climatologies of climate variables averaged from the six model simulations, the 6-model ensemble mean, is presented for the climate simulations rather than for any individual model. The model ensemble mean climatology of climate variables is a better representation of the corresponding climate change signal (also termed signal), since the averaging process reduces the internal variability of the climate system (also termed noise). This is particularly relevant where

¹ Virtual Climate Station Network, a set of New Zealand climate data based on a 5 km by 5 km grid across the country. Data have been interpolated from 'real' climate station records (TAIT, A., HENDERSON, R., TURNER, R. & ZHENG, X. G. 2006. Thin plate smoothing spline interpolation of daily rainfall for New Zealand using a climatological rainfall surface. *International Journal of Climatology*, 26, 2097-2115.)

the signal to noise ratio is small. Though only a small number of (six) model simulations were possible due to large computing resources required for running climate model simulations, they were very carefully selected to cover the range of the larger CMIP5 model ensemble.

Climate projections are presented as a 20-year average for two future periods: 2031-2050 (termed '2040') and 2081-2100 (termed '2090'). All maps show changes² relative to the baseline climate of 1986-2005 (termed '1995'), as used by IPCC (2013). Hence the projected changes by 2040 and 2090 should be thought of as 45-year and 95-year projected trends. Note that the projected changes use 20-year averages, which will not entirely represent and smoothen the natural variability of the selected period. The baseline maps (1986-2005) show modelled historical climate conditions from the same six models as the future climate change projection maps.

2.1.1 Representative Concentration Pathways

Assessing possible changes for our future climate due to human activity is challenging because climate projections strongly depend on estimates for future greenhouse gas concentrations. In turn, those concentrations depend on global greenhouse gas emissions that are driven by factors such as economic activity, population changes, technological advances and policies for mitigation and sustainable resource use. This range of uncertainty has been dealt with by the IPCC through consideration of 'scenarios' that describe concentrations of greenhouse gases in the atmosphere. The wide range of scenarios are associated with possible economic, political, and social developments during the 21st century. In the 2013 IPCC Fifth Assessment Report, a selection of these scenarios were called Representative Concentrations Pathways (RCPs).

These representative pathways are abbreviated as RCP2.6, RCP4.5, RCP6.0, and RCP8.5, in the order of increasing radiative forcing in Watts/m² of area from increasing greenhouse gases (i.e. the change in net energy in the atmosphere due to greenhouse gas concentrations). RCP2.6 requires net global emissions to reduce to zero around the 3rd quarter of this century, leading to low anthropogenic greenhouse gas concentrations (also requiring removal of CO₂ from the atmosphere), and called the 'mitigation' pathway (and the scenario closest to the aspirational goal of the 2015 Paris Agreement of reducing global temperature rise below 2°C above pre-industrial times), RCP4.5 and RCP6.0 are two 'stabilisation' pathways (where greenhouse gas concentrations stabilises by 2100), and RCP8.5 represents continuing high global emissions without effective mitigation, which will lead to high greenhouse gas concentrations (a 'high end' pathway).

Therefore, the RCPs represent the outcomes of a range of 21st-century climate policies.

Table 2-1 shows the projected global mean surface air temperature for each RCP. The full range of projected globally averaged temperature increases for all pathways for 2081-2100 (relative to 1986-2005) is 0.3 to 4.8°C (Figure 2-2). Warming will likely continue beyond 2100 under all RCPs except RCP2.6. Warming will continue to exhibit inter-annual-to-decadal variability and will not be regionally uniform.

² The exception in this report is the maps in section 6.2 which show the modelled probability of annual potential evapotranspiration deficit accumulation exceeding 300 mm. For this variable, maps simply show the future probability for the two future periods rather than the change in probability.

Table 2-1: Projected change in global mean surface air temperature for the mid- and late- 21st century relative to the reference period of 1986-2005 for different RCPs. After IPCC (2013).

Scenario	Alternative name	2046-2065 (mid-century)		2081-2100 (end-century)	
		Mean (°C)	Likely range (°C)	Mean (°C)	Likely range (°C)
RCP2.6	Mitigation pathway	1.0	0.4 to 1.6	1.0	0.3 to 1.7
RCP4.5	Stabilisation pathway	1.4	0.9 to 2.0	1.8	1.1 to 2.6
RCP6.0	Stabilisation pathway	1.3	0.8 to 1.8	2.2	1.4 to 3.1
RCP8.5	High end pathway	2.0	1.4 to 2.6	3.7	2.6 to 4.8

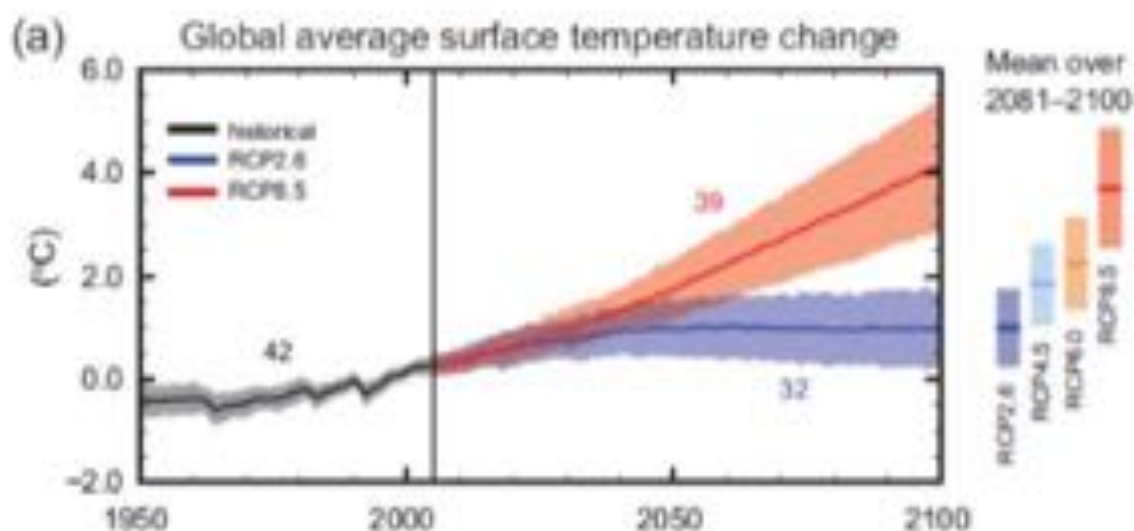


Figure 2-2: CMIP5 multi-model simulated time series from 1950-2100 for change in global annual mean surface temperature relative to 1986-2005. Time series of projections and a measure of uncertainty (shading) are shown for scenarios RCP2.6 (blue) and RCP8.5 (red). Black (grey shading) is the modelled historical evolution using historical reconstructed forcing. The mean and associated uncertainties averaged over 2081–2100 are given for all RCP scenarios as coloured vertical bars to the right of the graph (the mean projection is the solid line in the middle of the bars). The numbers of CMIP5 models used to calculate the multi-model mean is indicated on the graph. From IPCC (2013).

Cumulative CO₂ emissions will largely determine global mean surface warming by the late 21st century and beyond. Even if emissions are stopped, the inertia of many changes in global climate will continue for many centuries to come, with the longest lag effect being sea-level rise. This represents a substantial multi-century climate change commitment created by past, present and future emissions of CO₂ – particularly for coastal areas facing ongoing sea-level rise.

In this report, the downscaled results of the selected global climate models based on two RCPs (RCP4.5 and RCP8.5) are presented. The rationale for choosing these two scenarios was to present a 'high end' scenario if atmospheric greenhouse gas concentrations continue to rise at high rates (RCP8.5) and a scenario which could be realistic if moderate global action is taken towards mitigating greenhouse gas emissions (RCP4.5). Including all four RCP scenarios within the body of this report would make it unwieldy, but GIS datasets for climate projections for the four RCPs have been provided to the Councils. For sea-level rise, all four scenarios from the Ministry for the Environment (2017) coastal guidance, comprising RCP2.6, RCP4.5 and RCP8.5 (with a second high-end H⁺ scenario to cover the potential for runaway polar ice sheet instabilities), are covered by the sea-level rise increments used for the exposure assessment.

2.2 Maps and tabulated climate projections

Downscaled climate projection data is presented as 5 km x 5 km square pixels over New Zealand. The projections that are mapped and tabulated in this report contain some pixels around the coast where no projection data are displayed, resulting in some small gaps in the projection data at the coast (Figure 2-3). Data were downscaled only where low-resolution cells in the climate model consisted of land coverage and where they overlapped high-resolution cells on land. In most cases, interpolating over the mixed sea and land points creates artificial biases, for example, lower temperatures, so the data in that cell is removed (e.g. the white area over Mahia Peninsula or between Kaiaua Bay and Te Ikaarongamai Bay in Figure 2-3). For display purposes, NIWA has undertaken interpolation to continue the climate projections to the coast for the climate change and historic climate maps presented in sections 4-6. The nearest neighbour interpolation method was used to do this, where the value of the empty coastal cell was estimated using the value of the nearest neighbouring cells. Because the values at these locations are estimates generated simply for presentation purposes (i.e. not a direct output of the climate change model), mapped climate change values at these particular locations may go unmentioned in this report.

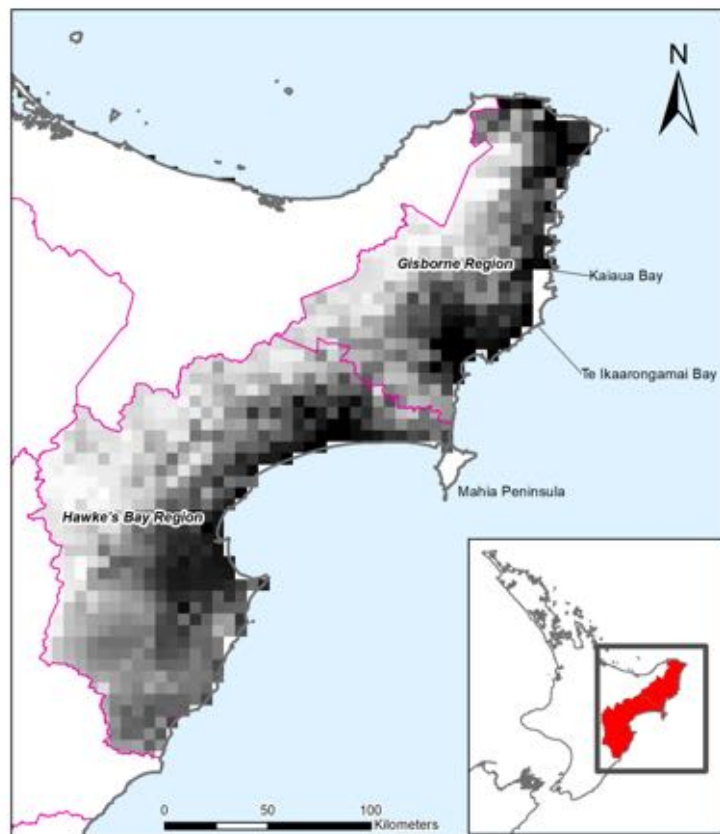


Figure 2-3: Map showing the resolution and spatial coverage of modelled historic and future climate data (grey-black pixels) in the Tairāwhiti and Hawke's Bay regions. Note the absence of modelled data along parts of the coast, particularly over Mahia Peninsula and between Kaiaua Bay and Te Ikaarongamai Bay. Inset map shows extent of the main map within the North Island of New Zealand, with the Hawke's Bay and Tairāwhiti regions coloured red.

2.3 Hydrological modelling

To assess the potential impacts of climate change on agricultural water resources and flooding, a hydrological model is required that can simulate soil moisture and river flows continuously and under a range of different climatic conditions, both historical and future. Ideally the model would also simulate complex groundwater fluxes but there is no national hydrological model capable of this at present. Because climate change implies that environmental conditions are shifting from what has been observed historically, it is advantageous to use a physically based hydrological model over one that is more empirical, with the assumption that a better representation of the biophysical processes will allow the model to perform better outside the range of conditions under which it is calibrated.

The hydrological model used in Section 7 is NIWA's TopNet model (Clark et al., 2008), which is routinely used for surface water hydrological modelling applications in New Zealand. It is a spatially semi-distributed, time-stepping model of water balance, that is used commonly in New Zealand for catchment, regional and national scale hydrological modelling. It is driven by time-series of precipitation and temperature, and of additional weather elements where available. TopNet simulates water storage in the snowpack, plant canopy, rooting zone, shallow subsurface, lakes and rivers. It produces time-series of modelled river flow (without consideration of water abstraction, impoundments or discharges) throughout the modelled river network, as well as evapotranspiration,

and does not consider irrigation. TopNet has two major components, namely a basin module and a flow routing module.

The model combines TOPMODEL hydrological model concepts (Beven et al., 1995) with a kinematic wave channel routing algorithm (Goring, 1994) and a simple temperature based empirical snow model (Clark et al., 2008). As a result, TopNet can be applied across a range of temporal and spatial scales over large watersheds using smaller sub-basins as model elements (Ibbitt and Woods, 2002, Bandaragoda et al., 2004). Considerable effort has been made during the development of TopNet to ensure that the model has a strong physical basis and that the dominant rainfall-runoff dynamics are adequately represented in the model (McMillan et al., 2010). TopNet model equations and information requirements are provided by Clark et al. (2008) and McMillan et al. (2013).

For the development of the national version of TopNet used here, spatial information in TopNet was provided by national datasets as follows:

- Catchment topography based on a nationally available 30 m Digital Elevation Model (DEM).
- Physiographical data based on the Land Cover Database version two and Land Resource Inventory (Newsome et al., 2012).
- Soil data based on the Fundamental Soil Layer information (Newsome et al., 2012).
- Hydrological properties (based on the River Environment Classification version one (REC1) (Snelder and Biggs, 2002).

The method for deriving TopNet's parameters based on GIS data sources in New Zealand is given in Table 1 of Clark et al. (2008). Due to the paucity of some spatial information at national/regional scales, some soil parameters are set uniformly across New Zealand.

To carry out the simulations required for this study, TopNet was run continuously from 1971 to 2100, with the spin-up period 1971 excluded from the analysis. The climate inputs were stochastically disaggregated from daily to hourly time steps. As the GCM simulations are "free-running" (based only on initial conditions, not updated with observations), comparisons between present and future hydrological conditions can be made directly (as each GCM is characterised by specific physical assumptions and parameterisation), but this also means that simulated hydrological hindcasts do not track observational records.

Hydrological simulations are based on the REC 1 network aggregated up to Strahler11 catchment order three (approximate average catchment area of 7 km²) used within previous national and regional scale assessments (Pearce et al., 2017, Pearce et al., 2018); residual coastal catchments of smaller stream orders remain included. The simulation results comprise hourly time-series of various hydrological variables for each computational sub-catchment, and for each of the six GCMs and two RCPs considered. To manage the volume of output data, only river flows information was preserved; all the other state variables and fluxes can be regenerated on demand.

Hydrological projections are presented as the average for two future periods: 2036-2056 (termed 'mid-century') and 2086-2099 (termed 'late-century'). All maps show changes relative to the baseline climate (1986-2005 average). The periods analysed are slightly different from the corresponding time slices of the atmospheric modelling because the modelling was done before this project was initiated. We do not expect that the conclusions drawn would be substantively different if the

periods were aligned. Hydrological projections were analysed for the following hydrological statistics: – Mean annual discharge; – Mean annual low flow; – The Q5% flow³; and – The mean annual flood⁴ (MAF).

Because of TopNet assumptions, soil and land use characteristics within each computational subcatchment are homogenised. Essentially this means that the soil characteristics and physical properties of different land uses, such as pasture and forest, will be spatially averaged, and the hydrological model outputs will approximate conditions across land uses. The data used in the hydrology section of the report is consistent with Collins and Zammit (2016).

2.4 Sea-level rise data analysis

NIWA quality-analysed (QA) sea-level data from both the Napier (1989–2019) and Gisborne (2010–2019) sea-level records. The quality-control (QC) was undertaken relative to National Environmental Monitoring Standards⁵ (NEMS) and to the Intergovernmental Oceanographic Commission Manual for the Quality Control of in situ Sea Level Observations⁶. Data was assigned one of four QC codes: 100 = missing data, 200 = data that was shifted in time to align with data either side (daylight-saving adjustment), 300 = synthetic data (sections of length ≤ 3 hours were filled by linear interpolation, sections of lengths between 3 and 24-hours were filled using linear interpolation of residuals plus predicted astronomical tide), 500 = good-quality original data.

The QC records were then averaged using a 15-minute running average which was applied to remove the effects of infra-gravity waves and the data was decimated to 1-hourly intervals. These datasets were then used to calculate the mean sea level (MSL), tidal harmonic analysis, and extreme sea-level analysis.

MSL was calculated over two epochs: the full records at Gisborne (2011–2019) and Napier (1989–2019) to the end of 2019, and the 1986–2005 epoch (Napier only), which was used as baseline epoch for sea-level rise projections by the IPCC AR5 assessment and for NZ (Ministry for the Environment, 2017).

Tidal harmonic analyses were undertaken with 69 constituents including the solar annual and semi-annual tidal constituents, using UniTide (Foreman et al., 2009). This software does a good job of fitting tides even in highly frictional environments such as shallow river systems where the tides can be highly non-linear.

Extreme sea-level analyses used the skew-surge⁷ joint-probability method (SSJPM) (Batstone et al., 2013) to determine extreme storm-tide frequency and magnitude. Joint-probability methods provide more robust low-frequency magnitude estimates for short-duration records than direct maxima methods — because they overcome the main theoretical limitations of extreme value theory application to measured sea-level maxima—splitting the sea level into its deterministic (predictable) tidal and stochastic (e.g., unpredictable, storm-driven) non-tidal components, and analysing the two components separately before recombining. Storm-tide return periods can be estimated from relatively short records because all skew surges are considered, not just those that lead to extreme levels. A limitation of the SSJPM and other joint-probability methods is that it assumes tide and skew

³ Flow that is exceeded 5% of the time

⁴ The mean of the series of each year's highest daily mean flow

⁵ <http://www.nems.org.nz/assets/Documents/NEMS-14/Water-Level-v3.0.pdf>

⁶ <https://repository.oceanbestpractices.org/handle/11329/1348>

⁷ A skew surge is the difference between the maximum observed sea level and the maximum predicted tide regardless of their timing during the tidal cycle

surge are independent, which has been shown to be true in the UK (Williams et al., 2016) but has not been fully investigated in NZ, although comparisons with direct maxima methods for > 50-year-long records give similar results for return periods ≥ 10 years and also match observed maxima well, and thus support the validity of the independence assumption for long-return-period events (Stephens et al., 2020). To verify the results we have plotted the SSJPM results against the annual maxima (AM) plotted in their Gringorten (1963) plotting positions, a generalised extreme-value distribution fitted to the AM, and an empirical distribution of the observed peak sea levels at high tide. The verifications indicate that the SSJPM is robust.

Tidal exceedance curves were based on 100-year tidal projections calculated using the T_TIDE MatLAB package (Pawlowicz et al., 2002). A thresholding routine was then used to calculate tidal statistics and infer exceedance levels.

All vertical datums are available from LINZ.

2.5 Inundation exposure modelling

Research for the Deep South National Science Challenge covered national, regional and district-level risk exposure to inundation in low-lying coastal areas (Paulik et al., 2019b, Paulik et al., 2020) and areas exposed to fluvial and pluvial (rainfall) flooding (Paulik et al., 2019a), noting that the latter study does not include climate change effects (only the present-day risk exposure). The RiskScape asset database was used to measure potential exposure. RiskScape⁸ is a tool used to predict exposure to natural hazards. Exposure to extreme coastal flooding in Tairāwhiti and Hawke's Bay was expressed as land area, built assets and infrastructure in the zone potentially exposed to direct and indirect⁹ extreme flood levels in a 100-year return period storm-tide event (1% annual exceedance probability or AEP) at the present day, combined with different increments of sea-level rise (SLR) (0.5 m, 1 m and 1.5 m of SLR are considered here). Maps showing the areas in the Tairāwhiti and Hawke's Bay regions exposed to a 1% AEP storm tide event at the present day and with different increments of sea-level rise are presented in Appendix A. It is noted that the coverage of the coastal flood mapping is limited to locations where high-resolution digital elevation models (DEMs) were available (Paulik et al., 2020). The exposure of assets in locations without available high-resolution DEMs are therefore not quantified in this report. Refer to Appendix A for additional detail regarding data coverage.

The timeframes for these SLR increments to emerge, based on the four SLR scenarios in the MfE coastal guidance (Ministry for the Environment, 2017) are shown in Table 2-2. These years of emergence do not include vertical land movement at any local site, with ongoing subsidence exacerbating the effective SLR, and bring forward in time when these SLR increments are reached. Note that only the potential inundation-exposed area of buildings was provided, rather than the total footprint area of all buildings fully or partially exposed.

⁸ <https://niwa.co.nz/natural-hazards/research-projects/riskscape-software>

⁹ Indirect refers to several possible situations where land areas do not have a direct overland flow of seawater, but could be exposed to residual risk (e.g. breaches of a stopbank or seawall, seepage, groundwater rise with SLR, tide gates unable to shut due to debris, combinations with river flooding).

Table 2-2: Approximate years (nearest 5 years) when specific SLR increments would be reached for wider NZ. Based on the 4 scenarios in the MfE (2017) coastal guidance: Table 11, and relative to a baseline MSL over the period 1986–2005 – see Appendix E, MfE(2017).

SLR increment	RCP8.5 H ⁺	RCP8.5 M	RCP4.5 M	RCP2.6 M
0.5 m	2060	2075	2090	2110
1.0 m	2100	2115	2170	>2200
1.5 m	2130	2160	>2200	>2200
2.0 m	2155	2200	>2200	>2200

The same asset database was intersected with a flood hazard area map that was created using publicly available flood hazard maps from local government organisations and flood-prone soil maps from Manaaki Whenua Landcare Research. This exercise included all areas inundated by past floods and areas considered to be at risk from flooding. Some flood prone areas may not be correctly identified and there was no specific return period assigned to this flood hazard area. This exercise did not consider potential changes to flood events with climate change, due to the unavailability of extreme flood projections at present. However, it provides a useful baseline for understanding all areas currently exposed to flood hazards in the Tairāwhiti and Hawke’s Bay regions. Maps of the flood hazard area in the Tairāwhiti and Hawke’s Bay regions are presented in Appendix A.

Elements exposed to coastal and flood hazards include both tangible and intangible assets. Included in the analysis for this report were:

- Land cover
 - Exotic forest
 - Forest – harvested
 - High producing exotic grassland
 - Low producing grassland
 - Orchard, vineyard or other perennial crop
 - Regional parks (for Hawke’s Bay)
 - Reserves (for Tairāwhiti – amenity, heritage, neighbourhood and recreational reserves)
- Transport infrastructure
 - Roads
 - Railway
 - Airports
 - Cycle lanes

- Water infrastructure
 - Stopbanks
 - Drains
 - Pipelines
 - Culverts
 - Floodgates
 - Headwalls
 - Pump stations
 - Deflection banks
 - Dams
 - Three waters¹⁰ nodes¹¹
 - Three waters pipelines
- Other infrastructure
 - Transmission lines
- Buildings
 - Total number (#)
 - Replacement value (\$ million)
 - Population (#)

2.6 Limitations

As with any modelling exercise, there are limitations on the results and use of the data. This section outlines some of these limitations and caveats that should be considered when using the results in this report.

- The maps and tables presented in this report show the average of six dynamically downscaled global climate models. This is a relatively small number of models and the full distribution of potential future outcomes is not available. In particular, the extremes of the distributions are not accurately represented in small ensembles.
- The average of six models is used in this report, which gives no indication of the range of the models' results. However, the six models chosen represented historic climate conditions in New Zealand well, and span a range of future outcomes. Using the average reduces the errors of the individual models.

¹⁰ Three-waters infrastructure refers to drinking water, wastewater and stormwater infrastructure.

¹¹ Three-waters nodes refer to infrastructure components such as connectors, aerators, bio-filters, valves, vents, treatment plants, pumps, etc. A full list of three-waters nodes included in this analysis is found in Paulik et al. (2019a).

- The time periods chosen for historic and future projection span 20-year periods. This is seen as a relatively short timeframe to understand average conditions in the historic period and in the future, as there is likely an influence of underlying climate variability (e.g. multi-annual to multi-decadal signals from climate drivers like the El Niño-Southern Oscillation etc.). However, the IPCC uses 20-year periods, so we have followed that approach for consistency.
- Care needs to be taken when interpreting grid-point-scale projections such as those presented in the tables in this report. The data have been bias-corrected, downscaled and interpolated from the approximately 30 km regional climate model grid to the 5 km grid across New Zealand using physically based models. Therefore, the data from these grid points may be slightly different to on-the-ground observations. It is useful to look at broader patterns between grid points, e.g. coast vs. inland, and the magnitude of change at different time periods and scenarios, when considering the values.

Although there are limitations and caveats to the approach used here, these climate change projections are the best currently available for New Zealand. A considerable amount of research effort has been dedicated to undertaking the modelling and validation of the results, and the projections provide context to base risk assessments and adaptation plans on.

3 Current and future climate of Tairāwhiti/Hawke's Bay

In comparison with regions exposed to the west, Tairāwhiti experiences a greater number of weather and climatic extremes. Its position as the easternmost region of New Zealand often results in differing weather conditions from those elsewhere, in that synoptic features over the ocean to the east of New Zealand sometimes affect Tairāwhiti alone among New Zealand regions. The climate is generally congenial with a large number of sunshine hours per year and a low mean wind speed. However, rainfall is unevenly distributed throughout the year with a prominent winter maximum and a shortage of rainfall during spring (Chappell, 2016).

The climate of Hawke's Bay is influenced largely by the orography and the airstreams crossing New Zealand. It is a region of highly variable and sporadic rainfall, and large and occasionally sudden temperature variations. Hawke's Bay is a sunny region with most areas having over 2000 hours per year. Hawke's Bay is less windy than many other coastal areas of New Zealand, experiencing a high frequency of very light winds. Consequently, a large number of frosts occur during the cooler months of the year. Much of the rain in Hawke's Bay occurs when the wind directions are predominantly easterly or southerly. Rainfall is extremely variable in spring and summer when westerly winds prevail over the country. In most years insufficient rainfall (dry spells) results in a total depletion of soil moisture to the extent that plant growth ceases. The high country areas of Hawke's Bay are exposed and gales occur frequently. Flurries of snow are frequent during the winter months in cold southerly conditions.

More information about the historic climate of Tairāwhiti and Hawke's Bay, outside of the information in this report, can be found in Chappell (2013, 2016).

4 Temperature

4.1 Mean temperature

Historic (average over 1986-2005) and future (average over 2031-2050 and 2081-2100) maps for mean temperature are shown in this section. The historic maps show annual and seasonal mean temperature in units of degrees Celsius (°C) and the future projection maps show the change in mean temperature compared with the present day, in units of °C. Note that the historic maps are on a different colour scale to the future projection maps.

For the modelled historic period, coastal portions of the Tairāwhiti and Hawke's Bay regions have the highest annual and seasonal mean temperatures whereas areas furthest inland have the lowest mean temperatures, particularly those at high elevations (Figure 4-1 to Figure 4-4). Temperatures are generally higher for Tairāwhiti than for Hawke's Bay.

Representative concentration pathway (RCP) 4.5

By 2040, annual and seasonal mean temperatures are projected to increase by 0.5-1.0°C under RCP4.5 in both regions (Figure 4-5 to Figure 4-8).

By 2090, annual mean temperatures for both regions are projected to increase by 1.0-1.5°C, with the exception of the Whangaparaoa and Waikura catchments in the northwest of the Tairāwhiti Region, where projected warming is 0.5-1.0°C (Figure 4-5 and Figure 4-6). At the seasonal scale, projected increases to mean temperature generally range from 0.5-1.5°C, although autumn temperatures in both regions (as well as spring temperatures in the Hawke's Bay region) are projected to increase by

a narrower range (1.0-1.5°C) (Figure 4-9 and Figure 4-10). The highest projected increases by 2090 under RCP4.5 are in the range of 1.5-2.0°C, and are restricted to the westernmost portion of Hawke's Bay during summer (Figure 4-10).

Representative concentration pathway (RCP) 8.5

By 2040, annual mean temperatures are projected to increase by 0.5-1.0°C in both regions (similar to RCP4.5; Figure 4-5 and Figure 4-6). This is also the case for majority of both regions at the seasonal scale, although western parts of the Hawke's Bay region are projected to increase by 1.0-1.5°C during summer and autumn, as is the northeastern portion of Tairāwhiti during autumn (Figure 4-11 and Figure 4-12).

By 2090, annual mean temperatures under RCP8.5 are projected to be around 2.5-3.0°C higher for most western/inland parts of both regions, and for coastal locations between Poverty Bay and Wairoa (Figure 4-5 and Figure 4-6). Remaining coastal locations are projected to warm by 2.0-2.5°C. The Whangaparoa and Waikura catchments (in northern Tairāwhiti) are projected to warm by the smallest amount (1.5-2.0°C; Figure 4-5), while the westernmost portion of the Hawke's Bay region is projected to warm the most (3.0-3.5°C; Figure 4-6). At the seasonal scale, projected increases to mean temperatures are generally higher for autumn with the majority of both regions projected to increase by 2.5-3.0°C (and as much as 3.0-3.5°C for westernmost locations; Figure 4-13 and Figure 4-14). Conversely, projected warming is generally lower for winter, with the majority of both regions projected to increase by 2.0-2.5°C. Spring and summer temperature increases also tend to be in the 2.0-3.0°C range, although western parts of the Hawke's Bay region during summer have the largest projected increases of all the seasons at 3.0-4.0°C (Figure 4-14). For all seasons, the smallest temperature increases in this scenario are projected for the Whangaparoa and Waikura catchments in northern Tairāwhiti (Figure 4-13).

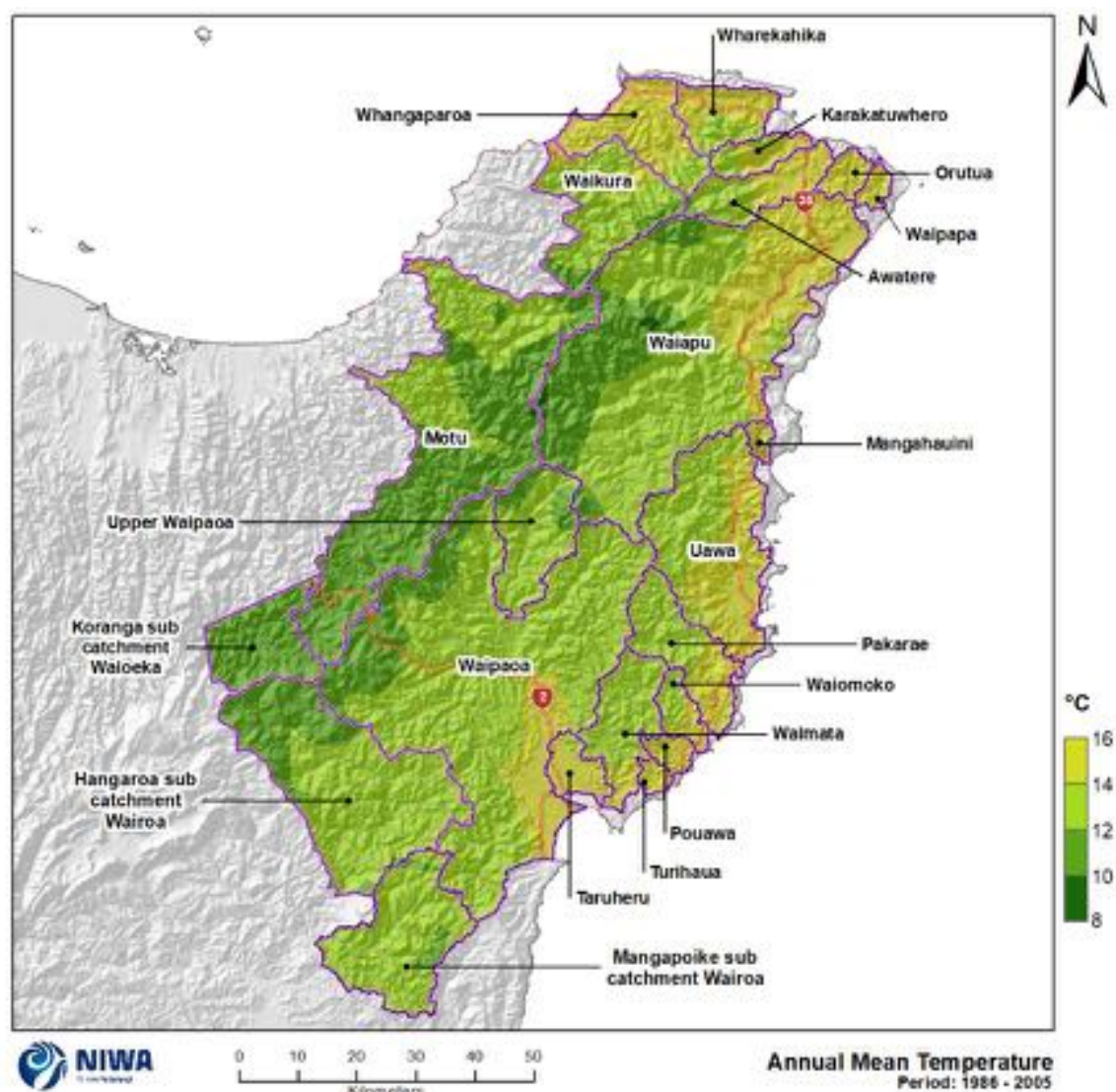


Figure 4-1: Modelled annual mean temperature for Tairāwhiti, average over 1986-2005. Results are based on dynamical downscaled projections using NIWA's Regional Climate Model. Resolution of projection is 5km x 5km.

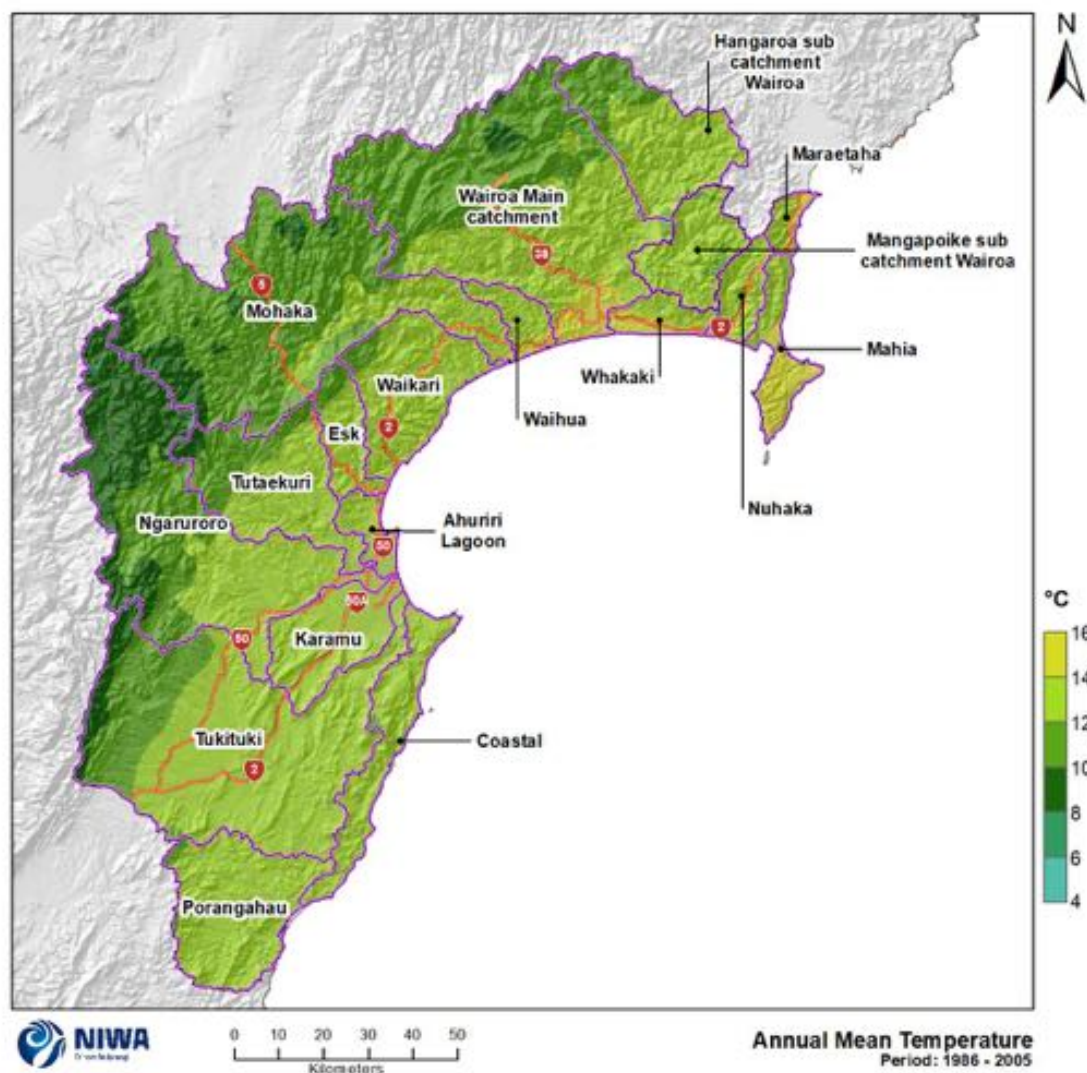


Figure 4-2: Modelled annual mean temperature for Hawke's Bay region, average over 1986-2005 . Results are based on dynamical downscaled projections using NIWA's Regional Climate Model. Resolution of projection is 5km x 5km.

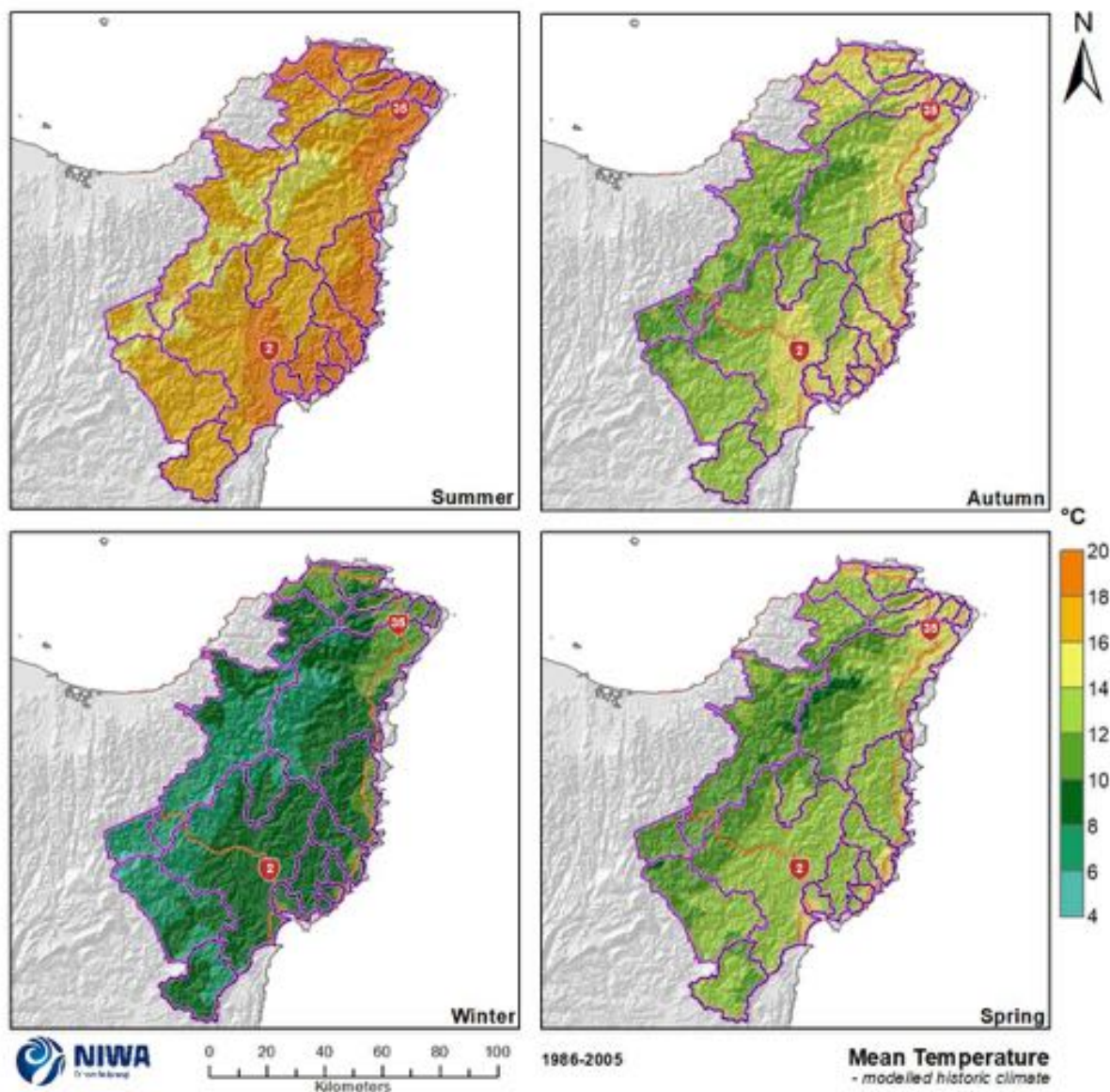


Figure 4-3: Modelled seasonal mean temperature for Tairāwhiti, average over 1986-2005 . Results are based on dynamical downscaled projections using NIWA's Regional Climate Model. Resolution of projection is 5km x 5km.

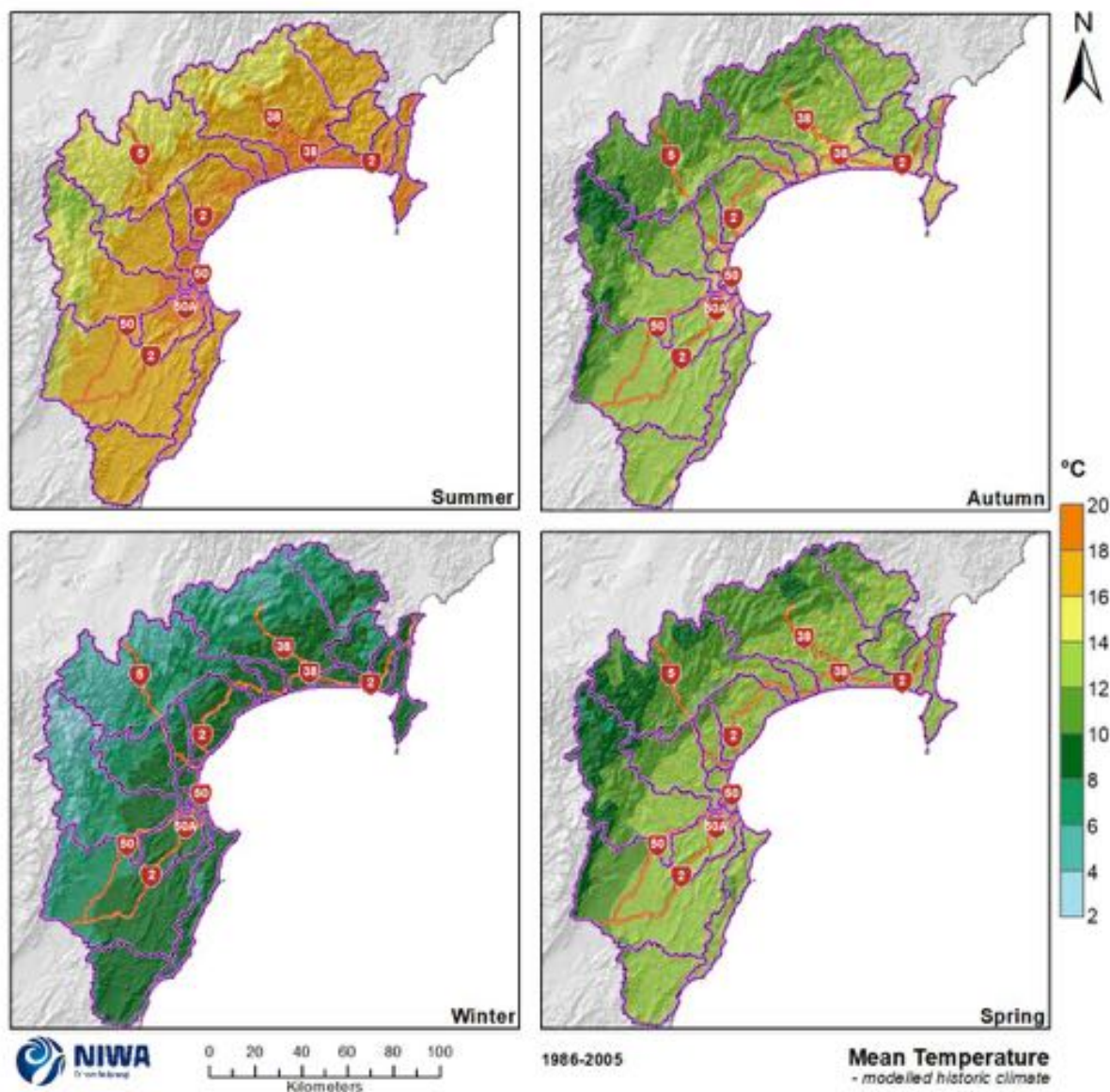


Figure 4-4: Modelled seasonal mean temperature for Hawke's Bay region, average over 1986-2005 . Results are based on dynamical downscaled projections using NIWA's Regional Climate Model. Resolution of projection is 5km x 5km.

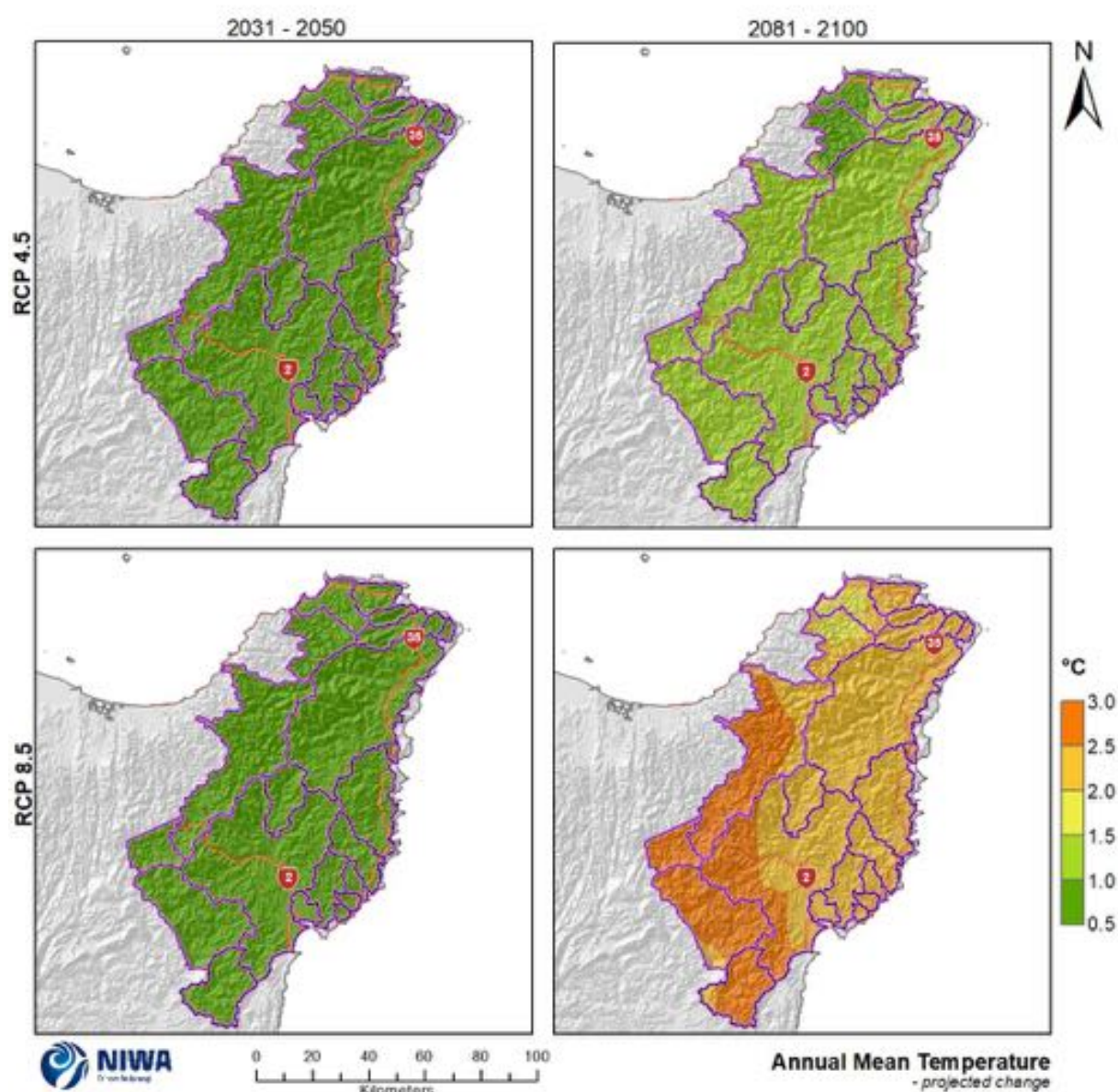


Figure 4-5: Projected annual mean temperature changes for Tairāwhiti by 2040 and 2090 under RCP4.5 and RCP8.5. Relative to 1986-2005 average, based on the average of six global climate models. Results are based on dynamical downscaled projections using NIWA's Regional Climate Model. Resolution of projection is 5km x 5km.

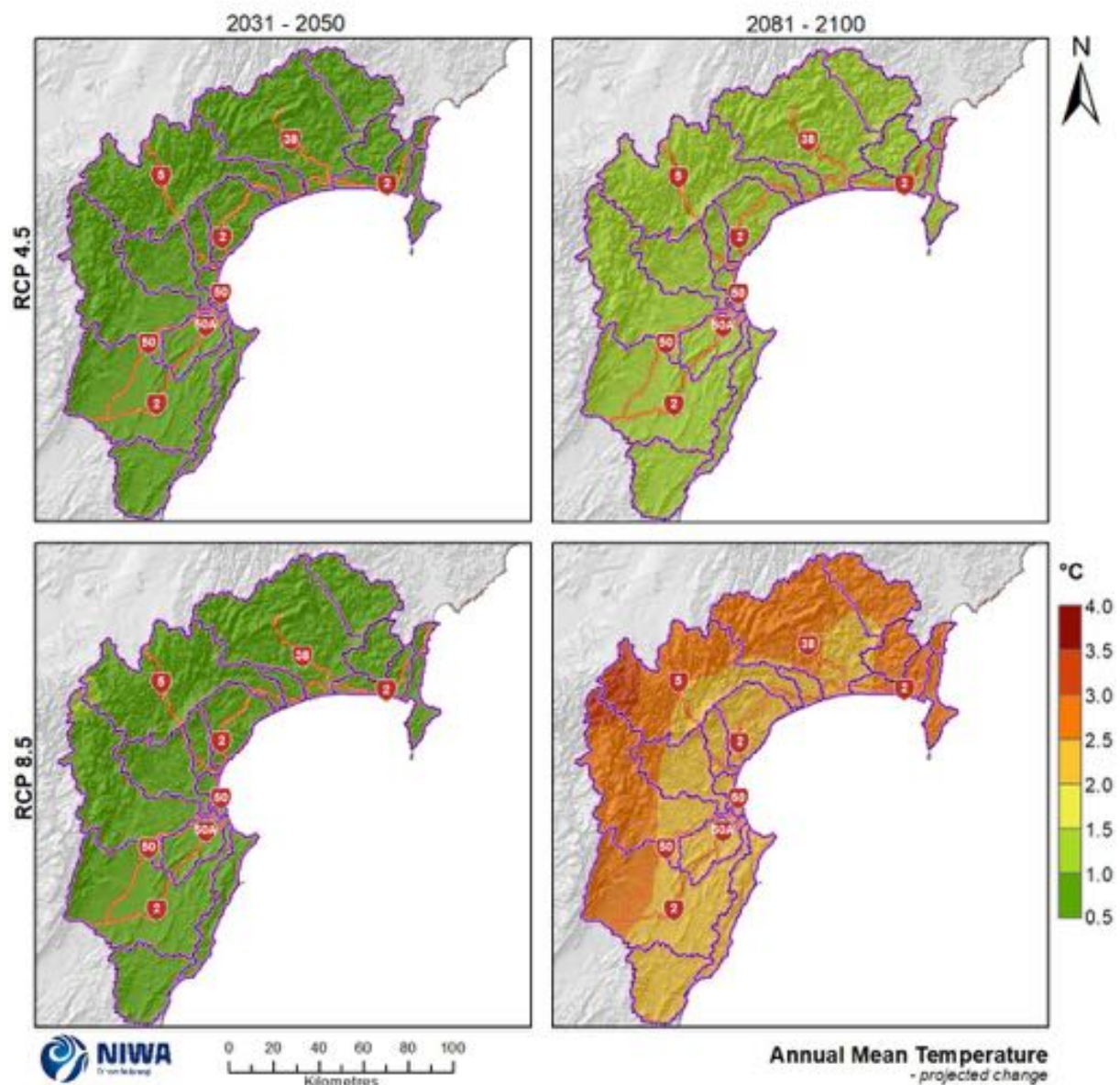


Figure 4-6: Projected annual mean temperature changes for Hawke's Bay by 2040 and 2090 under RCP4.5 and RCP8.5. Relative to 1986-2005 average, based on the average of six global climate models. Results are based on dynamical downscaled projections using NIWA's Regional Climate Model. Resolution of projection is 5km x 5km.

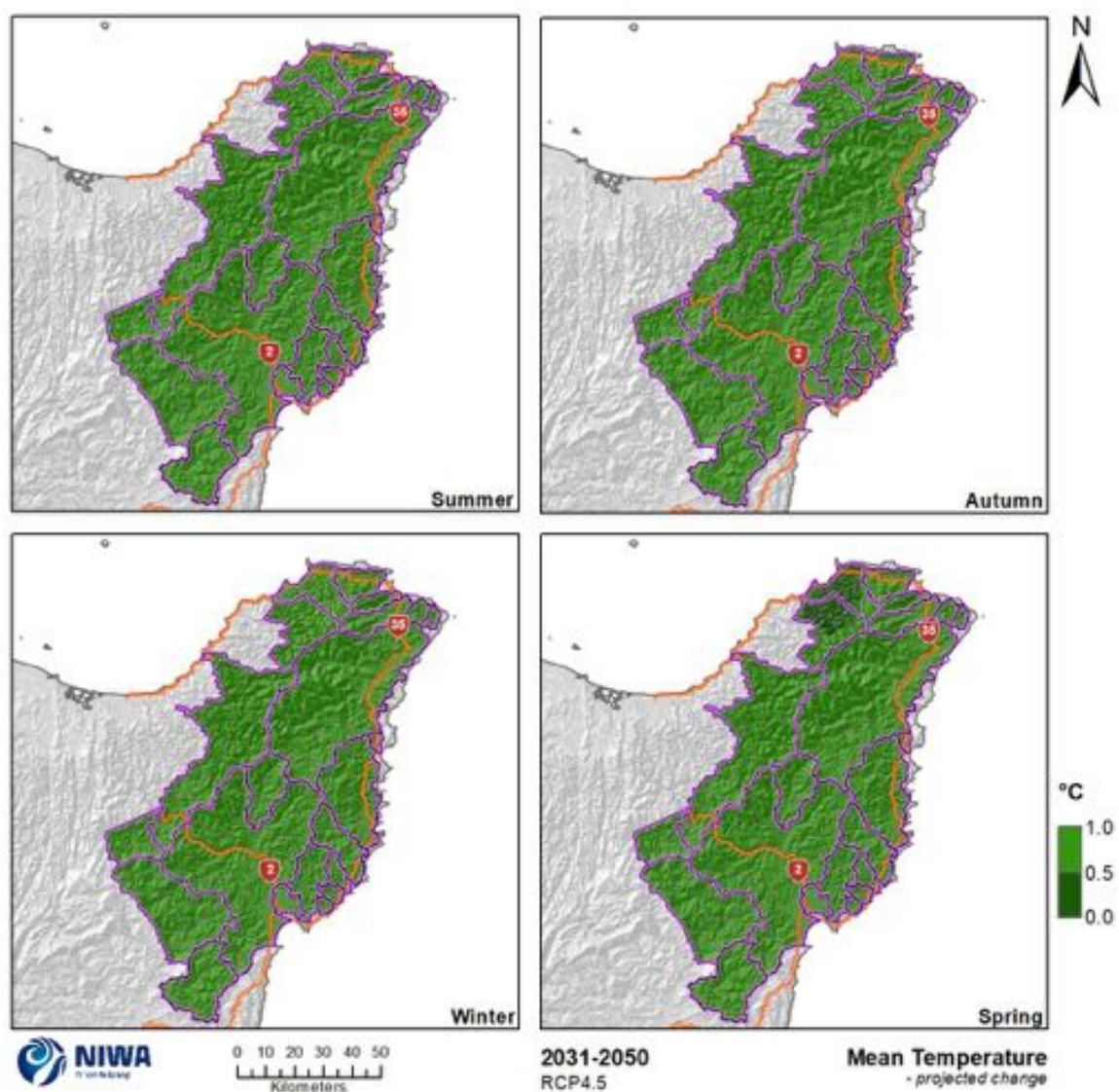


Figure 4-7: Projected seasonal mean temperature changes for Tairāwhiti by 2040 under RCP4.5. Relative to 1986-2005 average, based on the average of six global climate models. Results are based on dynamical downscaled projections using NIWA's Regional Climate Model. Resolution of projection is 5km x 5km.

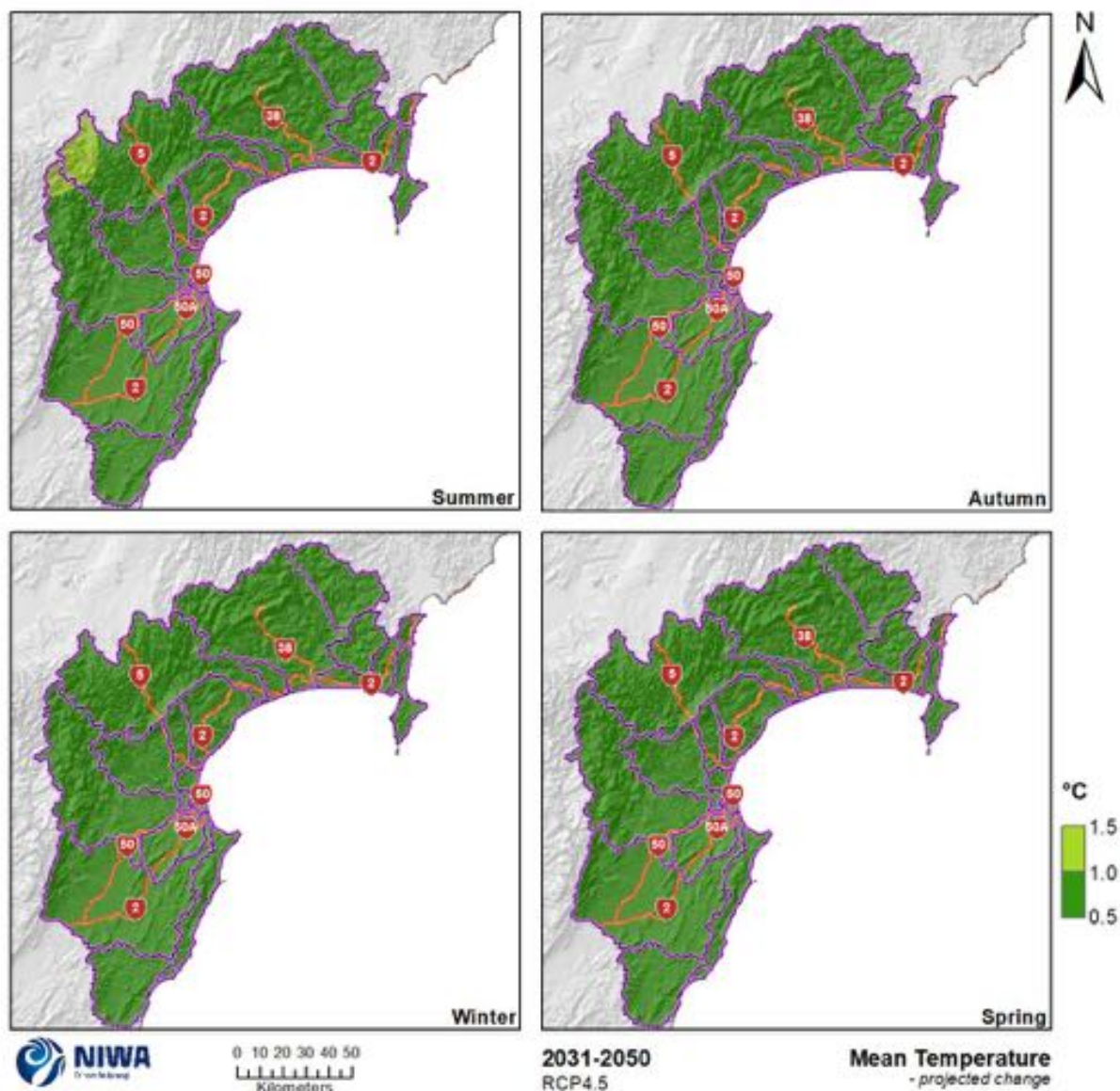


Figure 4-8: Projected seasonal mean temperature changes for the Hawke's Bay region by 2040 under RCP4.5. Relative to 1986-2005 average, based on the average of six global climate models. Results are based on dynamical downscaled projections using NIWA's Regional Climate Model. Resolution of projection is 5km x 5km.

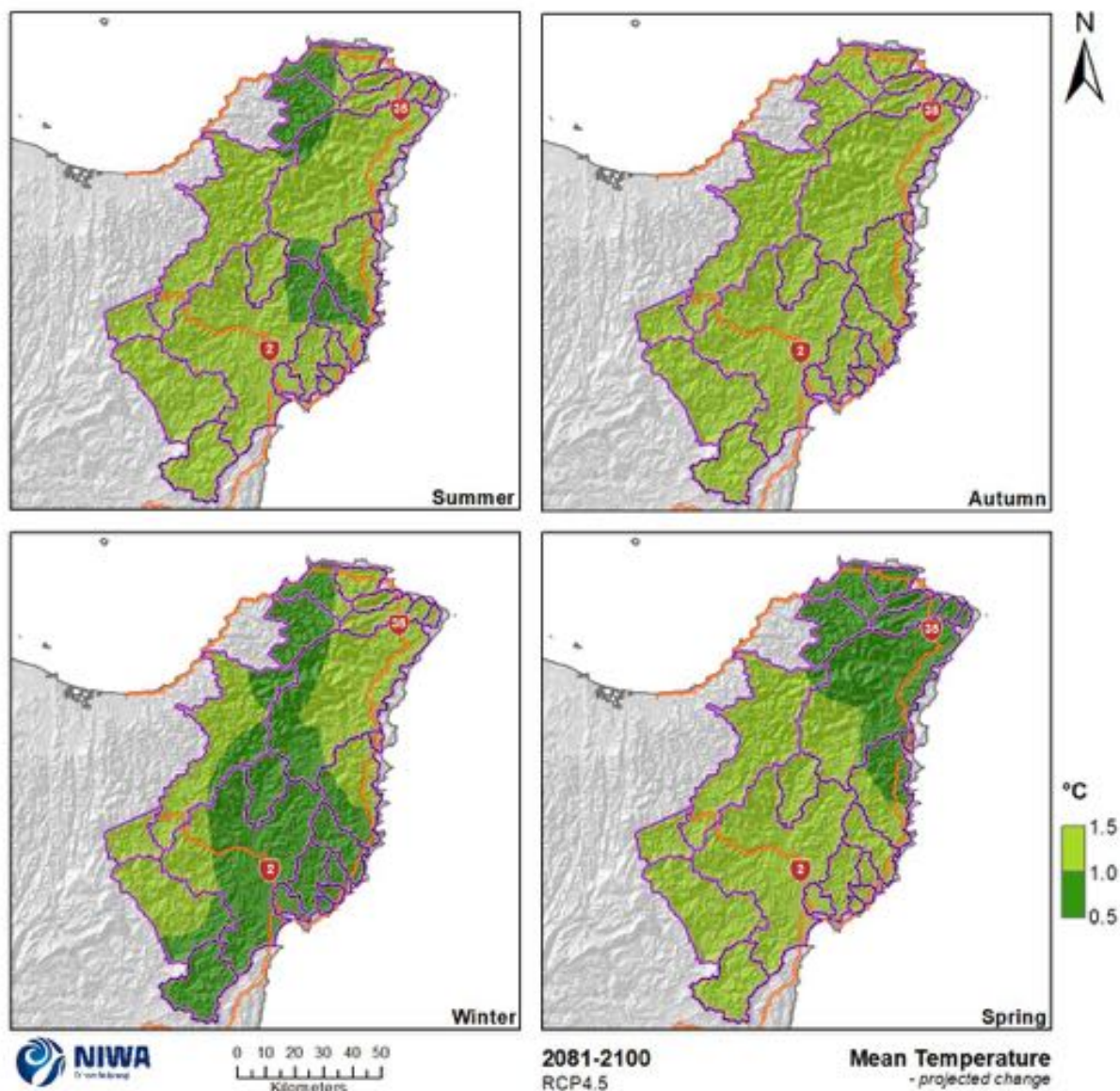


Figure 4-9: Projected seasonal mean temperature changes for Tairāwhiti by 2090 under RCP4.5. Relative to 1986-2005 average, based on the average of six global climate models. Results are based on dynamical downscaled projections using NIWA's Regional Climate Model. Resolution of projection is 5km x 5km.

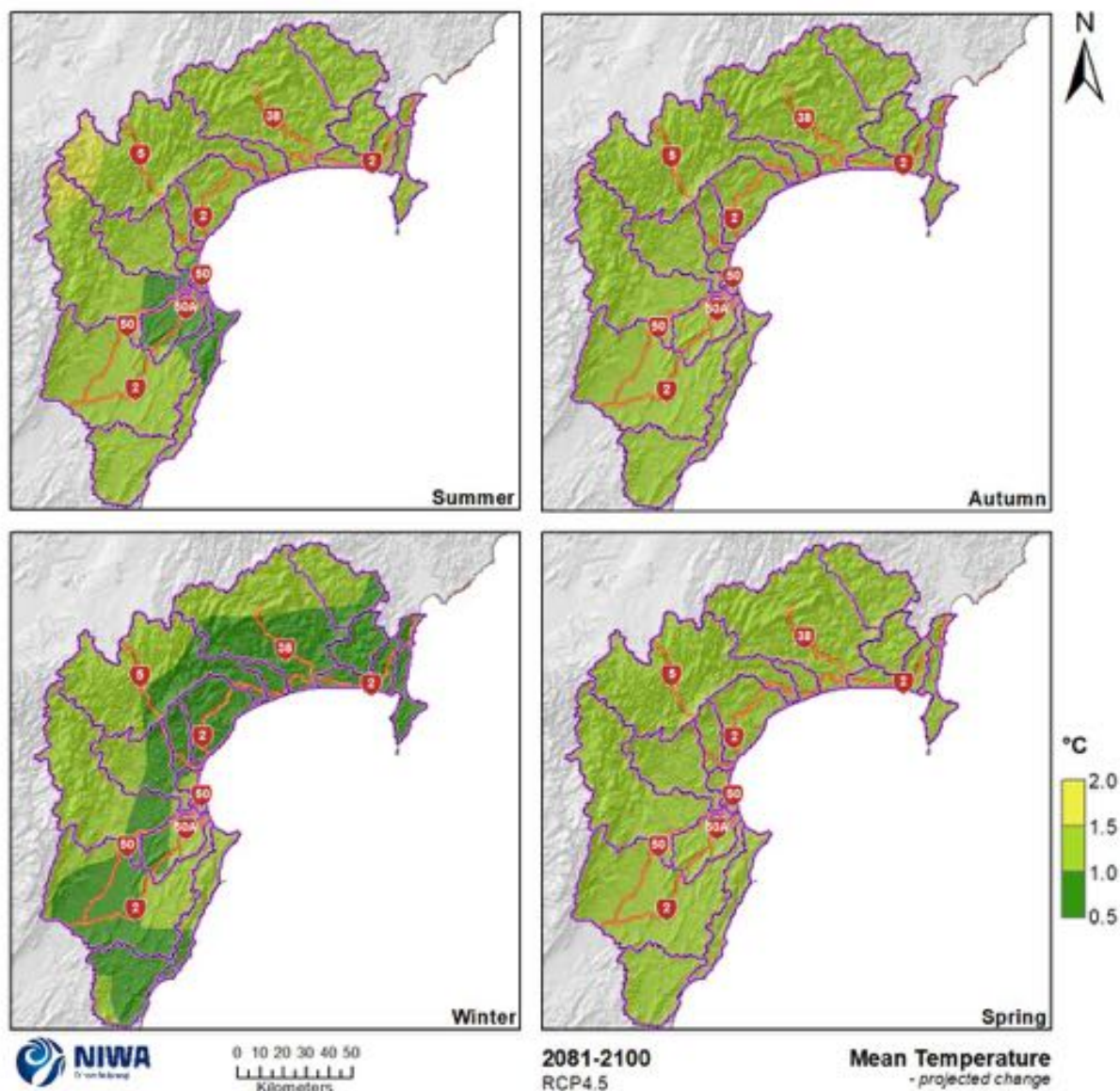


Figure 4-10: Projected seasonal mean temperature changes for the Hawke's Bay region by 2090 under RCP4.5. Relative to 1986-2005 average, based on the average of six global climate models. Results are based on dynamical downscaled projections using NIWA's Regional Climate Model. Resolution of projection is 5km x 5km.

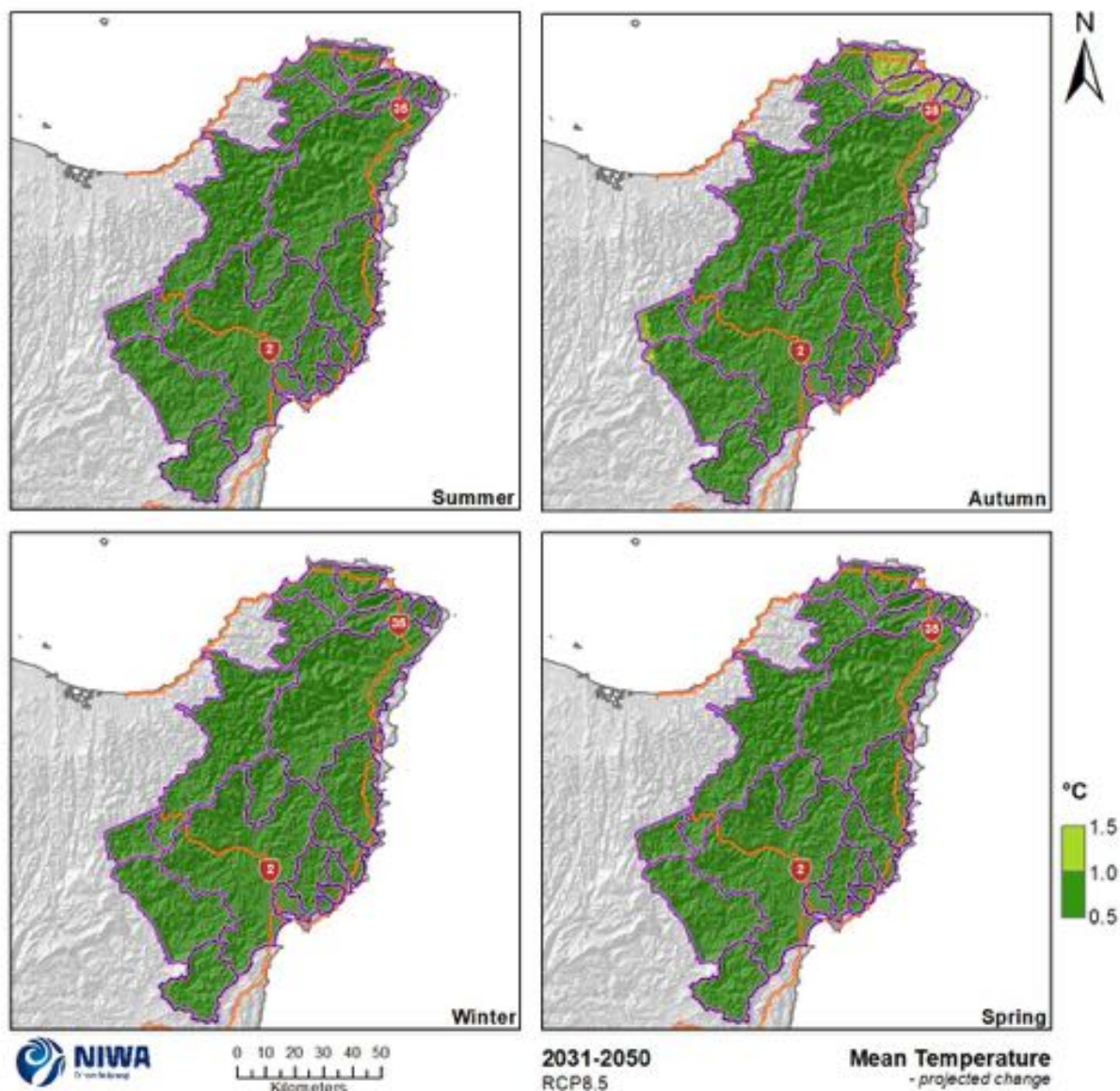


Figure 4-11: Projected seasonal mean temperature changes for Tairāwhiti by 2040 under RCP8.5. Relative to 1986-2005 average, based on the average of six global climate models. Results are based on dynamical downscaled projections using NIWA's Regional Climate Model. Resolution of projection is 5km x 5km.

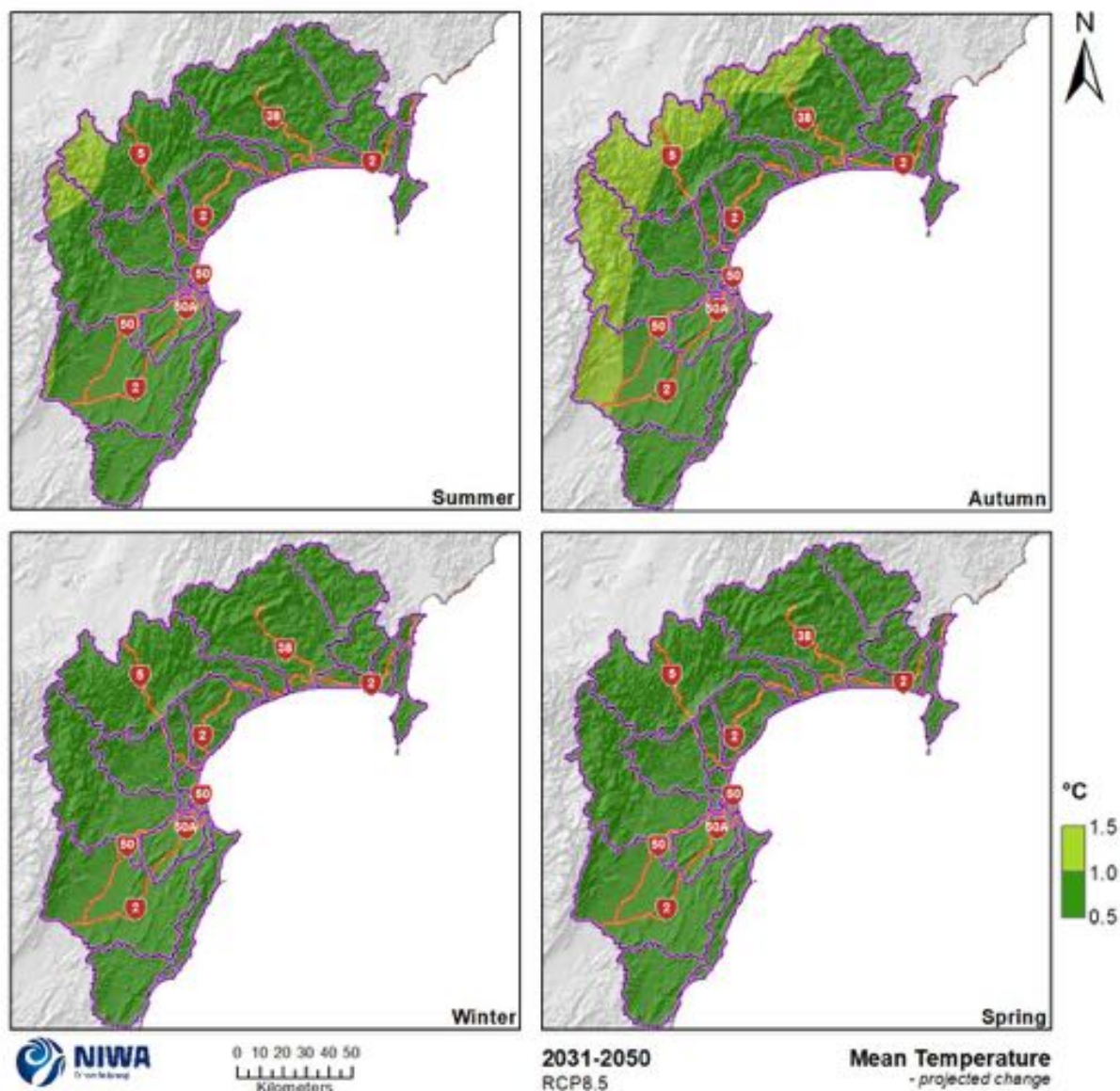


Figure 4-12: Projected seasonal mean temperature changes for the Hawke's Bay region by 2040 under RCP8.5. Relative to 1986-2005 average, based on the average of six global climate models. Results are based on dynamical downscaled projections using NIWA's Regional Climate Model. Resolution of projection is 5km x 5km.

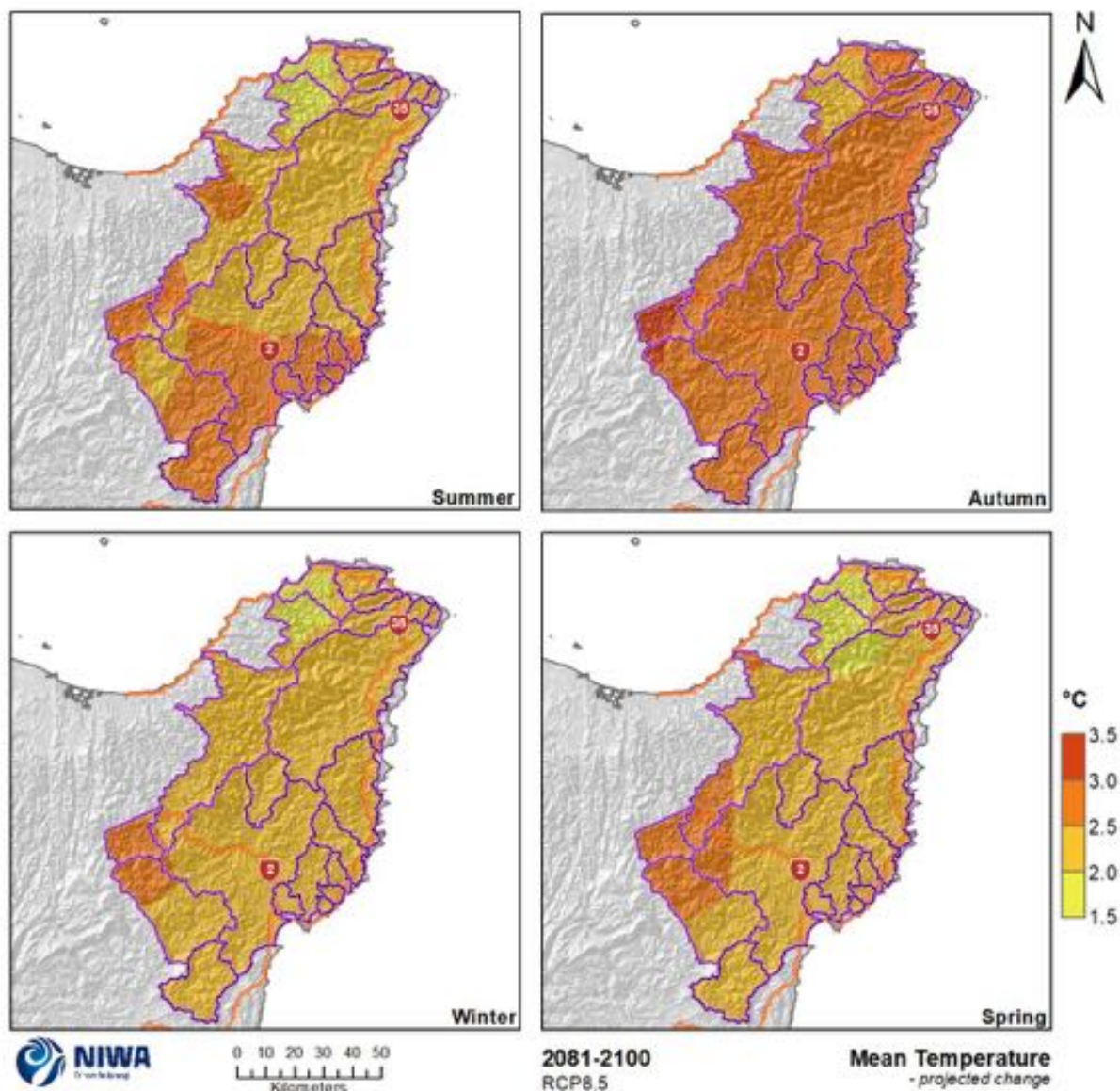


Figure 4-13: Projected seasonal mean temperature changes for Tairāwhiti by 2090 under RCP8.5. Relative to 1986-2005 average, based on the average of six global climate models. Results are based on dynamical downscaled projections using NIWA's Regional Climate Model. Resolution of projection is 5km x 5km.

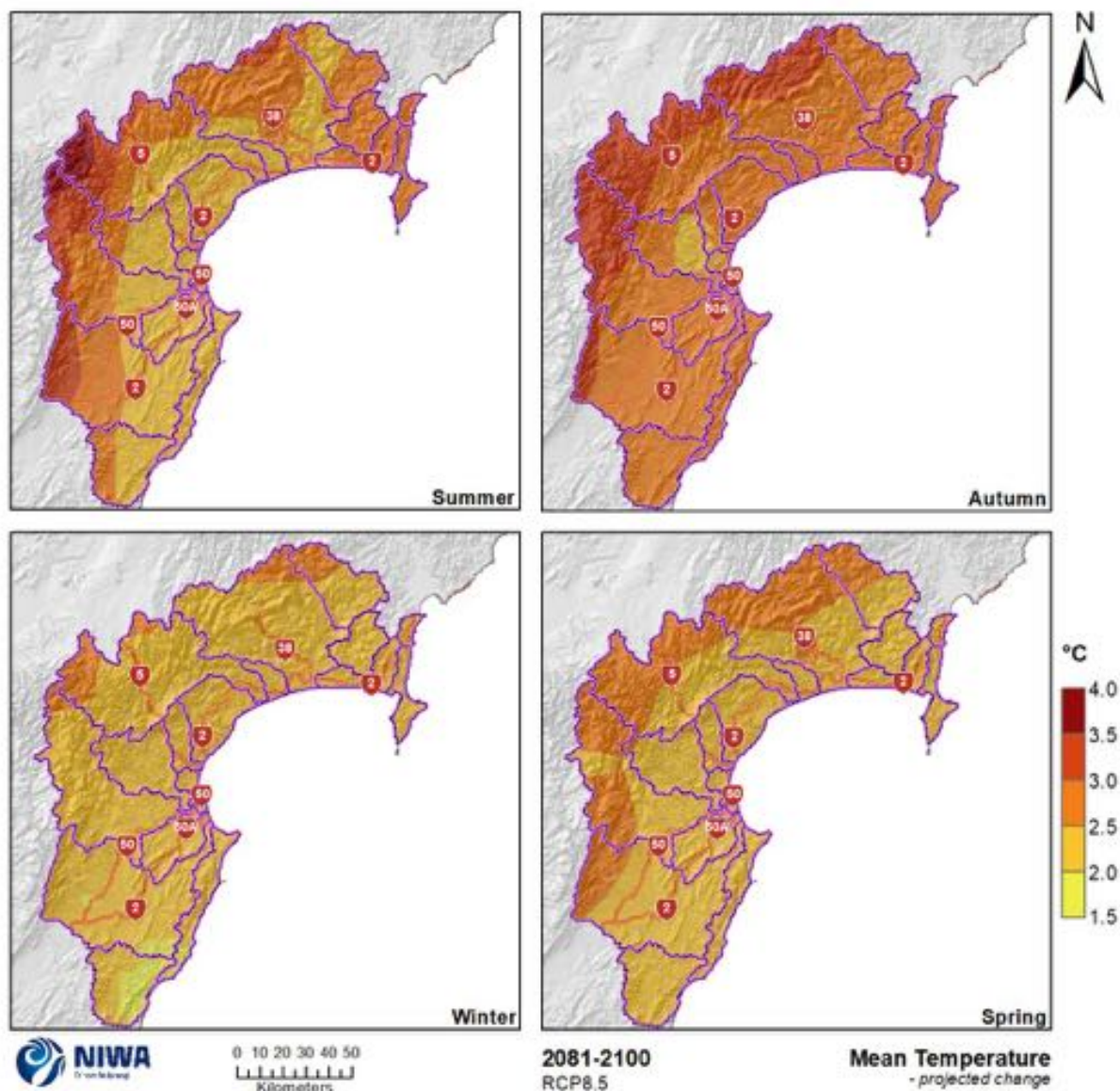


Figure 4-14: Projected seasonal mean temperature changes for the Hawke's Bay region by 2090 under RCP8.5. Relative to 1986-2005 average, based on the average of six global climate models. Results are based on dynamical downscaled projections using NIWA's Regional Climate Model. Resolution of projection is 5km x 5km.

4.2 Minimum temperature

Minimum temperatures are generally recorded in the early hours of the morning, and therefore are known as night-time temperatures. Historic (average over 1986-2005) and future (average over 2031-2050 and 2081-2100) maps for mean minimum temperature are shown in this section. The historic maps show annual and seasonal mean minimum temperature in units of degrees Celsius (°C) and the future projection maps show the change in mean minimum temperature compared with the historic period, in units of °C. Note that the historic maps are on a different colour scale to the future projection maps.

For the historic period, coastal portions of Tairāwhiti and Hawke's Bay have the highest annual and seasonal mean minimum temperatures (8-10°C at the annual scale; Figure 4-15 and Figure 4-16), particularly for the north of Tairāwhiti (10-12°C at the annual scale). Areas furthest inland have the lowest mean minimum temperatures, particularly in the Hawke's Bay region.

Representative concentration pathway (RCP) 4.5

By 2040, annual mean minimum temperatures are projected to increase by 0.5-1.0°C under RCP4.5 in both regions, with several isolated areas increasing by only 0.0-0.5°C (Figure 4-19 and Figure 4-20). At the seasonal scale, autumn minimum temperatures are projected to increase by 0.5-1.0°C for the entirety of both regions, while increases for the remaining three seasons range from 0.0 to 1.0°C (Figure 4-21 and Figure 4-22).

By 2090, projected changes to annual mean minimum temperatures are similar to 2040, with increases of 0.5-1.0°C for the majority of both regions, however there are no annual increases of less than 0.5°C, and several inland locations are projected to increase by slightly larger values 1.0-1.5°C (Figure 4-23 and Figure 4-24). Winter minimum temperatures are projected to increase by 0.5-1.0°C for the entirety of both regions while the remaining seasons are projected to generally have minimum temperature increases ranging from 0.5-1.5°C. Autumn however has more locations which are projected to experience increases on the higher end of this range (i.e. 1.0-1.5°C) compared to the other seasons. The lowest projected increases at the seasonal scale are 0.0-0.5°C, restricted to the Whangaparoa and Waikura catchments in the north of Tairāwhiti during spring.

Representative concentration pathway (RCP) 8.5

By 2040, annual mean minimum temperatures are projected to increase by 0.5-1.0°C under RCP8.5 in both regions, with several isolated areas increasing by only 0.0-0.5°C (similar to RCP4.5; Figure 4-19 and Figure 4-20). At the seasonal scale, projected increases are also similar to RCP4.5 by 2040, with autumn minimum temperatures projected to increase by 0.5-1.0°C for the entirety of both regions, and remaining seasons projected to increase by 0.0-1.0°C. It is noted however that most of the Hawke's Bay region is projected to have increases to spring minimum temperatures which are on the upper end of this range (0.5-1.0°C), with only a few locations projected to increase by 0.0-0.5°C (Figure 4-25 and Figure 4-26).

By 2090, projected increases to minimum temperatures are much greater than under RCP4.5, with increases of 1.5-2.0°C projected for the eastern majority of both regions, and 2.0-2.5°C for western locations (Figure 4-19 and Figure 4-20). The greatest projected warming (+2.5-3.0°C) is restricted to the west of the Mohaka catchment in the Hawke's Bay Region (i.e. at the western boundary of the region). At the seasonal scale, autumn minimum temperatures are projected to increase by the most across both regions (+2.0-3.0°C; Figure 4-27 and Figure 4-28). Winter is projected to generally

experience the smallest increases, with +1.0-1.5°C projected for southeast Tairāwhiti and eastern Hawke's Bay, and +1.5-2.0°C projected for most remaining locations. Summer and spring are generally projected to increase by 1.5-2.5°C although coastal portions of the Whangaparaoa and Waikura catchments in the north of Tairāwhiti have the smallest increases to minimum temperature projected for spring (+0.0-0.5°C).

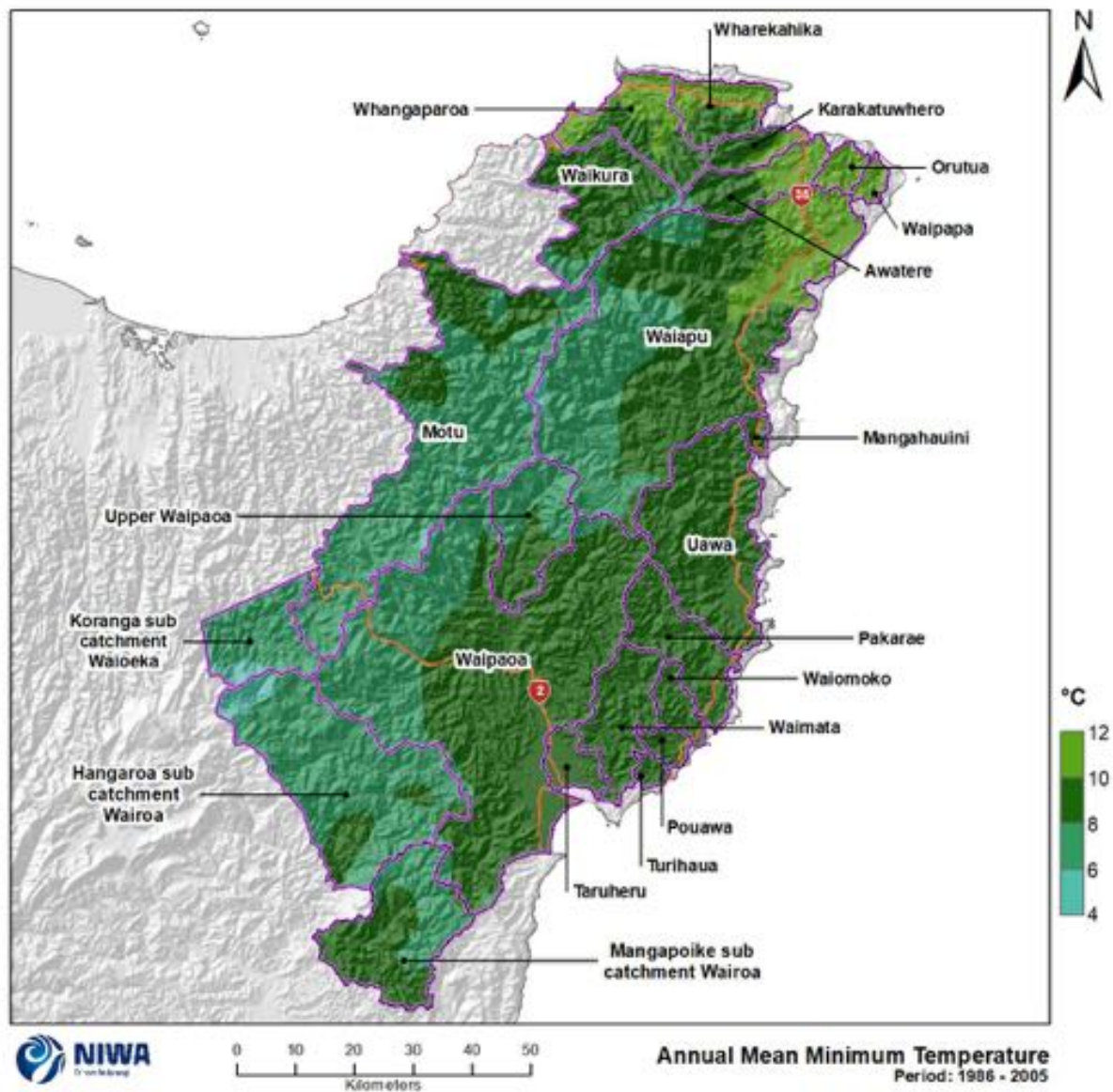


Figure 4-15: Modelled annual mean minimum temperature for Tairāwhiti, average over 1986-2005. Results are based on dynamical downscaled projections using NIWA's Regional Climate Model. Resolution of projection is 5km x 5km.

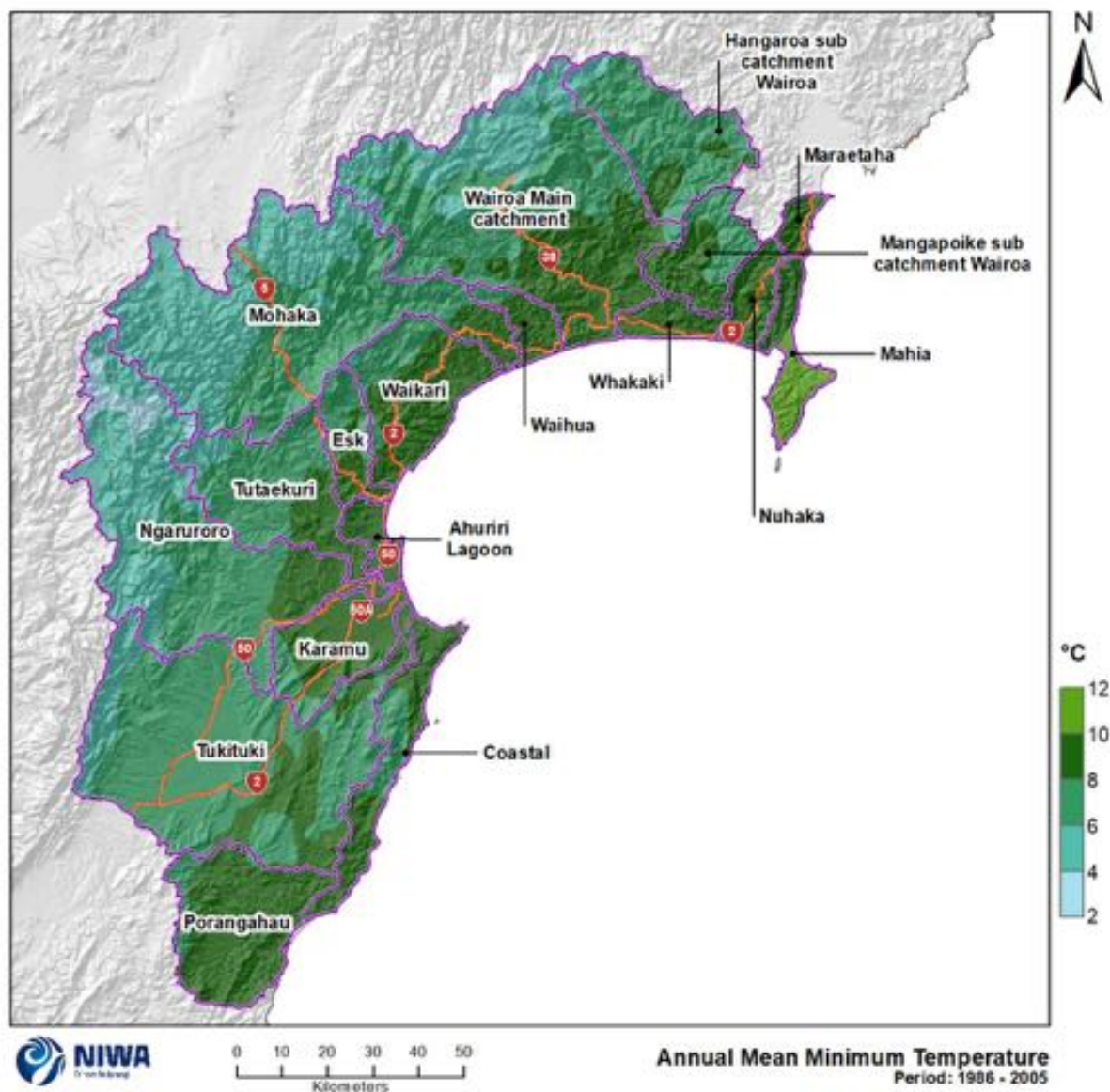


Figure 4-16: Modelled annual mean minimum temperature for Hawke's Bay region, average over 1986-2005. Results are based on dynamical downscaled projections using NIWA's Regional Climate Model. Resolution of projection is 5km x 5km.

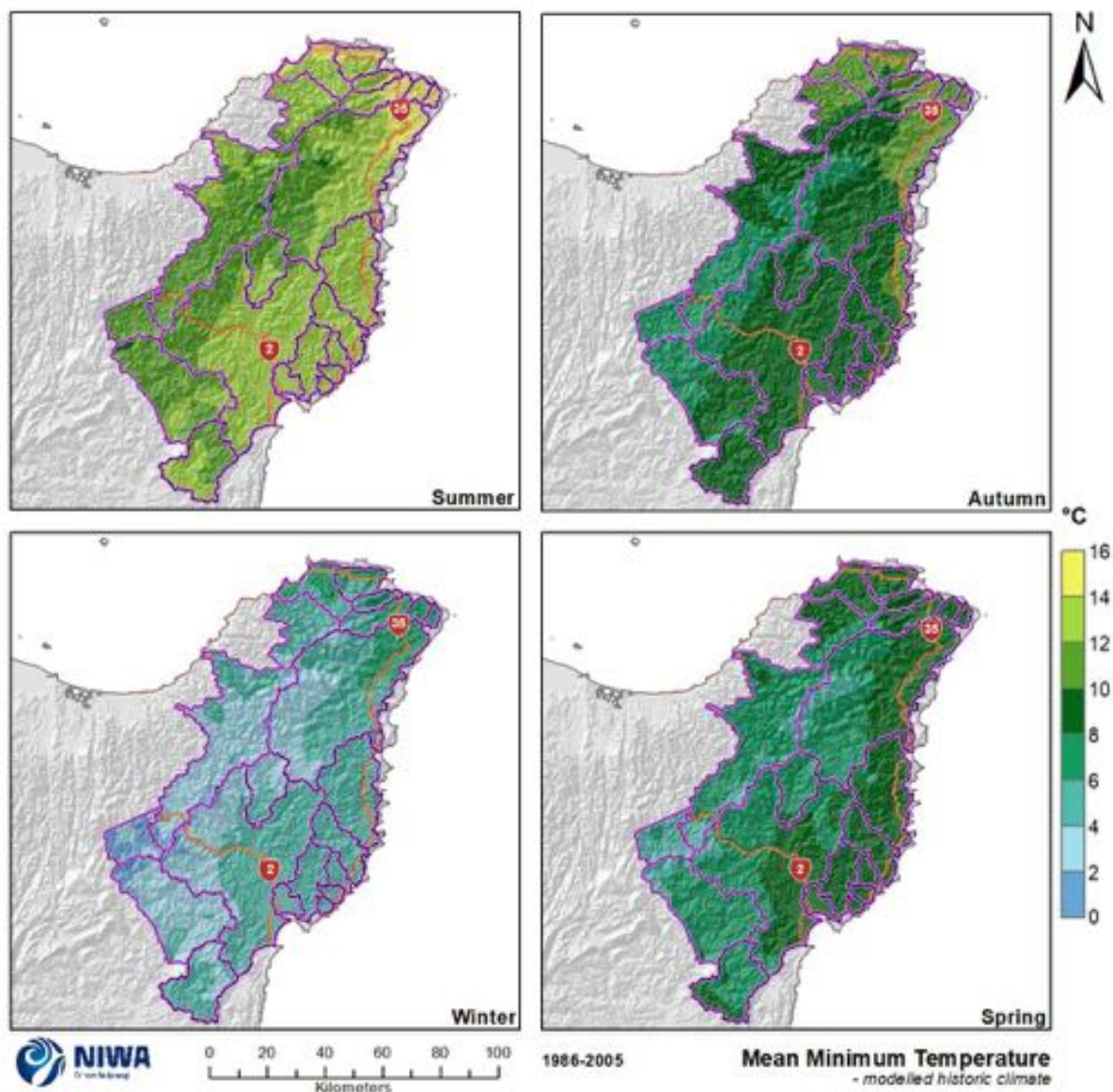


Figure 4-17: Modelled seasonal mean minimum temperature for Tairāwhiti, average over 1986-2005. Results are based on dynamical downscaled projections using NIWA's Regional Climate Model. Resolution of projection is 5km x 5km.

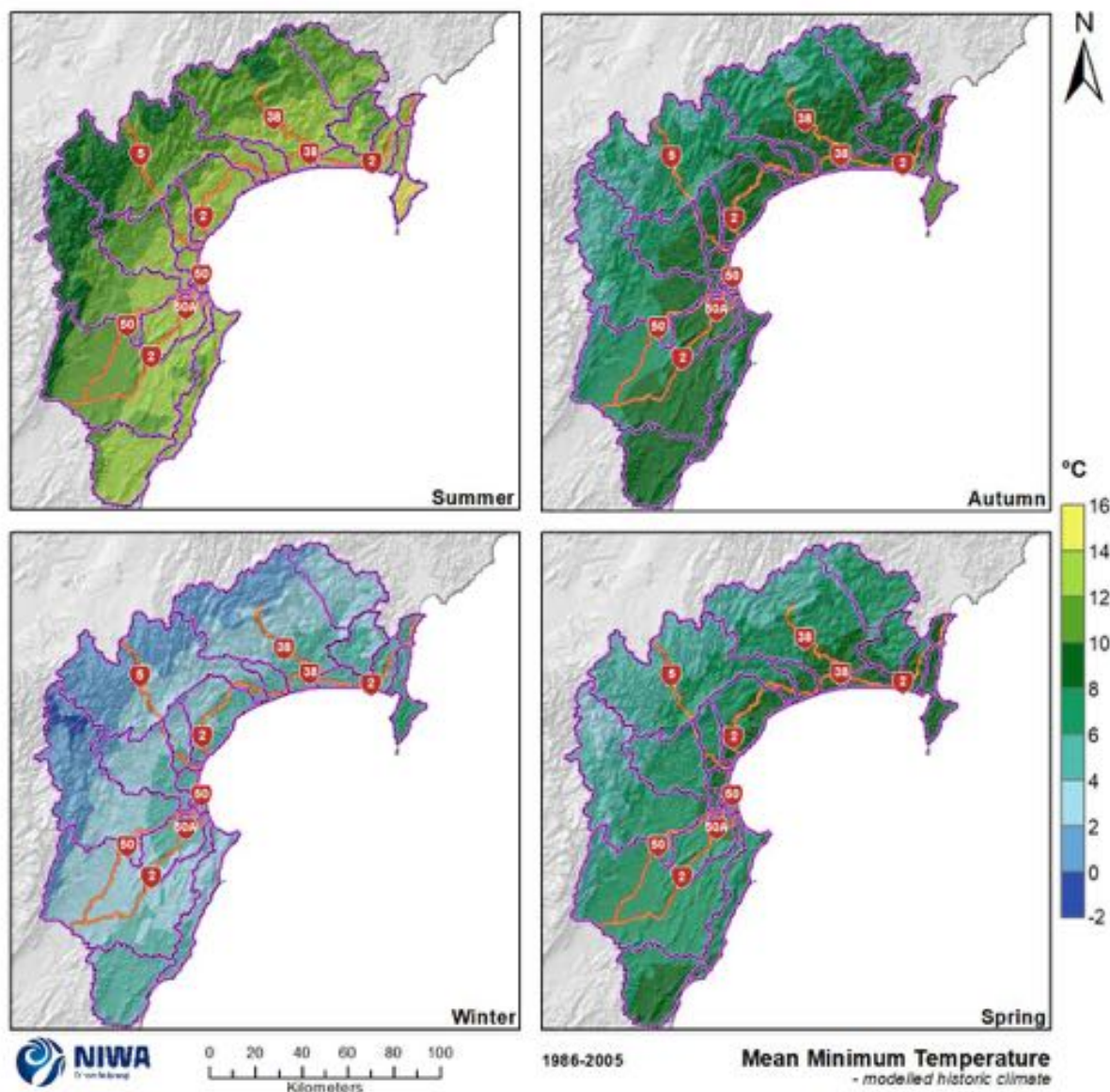


Figure 4-18: Modelled seasonal mean minimum temperature for Hawke's Bay region, average over 1986-2005. Results are based on dynamical downscaled projections using NIWA's Regional Climate Model. Resolution of projection is 5km x 5km.

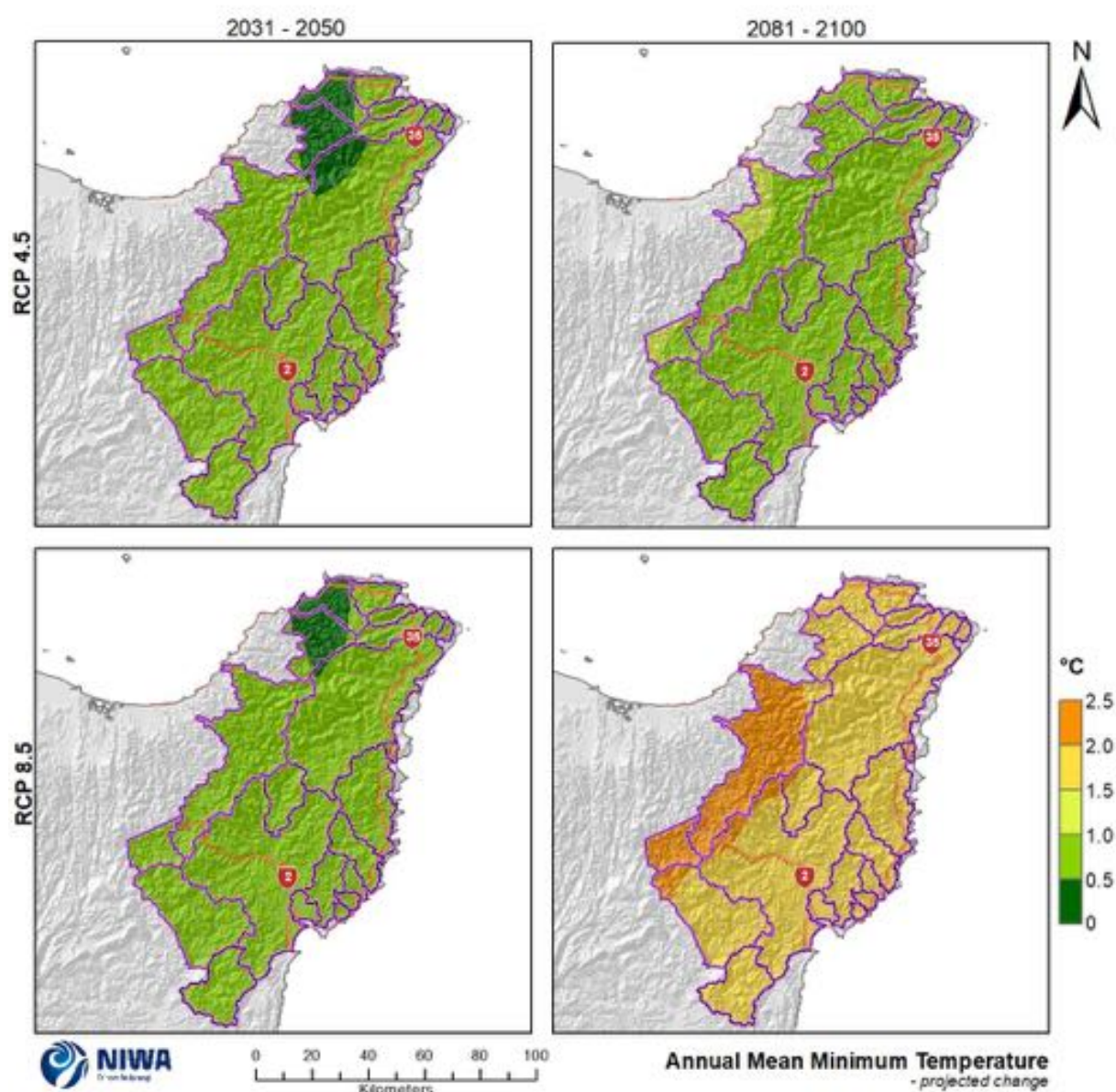


Figure 4-19: Projected annual mean minimum temperature changes for Tairāwhiti by 2040 and 2090 under RCP4.5 and RCP8.5. Relative to 1986-2005 average, based on the average of six global climate models. Results are based on dynamical downscaled projections using NIWA's Regional Climate Model. Resolution of projection is 5km x 5km.

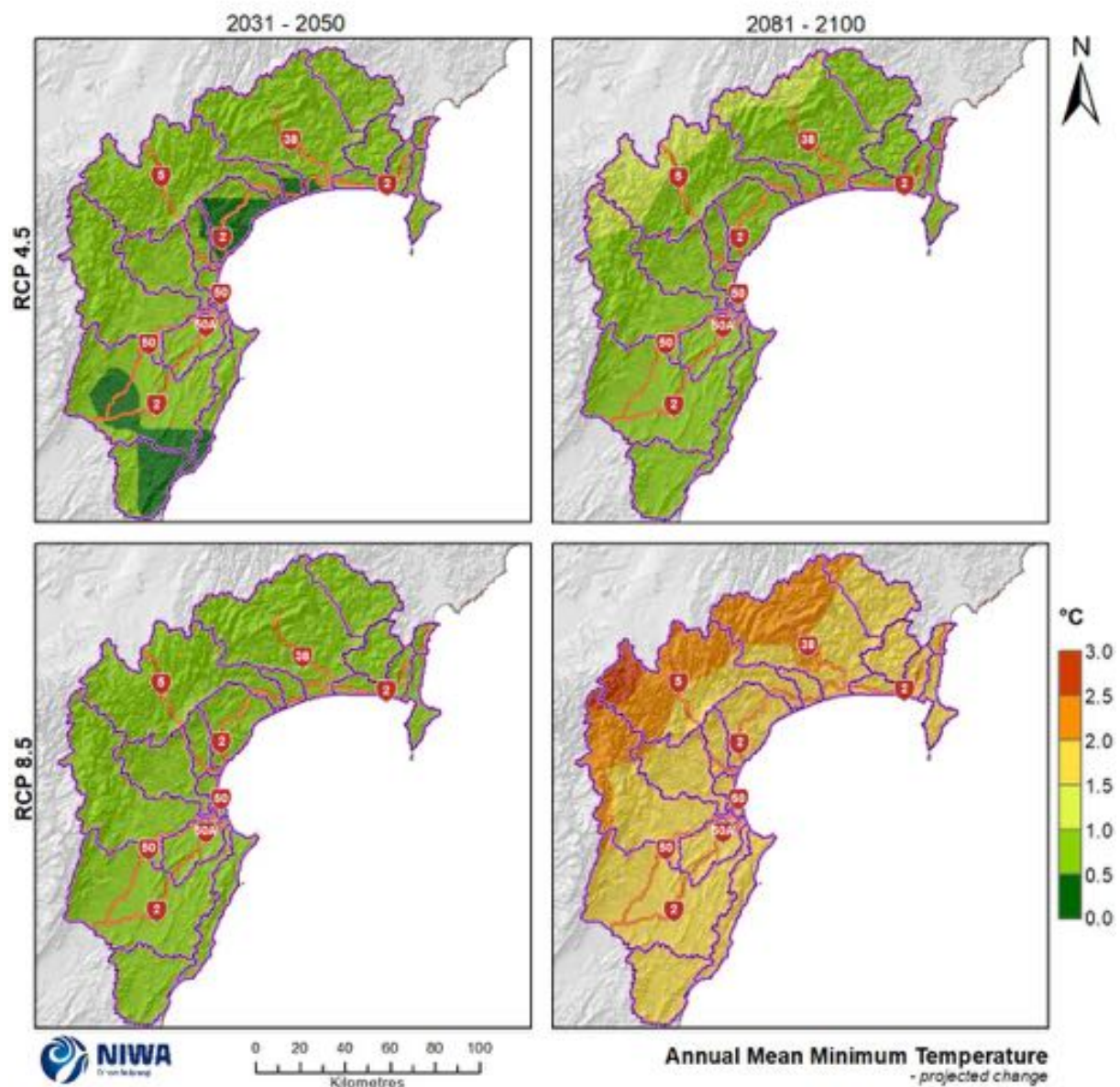


Figure 4-20: Projected annual mean minimum temperature changes for Hawke's Bay by 2040 and 2090 under RCP4.5 and RCP8.5. Relative to 1986-2005 average, based on the average of six global climate models. Results are based on dynamical downscaled projections using NIWA's Regional Climate Model. Resolution of projection is 5km x 5km.

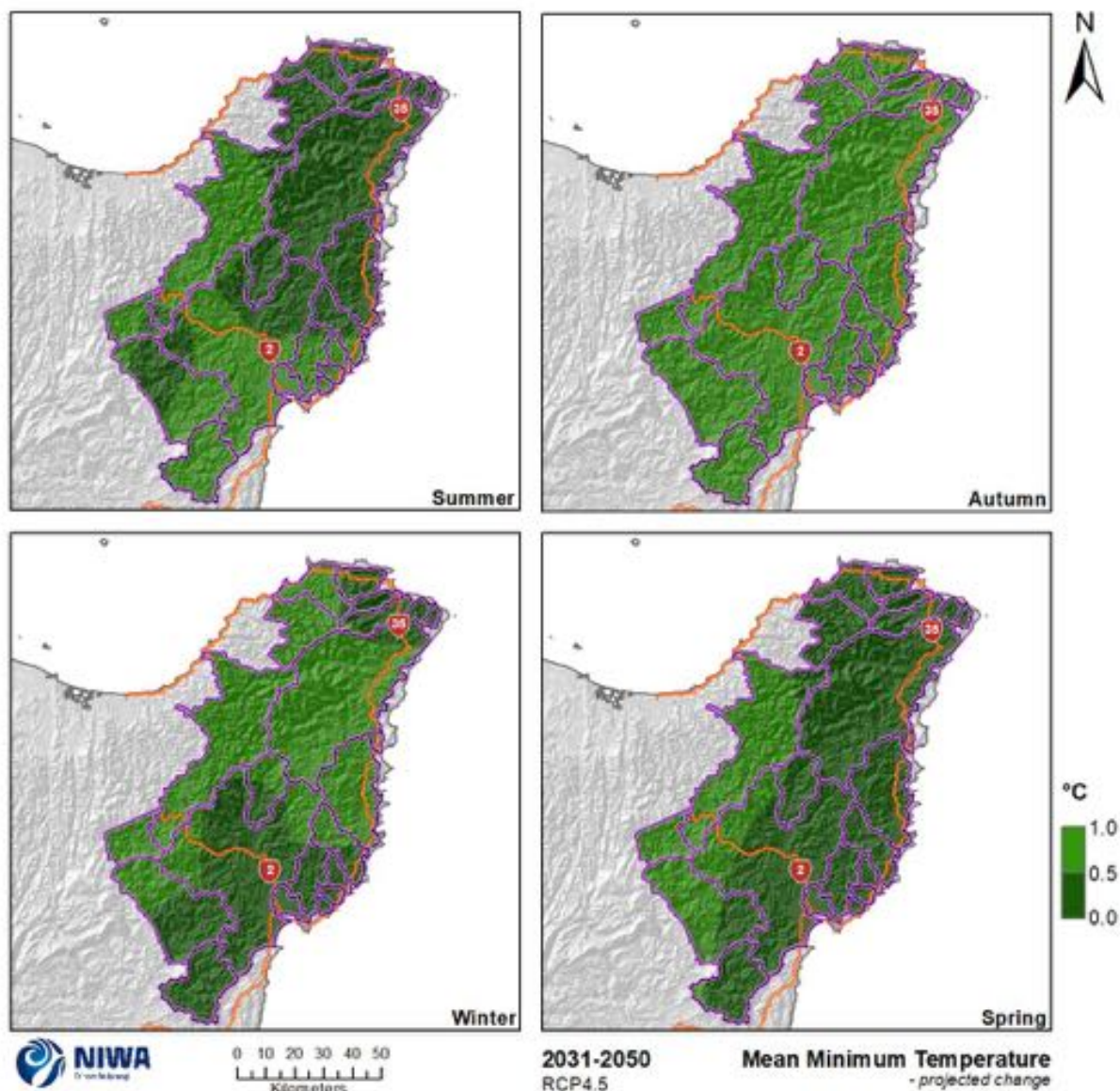


Figure 4-21: Projected seasonal mean minimum temperature changes for Tairāwhiti by 2040 under RCP4.5. Relative to 1986-2005 average, based on the average of six global climate models. Results are based on dynamical downscaled projections using NIWA's Regional Climate Model. Resolution of projection is 5km x 5km.

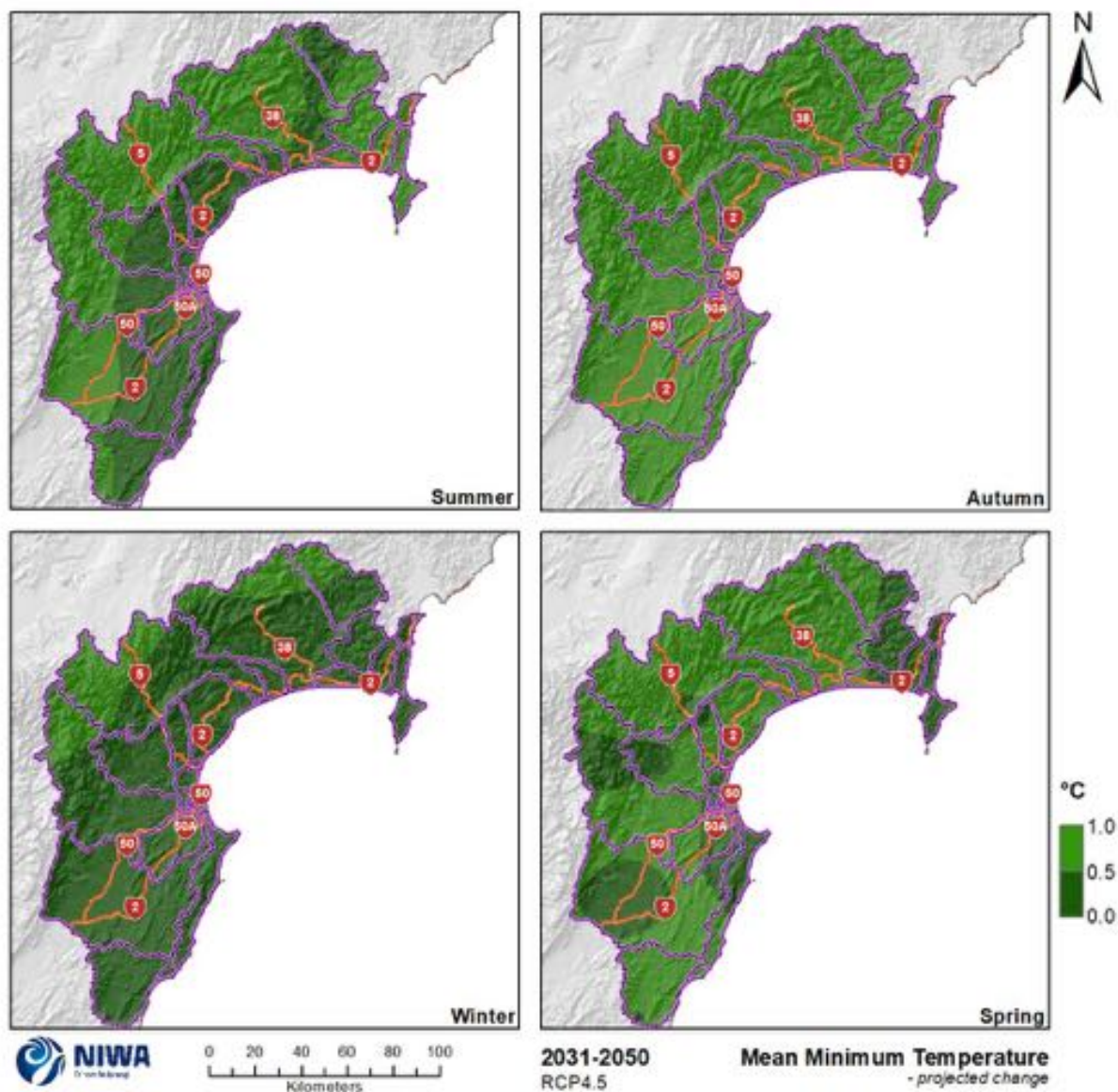


Figure 4-22: Projected seasonal mean minimum temperature changes for the Hawke's Bay region by 2040 under RCP4.5. Relative to 1986-2005 average, based on the average of six global climate models. Results are based on dynamical downscaled projections using NIWA's Regional Climate Model. Resolution of projection is 5km x 5km.

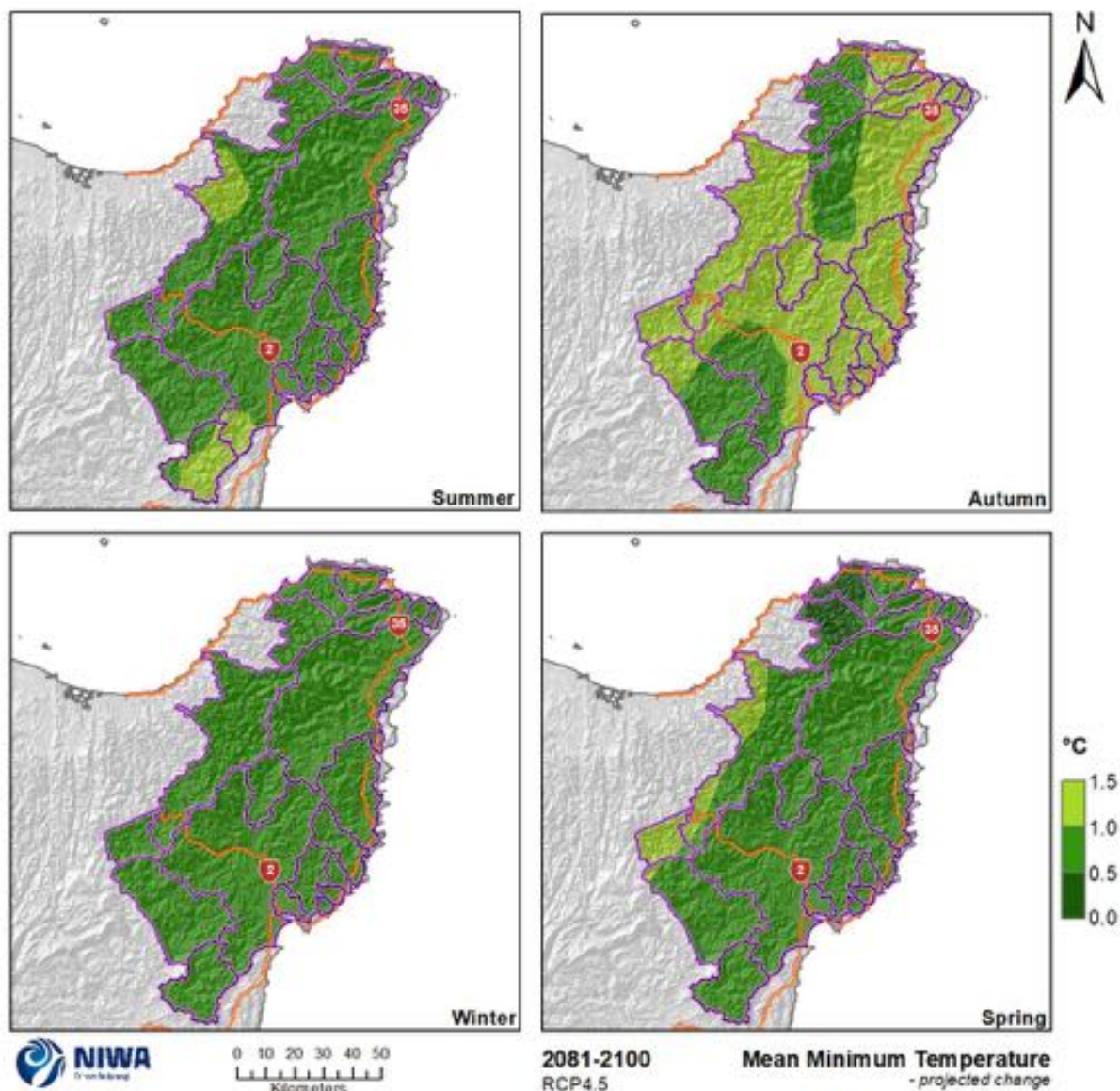


Figure 4-23: Projected seasonal mean minimum temperature changes for Tairāwhiti by 2090 under RCP4.5. Relative to 1986-2005 average, based on the average of six global climate models. Results are based on dynamical downscaled projections using NIWA's Regional Climate Model. Resolution of projection is 5km x 5km.

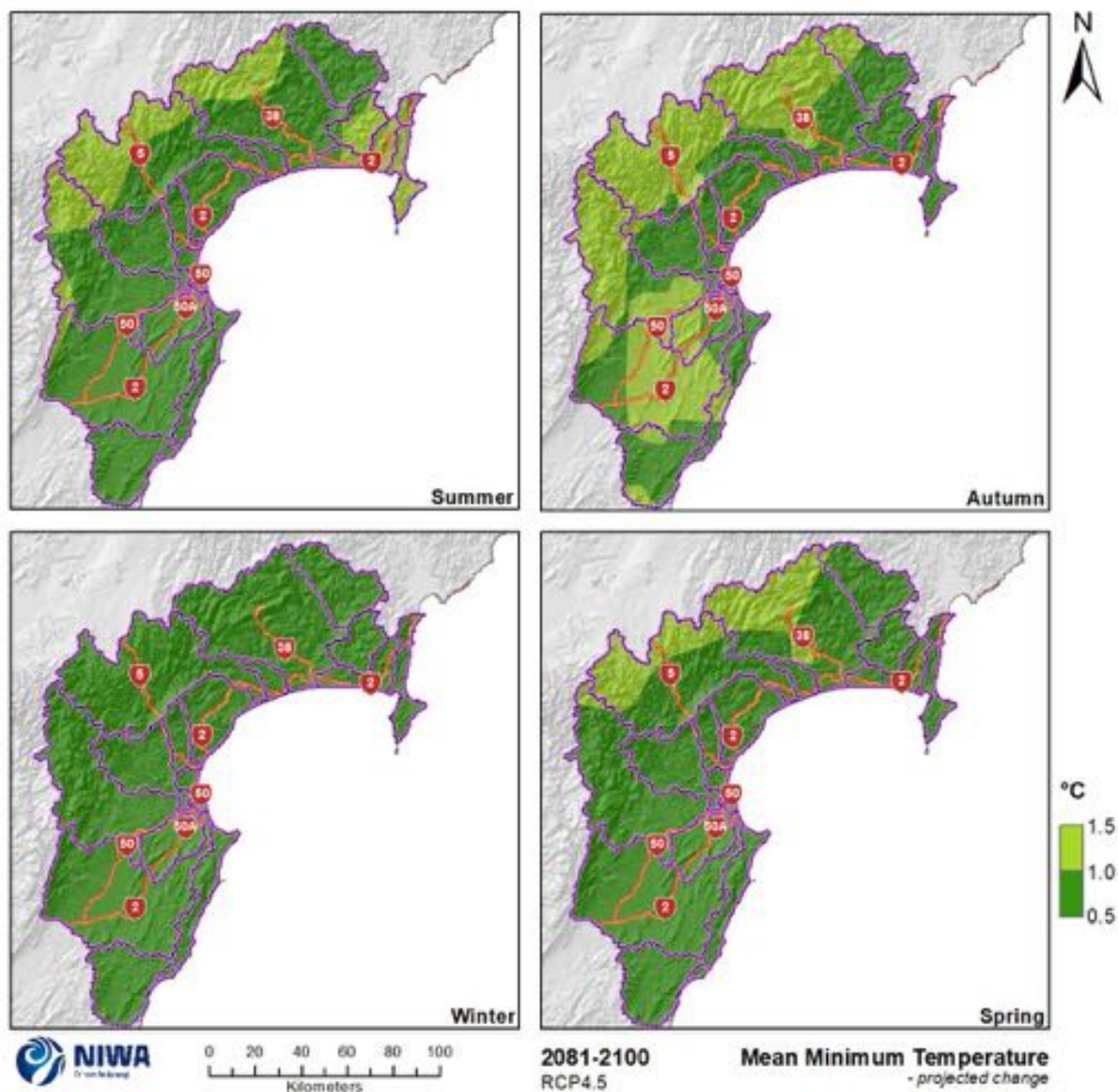


Figure 4-24: Projected seasonal mean minimum temperature changes for the Hawke's Bay region by 2090 under RCP4.5. Relative to 1986-2005 average, based on the average of six global climate models. Results are based on dynamical downscaled projections using NIWA's Regional Climate Model. Resolution of projection is 5km x 5km.

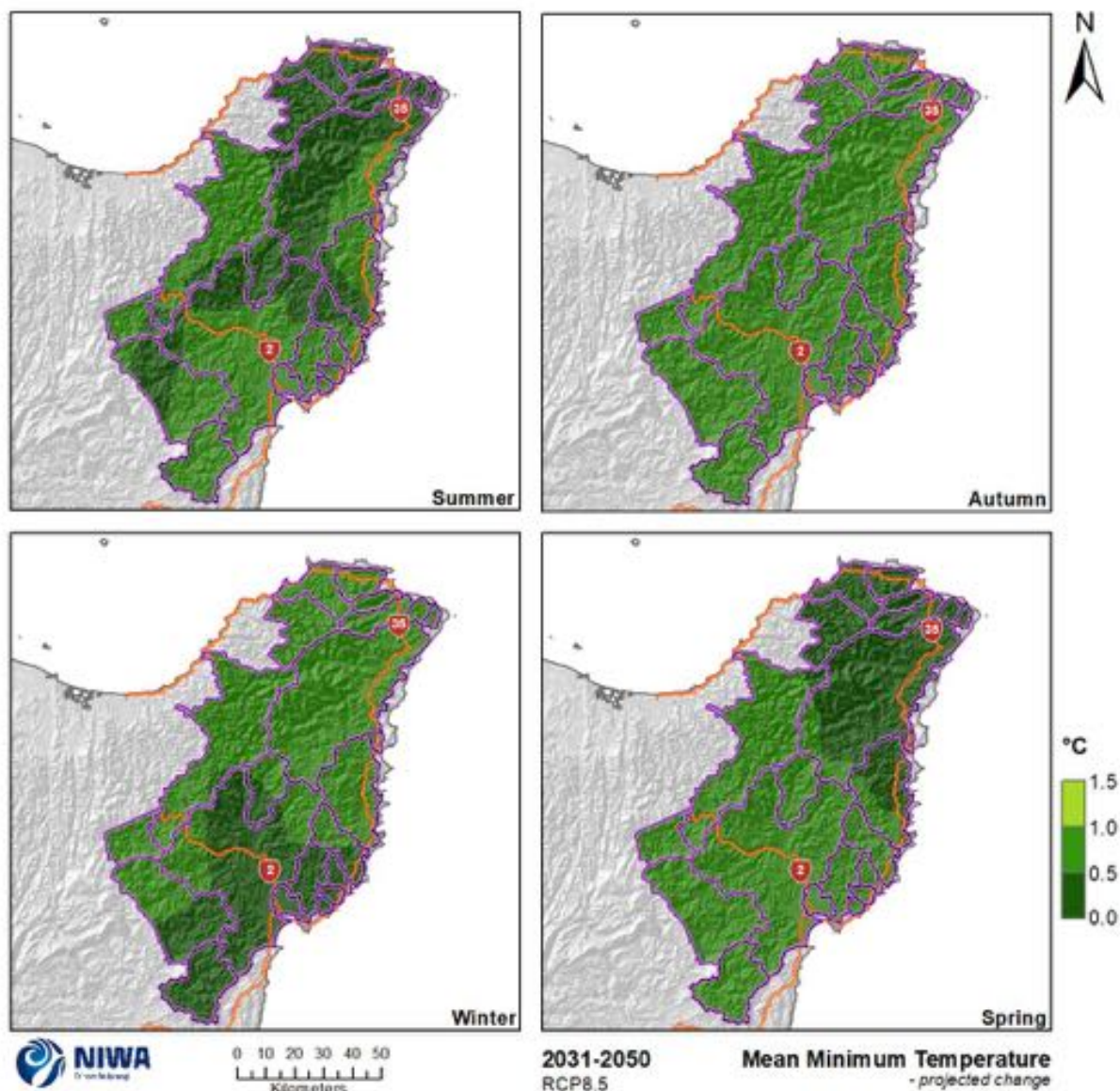


Figure 4-25: Projected seasonal mean minimum temperature changes for Tairāwhiti by 2040 under RCP8.5. Relative to 1986-2005 average, based on the average of six global climate models. Results are based on dynamical downscaled projections using NIWA's Regional Climate Model. Resolution of projection is 5km x 5km.

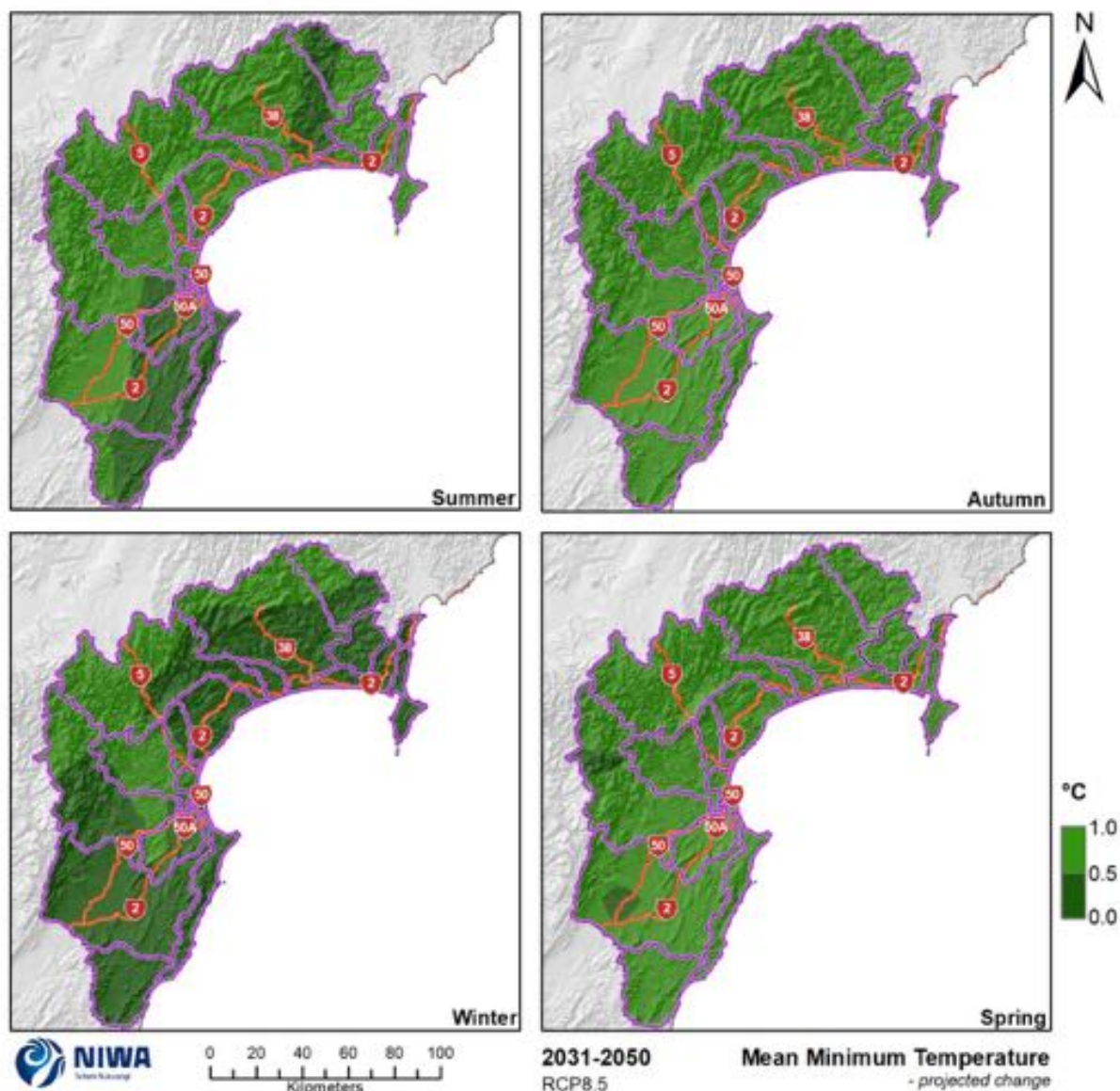


Figure 4-26: Projected seasonal mean minimum temperature changes for the Hawke's Bay region by 2040 under RCP8.5. Relative to 1986-2005 average, based on the average of six global climate models. Results are based on dynamical downscaled projections using NIWA's Regional Climate Model. Resolution of projection is 5km x 5km.

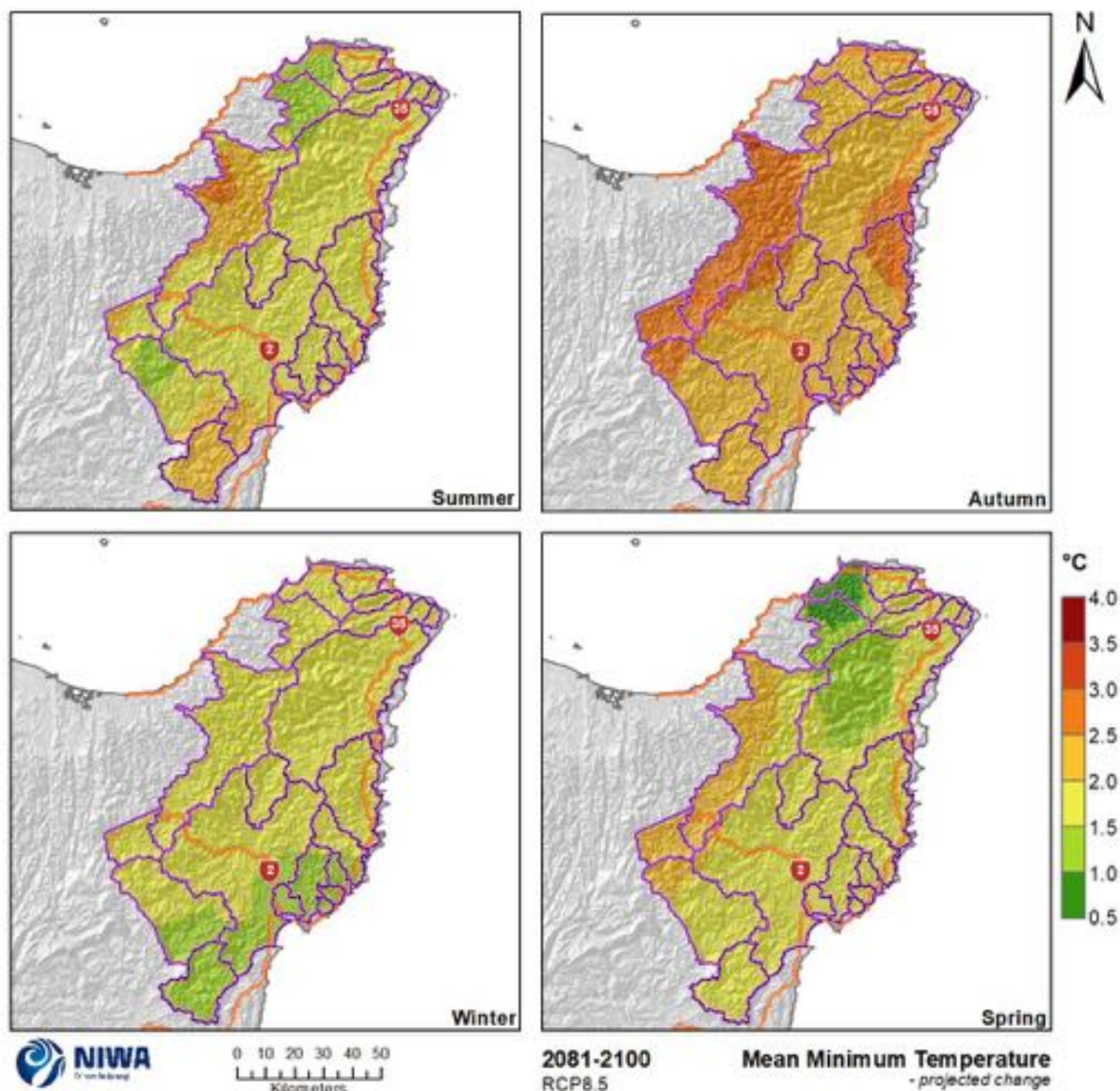


Figure 4-27: Projected seasonal mean minimum temperature changes for Tairāwhiti by 2090 under RCP8.5. Relative to 1986-2005 average, based on the average of six global climate models. Results are based on dynamical downscaled projections using NIWA's Regional Climate Model. Resolution of projection is 5km x 5km.

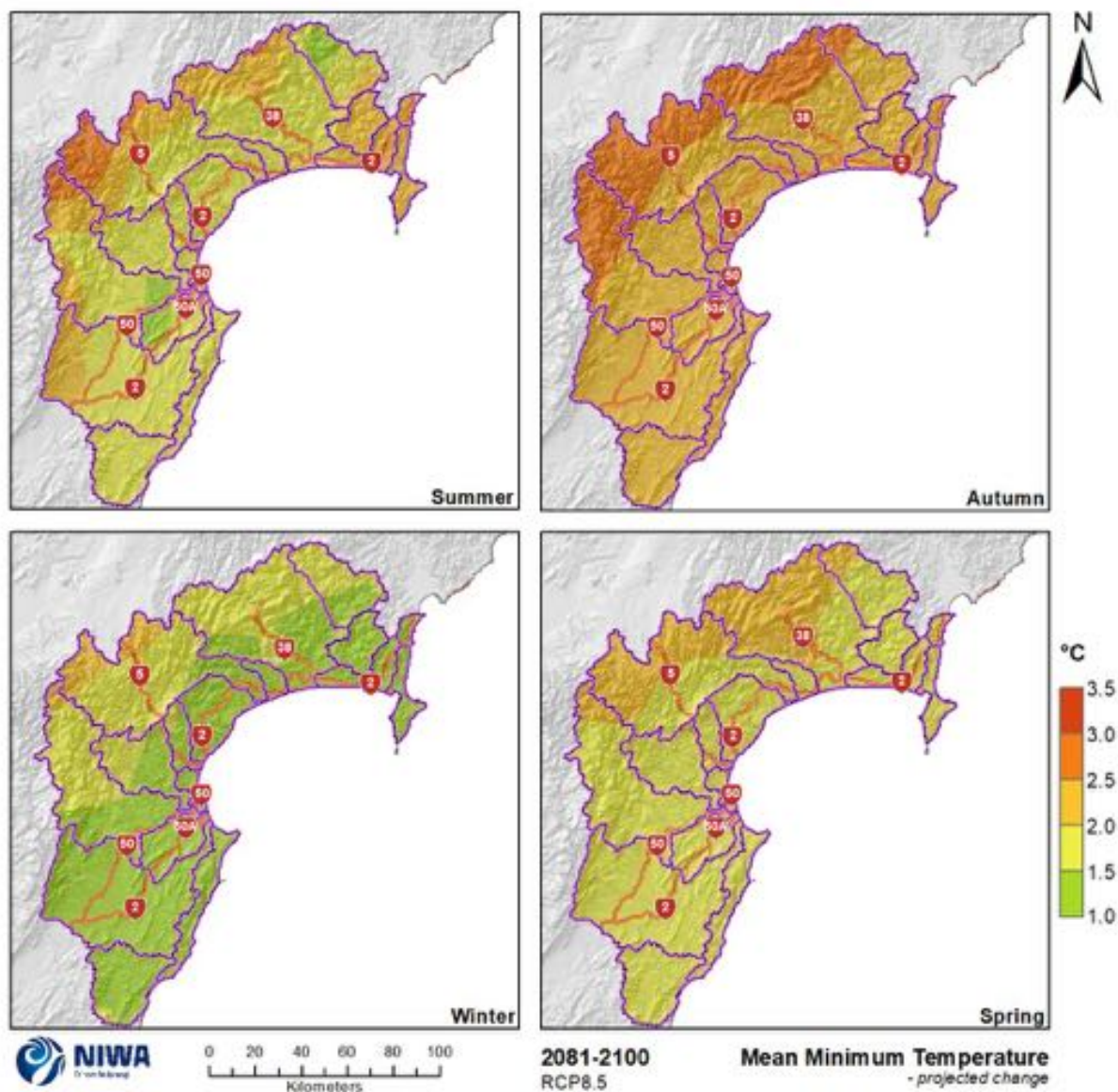


Figure 4-28: Projected seasonal mean minimum temperature changes for the Hawke's Bay region by 2090 under RCP8.5. Relative to 1986-2005 average, based on the average of six global climate models. Results are based on dynamical downscaled projections using NIWA's Regional Climate Model. Resolution of projection is 5km x 5km.

4.3 Frosts

A frost day is defined in this report when the modelled daily minimum temperature falls below 0°C. This is purely a temperature-derived metric for assessing the potential for frosts over the 5 km x 5 km climate model grid. Frost conditions are influenced at the local scale (i.e. finer scale than 5 km x 5 km) by temperature, topography, wind, and humidity, so the results presented in this section can be considered as the large-scale temperature conditions conducive to frosts.

Historic (average over 1986-2005) and future (average over 2031-2050 and 2081-2100) maps for frost days are shown in this section. The historic maps show annual average numbers of frost days and the future projection maps show the change in the annual number of frost days compared with the historic period. Note that the historic maps are on a different colour scale to the future projection maps.

For the modelled historic period, coastal portions of the Tairāwhiti and Hawke's Bay regions (where temperatures are generally higher) have the lowest number of frost days (Figure 4-29 and Figure 4-30). This is particularly true for coastal parts of northern Tairāwhiti where frosts are observed less than once per year on average. Inland and mountainous parts of both regions have the highest number of frost days, with Tairāwhiti reaching 10-25 days per year at many inland locations and even 25-50 days per year at several high elevation locations. For Hawke's Bay, many coastal locations experience between 1-10 frost days per year on average for the modelled historic period although several locations south of Hastings experience 10-25 frost days per year (e.g. Karamu catchment, eastern Tukituki catchment and the proximal coastline). Inland, mountainous parts of the Hawke's Bay region receive 25-75 frost days per year on average for the modelled historic period.

Representative concentration pathway (RCP) 4.5

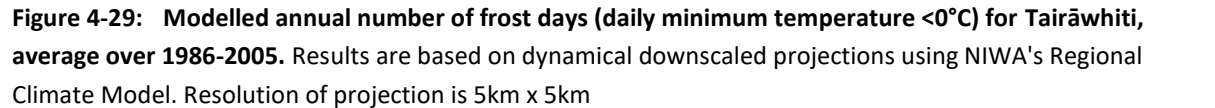
By 2040, decreases to frost days are projected for the entirety of both regions (Figure 4-31 and Figure 4-32). In Tairāwhiti, the projected decreases are very small for most coastal locations (less than one day), with the small magnitude of change largely attributed to the fact that frost days are rarely observed in those locations to begin with. Most inland locations in Tairāwhiti are projected to decrease by 1-5 days, although higher elevation inland locations (i.e. the Raukumara Range) are projected to decrease by 5-10 days. In Hawke's Bay, the eastern half of the region is projected to experience decreases of 1-5 frost days with only a few locations decreasing by less than one day. Inland, higher elevation locations are projected to experience decreases of 5-10 days or even 10-20 days for an isolated western part of the region.

By 2090, the pattern of change is very similar to that projected for 2040 under RCP4.5 except that the projected decreases of 5-10 days for the inland parts of both regions are slightly more widespread. There are also more locations in Hawke's Bay projected to decrease by 10-20 days (Figure 4-31 and Figure 4-32). Larger decreases are also projected for western extremes of both regions compared to projections for 2040.

Representative concentration pathway (RCP) 8.5

By 2040, the projected pattern of change under RCP8.5 is very similar to that projected for the same time period under RCP4.5 (Figure 4-31 and Figure 4-32).

By 2090, the projected decreases to frost days are generally more extreme than those projected under RCP4.5 (Figure 4-31 and Figure 4-32). In Tairāwhiti, small decreases of 1-5 days or even less than one day remain projected for many coastal locations due to the fact that there are limited frosts



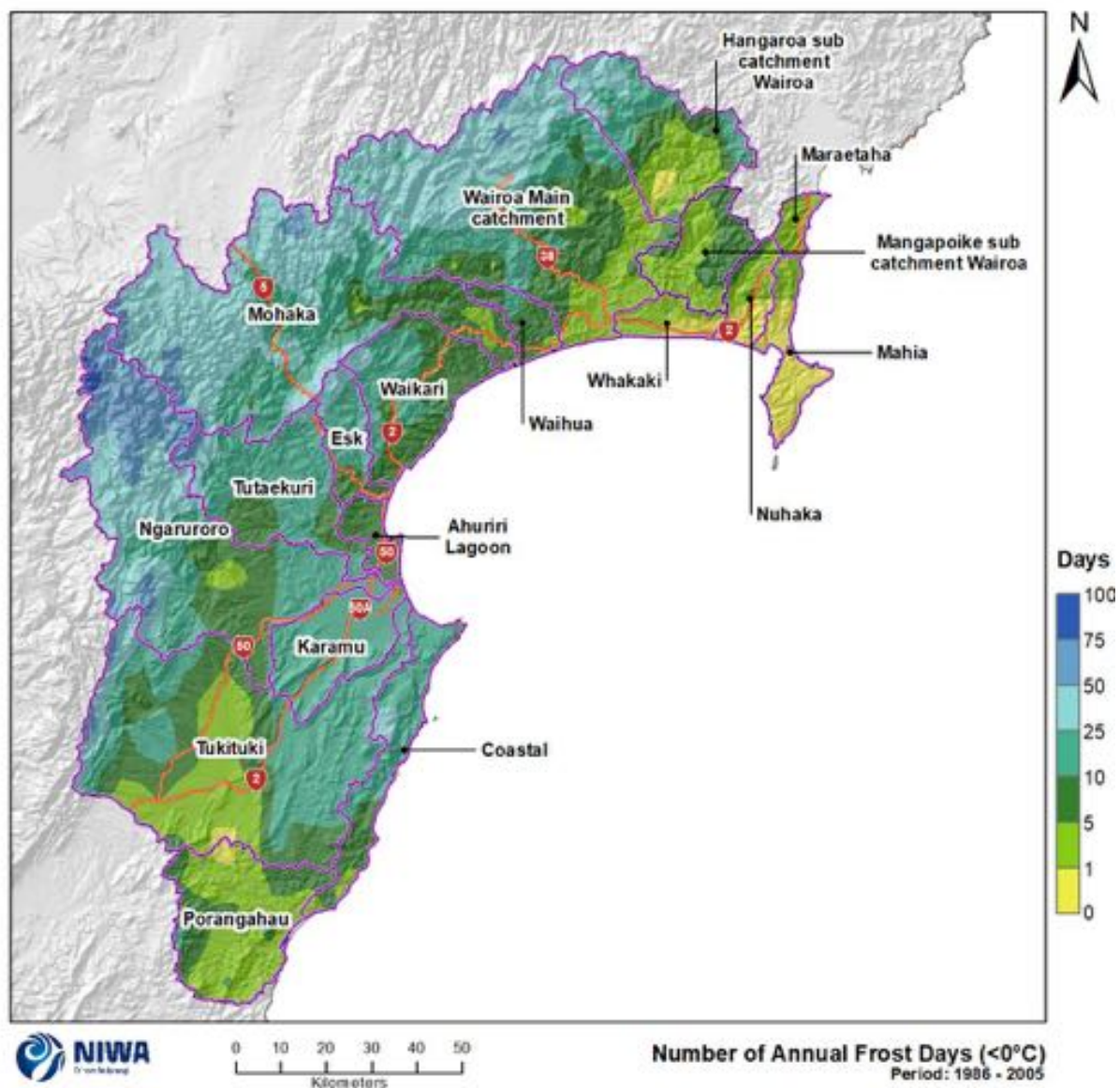


Figure 4-30: Modelled annual number of frost days (daily minimum temperature $<0^{\circ}\text{C}$) for Hawke's Bay region, average over 1986-2005 . Results are based on dynamical downscaled projections using NIWA's Regional Climate Model. Resolution of projection is 5km x 5km.

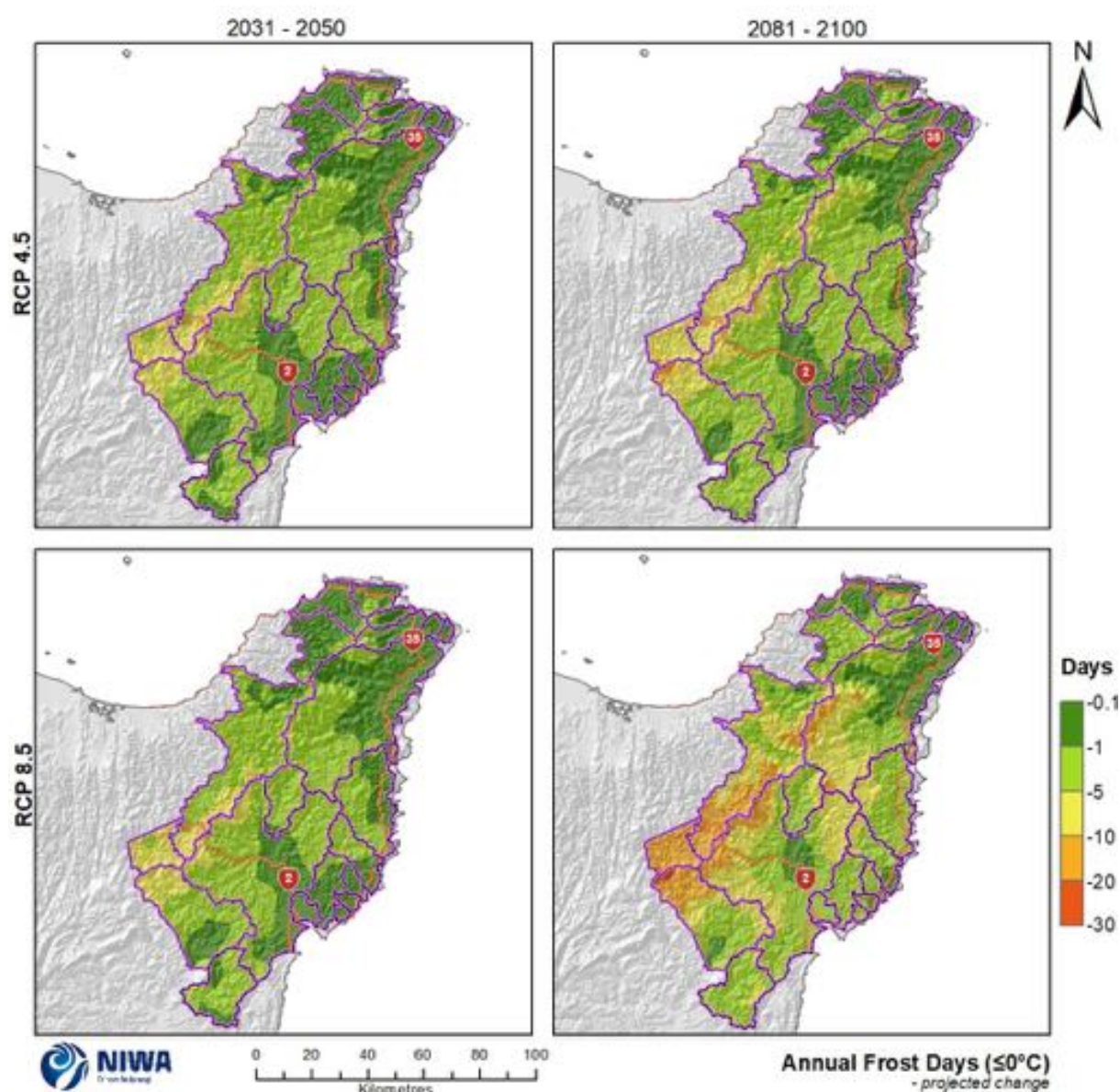


Figure 4-31: Projected annual number of frost days (daily minimum temperature <0°C) changes for Tairāwhiti by 2040 and 2090 under RCP4.5 and RCP8.5. Relative to 1986-2005 average, based on the average of six global climate models. Results are based on dynamical downscaled projections using NIWA's Regional Climate Model. Resolution of projection is 5km x 5km.

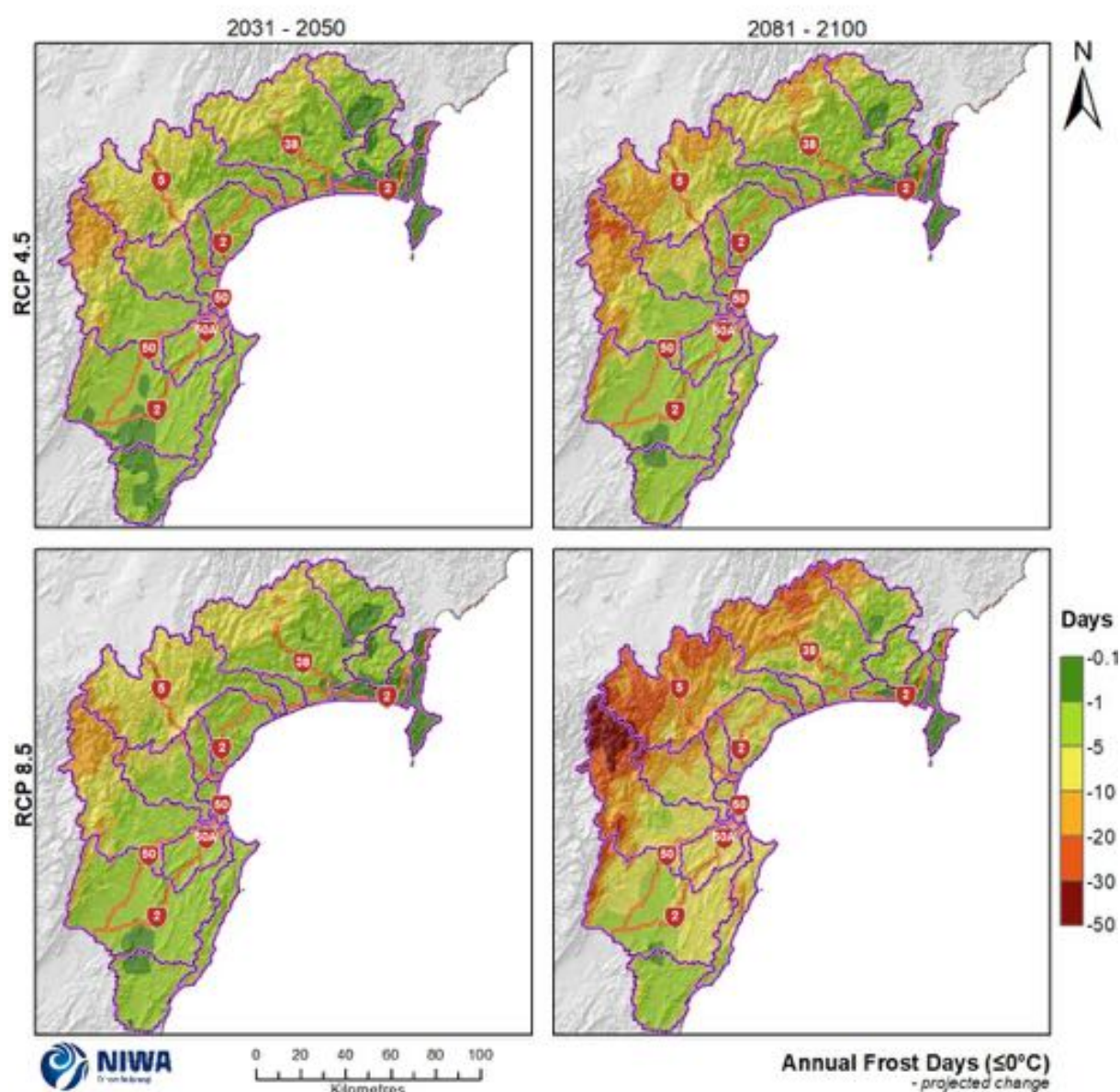


Figure 4-32: Projected annual number of frost days (daily minimum temperature <0°C) changes for Hawke's Bay by 2040 and 2090 under RCP4.5 and RCP8.5. Relative to 1986-2005 average, based on the average of six global climate models. Results are based on dynamical downscaled projections using NIWA's Regional Climate Model. Resolution of projection is 5km x 5km.

4.4 Heatwaves

The definition of a heatwave as considered here is a period of three or more consecutive days where the maximum daily temperature exceeds 25°C. This calculation is an aggregation of all days per year that are included in a heatwave (i.e., \geq three consecutive days with maximum temperature $> 25^\circ\text{C}$), no matter the length of the heatwave. The annual heatwave days are then averaged over the 20-year period of interest (e.g., 2031-2050) to get the average annual heatwave-day climatology (past) and future projections.

For the modelled historic period, eastern portions of Tairāwhiti and Hawke's Bay (where temperatures are generally warmer) have the highest number of heatwave days (Figure 4-33 and Figure 4-34). This is particularly true for coastal parts of southern Tairāwhiti as well as the lower reaches of the Waipaoa catchment (also in Tairāwhiti), and for part of Hawke Bay (near the mouth of the Wairoa River) where 20-30 heatwave days are experienced per year on average. Most remaining coastal locations receive 10-20 heatwave days per year. Many inland high elevation locations (which are cooler on average) experience 1-5 heatwave days per year for the modelled historic period, with some of these locations receiving less than one heatwave day per year on average.

Representative concentration pathway (RCP) 4.5

By 2040, the number of heatwave days observed per year is projected to increase for the entirety of both regions (albeit by a small magnitude at high elevations) (Figure 4-35 and Figure 4-36). These increases are greatest for coastal and eastern locations, with projected increases of 10-20 days for Tairāwhiti and much of the Hawke's Bay region, and increases of 5-10 days for the southeast of the Hawke's Bay region. Meanwhile, inland high elevation locations are only projected to increase by 1-5 days per year on average, and even less than one day for parts of Tairāwhiti.

By 2090, the projected increases to heatwave days are accentuated. Coastal and eastern parts of Tairāwhiti are projected to experience 10-40 additional heatwave days per year. Most of eastern Hawke's Bay is projected to increase by 10-20 days, with locations near Wairoa projected to increase by 20-40 days. Inland high elevation parts of both regions are projected to increase by 1-10 days, while isolated high elevation locations in Tairāwhiti are projected to increase by less than one day (Figure 4-35 and Figure 4-36).

Representative concentration pathway (RCP) 8.5

By 2040, the projected pattern of change to heatwave days under RCP8.5 is very similar to that projected for the same time period under RCP4.5, except that a greater portion of southeastern Hawke's Bay is projected to increase by 10-20 days rather than 5-10 days (Figure 4-35 and Figure 4-36).

By 2090 however, the projected increases to heatwave days are much more extreme than for the other scenarios. At least 20-40 additional heatwave days per year on average are projected for the majority of both regions, with most eastern locations projected to increase by 40-60 days per year. Parts of the Raukumara Range in Tairāwhiti however are projected to increase by a smaller amount (+1-20 days), as are isolated parts of western Hawke's Bay region (+10-20 days) (Figure 4-35 and Figure 4-36).

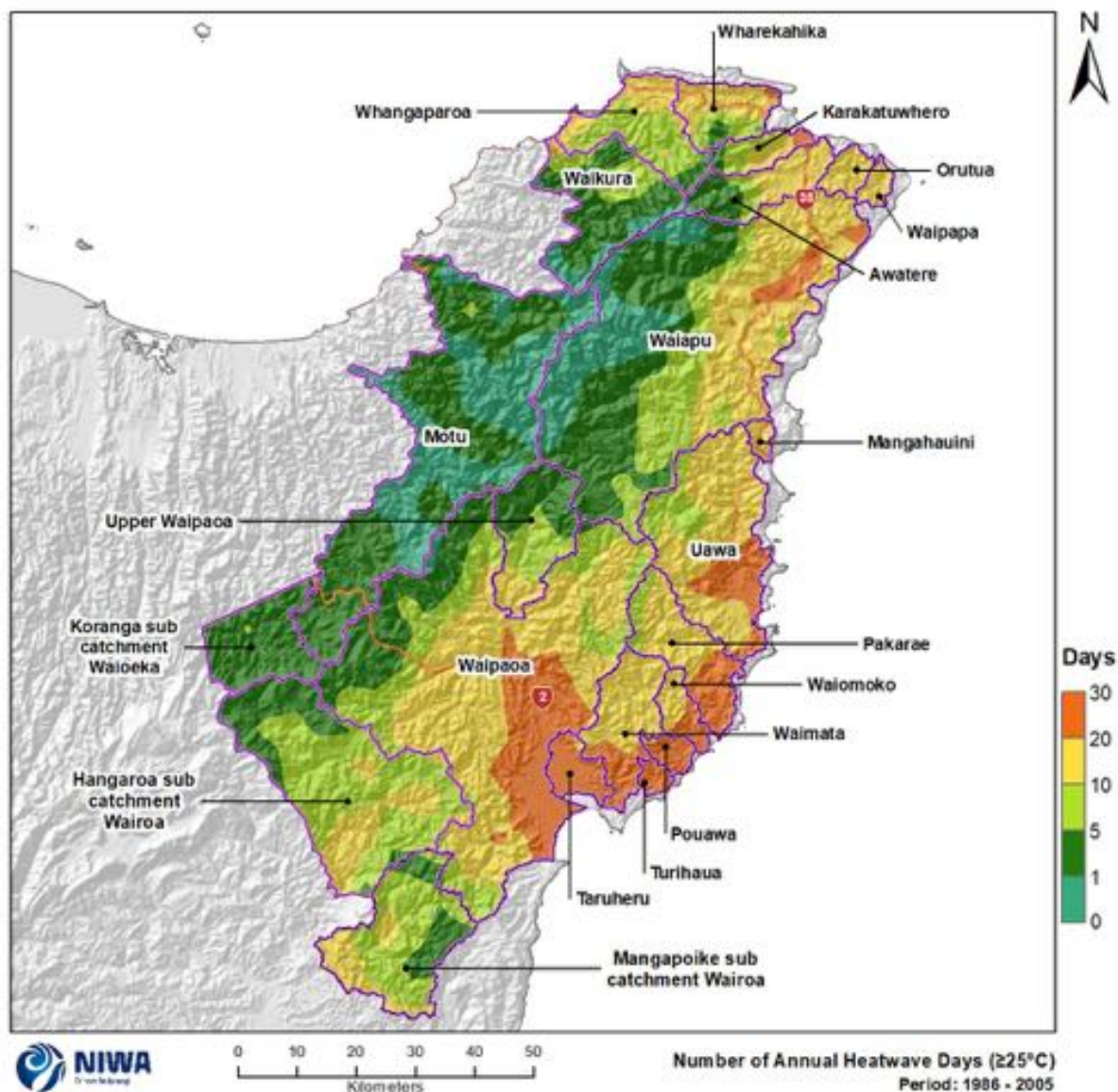


Figure 4-33: Modelled annual number of heatwave days (≥ three consecutive days with maximum temperatures > 25°C) for Tairāwhiti, average over 1986-2005. Results are based on dynamical downscaled projections using NIWA's Regional Climate Model. Resolution of projection is 5km x 5km.

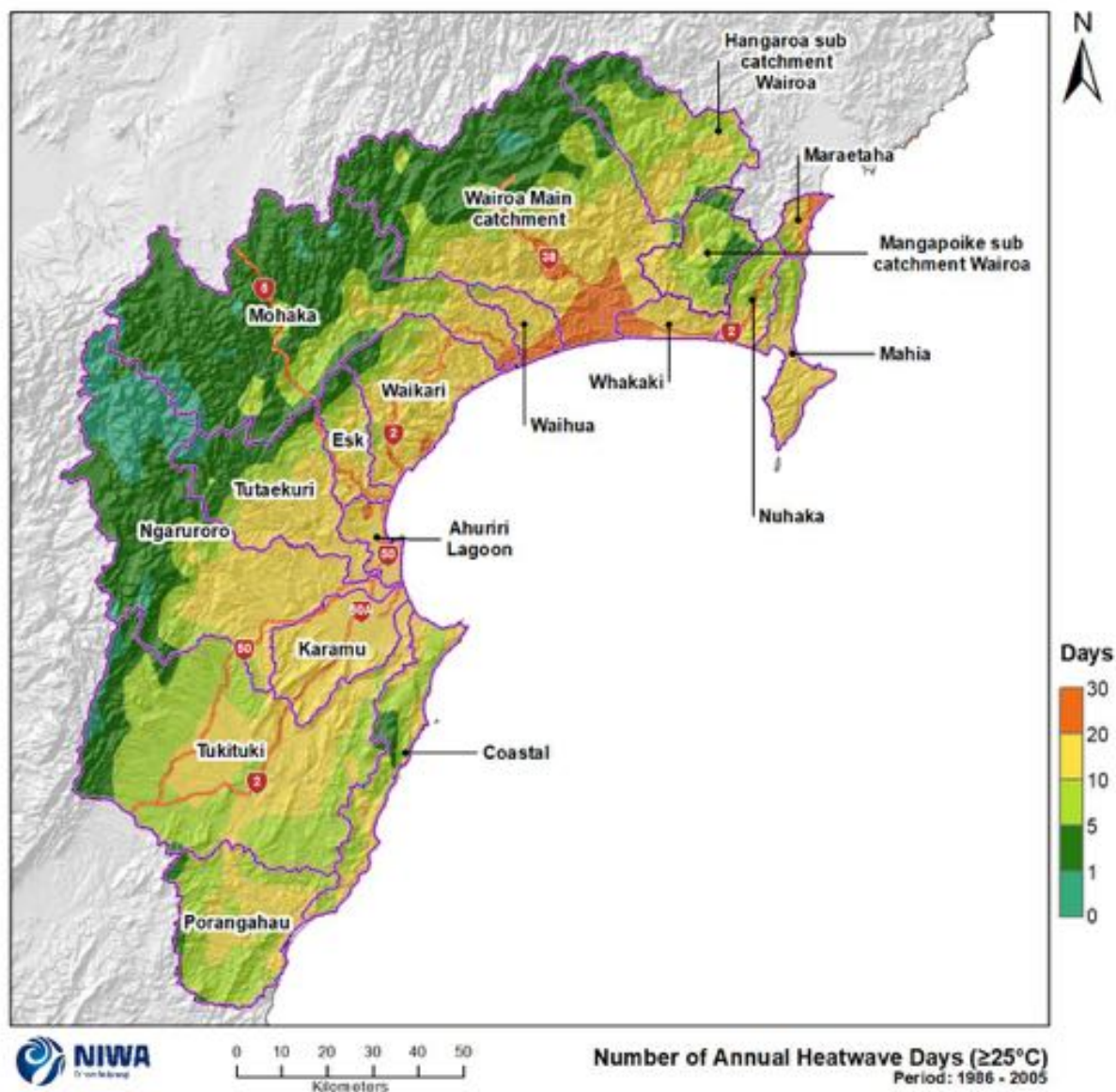


Figure 4-34: Modelled annual number of heatwave days (\geq three consecutive days with maximum temperatures $> 25^{\circ}\text{C}$) for Hawke's Bay region, average over 1986-2005 . Results are based on dynamical downscaled projections using NIWA's Regional Climate Model. Resolution of projection is 5km x 5km.

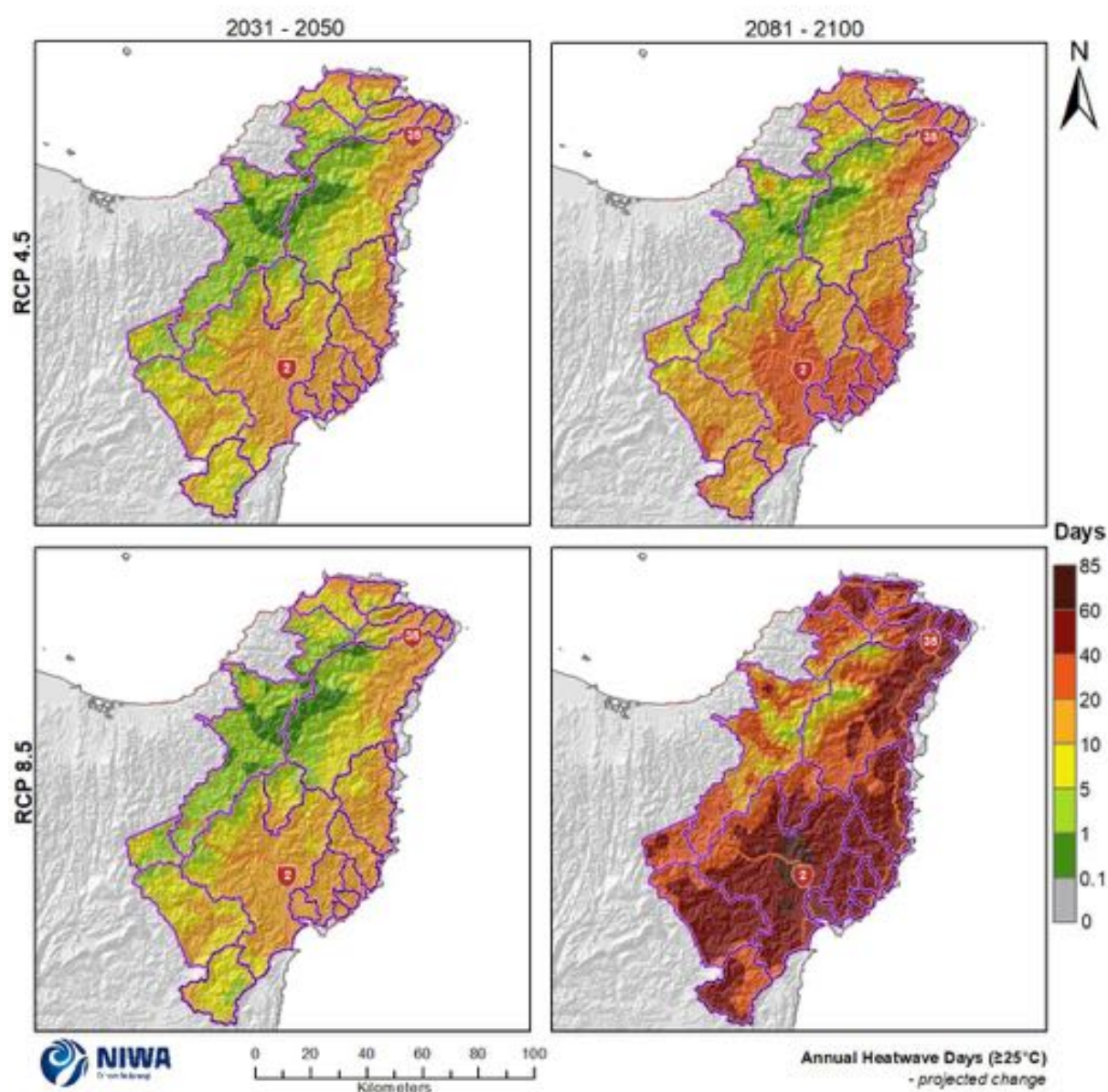


Figure 4-35: Projected annual number of heatwave days (≥ three consecutive days with maximum temperatures > 25°C) changes for Tairāwhiti by 2040 and 2090 under RCP4.5 and RCP8.5. Relative to 1986-2005 average, based on the average of six global climate models. Results are based on dynamical downscaled projections using NIWA's Regional Climate Model. Resolution of projection is 5km x 5km.

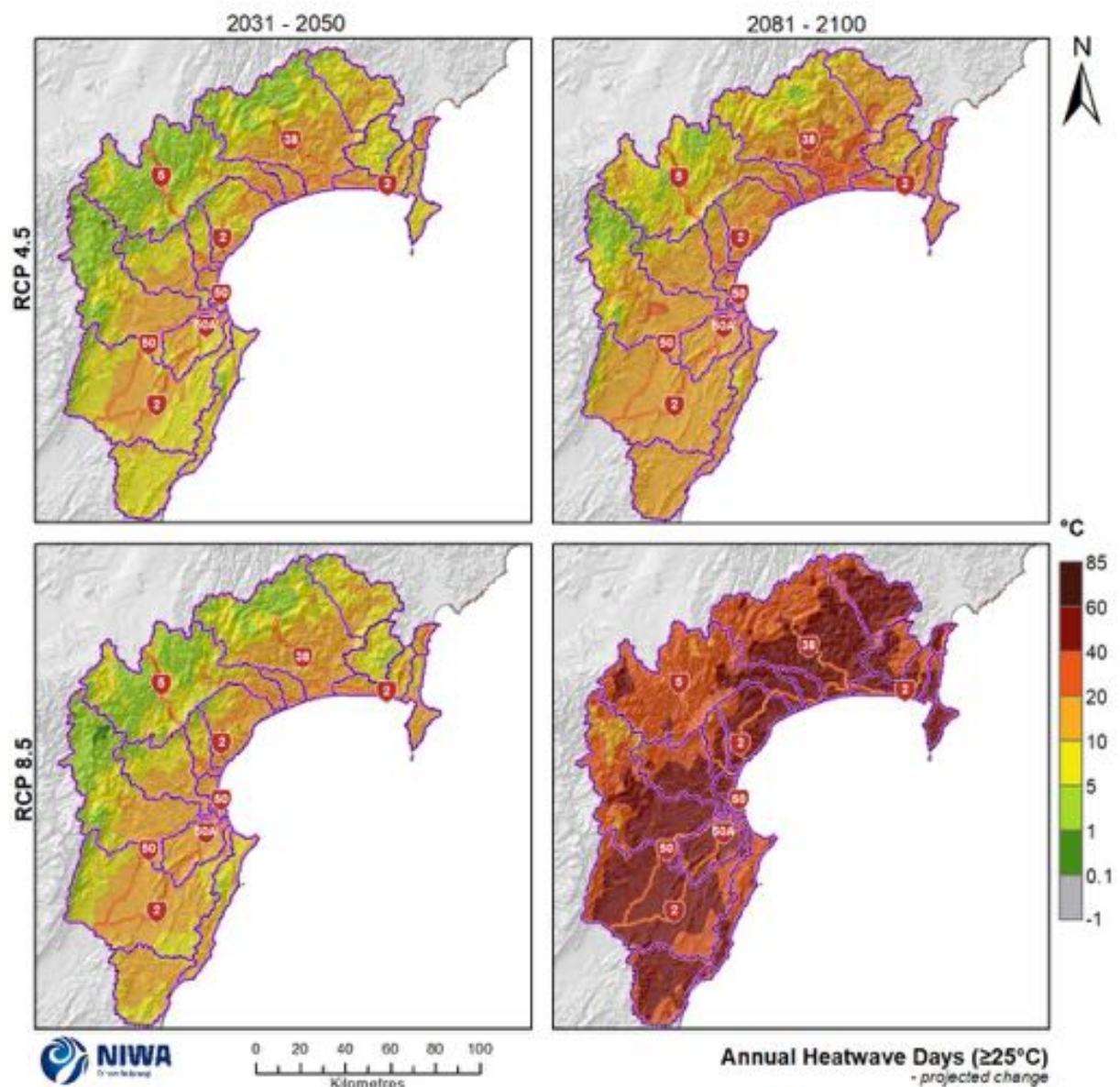


Figure 4-36: Projected annual number of heatwave days (≥ three consecutive days with maximum temperatures > 25°C) changes for Hawke's Bay by 2040 and 2090 under RCP4.5 and RCP8.5. Relative to 1986-2005 average, based on the average of six global climate models. Results are based on dynamical downscaled projections using NIWA's Regional Climate Model. Resolution of projection is 5km x 5km.

5 Rainfall

5.1 Rainfall totals

This section contains maps showing historic total rainfall and the future projected change in total rainfall. Historic rainfall maps are in units of mm per year or season (average over 1986-2005) and future (average over 2031-2050 and 2081-2100) maps show the percentage change in rainfall compared with the historic total. Note that the historic maps are on a different colour scale to the future projection maps.

For the modelled historic period, the highest annual rainfall totals are recorded in the high elevations of the Raukumara Ranges and other mountainous locations (>2000 mm/year) (Figure 5-1 and Figure 5-2). The lowest annual rainfall totals are recorded inland from Poverty Bay (1000-1500 mm; Figure 5-1) and for lower elevation locations in the Hawke's Bay region (750-1500 mm; Figure 5-2). Summer is the driest season and winter is the wettest, with seasonal patterns of high and low rainfall generally following annual patterns (Figure 5-3 and Figure 5-4).

Representative concentration pathway (RCP) 4.5

By 2040, projected change to annual rainfall is small, with a few northern and coastal locations projected to increase by 0-5%, but with decreases of 0-5% projected for the larger portion of both regions (Figure 5-5 and Figure 5-6). The seasonality of rainfall however is projected to increase for parts of both regions (Figure 5-7 and Figure 5-8). For Tairāwhiti, decreases of 5-15% are projected for summer (highest to the north), while increases of 5-15% are projected for northwestern and northeastern locations during winter and autumn respectively. The seasonal changes projected for the Hawke's Bay region are not as extreme as for northern parts of Tairāwhiti. There, winter is the only season with projected increases that exceed 5% (and with a limited spatial extent at this magnitude), while spring is projected to experience slightly larger decreases compared to the other seasons for this region (5-10% decrease for many locations).

By 2090, projected annual change is not dissimilar to that projected for the 2040 period, with many locations projected to experience small decreases to rainfall (0-5%). However, fewer locations are projected to experience increases to annual rainfall totals (compared to the 2040 period), and larger portions of both regions are projected to experience decreases of a larger magnitude (i.e. in the 5-10% range; Figure 5-5 and Figure 5-6). Again, there are more noticeable changes projected at the seasonal scale (Figure 5-9 and Figure 5-10). Generally speaking, the projections for most locations during autumn, winter, and spring indicate a greater magnitude of drying than for 2040. Additionally, any projected increases to rainfall during these seasons is more spatially limited and generally of lower magnitude than those projected for 2040 under the same RCP scenario. For summer, the rather extensive drying projected for Tairāwhiti by 2040 is not projected for the region by 2090, and instead increases or decreases in the 0-5% range are indicated for this period. The largest projected rainfall decreases are for spring, with the majority of both regions projected to decrease by 5-15%. The largest projected increases are over or west of mountainous locations in the western parts of both regions during winter, and for southeastern Hawke's Bay (including Napier and Hastings) during summer (+5-10%).

Representative concentration pathway (RCP) 8.5

By 2040, the projected pattern of change to annual rainfall is very similar to that projected for RCP4.5, albeit with only a few more locations projected to see rainfall decreases in the 5-10% range

(Figure 5-5 and Figure 5-6). There is a stronger pattern of change at the seasonal scale, with the greatest and most extensive drying projected for spring (5-15%; similar to RCP4.5 by 2040) (Figure 5-11 and Figure 5-12). Winter is generally projected to experience 0-10% more rainfall over or to the west of the mountain ranges in both regions, and 0-10% less rainfall in most remaining locations. Projections for autumn and summer are generally for increases or decreases in the 0-5% range, with a few locations projected to experience 5-10% more rainfall.

By 2090, a much stronger pattern of drying is evident. At the annual scale, many locations are projected to experience decreases of 5-15%, with smaller decreases in the 0-5% range projected for many coastal locations (Figure 5-5 and Figure 5-6). At the seasonal scale, decreases in the 0-15% range are projected for the majority of both regions, with spring projected to see the largest decreases (5-20%) (Figure 5-13 and Figure 5-14). Increases to rainfall amounts are projected over or to the west of the mountainous parts of both regions during winter, and for northern Tairāwhiti during autumn. Of these, the largest increases (5-15%) are projected for high elevations in the westernmost portion of Hawke's Bay during winter. Additionally, small increases in the 0-5% range remain projected for some coastal parts of Hawke's Bay during summer and autumn.

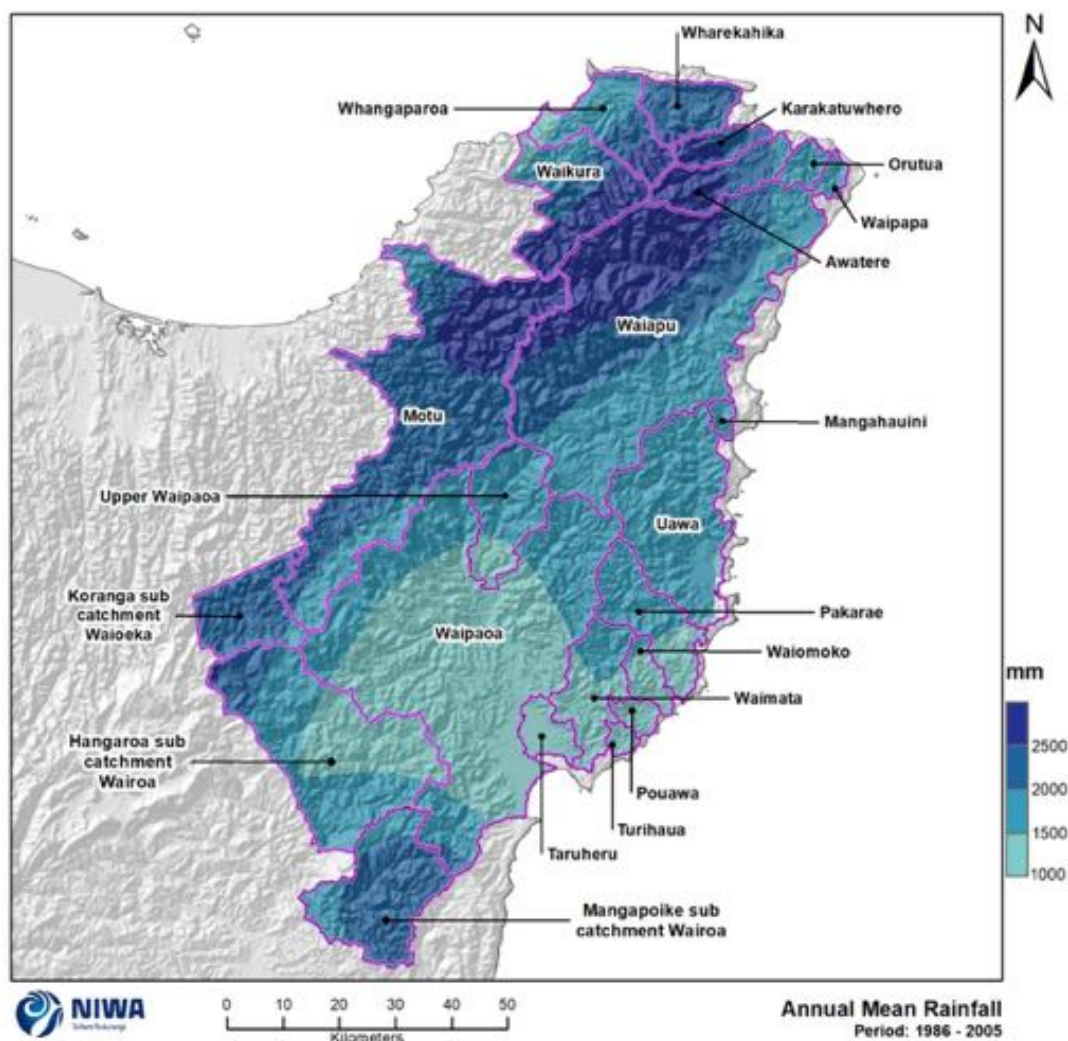


Figure 5-1: Modelled annual rainfall (mm) for Tairāwhiti, average over 1986-2005. Results are based on dynamical downscaled projections using NIWA's Regional Climate Model. Resolution of projection is 5km x 5km.

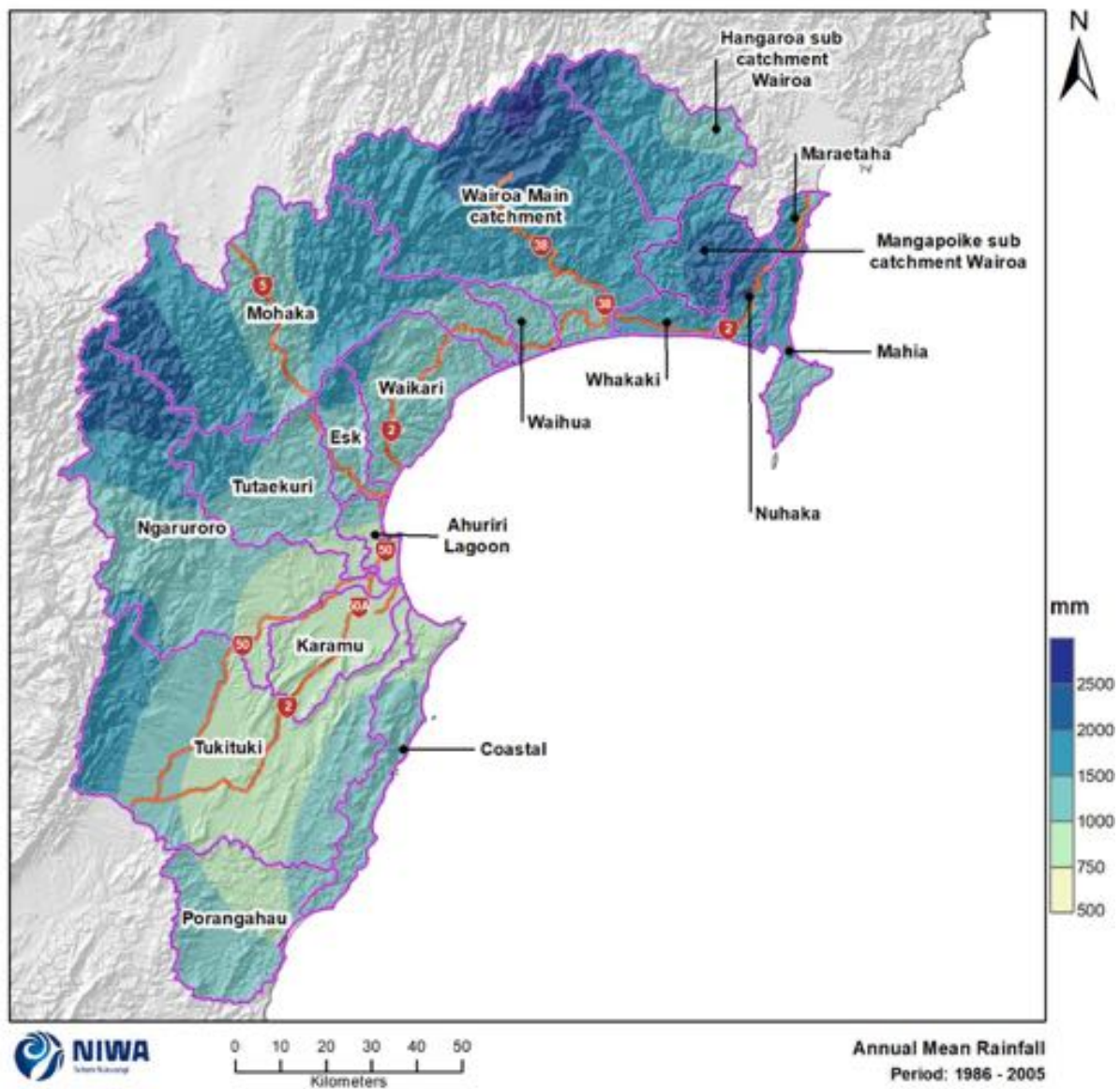


Figure 5-2: Modelled annual rainfall (mm) for Hawke's Bay, average over 1986-2005. Results are based on dynamical downscaled projections using NIWA's Regional Climate Model. Resolution of projection is 5km x 5km.

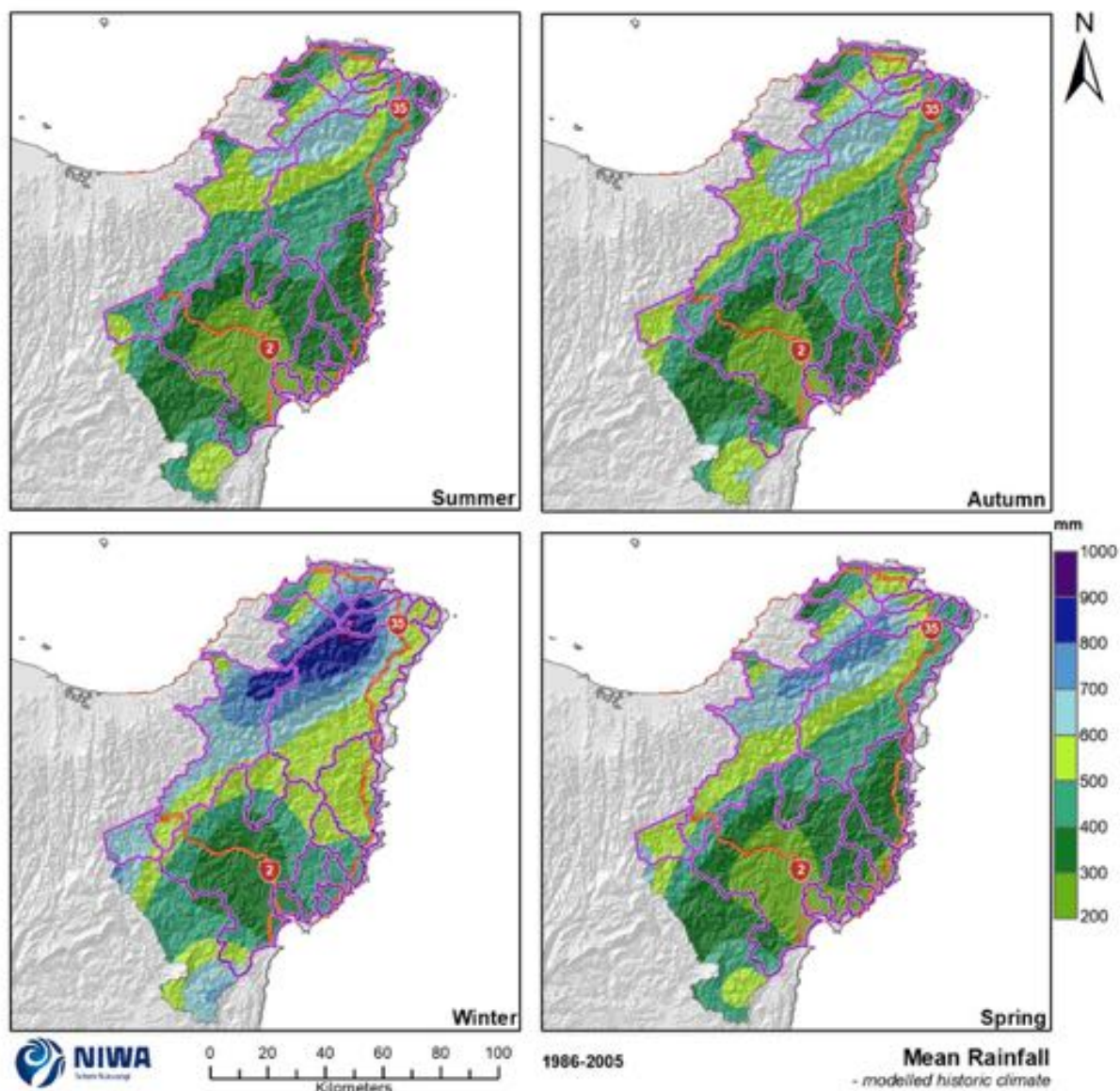


Figure 5-3: Modelled seasonal rainfall (mm) for Tairāwhiti, average over 1986-2005. Results are based on dynamical downscaled projections using NIWA's Regional Climate Model. Resolution of projection is 5km x 5km.

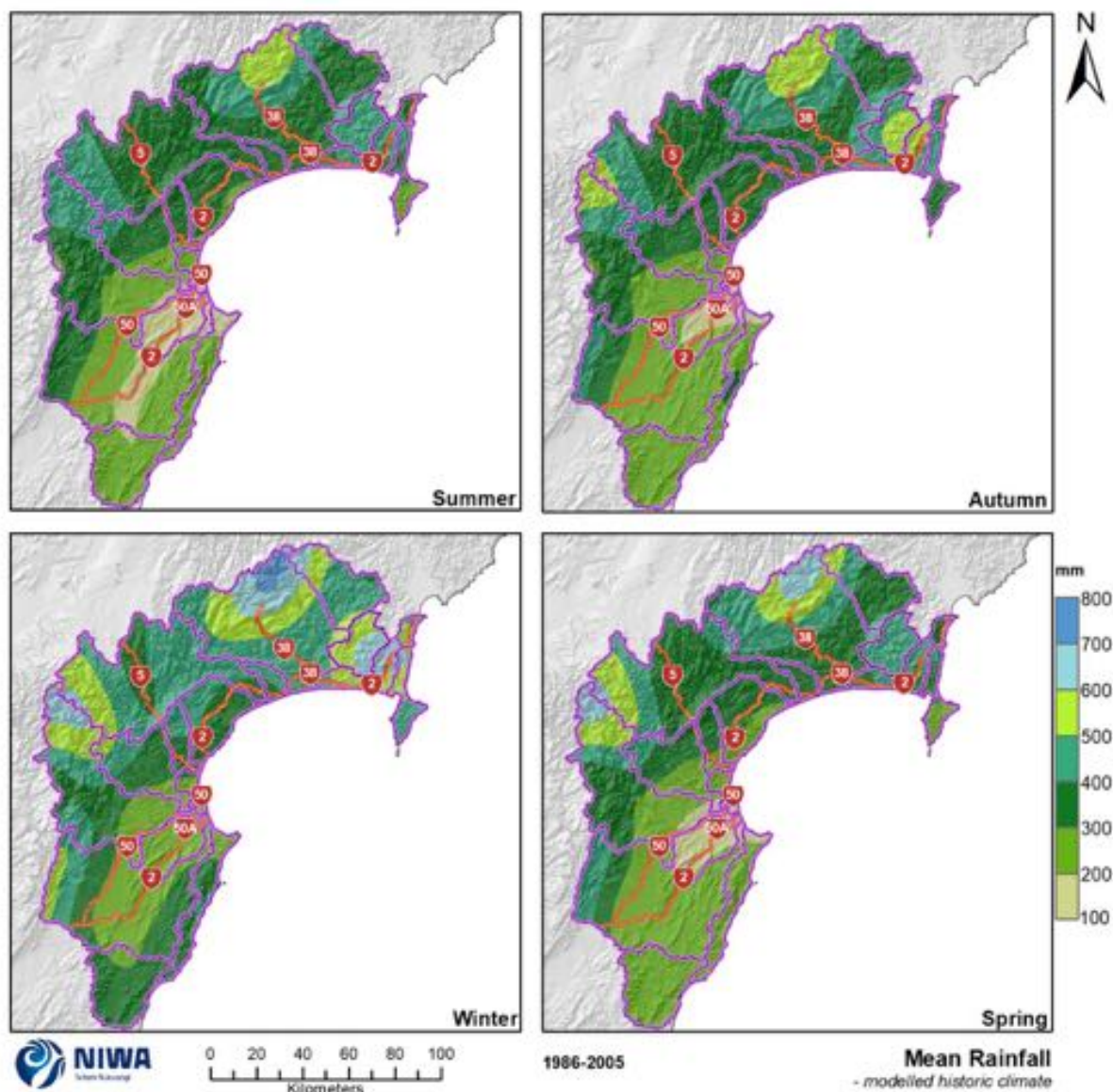


Figure 5-4: Modelled seasonal rainfall (mm) for Hawke's Bay, average over 1986-2005. Results are based on dynamical downscaled projections using NIWA's Regional Climate Model. Resolution of projection is 5km x 5km.

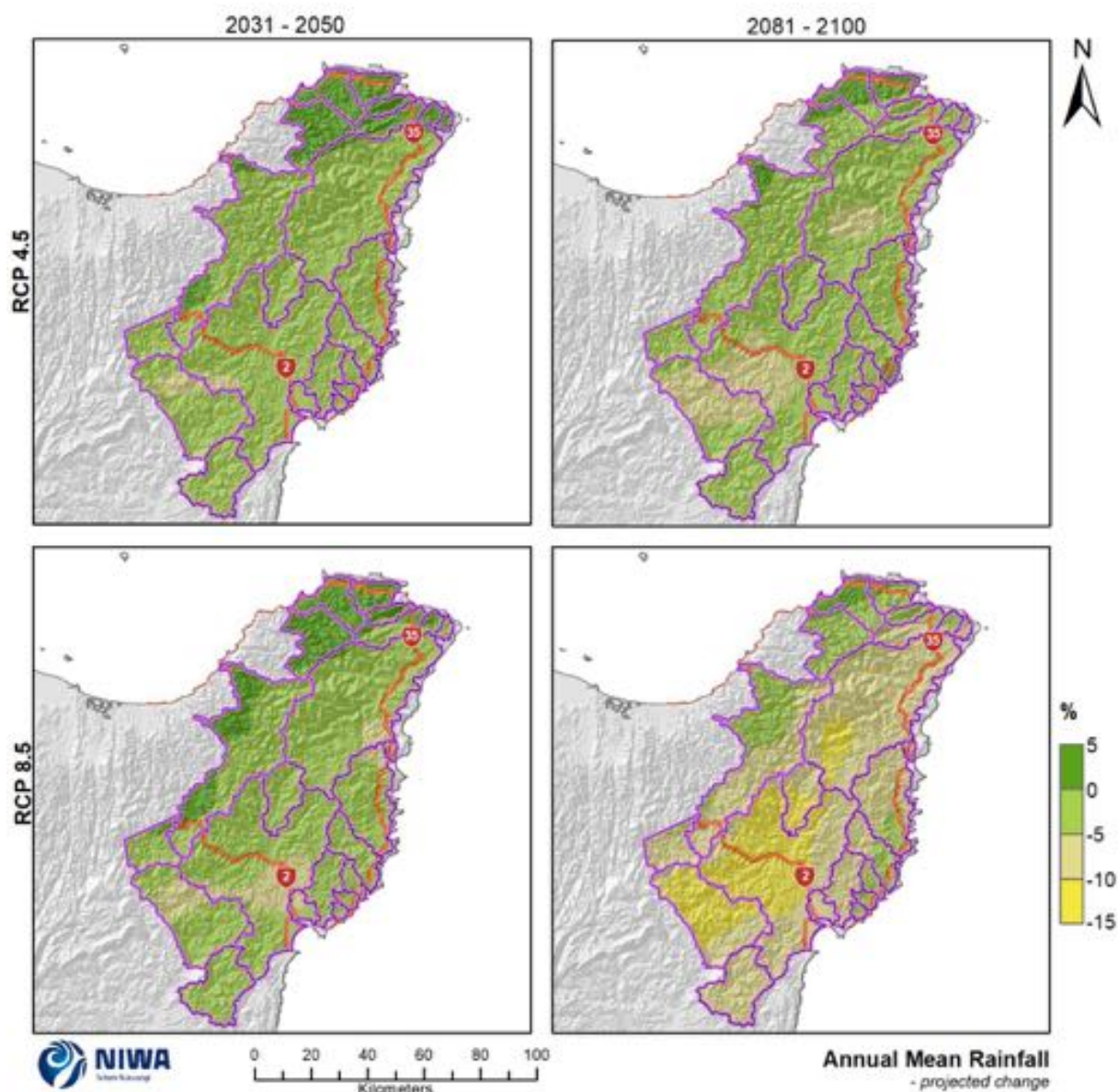


Figure 5-5: Projected annual rainfall changes (%) for Tairāwhiti. Relative to 1986-2005 average, based on the average of six global climate models. Results are based on dynamical downscaled projections using NIWA's Regional Climate Model. Resolution of projection is 5km x 5km.

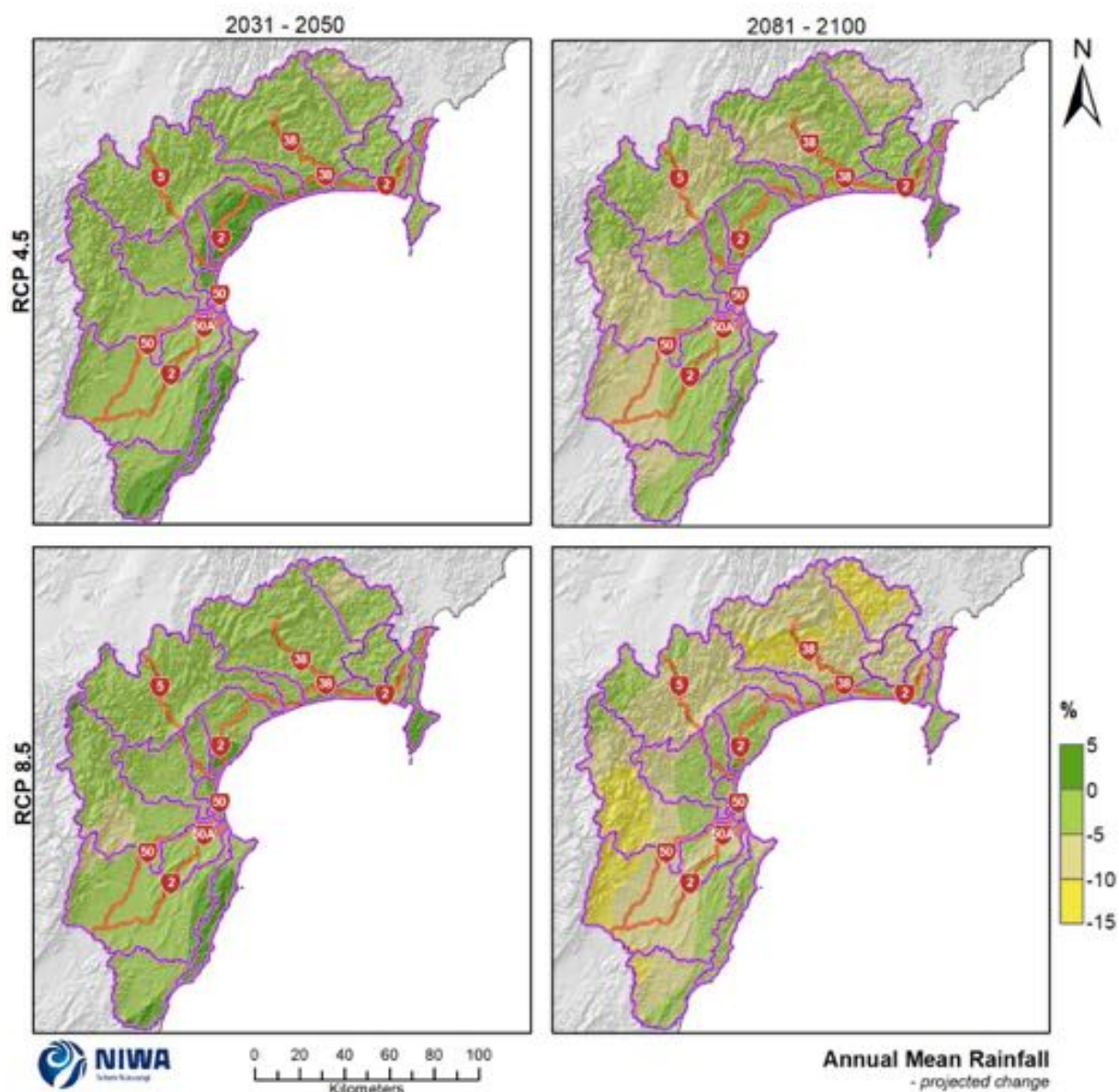


Figure 5-6: Projected annual rainfall changes (%) for Hawke's Bay. Relative to 1986-2005 average, based on the average of six global climate models. Results are based on dynamical downscaled projections using NIWA's Regional Climate Model. Resolution of projection is 5km x 5km.

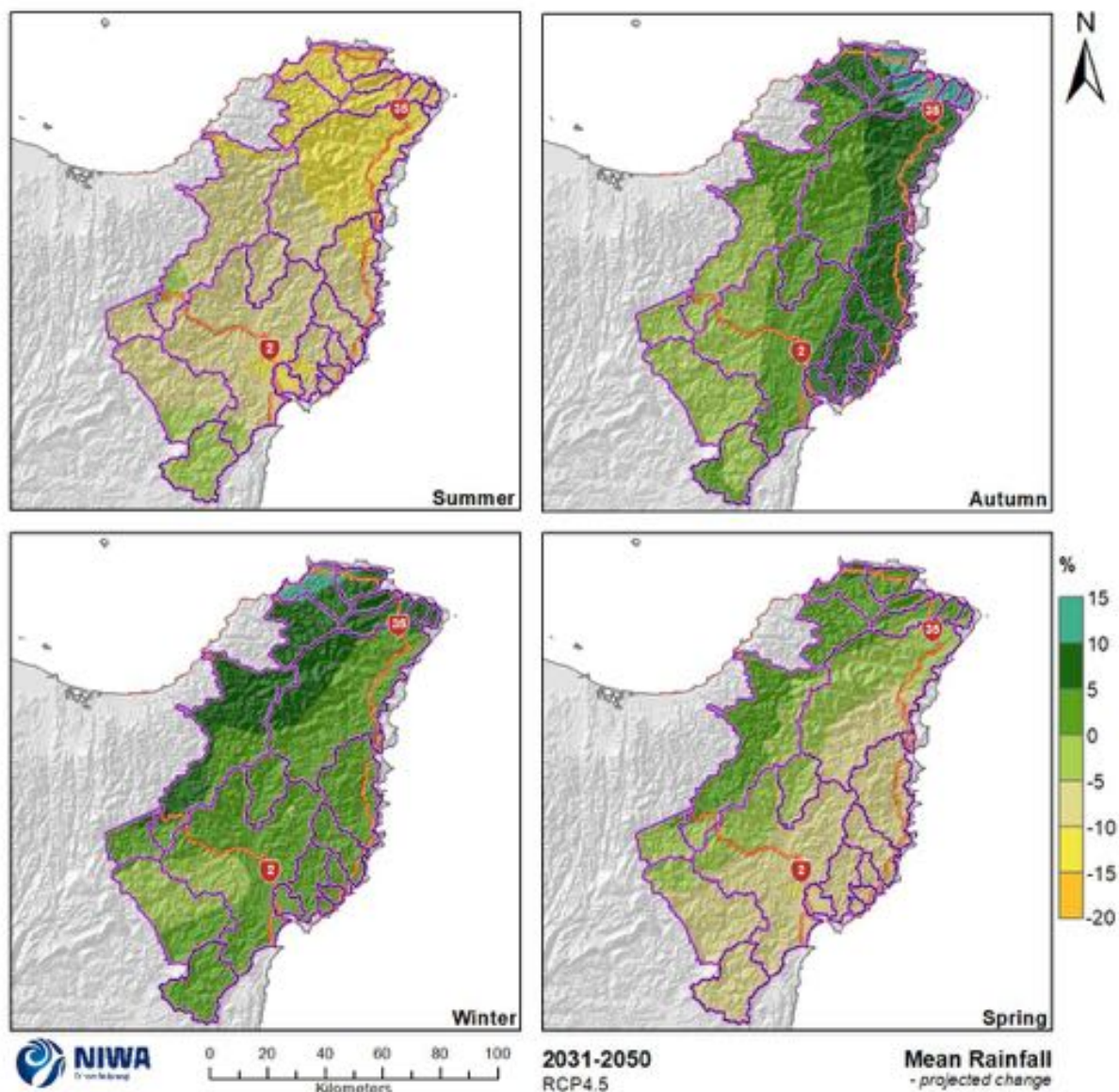


Figure 5-7: Projected seasonal rainfall changes (%) for Tairāwhiti by 2040 for RCP4.5. Relative to 1986-2005 average, based on the average of six global climate models. Results are based on dynamical downscaled projections using NIWA's Regional Climate Model. Resolution of projection is 5km x 5km.

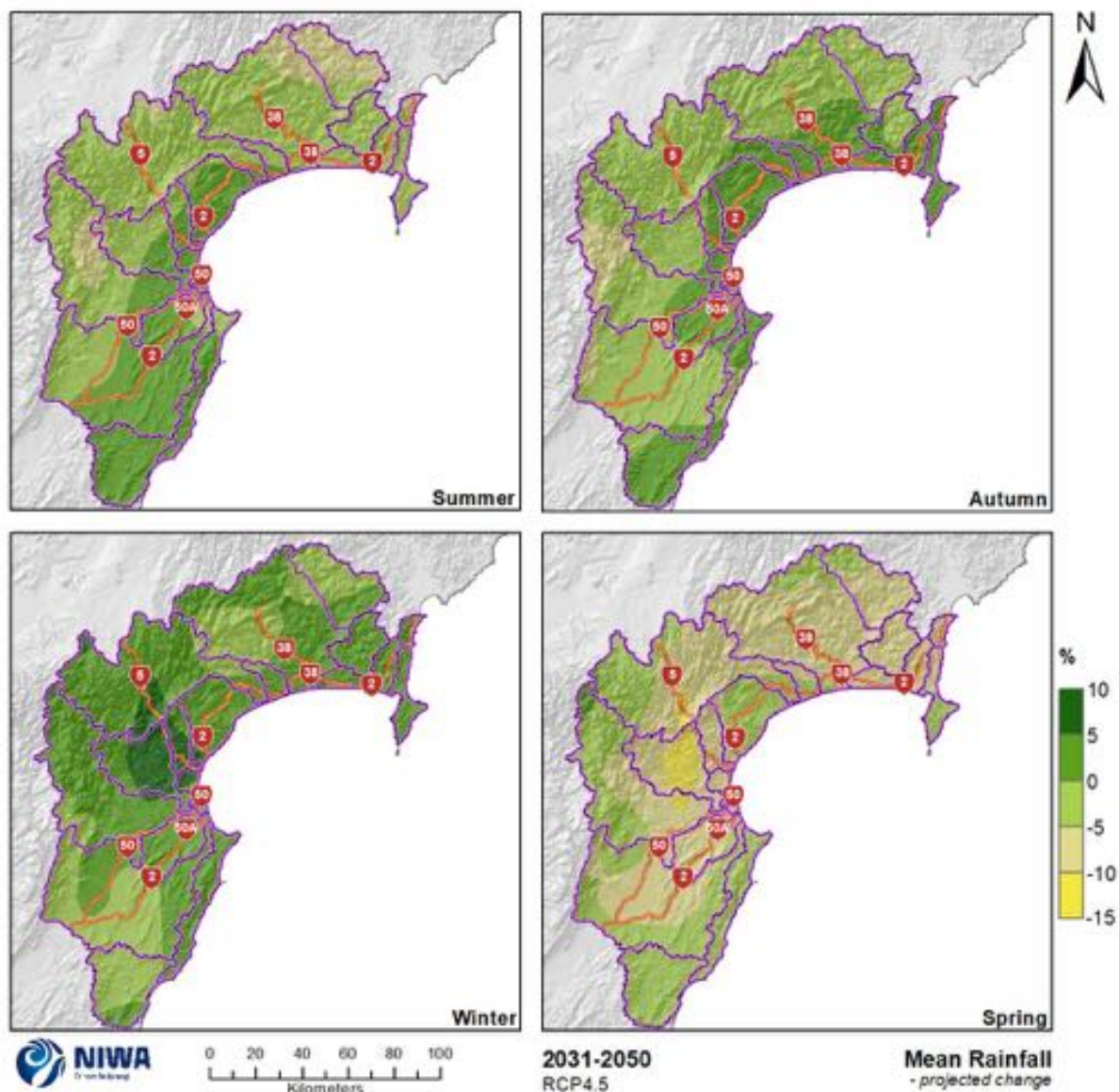


Figure 5-8: Projected seasonal rainfall changes (%) for Hawke's Bay by 2040 for RCP4.5. Relative to 1986-2005 average, based on the average of six global climate models. Results are based on dynamical downscaled projections using NIWA's Regional Climate Model. Resolution of projection is 5km x 5km.

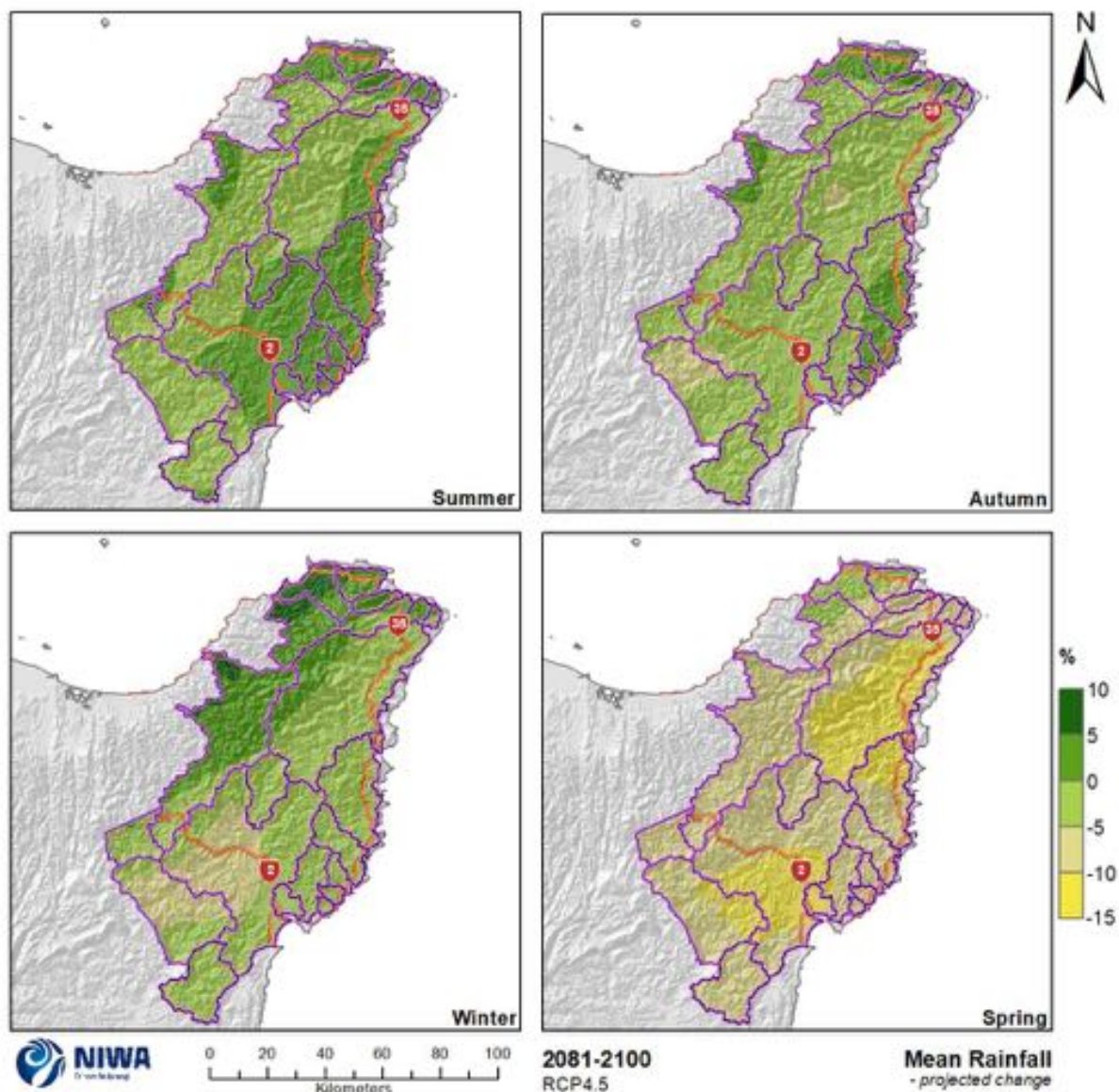


Figure 5-9: Projected seasonal rainfall changes (%) for Tairāwhiti by 2090 for RCP4.5. Relative to 1986-2005 average, based on the average of six global climate models. Results are based on dynamical downscaled projections using NIWA's Regional Climate Model. Resolution of projection is 5km x 5km.

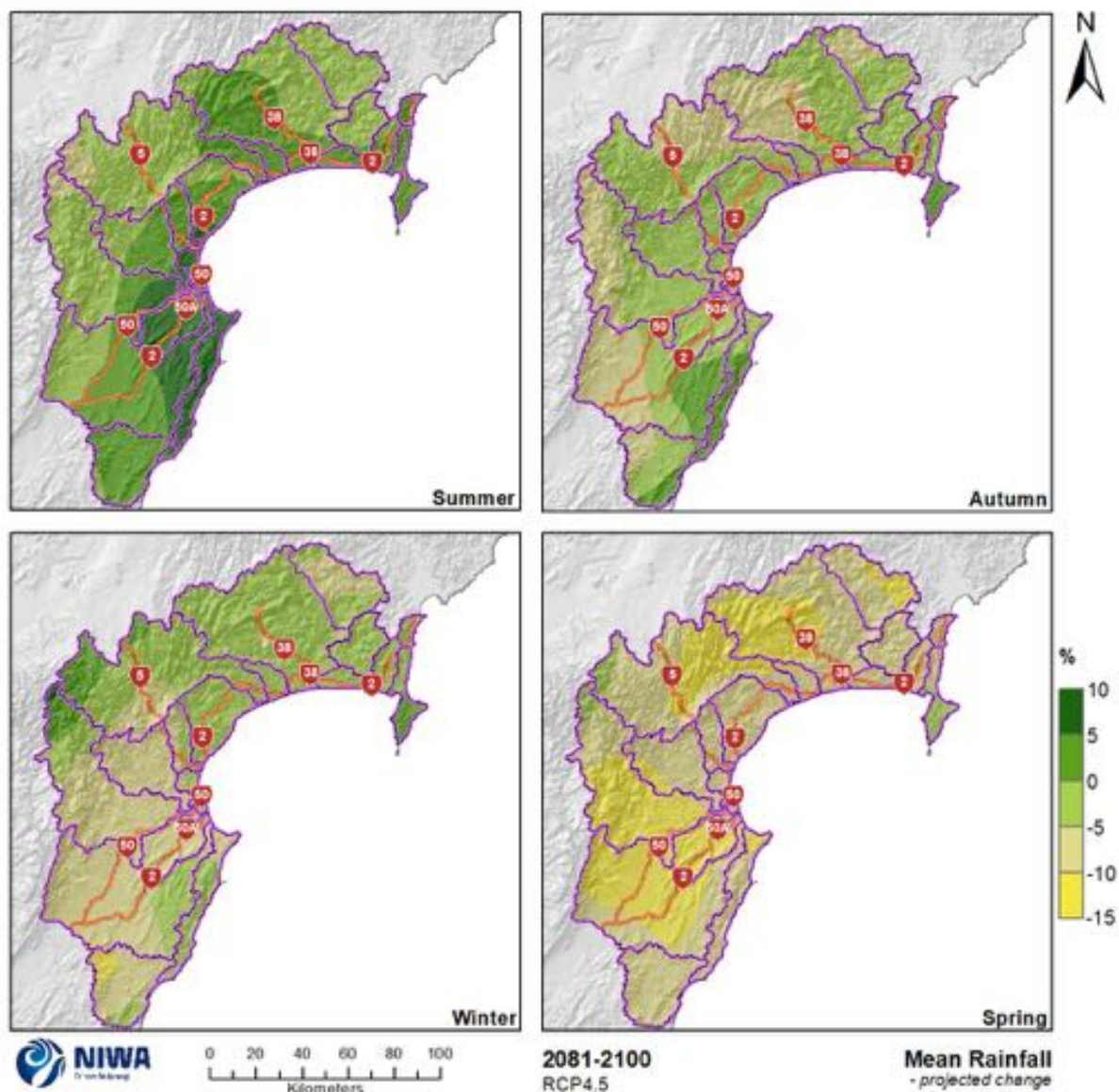


Figure 5-10: Projected seasonal rainfall changes (%) for Hawke's Bay by 2090 for RCP4.5. Relative to 1986-2005 average, based on the average of six global climate models. Results are based on dynamical downscaled projections using NIWA's Regional Climate Model. Resolution of projection is 5km x 5km.

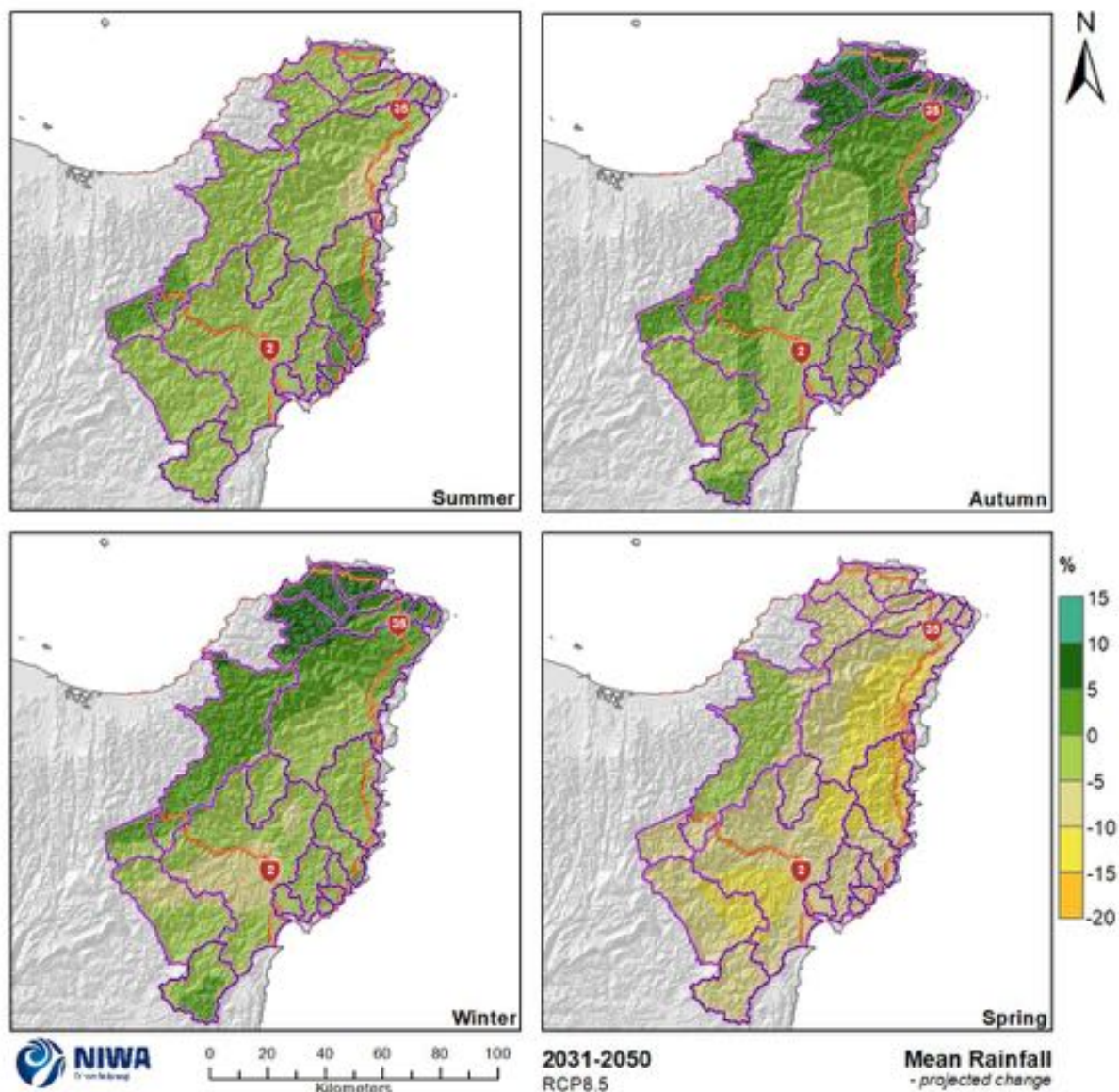


Figure 5-11: Projected seasonal rainfall changes (%) for Tairāwhiti by 2040 for RCP8.5. Relative to 1986-2005 average, based on the average of six global climate models. Results are based on dynamical downscaled projections using NIWA's Regional Climate Model. Resolution of projection is 5km x 5km.

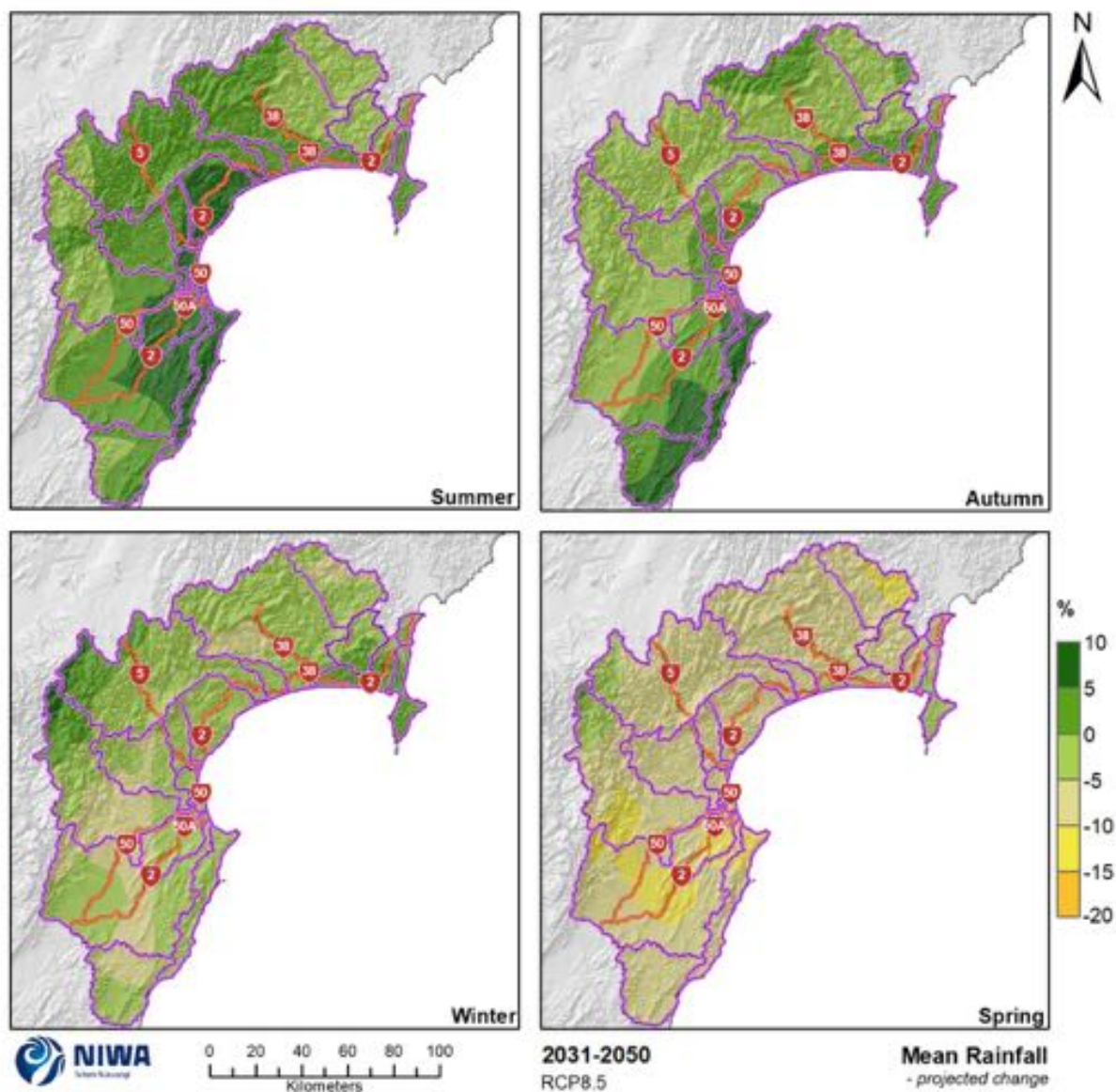


Figure 5-12: Projected seasonal rainfall changes (%) for Hawke's Bay by 2040 for RCP8.5. Relative to 1986-2005 average, based on the average of six global climate models. Results are based on dynamical downscaled projections using NIWA's Regional Climate Model. Resolution of projection is 5km x 5km.

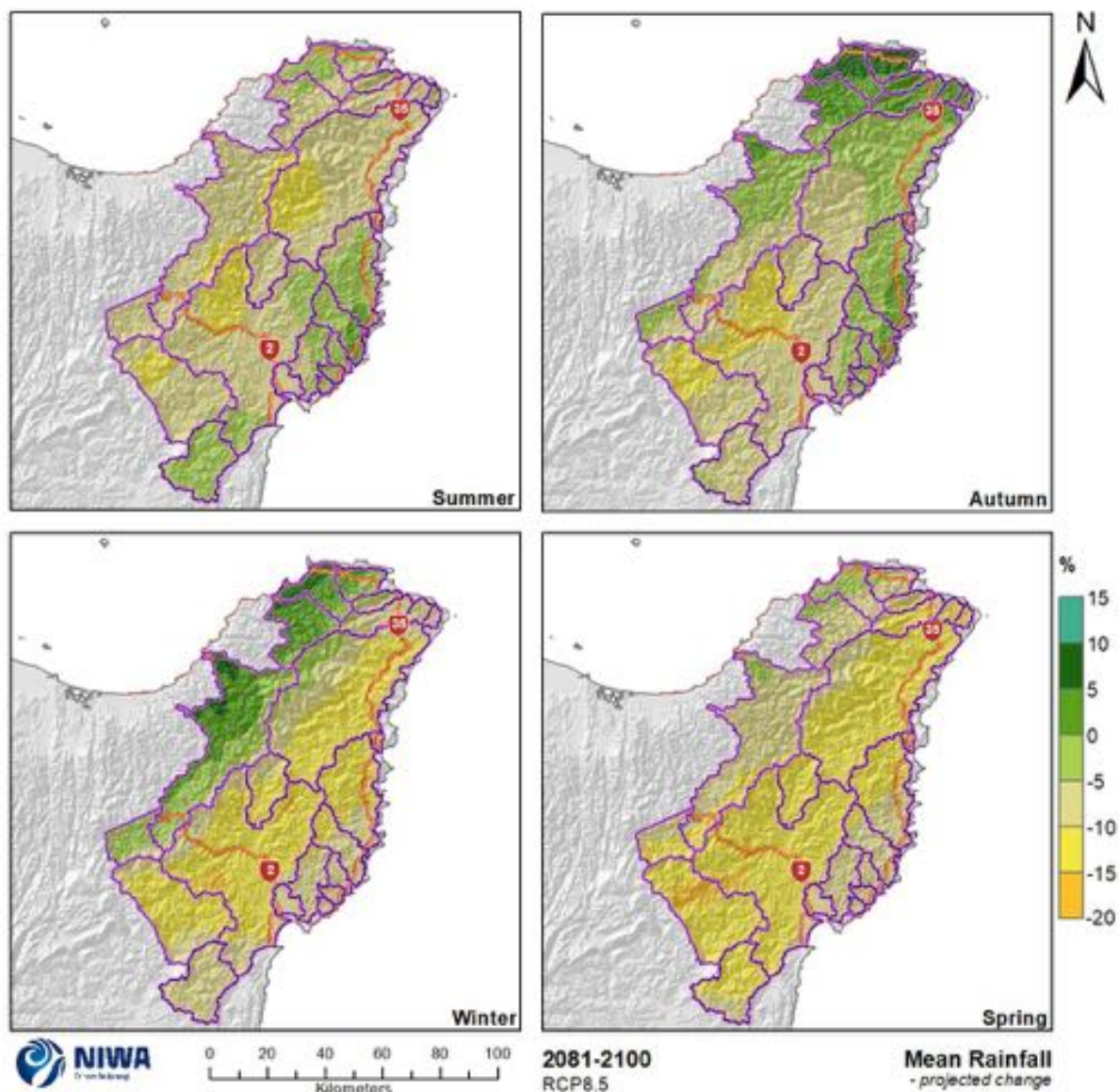


Figure 5-13: Projected seasonal rainfall changes (%) for Tairāwhiti by 2090 for RCP8.5. Relative to 1986-2005 average, based on the average of six global climate models. Results are based on dynamical downscaled projections using NIWA's Regional Climate Model. Resolution of projection is 5km x 5km.

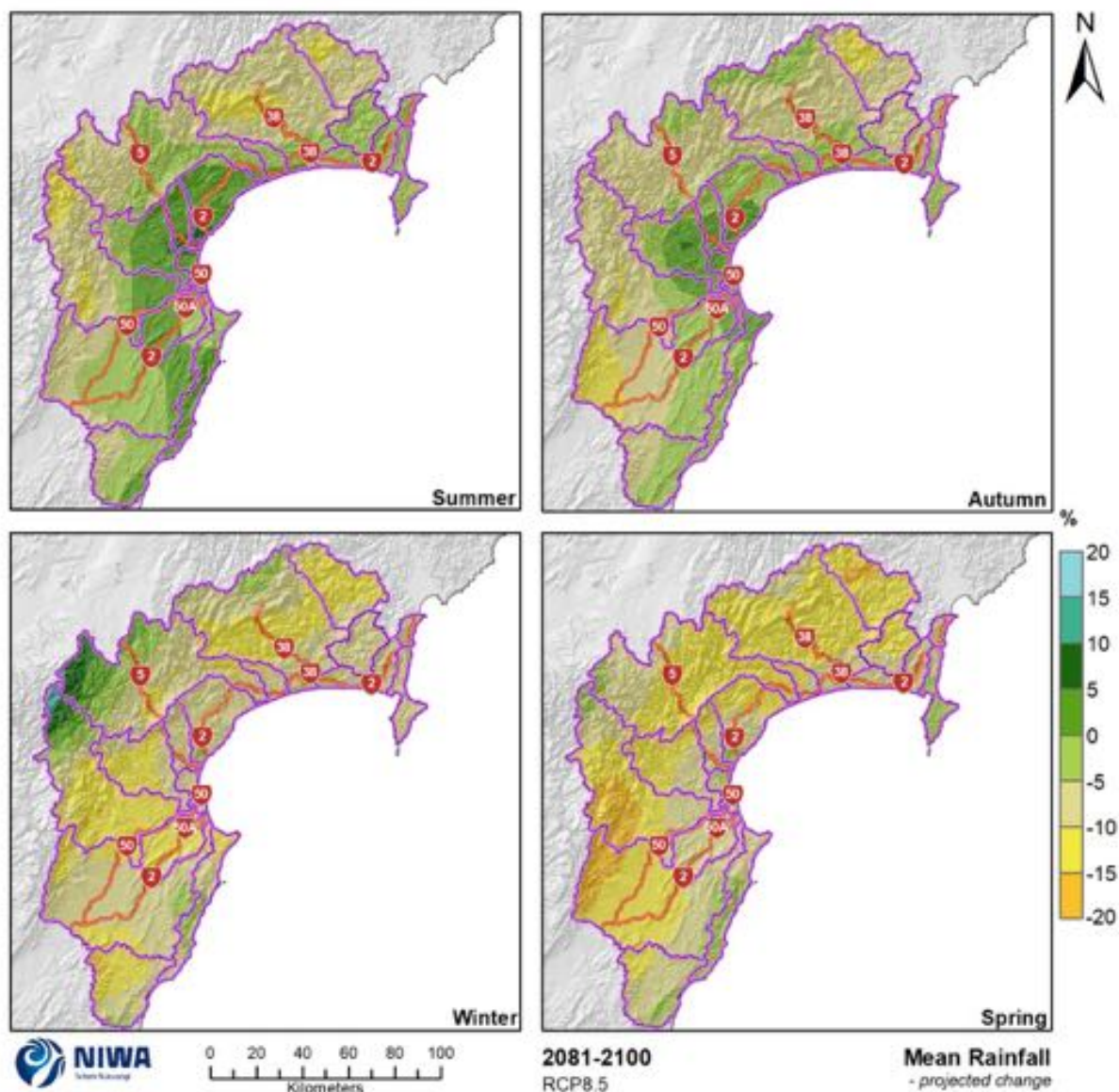


Figure 5-14: Projected seasonal rainfall changes (%) for Hawke's Bay by 2090 for RCP8.5. Relative to 1986-2005 average, based on the average of six global climate models. Results are based on dynamical downscaled projections using NIWA's Regional Climate Model. Resolution of projection is 5km x 5km.

5.2 Extreme, rare rainfall events

Extreme rainfall events are often considered in the context of return periods (e.g. 1-in-100-year rainfall events). A return period, also known as an average recurrence interval (ARI), is an estimate of the likelihood of an event. It is a statistical measure typically based on historical data and probability distributions which calculate how often an event of a certain magnitude may occur. Return periods are often used in risk analysis and infrastructure design.

The theoretical return period is the inverse of the probability that the event will be exceeded in any one year. For example, a 1-in-10-year rainfall event has a $1/10 = 0.1$ or 10% chance of being exceeded in any one year, and a 1-in-100-year rainfall event has a $1/100 = 0.01$ or 1% chance of being exceeded in any one year. However, this does not mean that a 1-in-100-year rainfall event will happen regularly every 100 years, or only once in 100 years. With a changing climate, the return periods used below should be thought of only within the 20-year period in which they are defined. For instance, if extreme heavy rainfall events are becoming a lot more frequent under climate change then the 1-in-100-year rainfall event for 2040 as defined as the 2031-2050 period will be less than the 1-in-100-year rainfall event when defined under 2001-2080, because the latter is dominated by the more frequent heavy events during the 2070s. The events with larger return periods (i.e. 1-in-100-year events) have larger rainfall amounts for the same duration as events with smaller return periods (i.e. 1-in-2-year events) because larger events occur less frequently (on average).

NIWA's High Intensity Rainfall Design System (HIRDS version 4) allows rainfall event totals (depth; measured in mm) at various recurrence intervals to be calculated for any location in New Zealand (Carey-Smith et al., 2018). The rainfall event durations presented in HIRDS range from 10 minutes to 120 hours. HIRDS calculates historic rainfall event totals for given recurrence intervals as well as future potential rainfall event totals for given recurrence intervals based on climate change scenarios. The future rainfall increases calculated by the HIRDS v4 tool are based on a per cent change per degree of warming, which is averaged across New Zealand. The short duration, rare events have the largest relative increases of around 14% per degree of warming, while the longest duration events increase by about 5 to 6%. HIRDS v4 can be accessed at <https://hirds.niwa.co.nz/>, and more background information to the HIRDS methodology can be found at <https://www.niwa.co.nz/information/services/hirds/help>.

HIRDS rainfall projections for selected sites in the Tairāwhiti and Hawke's Bay regions (Figure 5-15 and Figure 5-16) are presented in this section. For each site there are two tables; the first table presents data for 1-in-50-year rainfall events, and the second table presents data for 1-in-100-year rainfall events, with each of these tables listing the modelled historical and projected rainfall depths for one to 48-hour rain events. The results for Tairāwhiti are presented in Tables 5-1 to 5-32 and the results for Hawke's Bay are presented in Tables 5-33 to 5-54.

For each of the selected locations (in both regions), rainfall depths are projected to increase across all the future scenarios, and both return periods. For example, Table 5-1 shows that the projected rainfall depth for a 12-hour rainfall event at the Waikura Valley site (50-year ARI) is projected to increase under RCP4.5 from 286mm (historical depth) to 307 mm by 2040, and 320 mm by 2090. Under RCP8.5 and for the same rainfall event duration, the projected amounts are 310 mm by 2040, and 359 mm by 2090, which indicate a 24 mm and 73 mm rise respectively compared with historical depth.



Figure 5-15: Selected sites in the Tairāwhiti region for location specific rainfall intensity projections.

Table 5-1: Modelled historical and projected rainfall depths (mm) for Waikura Valley for different event durations with a 50-year return period (ARI) Source: HIRDS v4.

Rainfall event duration	Historical depth (mm)	Projected depth (mm)			
		Mid-century average (2031-2050)		Late-century average (2081-2100)	
		RCP4.5	RCP8.5	RCP4.5	RCP8.5
1-hour	59.4	65.3	66.2	69.1	80
6-hour	196	213	215	223	253
12-hour	286	307	310	320	359
24-hour	390	414	418	430	474
48-hour	494	521	525	538	588

Table 5-2: Modelled historical and projected rainfall depths (mm) for Waikura Valley for different event durations with a 100-year return period (ARI) Source: HIRDS v4.

Rainfall event duration	Historical depth (mm)	Projected depth (mm)			
		Mid-century average (2031-2050)		Late-century average (2081-2100)	
		RCP4.5	RCP8.5	RCP4.5	RCP8.5
1-hour	67.6	74.4	75.4	78.7	91.3
6-hour	221	240	243	252	287
12-hour	321	345	349	360	405
24-hour	437	464	469	482	534
48-hour	551	582	586	601	658

Table 5-3: Modelled historical and projected rainfall depths (mm) for East Cape at Lighthouse for different event durations with a 50-year return period (ARI) Source: HIRDS v4.

Rainfall event duration	Historical depth (mm)	Projected depth (mm)			
		Mid-century average (2031-2050)		Late-century average (2081-2100)	
		RCP4.5	RCP8.5	RCP4.5	RCP8.5
1-hour	57.6	63.3	64.2	67	77.6
6-hour	140	151	153	159	180
12-hour	181	194	196	202	227
24-hour	223	237	239	246	272
48-hour	263	277	280	287	313

Table 5-4: Modelled historical and projected rainfall depths (mm) for East Cape at Lighthouse for different event durations with a 100-year return period (ARI) Source: HIRDS v4.

Rainfall event duration	Historical depth (mm)	Projected depth (mm)			
		Mid-century average (2031-2050)		Late-century average (2081-2100)	
		RCP4.5	RCP8.5	RCP4.5	RCP8.5
1-hour	66.9	73.6	74.6	77.9	90.4
6-hour	160	174	176	182	208
12-hour	206	221	224	231	260
24-hour	253	269	272	279	309
48-hour	296	313	315	323	354

Table 5-5: Modelled historical and projected rainfall depths (mm) for Ruatoria Telemetry Station at Barry Ave for different event durations with a 50-year return period (ARI) Source: HIRDS v4.

Rainfall event duration	Historical depth (mm)	Projected depth (mm)			
		Mid-century average (2031-2050)		Late-century average (2081-2100)	
		RCP4.5	RCP8.5	RCP4.5	RCP8.5
1-hour	61.5	67.6	68.5	71.5	82.9
6-hour	165	179	181	188	213
12-hour	231	248	250	258	290
24-hour	308	328	330	340	375
48-hour	391	413	416	426	466

Table 5-6: Modelled historical and projected rainfall depths (mm) for Ruatoria Telemetry Station at Barry Ave for different event durations with a 100-year return period (ARI) Source: HIRDS v4.

Rainfall event duration	Historical depth (mm)	Projected depth (mm)			
		Mid-century average (2031-2050)		Late-century average (2081-2100)	
		RCP4.5	RCP8.5	RCP4.5	RCP8.5
1-hour	70.7	77.8	78.9	82.3	95.5
6-hour	188	204	206	214	244
12-hour	261	281	283	293	329
24-hour	348	370	373	384	425
48-hour	439	463	467	479	524

Table 5-7: Modelled historical and projected rainfall depths (mm) for Puketoro Telemetry Station for different event durations with a 50-year return period (ARI) Source: HIRDS v4.

Rainfall event duration	Historical depth (mm)	Projected depth (mm)			
		Mid-century average (2031-2050)		Late-century average (2081-2100)	
		RCP4.5	RCP8.5	RCP4.5	RCP8.5
1-hour	40.2	44.2	44.8	46.8	54.2
6-hour	140	152	154	159	181
12-hour	208	224	226	233	262
24-hour	294	313	316	324	358
48-hour	395	416	419	430	470

Table 5-8: Modelled historical and projected rainfall depths (mm) for Puketoro Telemetry Station for different event durations with a 100-year return period (ARI) Source: HIRDS v4.

Rainfall event duration	Historical depth (mm)	Projected depth (mm)			
		Mid-century average (2031-2050)		Late-century average (2081-2100)	
		RCP4.5	RCP8.5	RCP4.5	RCP8.5
1-hour	45.3	49.8	50.5	52.7	61.1
6-hour	157	170	172	179	203
12-hour	232	250	252	261	293
24-hour	327	348	351	361	400
48-hour	437	461	465	477	522

Table 5-9: Modelled historical and projected rainfall depths (mm) for Te Puia for different event durations with a 50-year return period (ARI) Source: HIRDS v4.

Rainfall event duration	Historical depth (mm)	Projected depth (mm)			
		Mid-century average (2031-2050)		Late-century average (2081-2100)	
		RCP4.5	RCP8.5	RCP4.5	RCP8.5
1-hour	61.3	67.4	68.4	71.3	82.7
6-hour	184	199	201	209	237
12-hour	253	272	275	284	318
24-hour	330	351	354	364	402
48-hour	406	428	431	442	483

Table 5-10: Modelled historical and projected rainfall depths (mm) for Te Puia for different event durations with a 100-year return period (ARI) Source: HIRDS v4.

Rainfall event duration	Historical depth (mm)	Projected depth (mm)			
		Mid-century average (2031-2050)		Late-century average (2081-2100)	
		RCP4.5	RCP8.5	RCP4.5	RCP8.5
1-hour	70.3	77.4	78.4	81.8	94.9
6-hour	209	227	229	238	271
12-hour	287	308	312	322	362
24-hour	373	396	400	411	455
48-hour	457	482	486	498	545

Table 5-11: Modelled historical and projected rainfall depths (mm) for Te Rata Telemetry Station for different event durations with a 50-year return period (ARI) Source: HIRDS v4.

Rainfall event duration	Historical depth (mm)	Projected depth (mm)			
		Mid-century average (2031-2050)		Late-century average (2081-2100)	
		RCP4.5	RCP8.5	RCP4.5	RCP8.5
1-hour	38.4	42.3	42.9	44.7	51.8
6-hour	120	130	132	137	155
12-hour	174	187	189	195	218
24-hour	241	256	259	266	294
48-hour	321	339	342	350	383

Table 5-12: Modelled historical and projected rainfall depths (mm) for Te Rata Telemetry Station for different event durations with a 100-year return period (ARI) Source: HIRDS v4.

Rainfall event duration	Historical depth (mm)	Projected depth (mm)			
		Mid-century average (2031-2050)		Late-century average (2081-2100)	
		RCP4.5	RCP8.5	RCP4.5	RCP8.5
1-hour	43.4	47.7	48.4	50.5	58.6
6-hour	135	146	148	154	175
12-hour	195	209	211	218	245
24-hour	269	286	289	297	329
48-hour	357	377	380	390	427

Table 5-13: Modelled historical and projected rainfall depths (mm) for Tutamoe Station Telemetry Station for different event durations with a 50-year return period (ARI) Source: HIRDS v4.

Rainfall event duration	Historical depth (mm)	Projected depth (mm)			
		Mid-century average (2031-2050)		Late-century average (2081-2100)	
		RCP4.5	RCP8.5	RCP4.5	RCP8.5
1-hour	38.3	42.1	42.7	44.5	51.6
6-hour	117	126	128	133	151
12-hour	168	180	182	188	211
24-hour	234	248	251	258	285
48-hour	314	331	334	342	374

Table 5-14: Modelled historical and projected rainfall depths (mm) for Tutamoe Station Telemetry Station for different event durations with a 100-year return period (ARI) Source: HIRDS v4.

Rainfall event duration	Historical depth (mm)	Projected depth (mm)			
		Mid-century average (2031-2050)		Late-century average (2081-2100)	
		RCP4.5	RCP8.5	RCP4.5	RCP8.5
1-hour	43.8	48.2	48.9	51	59.2
6-hour	132	143	145	150	171
12-hour	189	204	206	213	239
24-hour	262	279	281	290	321
48-hour	350	370	373	382	418

Table 5-15: Modelled historical and projected rainfall depths (mm) for Hikuwai River at Willowflat for different event durations with a 50-year return period (ARI) Source: HIRDS v4

Rainfall event duration	Historical depth (mm)	Projected depth (mm)			
		Mid-century average (2031-2050)		Late-century average (2081-2100)	
		RCP4.5	RCP8.5	RCP4.5	RCP8.5
1-hour	61.9	68.1	69	72	83.5
6-hour	186	202	204	211	240
12-hour	256	275	278	287	321
24-hour	329	349	352	362	400
48-hour	392	413	416	427	467

Table 5-16: Modelled historical and projected rainfall depths (mm) for Hikuwai River at Willowflat for different event durations with a 100-year return period (ARI) Source: HIRDS v4.

Rainfall event duration	Historical depth (mm)	Projected depth (mm)			
		Mid-century average (2031-2050)		Late-century average (2081-2100)	
		RCP4.5	RCP8.5	RCP4.5	RCP8.5
1-hour	72.2	79.4	80.5	84	97.5
6-hour	213	231	234	243	277
12-hour	292	314	317	327	368
24-hour	372	396	400	411	455
48-hour	441	465	469	481	526

Table 5-17: Modelled historical and projected rainfall depths (mm) for Matawai Telemetry Station for different event durations with a 50-year return period (ARI) Source: HIRDS v4.

Rainfall event duration	Historical depth (mm)	Projected depth (mm)			
		Mid-century average (2031-2050)		Late-century average (2081-2100)	
		RCP4.5	RCP8.5	RCP4.5	RCP8.5
1-hour	41.6	45.7	46.3	48.3	56
6-hour	115	125	126	131	149
12-hour	158	170	172	177	199
24-hour	208	221	223	229	253
48-hour	261	276	278	285	311

Table 5-18: Modelled historical and projected rainfall depths (mm) for Matawai Telemetry Station for different event durations with a 100-year return period (ARI) Source: HIRDS v4.

Rainfall event duration	Historical depth (mm)	Projected depth (mm)			
		Mid-century average (2031-2050)		Late-century average (2081-2100)	
		RCP4.5	RCP8.5	RCP4.5	RCP8.5
1-hour	47	51.7	52.4	54.7	63.4
6-hour	130	141	142	148	168
12-hour	178	191	193	199	224
24-hour	233	248	250	257	285
48-hour	292	308	311	319	349

Table 5-19: Modelled historical and projected rainfall depths (mm) for Panikau Rd – Reed Rd for different event durations with a 50-year return period (ARI) Source: HIRDS v4.

Rainfall event duration	Historical depth (mm)	Projected depth (mm)			
		Mid-century average (2031-2050)		Late-century average (2081-2100)	
		RCP4.5	RCP8.5	RCP4.5	RCP8.5
1-hour	53	58.3	59.1	61.7	71.5
6-hour	166	180	182	189	214
12-hour	237	255	257	266	298
24-hour	319	339	341	351	388
48-hour	397	419	422	433	473

Table 5-20: Modelled historical and projected rainfall depths (mm) for Panikau Rd – Reed Rd for different event durations with a 100-year return period (ARI) Source: HIRDS v4.

Rainfall event duration	Historical depth (mm)	Projected depth (mm)			
		Mid-century average (2031-2050)		Late-century average (2081-2100)	
		RCP4.5	RCP8.5	RCP4.5	RCP8.5
1-hour	61.7	67.9	68.8	71.8	83.3
6-hour	190	206	209	216	246
12-hour	270	290	293	303	340
24-hour	360	383	387	398	440
48-hour	446	471	474	486	532

Table 5-21: Modelled historical and projected rainfall depths (mm) for Waipaoa River at Kanakanaia for different event durations with a 50-year return period (ARI) Source: HIRDS v4.

Rainfall event duration	Historical depth (mm)	Projected depth (mm)			
		Mid-century average (2031-2050)		Late-century average (2081-2100)	
		RCP4.5	RCP8.5	RCP4.5	RCP8.5
1-hour	37.3	41	41.6	43.4	50.3
6-hour	97.4	106	107	111	126
12-hour	133	143	144	149	167
24-hour	174	185	187	192	212
48-hour	216	228	230	236	258

Table 5-22: Modelled historical and projected rainfall depths (mm) for Waipaoa River at Kanakanaia for different event durations with a 100-year return period (ARI) Source: HIRDS v4.

Rainfall event duration	Historical depth (mm)	Projected depth (mm)			
		Mid-century average (2031-2050)		Late-century average (2081-2100)	
		RCP4.5	RCP8.5	RCP4.5	RCP8.5
1-hour	43.5	47.9	48.6	50.7	58.8
6-hour	112	122	123	128	146
12-hour	153	164	166	171	193
24-hour	199	212	213	220	243
48-hour	246	260	262	268	294

Table 5-23: Modelled historical and projected rainfall depths (mm) for Wharekopae School for different event durations with a 50-year return period (ARI) Source: HIRDS v4.

Rainfall event duration	Historical depth (mm)	Projected depth (mm)			
		Mid-century average (2031-2050)		Late-century average (2081-2100)	
		RCP4.5	RCP8.5	RCP4.5	RCP8.5
1-hour	33.9	37.3	37.8	39.5	45.8
6-hour	105	114	115	119	136
12-hour	149	160	162	167	187
24-hour	200	212	214	220	243
48-hour	252	266	268	275	300

Table 5-24: Modelled historical and projected rainfall depths (mm) for Wharekopae School for different event durations with a 100-year return period (ARI) Source: HIRDS v4.

Rainfall event duration	Historical depth (mm)	Projected depth (mm)			
		Mid-century average (2031-2050)		Late-century average (2081-2100)	
		RCP4.5	RCP8.5	RCP4.5	RCP8.5
1-hour	38.6	42.5	43	44.9	52.1
6-hour	119	129	130	135	154
12-hour	168	181	183	189	212
24-hour	225	240	242	249	275
48-hour	284	299	302	309	338

Table 5-25: Modelled historical and projected rainfall depths (mm) for Caesar Rd No. 1 Bore for different event durations with a 50-year return period (ARI) Source: HIRDS v4.

Rainfall event duration	Historical depth (mm)	Projected depth (mm)			
		Mid-century average (2031-2050)		Late-century average (2081-2100)	
		RCP4.5	RCP8.5	RCP4.5	RCP8.5
1-hour	42	46.2	46.8	48.9	56.6
6-hour	105	114	115	119	135
12-hour	143	154	156	161	180
24-hour	188	200	202	208	229
48-hour	235	247	249	256	279

Table 5-26: Modelled historical and projected rainfall depths (mm) for Caesar Rd No. 1 Bore for different event durations with a 100-year return period (ARI) Source: HIRDS v4.

Rainfall event duration	Historical depth (mm)	Projected depth (mm)			
		Mid-century average (2031-2050)		Late-century average (2081-2100)	
		RCP4.5	RCP8.5	RCP4.5	RCP8.5
1-hour	48.9	53.8	54.5	56.9	66
6-hour	121	131	132	137	156
12-hour	164	177	179	185	207
24-hour	215	229	231	238	263
48-hour	267	281	284	291	318

Table 5-27: Modelled historical and projected rainfall depths (mm) for Cameron Rd No. 1 Bore for different event durations with a 50-year return period (ARI) Source: HIRDS v4.

Rainfall event duration	Historical depth (mm)	Projected depth (mm)			
		Mid-century average (2031-2050)		Late-century average (2081-2100)	
		RCP4.5	RCP8.5	RCP4.5	RCP8.5
1-hour	42.8	47	47.7	49.8	57.7
6-hour	104	113	114	118	134
12-hour	142	152	154	159	178
24-hour	186	197	199	205	226
48-hour	231	244	246	252	276

Table 5-28: Modelled historical and projected rainfall depths (mm) for Cameron Rd No. 1 Bore for different event durations with a 100-year return period (ARI) Source: HIRDS v4.

Rainfall event duration	Historical depth (mm)	Projected depth (mm)			
		Mid-century average (2031-2050)		Late-century average (2081-2100)	
		RCP4.5	RCP8.5	RCP4.5	RCP8.5
1-hour	49.5	54.5	55.3	57.7	66.9
6-hour	119	129	131	136	155
12-hour	162	174	176	182	204
24-hour	211	225	227	233	258
48-hour	262	277	279	286	313

Table 5-29: Modelled historical and projected rainfall depths (mm) for Te Arai River at Pykes Weir for different event durations with a 50-year return period (ARI) Source: HIRDS v4.

Rainfall event duration	Historical depth (mm)	Projected depth (mm)			
		Mid-century average (2031-2050)		Late-century average (2081-2100)	
		RCP4.5	RCP8.5	RCP4.5	RCP8.5
1-hour	44.7	49.1	49.8	52	60.2
6-hour	118	128	130	135	153
12-hour	166	178	180	185	208
24-hour	226	241	243	249	276
48-hour	302	319	321	330	360

Table 5-30: Modelled historical and projected rainfall depths (mm) for Te Arai River at Pykes Weir for different event durations with a 100-year return period (ARI) Source: HIRDS v4.

Rainfall event duration	Historical depth (mm)	Projected depth (mm)			
		Mid-century average (2031-2050)		Late-century average (2081-2100)	
		RCP4.5	RCP8.5	RCP4.5	RCP8.5
1-hour	51.4	56.5	57.3	59.8	69.4
6-hour	135	147	148	154	175
12-hour	188	203	205	212	238
24-hour	257	273	276	284	314
48-hour	342	361	364	373	408

Table 5-31: Modelled historical and projected rainfall depths (mm) for Mangapoike at Reservoir for different event durations with a 50-year return period (ARI) Source: HIRDS v4.

Rainfall event duration	Historical depth (mm)	Projected depth (mm)			
		Mid-century average (2031-2050)		Late-century average (2081-2100)	
		RCP4.5	RCP8.5	RCP4.5	RCP8.5
1-hour	45.1	49.6	50.3	52.5	60.8
6-hour	149	161	163	169	192
12-hour	228	244	247	255	286
24-hour	334	355	358	368	406
48-hour	464	490	494	506	553

Table 5-32: Modelled historical and projected rainfall depths (mm) for Mangapoike at Reservoir for different event durations with a 100-year return period (ARI) Source: HIRDS v4.

Rainfall event duration	Historical depth (mm)	Projected depth (mm)			
		Mid-century average (2031-2050)		Late-century average (2081-2100)	
		RCP4.5	RCP8.5	RCP4.5	RCP8.5
1-hour	51.6	56.7	57.5	60	69.6
6-hour	169	183	185	192	219
12-hour	257	276	279	288	324
24-hour	375	399	403	414	458
48-hour	520	549	553	567	620

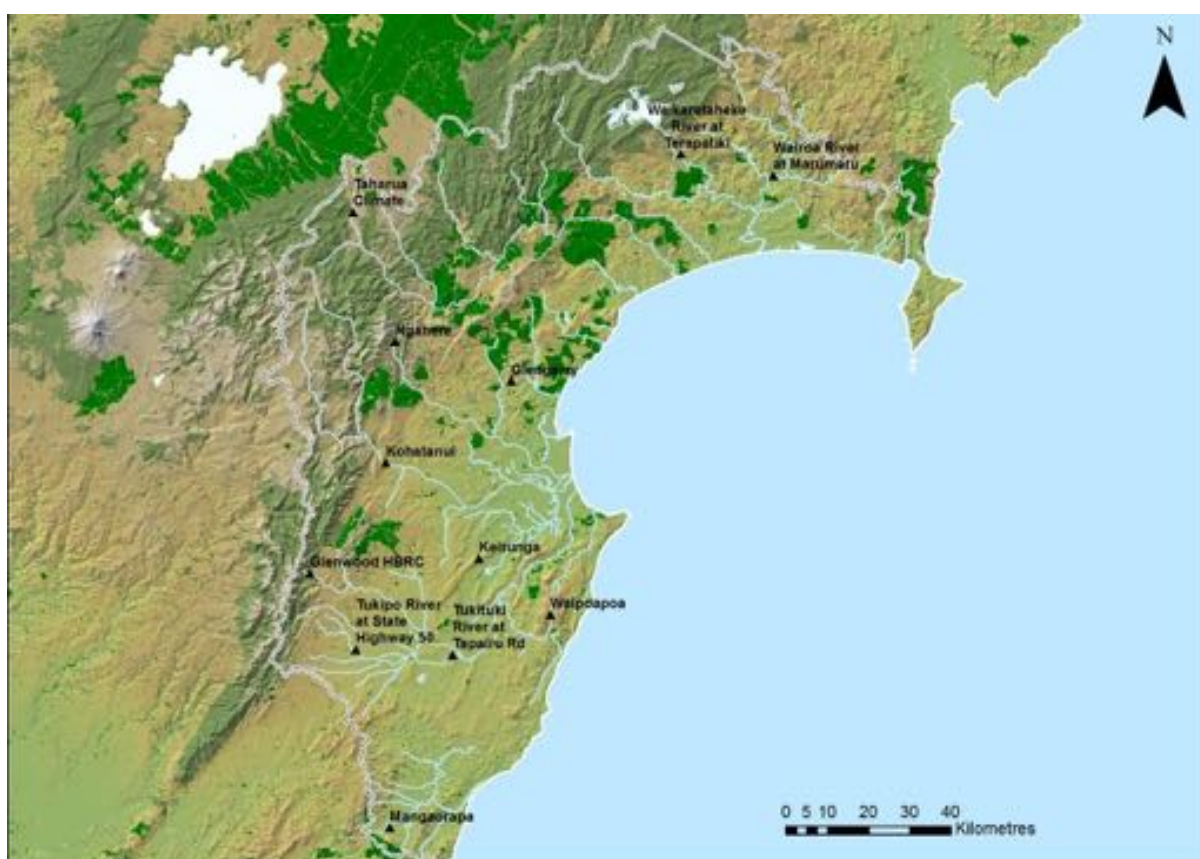


Figure 5-16: Selected sites in the Hawke's Bay region for location specific rainfall intensity projections.

Table 5-33: Modelled historical and projected rainfall depths (mm) for Waikaretaheke River at Terapatiki for different event durations with a 50-year return period (ARI) Source: HIRDS v4.

Rainfall event duration	Historical depth (mm)	Projected depth (mm)			
		Mid-century average (2031-2050)		Late-century average (2081-2100)	
		RCP4.5	RCP8.5	RCP4.5	RCP8.5
1-hour	38.9	42.7	43.3	45.2	52.4
6-hour	108	116	118	122	139
12-hour	154	166	167	173	194
24-hour	213	227	229	235	260
48-hour	280	296	298	305	334

Table 5-34: Modelled historical and projected rainfall depths (mm) for Waikaretaheke River at Terapatiki for different event durations with a 100-year return period (ARI) Source: HIRDS v4.

Rainfall event duration	Historical depth (mm)	Projected depth (mm)			
		Mid-century average (2031-2050)		Late-century average (2081-2100)	
		RCP4.5	RCP8.5	RCP4.5	RCP8.5
1-hour	44.3	48.8	49.4	51.6	59.9
6-hour	122	132	134	139	158
12-hour	175	188	190	196	221
24-hour	241	257	259	267	295
48-hour	317	334	337	345	378

Table 5-35: Modelled historical and projected rainfall depths (mm) for Wairoa River at Marumaru for different event durations with a 50-year return period (ARI) Source: HIRDS v4.

Rainfall event duration	Historical depth (mm)	Projected depth (mm)			
		Mid-century average (2031-2050)		Late-century average (2081-2100)	
		RCP4.5	RCP8.5	RCP4.5	RCP8.5
1-hour	40.8	44.8	45.4	47.4	55
6-hour	111	120	122	126	143
12-hour	157	168	170	175	197
24-hour	214	227	229	235	260
48-hour	281	297	299	306	335

Table 5-36: Modelled historical and projected rainfall depths (mm) for Wairoa River at Marumaru for different event durations with a 100-year return period (ARI) Source: HIRDS v4.

Rainfall event duration	Historical depth (mm)	Projected depth (mm)			
		Mid-century average (2031-2050)		Late-century average (2081-2100)	
		RCP4.5	RCP8.5	RCP4.5	RCP8.5
1-hour	46.8	51.5	52.2	54.5	63.2
6-hour	127	137	139	144	164
12-hour	178	191	193	200	224
24-hour	242	258	260	268	296
48-hour	318	336	338	347	380

Table 5-37: Modelled historical and projected rainfall depths (mm) for Taharua Climate for different event durations with a 50-year return period (ARI) Source: HIRDS v4.

Rainfall event duration	Historical depth (mm)	Projected depth (mm)			
		Mid-century average (2031-2050)		Late-century average (2081-2100)	
		RCP4.5	RCP8.5	RCP4.5	RCP8.5
1-hour	34.2	37.6	38.1	39.7	46.1
6-hour	105	114	115	119	136
12-hour	147	158	159	164	184
24-hour	194	206	208	214	236
48-hour	242	256	258	264	289

Table 5-38: Modelled historical and projected rainfall depths (mm) for Taharua Climate for different event durations with a 100-year return period (ARI) Source: HIRDS v4.

Rainfall event duration	Historical depth (mm)	Projected depth (mm)			
		Mid-century average (2031-2050)		Late-century average (2081-2100)	
		RCP4.5	RCP8.5	RCP4.5	RCP8.5
1-hour	39.1	43	43.6	45.5	52.8
6-hour	119	129	131	136	155
12-hour	166	178	180	186	209
24-hour	219	232	235	241	267
48-hour	272	287	289	297	325

Table 5-39: Modelled historical and projected rainfall depths (mm) for Ngahere for different event durations with a 50-year return period (ARI) Source: HIRDS v4.

Rainfall event duration	Historical depth (mm)	Projected depth (mm)			
		Mid-century average (2031-2050)		Late-century average (2081-2100)	
		RCP4.5	RCP8.5	RCP4.5	RCP8.5
1-hour	45.1	49.6	50.3	52.5	60.8
6-hour	127	138	139	144	164
12-hour	190	204	206	213	239
24-hour	280	298	300	309	341
48-hour	400	422	425	436	476

Table 5-40: Modelled historical and projected rainfall depths (mm) for Ngahere for different event durations with a 100-year return period (ARI) Source: HIRDS v4.

Rainfall event duration	Historical depth (mm)	Projected depth (mm)			
		Mid-century average (2031-2050)		Late-century average (2081-2100)	
		RCP4.5	RCP8.5	RCP4.5	RCP8.5
1-hour	51.8	57	57.8	60.3	70
6-hour	144	156	158	164	187
12-hour	215	231	233	241	270
24-hour	314	334	337	347	384
48-hour	446	471	474	486	532

Table 5-41: Modelled historical and projected rainfall depths (mm) for Glengarry for different event durations with a 50-year return period (ARI) Source: HIRDS v4.

Rainfall event duration	Historical depth (mm)	Projected depth (mm)			
		Mid-century average (2031-2050)		Late-century average (2081-2100)	
		RCP4.5	RCP8.5	RCP4.5	RCP8.5
1-hour	38.9	42.8	43.4	45.3	52.5
6-hour	109	118	119	123	140
12-hour	156	167	169	174	195
24-hour	217	230	232	239	264
48-hour	292	308	310	318	348

Table 5-42: Modelled historical and projected rainfall depths (mm) for Glengarry for different event durations with a 100-year return period (ARI) Source: HIRDS v4.

Rainfall event duration	Historical depth (mm)	Projected depth (mm)			
		Mid-century average (2031-2050)		Late-century average (2081-2100)	
		RCP4.5	RCP8.5	RCP4.5	RCP8.5
1-hour	44.7	49.2	49.9	52.1	60.4
6-hour	123	134	135	140	160
12-hour	176	189	191	198	222
24-hour	244	260	262	270	298
48-hour	327	346	348	357	391

Table 5-43: Modelled historical and projected rainfall depths (mm) for Kohatanui for different event durations with a 50-year return period (ARI) Source: HIRDS v4.

Rainfall event duration	Historical depth (mm)	Projected depth (mm)			
		Mid-century average (2031-2050)		Late-century average (2081-2100)	
		RCP4.5	RCP8.5	RCP4.5	RCP8.5
1-hour	48.4	53.2	53.9	56.3	65.2
6-hour	104	113	115	119	135
12-hour	137	147	149	153	172
24-hour	177	188	190	195	215
48-hour	225	238	239	245	268

Table 5-44: Modelled historical and projected rainfall depths (mm) for Kohatanui for different event durations with a 100-year return period (ARI) Source: HIRDS v4.

Rainfall event duration	Historical depth (mm)	Projected depth (mm)			
		Mid-century average (2031-2050)		Late-century average (2081-2100)	
		RCP4.5	RCP8.5	RCP4.5	RCP8.5
1-hour	55.8	61.4	62.3	65	75.4
6-hour	119	129	130	135	154
12-hour	155	166	168	174	195
24-hour	199	212	213	220	243
48-hour	252	265	268	274	300

Table 5-45: Modelled historical and projected rainfall depths (mm) for Keirunga for different event durations with a 50-year return period (ARI) Source: HIRDS v4.

Rainfall event duration	Historical depth (mm)	Projected depth (mm)			
		Mid-century average (2031-2050)		Late-century average (2081-2100)	
		RCP4.5	RCP8.5	RCP4.5	RCP8.5
1-hour	40.5	44.5	45.1	47.1	54.6
6-hour	88.9	96.4	97.5	101	115
12-hour	116	124	125	129	145
24-hour	146	155	157	161	178
48-hour	180	190	191	196	214

Table 5-46: Modelled historical and projected rainfall depths (mm) for Keirunga for different event durations with a 100-year return period (ARI) Source: HIRDS v4.

Rainfall event duration	Historical depth (mm)	Projected depth (mm)			
		Mid-century average (2031-2050)		Late-century average (2081-2100)	
		RCP4.5	RCP8.5	RCP4.5	RCP8.5
1-hour	46.6	51.2	51.9	54.2	62.9
6-hour	101	109	110	115	130
12-hour	130	140	141	146	164
24-hour	163	174	175	180	199
48-hour	199	210	212	218	238

Table 5-47: Modelled historical and projected rainfall depths (mm) for Glenwood for different event durations with a 50-year return period (ARI) Source: HIRDS v4.

Rainfall event duration	Historical depth (mm)	Projected depth (mm)			
		Mid-century average (2031-2050)		Late-century average (2081-2100)	
		RCP4.5	RCP8.5	RCP4.5	RCP8.5
1-hour	42.3	46.5	47.1	49.2	57
6-hour	114	124	125	130	148
12-hour	165	177	179	185	207
24-hour	231	246	248	255	281
48-hour	312	330	332	340	372

Table 5-48: Modelled historical and projected rainfall depths (mm) for Glenwood for different event durations with a 100-year return period (ARI) Source: HIRDS v4.

Rainfall event duration	Historical depth (mm)	Projected depth (mm)			
		Mid-century average (2031-2050)		Late-century average (2081-2100)	
		RCP4.5	RCP8.5	RCP4.5	RCP8.5
1-hour	48.8	53.7	54.5	56.9	66
6-hour	129	140	142	147	168
12-hour	185	199	201	208	233
24-hour	258	274	277	285	315
48-hour	345	365	367	377	412

Table 5-49: Modelled historical and projected rainfall depths (mm) for Tukipo River at SH 50 for different event durations with a 50-year return period (ARI) Source: HIRDS v4.

Rainfall event duration	Historical depth (mm)	Projected depth (mm)			
		Mid-century average (2031-2050)		Late-century average (2081-2100)	
		RCP4.5	RCP8.5	RCP4.5	RCP8.5
1-hour	45.1	49.6	50.3	52.5	60.8
6-hour	93.1	101	102	106	120
12-hour	120	129	130	134	151
24-hour	153	162	164	168	186
48-hour	191	202	203	208	228

Table 5-50: Modelled historical and projected rainfall depths (mm) for Tukipo River at SH 50 for different event durations with a 100-year return period (ARI) Source: HIRDS v4.

Rainfall event duration	Historical depth (mm)	Projected depth (mm)			
		Mid-century average (2031-2050)		Late-century average (2081-2100)	
		RCP4.5	RCP8.5	RCP4.5	RCP8.5
1-hour	52.3	57.6	58.4	61	70.7
6-hour	106	115	116	120	137
12-hour	135	145	147	152	170
24-hour	171	181	183	188	208
48-hour	212	224	225	231	253

Table 5-51: Modelled historical and projected rainfall depths (mm) for Tukituki River at Tapairu Road for different event durations with a 50-year return period (ARI) Source: HIRDS v4.

Rainfall event duration	Historical depth (mm)	Projected depth (mm)			
		Mid-century average (2031-2050)		Late-century average (2081-2100)	
		RCP4.5	RCP8.5	RCP4.5	RCP8.5
1-hour	39.6	43.6	44.2	46.1	53.5
6-hour	80.8	87.6	88.6	91.9	104
12-hour	103	111	112	116	130
24-hour	130	138	139	143	158
48-hour	160	169	170	174	190

Table 5-52: Modelled historical and projected rainfall depths (mm) for Tukituki River at Tapairu Road for different event durations with a 100-year return period (ARI) Source: HIRDS v4.

Rainfall event duration	Historical depth (mm)	Projected depth (mm)			
		Mid-century average (2031-2050)		Late-century average (2081-2100)	
		RCP4.5	RCP8.5	RCP4.5	RCP8.5
1-hour	45.9	50.5	51.2	53.4	62
6-hour	91.6	99.4	101	104	119
12-hour	116	125	126	130	146
24-hour	145	154	155	160	177
48-hour	177	187	188	193	211

Table 5-53: Modelled historical and projected rainfall depths (mm) for Mangaorapa for different event durations with a 50-year return period (ARI) Source: HIRDS v4.

Rainfall event duration	Historical depth (mm)	Projected depth (mm)			
		Mid-century average (2031-2050)		Late-century average (2081-2100)	
		RCP4.5	RCP8.5	RCP4.5	RCP8.5
1-hour	41.9	46.1	46.8	48.8	56.6
6-hour	95.5	103	105	109	123
12-hour	126	135	136	141	158
24-hour	162	172	173	178	197
48-hour	203	214	215	221	241

Table 5-54: Modelled historical and projected rainfall depths (mm) for Mangaorapa for different event durations with a 100-year return period (ARI) Source: HIRDS v4.

Rainfall event duration	Historical depth (mm)	Projected depth (mm)			
		Mid-century average (2031-2050)		Late-century average (2081-2100)	
		RCP4.5	RCP8.5	RCP4.5	RCP8.5
1-hour	48.8	53.7	54.4	56.8	65.9
6-hour	109	118	119	124	141
12-hour	142	153	154	159	179
24-hour	181	192	194	200	221
48-hour	225	238	239	246	269

5.3 Maximum 1-day rainfall

The annual maximum 1-day rainfall (otherwise known as Rx1day) is calculated as the wettest day of each year, which is then averaged over the 20-year period (e.g., 1986-2005 for the historic period and 2031-2050 and 2081-2100 for the future projections). Historic Rx1day maps are in units of mm per year (average over 1986-2005) and future (average over 2031-2050 and 2081-2100) maps show the change in the average future value of maximum 1-day rainfall compared with the historic value (units of mm). Note that the historic maps are on a different colour scale to the future projection maps. Table 5-55 and Table 5-56 list site specific projections for the Rx1day amount under the same RCP scenarios and for the same future time periods (locations shown in Figure 5-15 and Figure 5-16).

For the modelled historic period, the annual average Rx1day in Tairāwhiti is higher for coastal locations in the northern portion of Tairāwhiti, as well as locations over or west of the Raukumara Range. Notably high values (150-250 mm) are modelled for the northeast of the region. The lowest values in Tairāwhiti (mostly 50-100 mm) are located over the Waipaoa and neighbouring catchments in the southern portion of the region. In Hawke's Bay, the annual average Rx1day is generally in the 50-100 mm range (similar to southern Tairāwhiti) although some locations have values of 0-50 mm or 100-150 mm.

Representative concentration pathway (RCP) 4.5

By 2040, the pattern of change to the annual maximum 1-day rainfall is \pm 0-5 mm for much of both regions. For Hawke's Bay, there is an increasing signal for the east (0-5 mm), with decreasing values for the west (0-5 mm). Larger decreases of 5-10 mm are projected for a few western extremes in both regions, but these are relatively limited spatially. Relatively large increases of 5-15 mm are projected for a few locations, including the Waikura catchment at the northwestern end of the Raukumara Range and the Mangapoike subcatchment which lies at the boundary between both Tairāwhiti and Hawke's Bay.

By 2090, increases to the annual maximum 1-day rainfall amount are projected for the majority of both regions, with fewer locations projected to experience decreases (nearly all decreases are in the 0-5 mm range). Compared to the projections for 2040 (same RCP), a much larger portion of northern Tairāwhiti is projected to experience increases of more than 5 mm to the Rx1day amount. The northern end of the Raukumara Range continues to see the greatest projected increases for the two regions, with some locations (e.g. Waikura catchment) in this area increasing by >20 mm.

Representative concentration pathway (RCP) 8.5

By 2040, the annual maximum 1-day rainfall is projected to increase for most of Tairāwhiti and Hawke's Bay, although there are a few locations projected to decrease by 0-5 mm. For many locations, increases to the Rx1day are in the 0-10 mm range. The highest projected increases are situated over or just west of the Raukumara Range, exceeding 20 mm in some locations.

By 2090, the projected pattern of change is that of widespread increases to the annual maximum 1-day rainfall amount. Large increases exceeding 10 mm are projected for northern Tairāwhiti and over or just west of the mountain ranges that separate the two regions from Bay of Plenty (>20 mm increases in some locations). Similar large increases are also projected for the Mangapoike subcatchment (between the Tairāwhiti and Hawke's Bay regions).

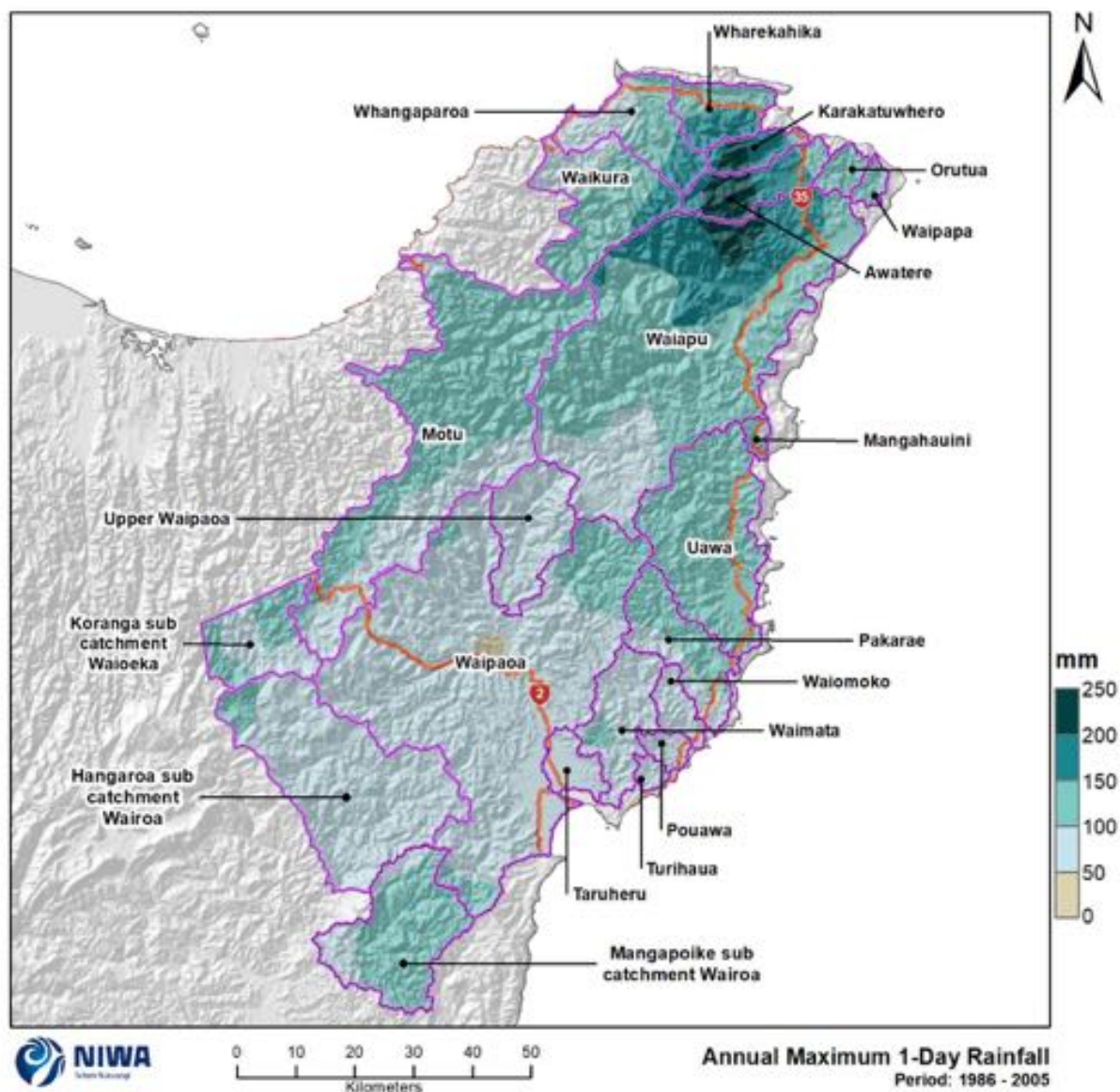


Figure 5-17: Modelled annual maximum daily rainfall (Rx1day) for Tairāwhiti, average over 1986-2005. Results are based on dynamical downscaled projections using NIWA's Regional Climate Model. Resolution of projection is 5km x 5km.

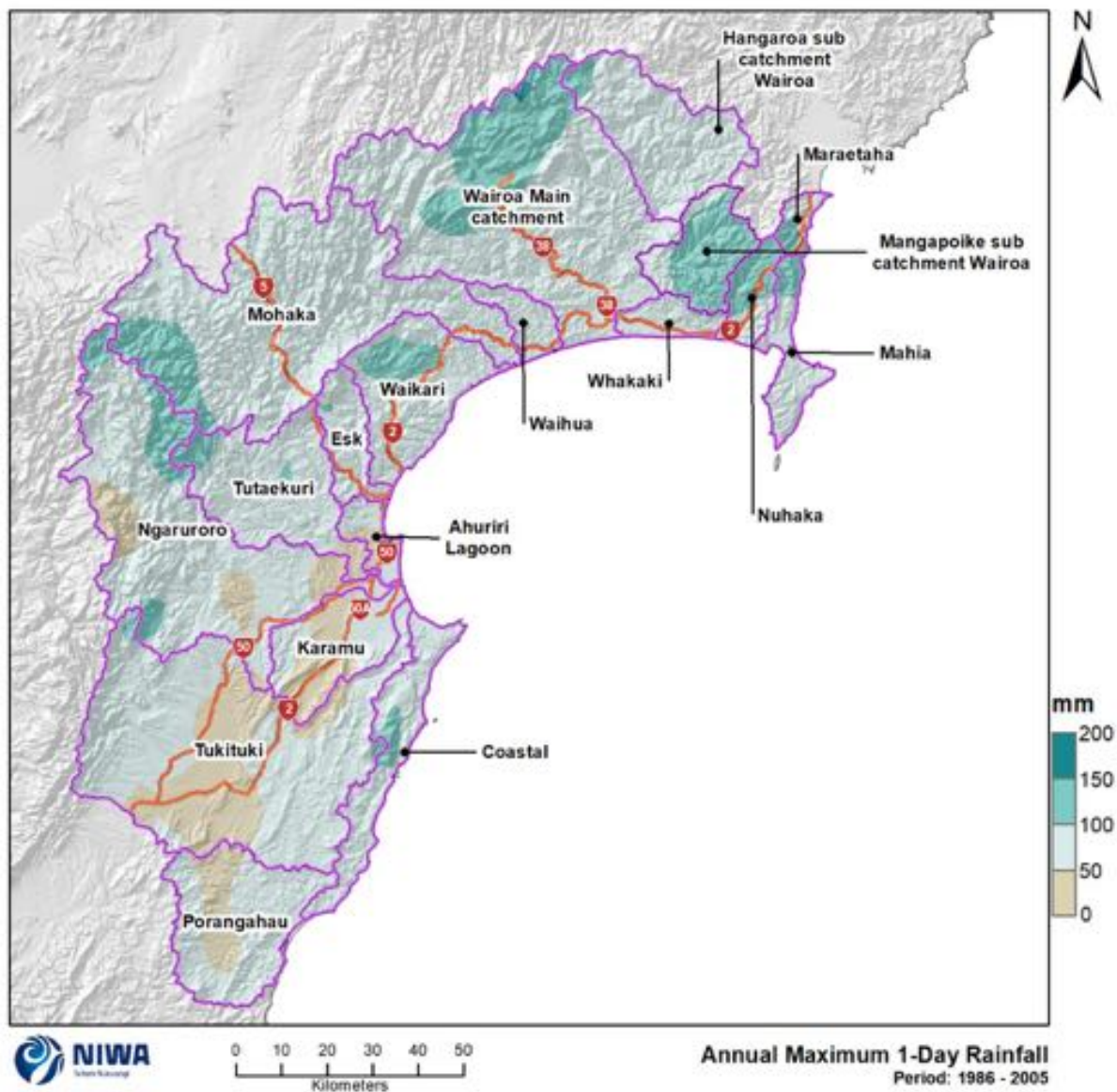


Figure 5-18: Modelled annual maximum daily rainfall (Rx1day) for Hawke's Bay region, average over 1986-2005 . Results are based on dynamical downscaled projections using NIWA's Regional Climate Model. Resolution of projection is 5km x 5km.

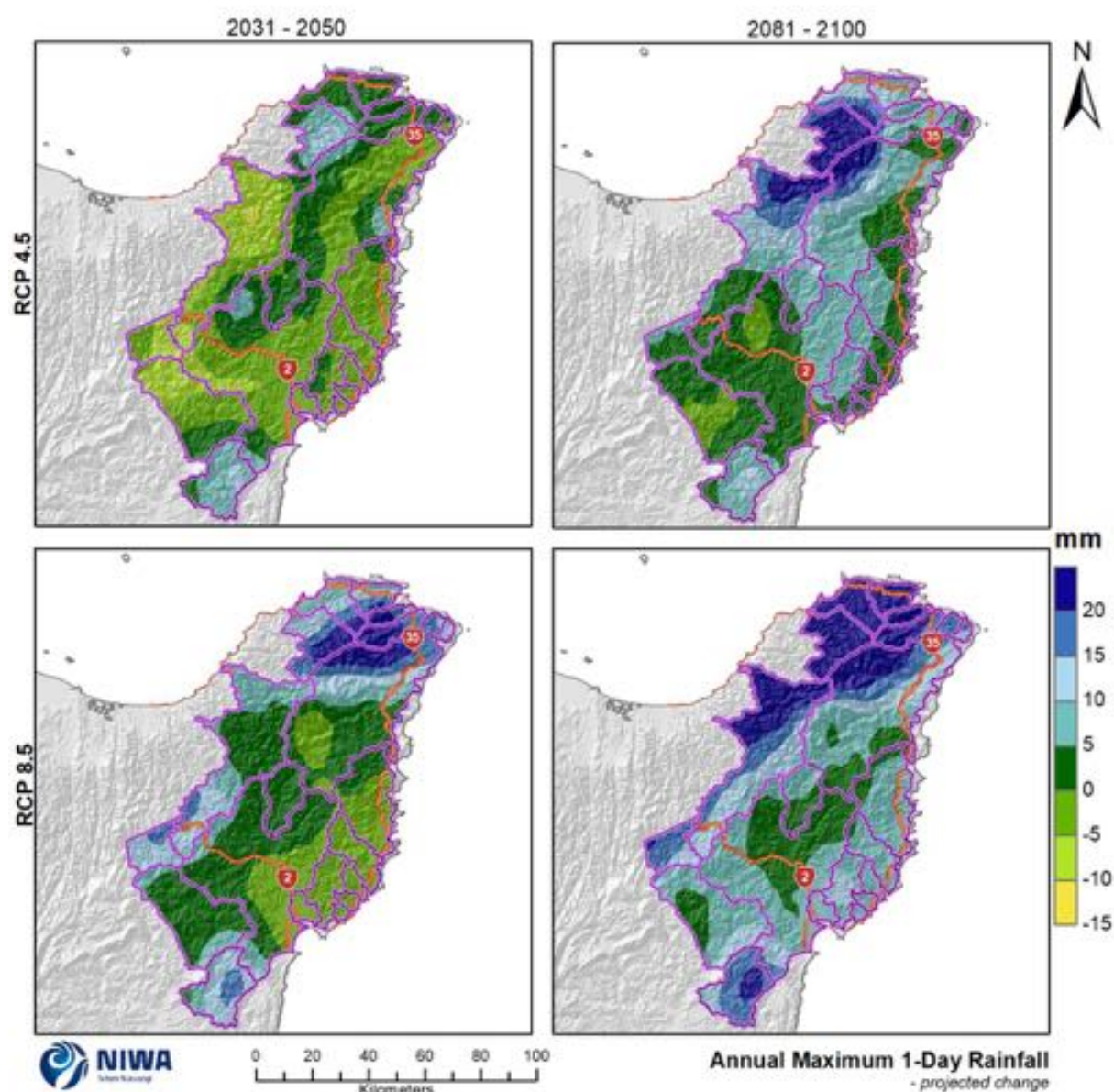


Figure 5-19: Projected annual maximum daily rainfall (Rx1day) changes for Tairāwhiti by 2040 and 2090 under RCP4.5 and RCP8.5. Relative to 1986-2005 average, based on the average of six global climate models. Results are based on dynamical downscaled projections using NIWA's Regional Climate Model. Resolution of projection is 5km x 5km.

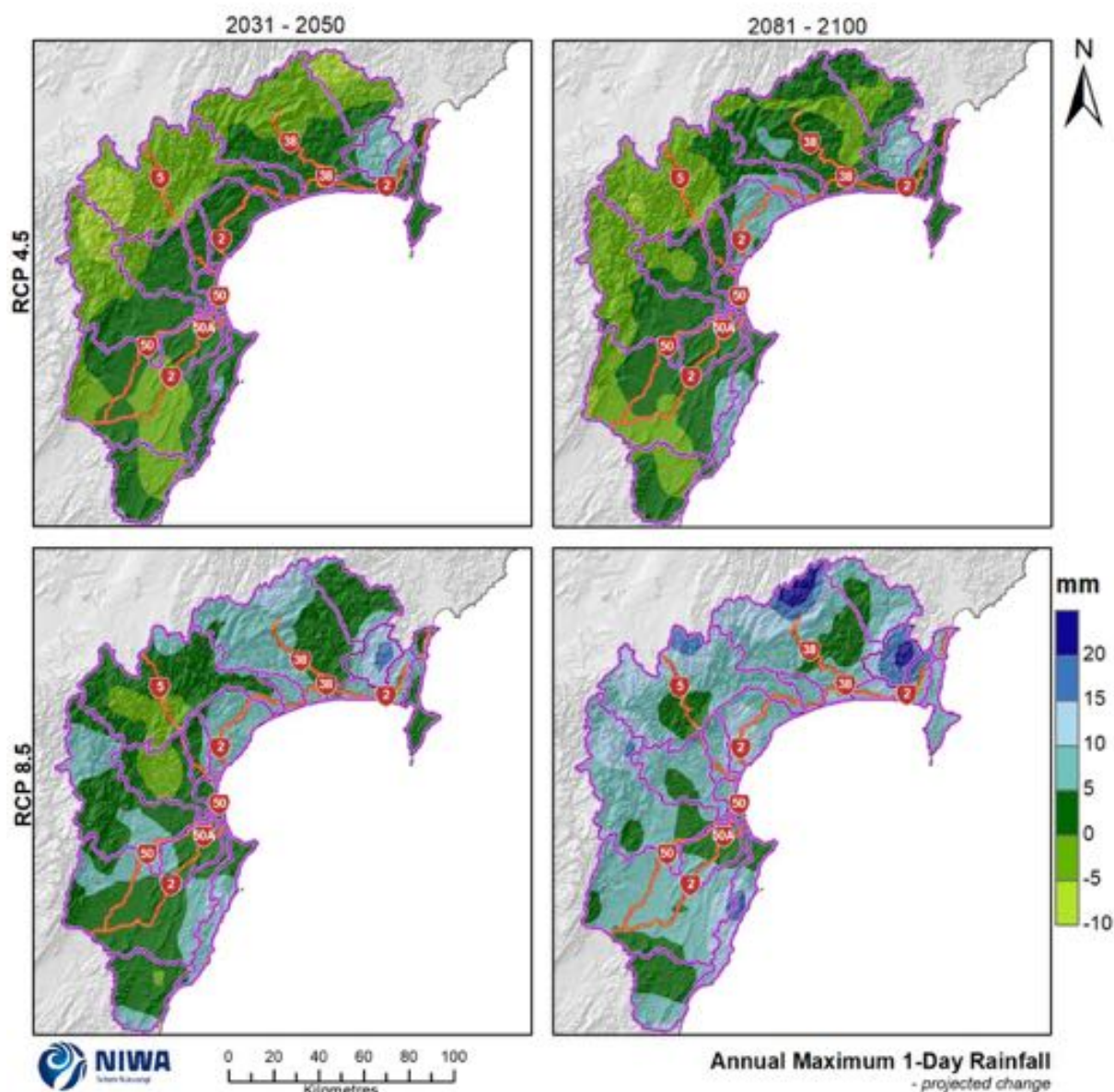


Figure 5-20: Projected annual maximum daily rainfall (Rx1day) changes for Hawke's Bay by 2040 and 2090 under RCP4.5 and RCP8.5. Relative to 1986-2005 average, based on the average of six global climate models. Results are based on dynamical downscaled projections using NIWA's Regional Climate Model. Resolution of projection is 5km x 5km.

Table 5-55: Modelled annual maximum daily rainfall (mm) for selected sites in Tairāwhiti. Future projections are shown as the total future projected maximum daily rainfall amount (mm) outside the parentheses, and future change inside the parentheses. Refer to Figure 5-15 for site locations.

Location	RCP	Mid-century average (2031-2050) (mm)	Late-century average (2081-2100) (mm)
East Cape at Lighthouse	RCP4.5	121.7 (+0.5)	125.2 (+4.0)
	RCP8.5	134.3 (+13.1)	137.1 (+15.9)
Hikuwai River at Willowflat	RCP4.5	104.8 (-2.1)	110.7 (+3.8)
	RCP8.5	104.9 (-2.0)	114.2 (+7.3)
Matawai Telemetry Station	RCP4.5	79.9 (-1.8)	84.2 (+2.6)
	RCP8.5	89.1 (+7.5)	89.8 (+8.2)
Puketoro Telemetry Station	RCP4.5	123.3 (+0.2)	134.7 (+11.6)
	RCP8.5	125.1 (+2.0)	131.6 (+8.5)
Ruatoria Telemetry Stn at Barry Ave	RCP4.5	126.4 (-1.4)	133.9 (+6.1)
	RCP8.5	137.7 (+9.9)	140.2 (+12.3)
Te Arai River at Pykes Weir	RCP4.5	80.3 (+2.5)	79.7 (+2.0)
	RCP8.5	82.5 (+4.7)	88.6 (+10.9)
Te Rata Telemetry Station	RCP4.5	94.2 (+0.4)	104.7 (+10.9)
	RCP8.5	96.1 (+2.3)	101.1 (+7.3)
Waikura Valley	RCP4.5	181.0 (+3.1)	190.1 (+12.2)
	RCP8.5	196.8 (+18.9)	206.7 (+28.8)
Waipaoa River at Kanakanaia	RCP4.5	53.5 (-1.5)	59.9 (+4.9)
	RCP8.5	54.3 (-0.7)	59.1 (+4.1)
Wharekopae School	RCP4.5	69.2 (-6.4)	77.1 (+1.5)
	RCP8.5	78.2 (+2.6)	82.1 (+6.5)
Tutamoe Station Telemetry Station	RCP4.5	97.5 (-0.3)	106.3 (+8.6)
	RCP8.5	97.4 (-0.3)	99.9 (+2.1)
Cameron Rd No.1 Bore GPB099	RCP4.5	76.9 (-0.4)	82.3 (+4.9)
	RCP8.5	74.7 (-2.7)	85.3 (+8.0)
Panikau Rd - Reed Rd	RCP4.5	98.5 (-2.2)	105.0 (+4.3)
	RCP8.5	98.1 (-2.6)	107.0 (+6.3)
Te Puia	RCP4.5	142.6 (+4.3)	139.5 (+1.2)
	RCP8.5	140.2 (+1.9)	143.1 (+4.8)
Mangapoike at Reservoir	RCP4.5	140.5 (+9.0)	139.7 (+8.3)
	RCP8.5	144.3 (+12.8)	150.2 (+18.7)
Caesar Rd No1 Bore GPG058	RCP4.5	78.9 (-0.9)	85.1 (+5.4)
	RCP8.5	77.1 (-2.7)	88.0 (+8.2)

Table 5-56: Modelled annual maximum daily rainfall (mm) for selected sites in Hawke's Bay. Future projections are shown as the total future projected maximum daily rainfall amount (mm) outside the parentheses, and future change inside the parentheses. Refer to Figure 5-16 for site locations.

Location	RCP	Mid-century average (2031-2050) (mm)	Late-century average (2081-2100) (mm)
Glengarry	RCP4.5	81.0 (+2.3)	80.0 (+1.3)
	RCP8.5	80.2 (+1.5)	85.6 (+6.9)
Glenwood HBRC	RCP4.5	77.9 (-1.4)	76.7 (-2.6)
	RCP8.5	84.9 (+5.6)	87.5 (+8.2)
Keirunga	RCP4.5	45.8 (+0.3)	48.5 (+3.0)
	RCP8.5	50.9 (+5.4)	52.5 (+7.0)
Kohatanui	RCP4.5	66.9 (+2.4)	65.7 (+1.2)
	RCP8.5	69.8 (+5.3)	69.6 (+5.1)
Mangaorapa	RCP4.5	55.3 (+4.2)	52.9 (+1.8)
	RCP8.5	57.2 (+6.1)	59.8 (+8.7)
Ngahere	RCP4.5	106.5 (-3.3)	109.3 (-0.5)
	RCP8.5	112.4 (+2.6)	122.1 (+12.3)
Taharua Climate	RCP4.5	86.2 (-6.3)	89.1 (-3.5)
	RCP8.5	93.2 (+0.7)	104.1 (+11.5)
Tukipo River at State Highway 50	RCP4.5	52.4 (+0.5)	51.5 (-0.3)
	RCP8.5	55.2 (+3.3)	57.7 (+5.8)
Tukituki River at Tapairu Rd	RCP4.5	52.6 (-3.2)	56.0 (+0.3)
	RCP8.5	57.9 (+2.1)	61.4 (+5.6)
Waikaretaheke River at Terapatiki	RCP4.5	79.8 (-0.6)	83.7 (+3.3)
	RCP8.5	86.6 (+6.2)	85.8 (+5.4)
Waipoapoa	RCP4.5	113.8 (+5.5)	119.4 (+11.1)
	RCP8.5	121.7 (+13.4)	126.8 (+18.4)
Wairoa River at Marumaru	RCP4.5	82.6 (+2.0)	79.7 (-0.9)
	RCP8.5	81.3 (+0.7)	84.9 (+4.3)

5.4 Maximum 5-day rainfall

The annual maximum 5-day rainfall (otherwise known as Rx5day) is calculated as the wettest 5-day period of each year, which is then averaged over the 20-year period (e.g., 1986-2005 for the historic period and 2031-2050 and 2081-2100 for the future projections). Historic Rx5day maps are in units of mm per year (average over 1986-2005) and future (average over 2031-2050 and 2081-2100) maps show the change in 5-day rainfall compared with the historic total (units of mm). Note that the historic maps are on a different colour scale to the future projection maps. Table 5-57 and Table 5-58 list site specific projections for the Rx5day amount under the same RCP scenarios and for the same future time periods (locations shown in Figure 5-15 and Figure 5-16).

For the historic period, the highest annual Rx5day values are located to the north of Tairāwhiti (>200 mm) with values of less than 200 mm for locations south of there, including most of the Hawke's Bay Region (Figure 5-21 and Figure 5-22). The lowest Rx5day totals (<100 mm) are modelled for part of the Waipaoa catchment, and for southeastern parts of Hawke's Bay.

Representative concentration pathway (RCP) 4.5

By 2040, decreases to the Rx5day value are projected for many eastern/coastal parts of Tairāwhiti (0-10 mm), with larger projected decreases near East Cape (10-20 mm). Some inland parts of both regions are also projected to see decreases (generally 0-5 mm) however most remaining locations (which includes most of Hawke's Bay) are projected to increase. The largest increases (>20 mm) are projected for the area just inland from Mahia Peninsula, at the border between the two regions (i.e. centred over Mangapoike catchment) (Figure 5-23 and Figure 5-24).

By 2090, relatively large decreases to the Rx5day value remain projected for an eastern portion of Tairāwhiti (5-15 mm lower; near Waipiro Bay). In the Hawke's Bay region, parts of the Mohaka, Waikari, and nearby catchments (mid-Hawke Bay and inland) are also projected to see decreases in the 5-15 mm range. Conversely, large increases to the Rx5day value (10-20 mm) are projected for the western side of the Raukumara Range in Tairāwhiti, with increases of more than 20 mm projected for the northern portion of this area. The area just inland from Mahia Peninsula continues to see relatively large projected increases (5-20 mm), as does a small area just north of Poverty Bay. Most remaining locations (including most of Hawke's Bay) are however projected to increase or decrease by only 0-5 mm (Figure 5-23 and Figure 5-24).

Representative concentration pathway (RCP) 8.5

By 2040, most of eastern Tairāwhiti is projected to see decreases to the Rx5day amount (0-15 mm), although locations over or just west of the Raukumara and Huiarau ranges are projected to increase by large amounts (>20 mm in some parts of these ranges). Again, the area just inland from Mahia Peninsula is projected to see large increases to the Rx5day amount. Most of the Hawke's Bay region is projected to see increases. These increases generally exceed 5 mm along the coast and over or west of the mountain ranges (Figure 5-23 and Figure 5-24).

By 2090, locations over or just west of the Raukumara and Huiarau ranges remain projected to increase by large amounts (>20 mm in some parts) and similarly large increases are projected once again for several coastal parts of Hawke's Bay Region, including the area just inland from Mahia (i.e. at the border of both regions). Several locations east of the Raukumara Range are projected to experience decreases of 5-15 mm to the Rx5day value (Figure 5-23 and Figure 5-24). It is noted that decreases of this magnitude are among the largest decreases projected for this scenario/period

across the entire country (most other locations are actually projected to increase; see Figure 5-25 for national scale map).

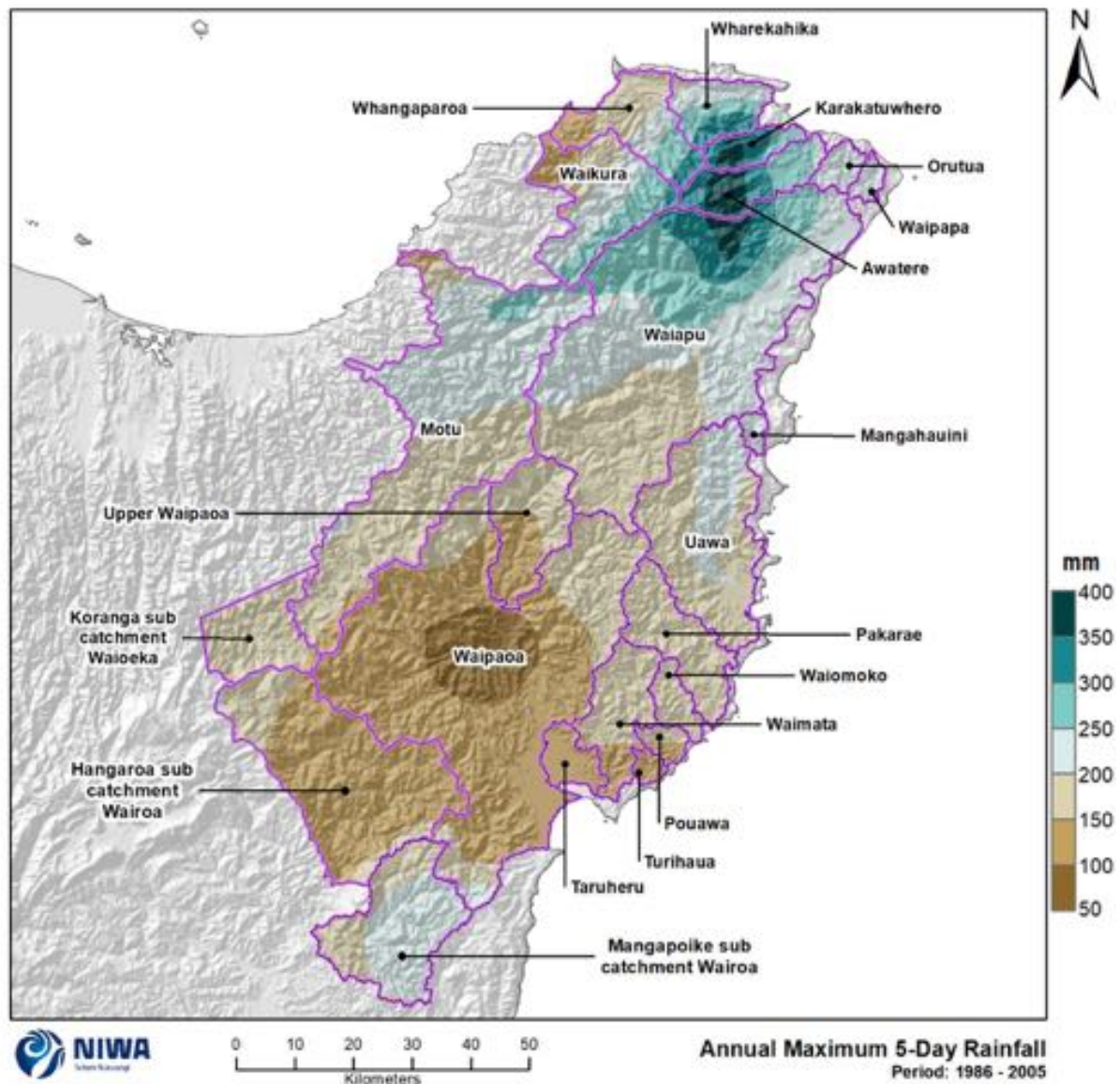


Figure 5-21: Modelled annual maximum 5-day rainfall (Rx5day) for Tairāwhiti, average over 1986-2005. Results are based on dynamical downscaled projections using NIWA's Regional Climate Model. Resolution of projection is 5km x 5km.

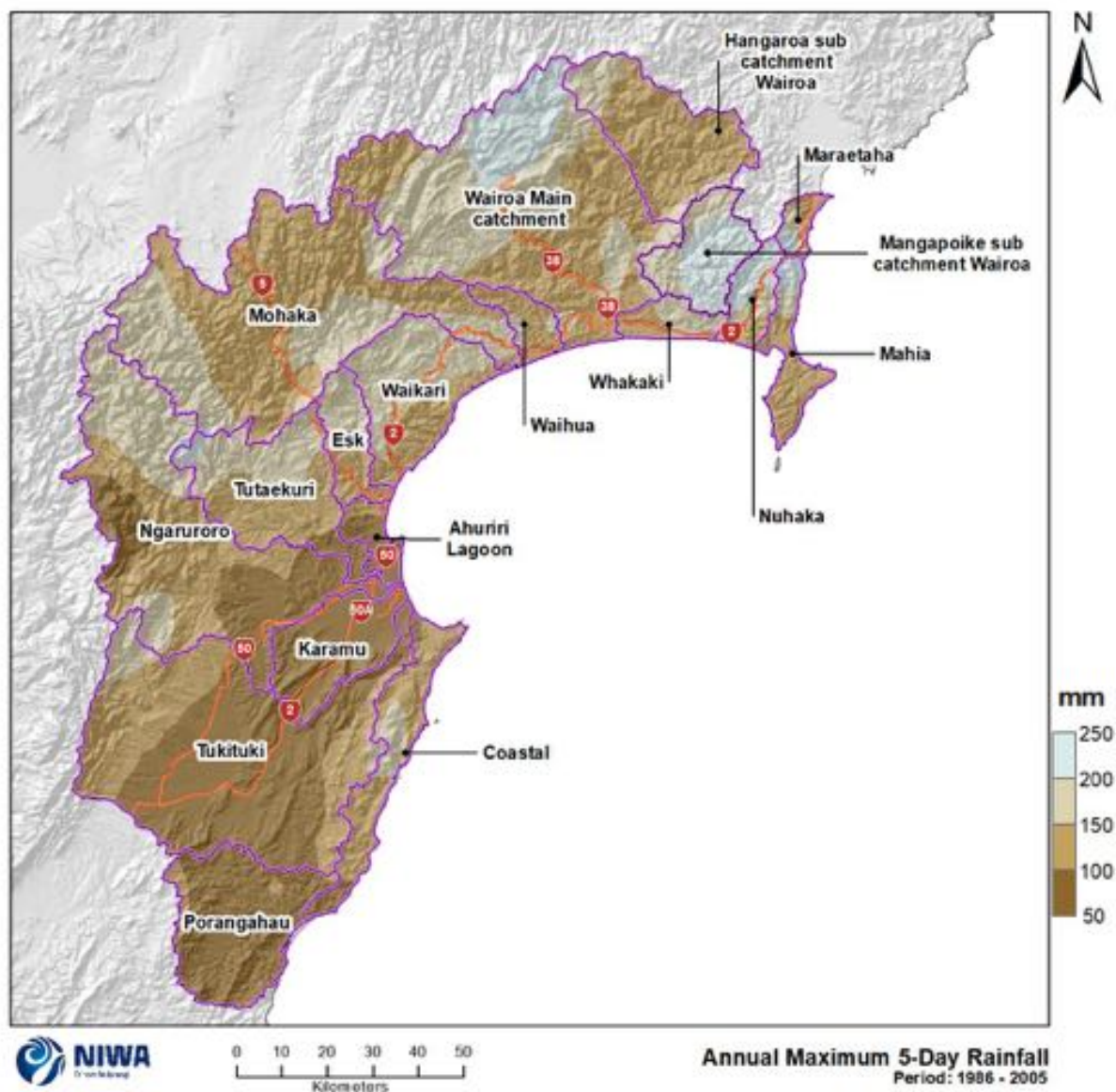


Figure 5-22: Modelled annual maximum 5-day rainfall (Rx5day) for Hawke's Bay region, average over 1986-2005 . Results are based on dynamical downscaled projections using NIWA's Regional Climate Model. Resolution of projection is 5km x 5km.

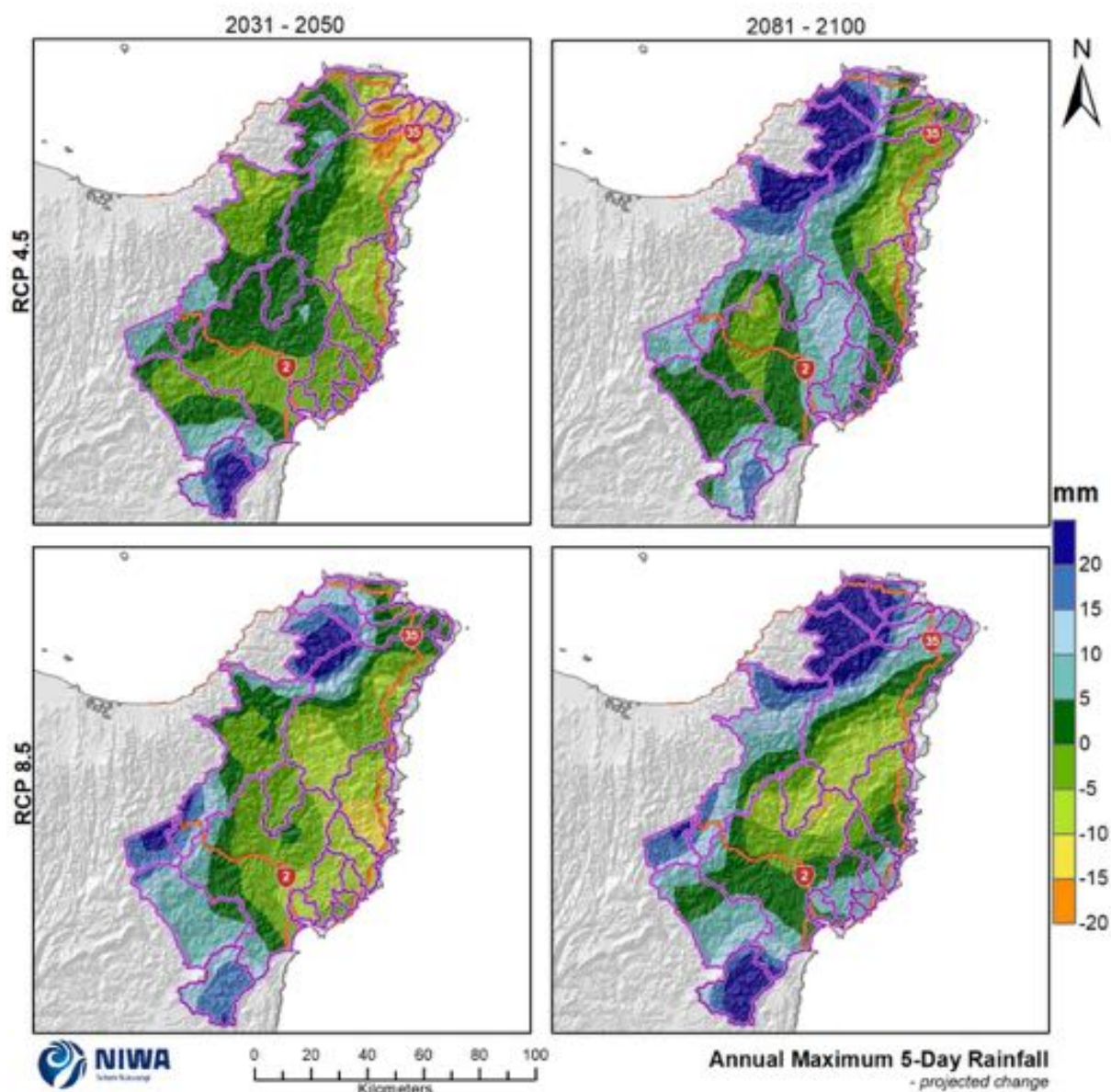


Figure 5-23: Projected annual maximum 5-day rainfall (Rx5day) changes for Tairāwhiti by 2040 and 2090 under RCP4.5 and RCP8.5. Relative to 1986-2005 average, based on the average of six global climate models. Results are based on dynamical downscaled projections using NIWA's Regional Climate Model. Resolution of projection is 5km x 5km.

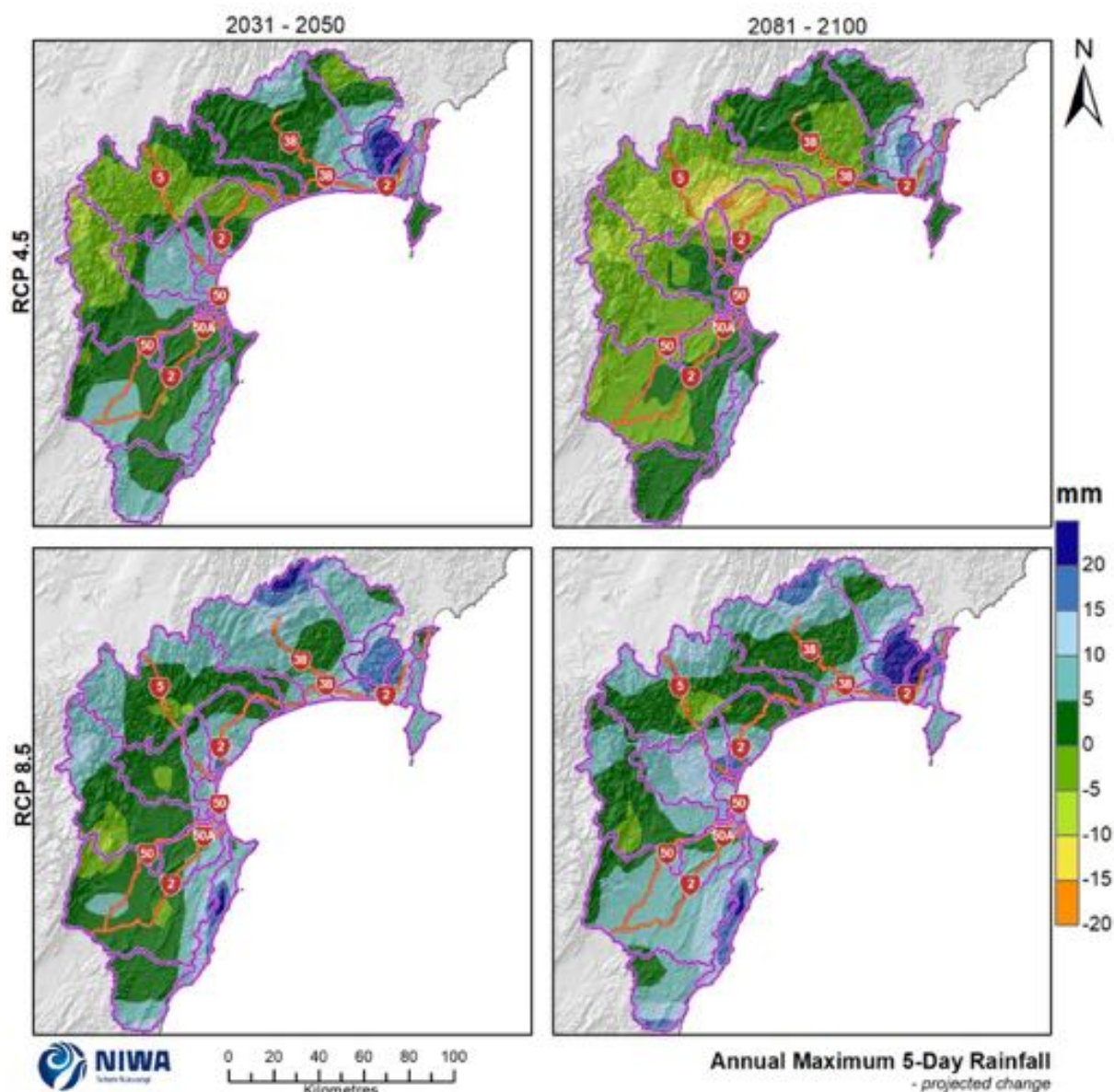


Figure 5-24: Projected annual maximum 5-day rainfall (Rx5day) changes for Hawke's Bay by 2040 and 2090 under RCP4.5 and RCP8.5. Relative to 1986-2005 average, based on the average of six global climate models. Results are based on dynamical downscaled projections using NIWA's Regional Climate Model. Resolution of projection is 5km x 5km.

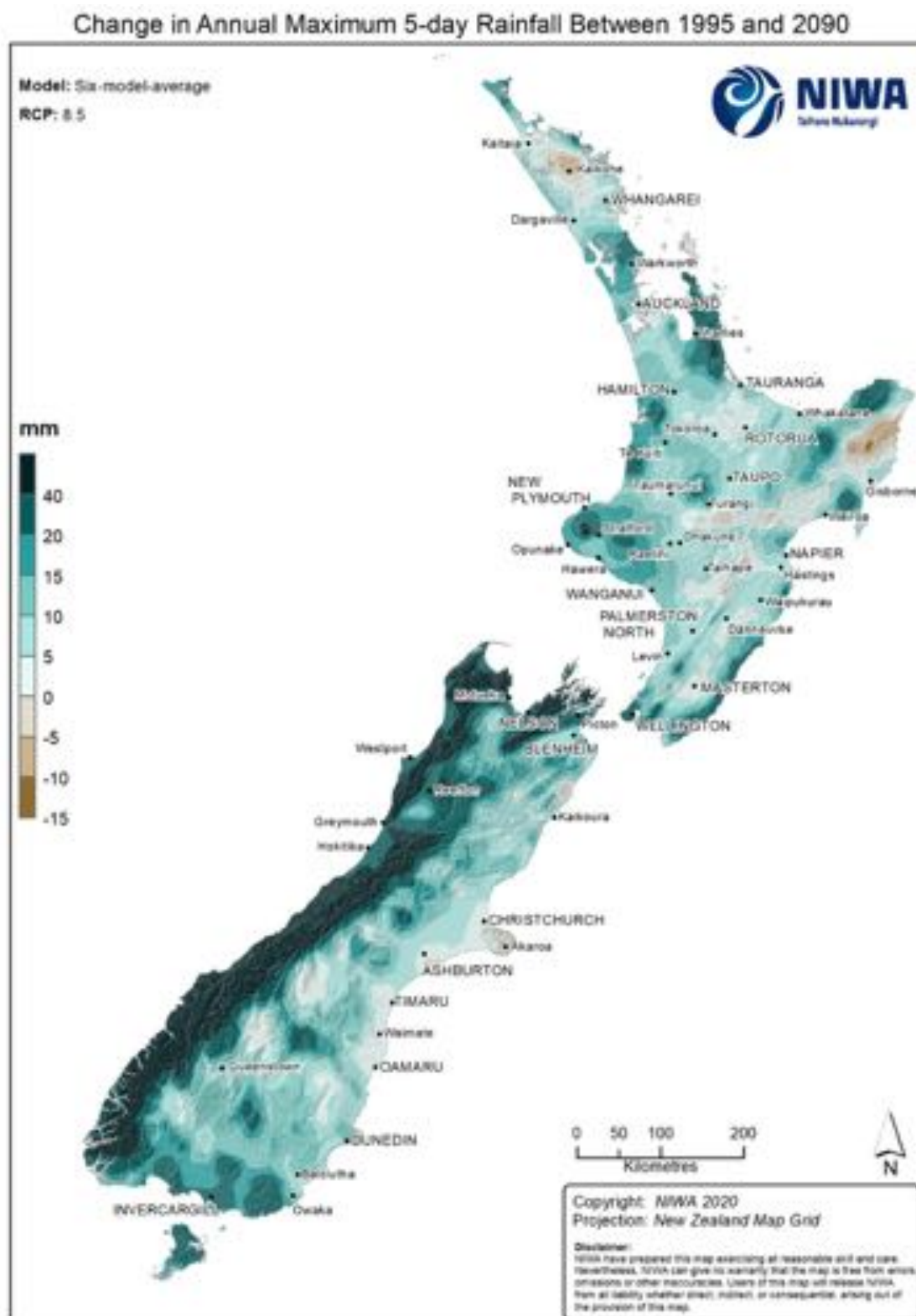


Figure 5-25: Projected annual maximum 5-day rainfall (Rx5day) changes for New Zealand by 2090 under RCP8.5. Relative to 1986-2005 average, based on the average of six global climate models. Results are based on dynamical downscaled projections using NIWA's Regional Climate Model. Resolution of projection is 5km x 5km.

Table 5-57: Modelled annual maximum 5-day rainfall (mm) for selected sites in Tairāwhiti. Future projections are shown as the total future projected maximum 5-day rainfall amount (mm) outside the parentheses, and future change (mm) inside the parentheses. Refer to Figure 5-15 for site locations.

Location	RCP	Mid-century average (2031-2050) (mm)	Late-century average (2081-2100) (mm)
East Cape at Lighthouse	RCP4.5	197.2 (-10.7)	206.7 (-1.3)
	RCP8.5	207.8 (-0.1)	216.0 (+8.0)
Hikawai River at Willowflat	RCP4.5	178.1 (-6.5)	182.3 (-2.3)
	RCP8.5	174.3 (-10.3)	185.2 (+0.6)
Matawai Telemetry Station	RCP4.5	149.6 (+2.9)	148.0 (+1.3)
	RCP8.5	155.6 (+8.9)	153.1 (+6.4)
Puketoro Telemetry Station	RCP4.5	217.8 (+2.4)	224.3 (+9.0)
	RCP8.5	215.2 (-0.2)	219.0 (+3.6)
Ruatoria Telemetry Stn at Barry Ave	RCP4.5	212.4 (-9.1)	218.2 (-3.3)
	RCP8.5	216.9 (-4.6)	223.4 (+1.9)
Te Arai River at Pykes Weir	RCP4.5	149.1 (+8.6)	147.8 (+7.3)
	RCP8.5	147.1 (+6.6)	152.8 (+12.3)
Te Rata Telemetry Station	RCP4.5	174.6 (+2.4)	180.0 (+7.7)
	RCP8.5	169.2 (-3.1)	169.1 (-3.1)
Waikura Valley	RCP4.5	306.8 (-7.9)	326.1 (+11.3)
	RCP8.5	322.9 (+8.2)	339.6 (+24.9)
Waipaoa River at Kanakanaia	RCP4.5	96.3 (-0.2)	100.8 (+4.4)
	RCP8.5	94.8 (-1.6)	95.9 (-0.6)
Wharekopae School	RCP4.5	130.1 (-1.1)	135.8 (+4.6)
	RCP8.5	141.4 (+10.3)	136.8 (+5.6)
Tutamoe Station Telemetry Station	RCP4.5	173.6 (-1.7)	181.9 (+6.6)
	RCP8.5	167.4 (-8.0)	165.3 (-10.1)
Cameron Rd No.1 Bore GPB099	RCP4.5	115.1 (-1.6)	124.0 (+7.2)
	RCP8.5	109.8 (-6.9)	121.9 (+5.2)
Panikau Rd - Reed Rd	RCP4.5	169.7 (-4.1)	177.1 (+3.3)
	RCP8.5	165.3 (-8.5)	177.2 (+3.4)
Te Puia	RCP4.5	214.3 (-5.2)	210.4 (-9.0)
	RCP8.5	214.7 (-4.7)	211.1 (-8.3)
Mangapoike at Reservoir	RCP4.5	253.6 (+23.6)	244.5 (+14.5)
	RCP8.5	246.0 (+16)	255.0 (+25)
Caesar Rd No1 Bore GPG058	RCP4.5	116.8 (-2.0)	125.7 (+6.9)
	RCP8.5	111.6 (-7.2)	123.9 (+5.1)

Table 5-58: Modelled annual maximum 5-day rainfall (mm) for selected sites in Hawke's Bay. Future projections are shown as the total future projected maximum 5-day rainfall amount (mm) outside the parentheses, and future change (mm) inside the parentheses. Refer to Figure 5-16 for site locations.

Location	RCP	Mid-century average (2031-2050) (mm)	Late-century average (2081-2100) (mm)
Glengarry	RCP4.5	144.8 (+8.3)	138.6 (+2.1)
	RCP8.5	142.2 (+5.7)	151.3 (+14.8)
Glenwood HBRC	RCP4.5	152.0 (+0.7)	145.7 (-5.6)
	RCP8.5	152.1 (+0.8)	156.2 (+4.9)
Keirunga	RCP4.5	86.1 (+3.0)	83.0 (+0.0)
	RCP8.5	87.6 (+4.6)	90.6 (+7.6)
Kohatanui	RCP4.5	119.2 (+1.3)	115.7 (-2.2)
	RCP8.5	116.4 (-1.5)	117.8 (-0.1)
Mangaorapa	RCP4.5	102.0 (+9.3)	96.0 (+3.4)
	RCP8.5	101.7 (+9.1)	107.6 (+14.9)
Ngahere	RCP4.5	205.3 (+0.0)	198.9 (-6.5)
	RCP8.5	209.0 (+3.6)	212.1 (+6.7)
Taharua Climate	RCP4.5	155.5 (-1.2)	153.0 (-3.7)
	RCP8.5	163.9 (+7.2)	163.6 (+6.9)
Tukipo River at State Highway 50	RCP4.5	94.1 (+6.8)	85.5 (-1.8)
	RCP8.5	91.7 (+4.4)	95.0 (+7.8)
Tukituki River at Tapairu Rd	RCP4.5	90.2 (+1.5)	88.2 (-0.6)
	RCP8.5	88.1 (-0.7)	97.0 (+8.2)
Waikaretaheke River at Terapatiki	RCP4.5	147.6 (+2.6)	145.1 (+0.0)
	RCP8.5	151.6 (+6.5)	145.2 (+0.2)
Waipoapoa	RCP4.5	190.1 (+8.3)	192.7 (+10.9)
	RCP8.5	202.2 (+20.4)	203.3 (+21.5)
Wairoa River at Marumaru	RCP4.5	158.5 (+8.4)	148.9 (-1.2)
	RCP8.5	154.4 (+4.3)	157.3 (+7.3)

5.5 Snow

At present, flurries of snow can be observed in both regions during winter months, and in cold, southerly conditions. These events are typically restricted to high country areas, and are rarely observed in populated locations (Chappell, 2013, Chappell, 2016). Modelled historic data shows very few locations that receive one day or more of snow per year on average, and these are restricted to high elevations in the Hawke's Bay region, with no locations reaching as high as five days. All locations with modelled historic snow days are projected to see even fewer snow days in the future. Changes in modelled snow amount require further analysis however model simulations generally suggest a reduction in this variable along with snow days (Ministry for the Environment, 2018).

6 Drought

6.1 Potential evapotranspiration deficit

One measure of meteorological drought¹² that is used in this section is 'potential evapotranspiration deficit' (PED). Evapotranspiration is the process where water held in the soil is gradually released to the atmosphere through a combination of direct evaporation and transpiration from plants. As the growing season advances, the amount of water lost from the soil through evapotranspiration typically exceeds rainfall, giving rise to an increase in soil moisture deficit. As soil moisture decreases, pasture production becomes moisture-constrained and evapotranspiration can no longer meet atmospheric demand.

The difference between this demand (evapotranspiration deficit) and the actual evapotranspiration is defined as the 'potential evapotranspiration deficit' (PED). In practice, PED represents the total amount of water required by irrigation, or that needs to be replenished by rainfall, to maintain plant growth at levels unconstrained by water shortage. As such, PED estimates provide a robust measure of drought intensity and duration. Days when water demand is not met, and pasture growth is reduced, are often referred to as days of potential evapotranspiration deficit.

PED is calculated as the difference between potential evapotranspiration (PET) and rainfall, for days of soil moisture under half of available water capacity (AWC), where an AWC of 150mm for silty-loamy soils is consistent with estimates in previous studies (e.g. Mullan et al., 2005). PED, in units of mm, can be thought of as the amount of missing rainfall needed in order to keep pastures growing at optimum levels. Higher PED totals indicate drier soils. An increase in PED of 30 mm or more corresponds to an extra week of reduced grass growth. Accumulations of PED greater than 300 mm indicate very dry conditions.

For the modelled historic period, the highest PED accumulation is experienced near Gisborne City, Napier and Hastings, as well as a few isolated coastal parts of Hawke's Bay (300-400 mm). Remaining coastal areas generally experience 200-300 mm of PED per year with the exception of the Mangapoike sub catchment (just inland from Mahia) which has relatively low accumulated PED for the modelled historic period (0-100 mm). PED declines inland at higher elevations, with most mountainous locations experiencing 0-100 mm of PED per year (Figure 6-1 and Figure 6-2).

For all future scenarios, annual PED accumulation is projected to increase across the entirety of both regions (Figure 6-3 and Figure 6-4).

Representative concentration pathway (RCP) 4.5

By 2040, annual PED accumulation is projected to increase most notably for eastern parts of Tairāwhiti and some southern parts of Hawke's Bay (+100-150 mm). Smaller increases are generally projected to the west, with higher elevations increasing by 25-75 mm (Figure 6-3 and Figure 6-4).

By 2090, the pattern of change is almost identical to that at 2040 (under the same RCP), except that more locations are projected to increase by 100-150 mm (rather than 75-100 mm as projected for 2040) (Figure 6-3 and Figure 6-4).

¹² Meteorological drought happens when dry weather patterns dominate an area and resulting rainfall is low. Hydrological drought occurs when low water supply becomes evident, especially in streams, reservoirs, and groundwater levels, usually after an extended period of meteorological drought.

Representative concentration pathway (RCP) 8.5

By 2040, the pattern of change is almost identical to that under RCP4.5 (for the same future period), with the largest increases projected for eastern parts of Tairāwhiti and some southern parts of Hawke's Bay (+100-150 mm), and smaller increases generally projected for higher elevation locations in the west (Figure 6-3 and Figure 6-4).

By 2090, the projected increases to annual PED accumulation are much greater than for the other scenarios. Much of eastern Tairāwhiti is projected to increase by 150-200 mm, with the largest projected increases of 200-250 mm located inland from Poverty Bay. Again, the lowest increases for Tairāwhiti are for western, high elevation locations, generally ranging from 50-100 mm, and even up to 150 mm in some locations. The majority of the Hawke's Bay Region is projected to experience increases between 100 and 200 mm (Figure 6-3 and Figure 6-4).

It is noted that the projected increases to PED accumulation for eastern Tairāwhiti are among the largest projected increases for New Zealand (Figure 6-5).

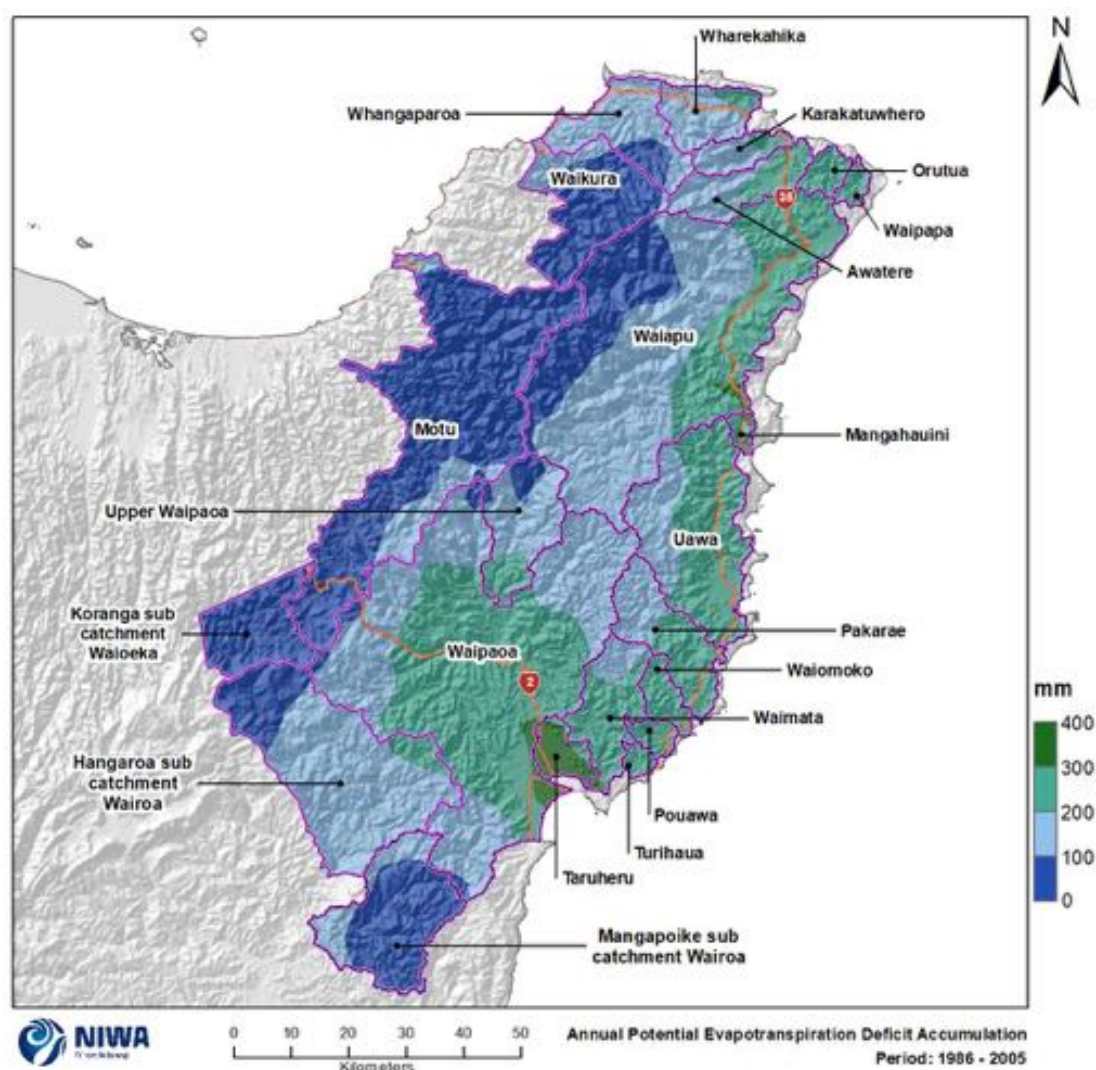


Figure 6-1: Modelled annual potential evapotranspiration deficit accumulation (mm) for Tairāwhiti, average over 1986-2005. Results are based on dynamical downscaled projections using NIWA's Regional Climate Model. Resolution of projection is 5km x 5km.

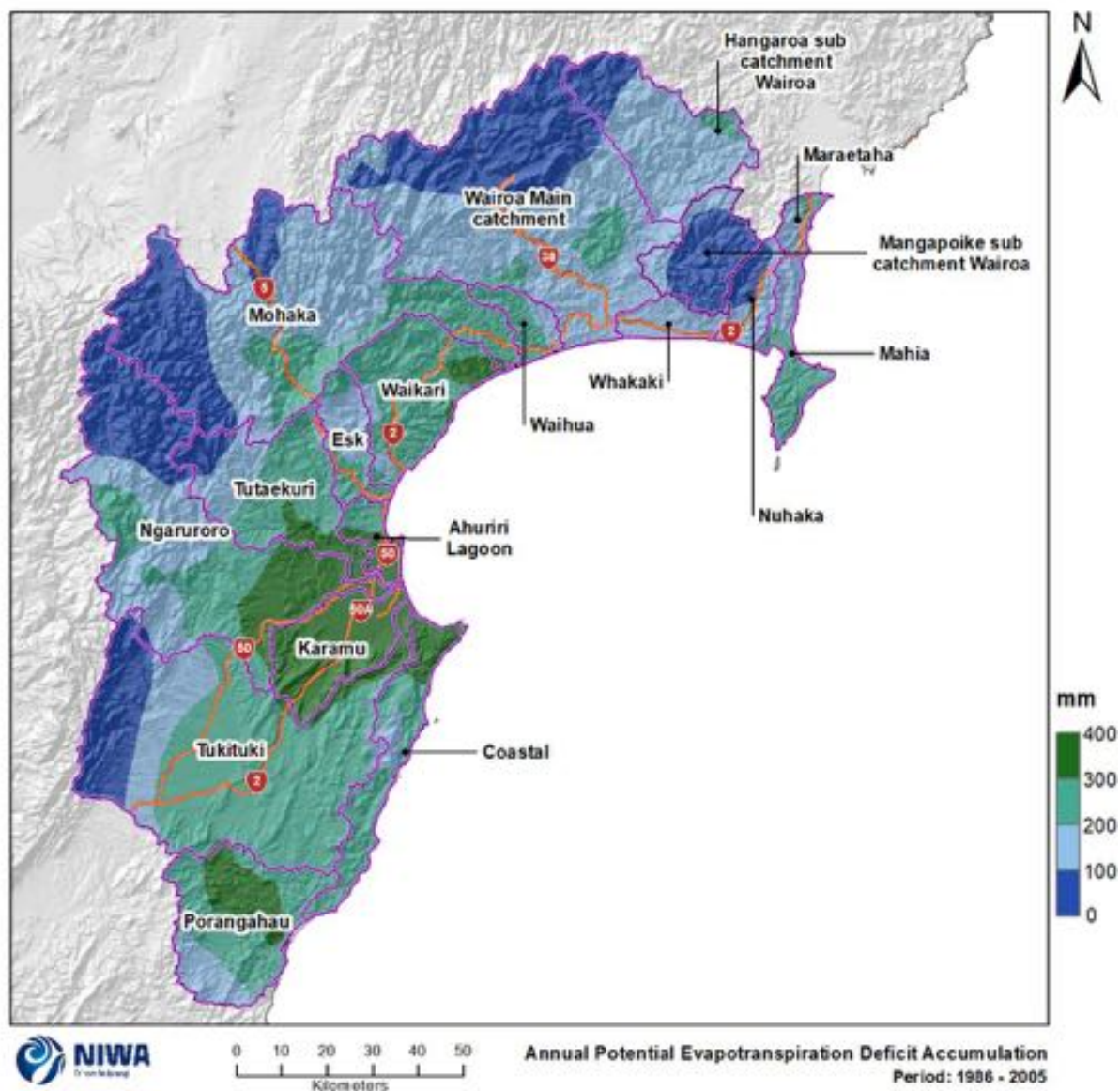


Figure 6-2: Modelled annual potential evapotranspiration deficit accumulation (mm) for Hawke's Bay region, average over 1986-2005 . Results are based on dynamical downscaled projections using NIWA's Regional Climate Model. Resolution of projection is 5km x 5km.

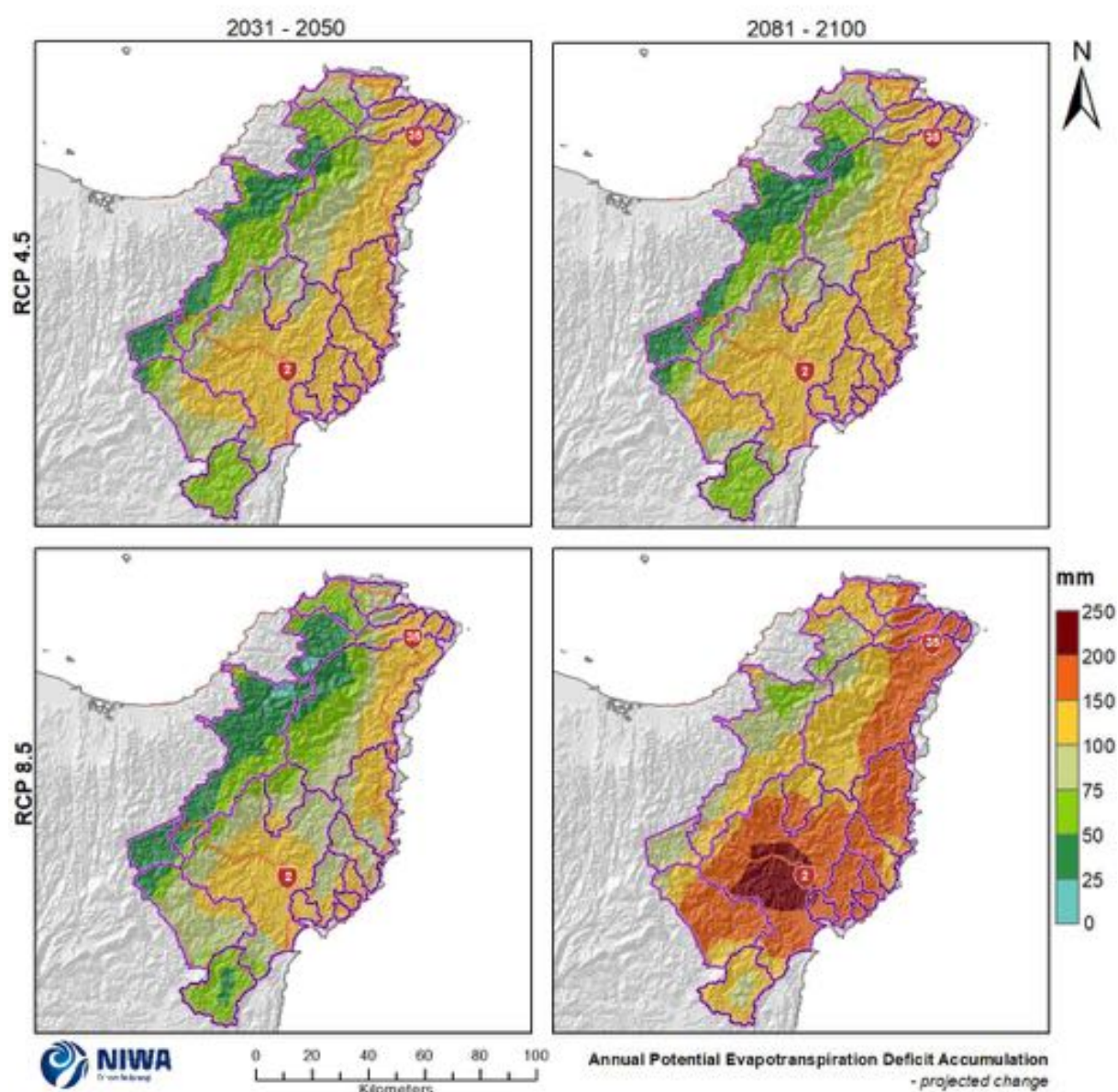


Figure 6-3: Projected annual potential evapotranspiration deficit accumulation (mm) changes for Tairāwhiti by 2040 and 2090 under RCP4.5 and RCP8.5. Relative to 1986-2005 average, based on the average of six global climate models. Results are based on dynamical downscaled projections using NIWA's Regional Climate Model. Resolution of projection is 5km x 5km.

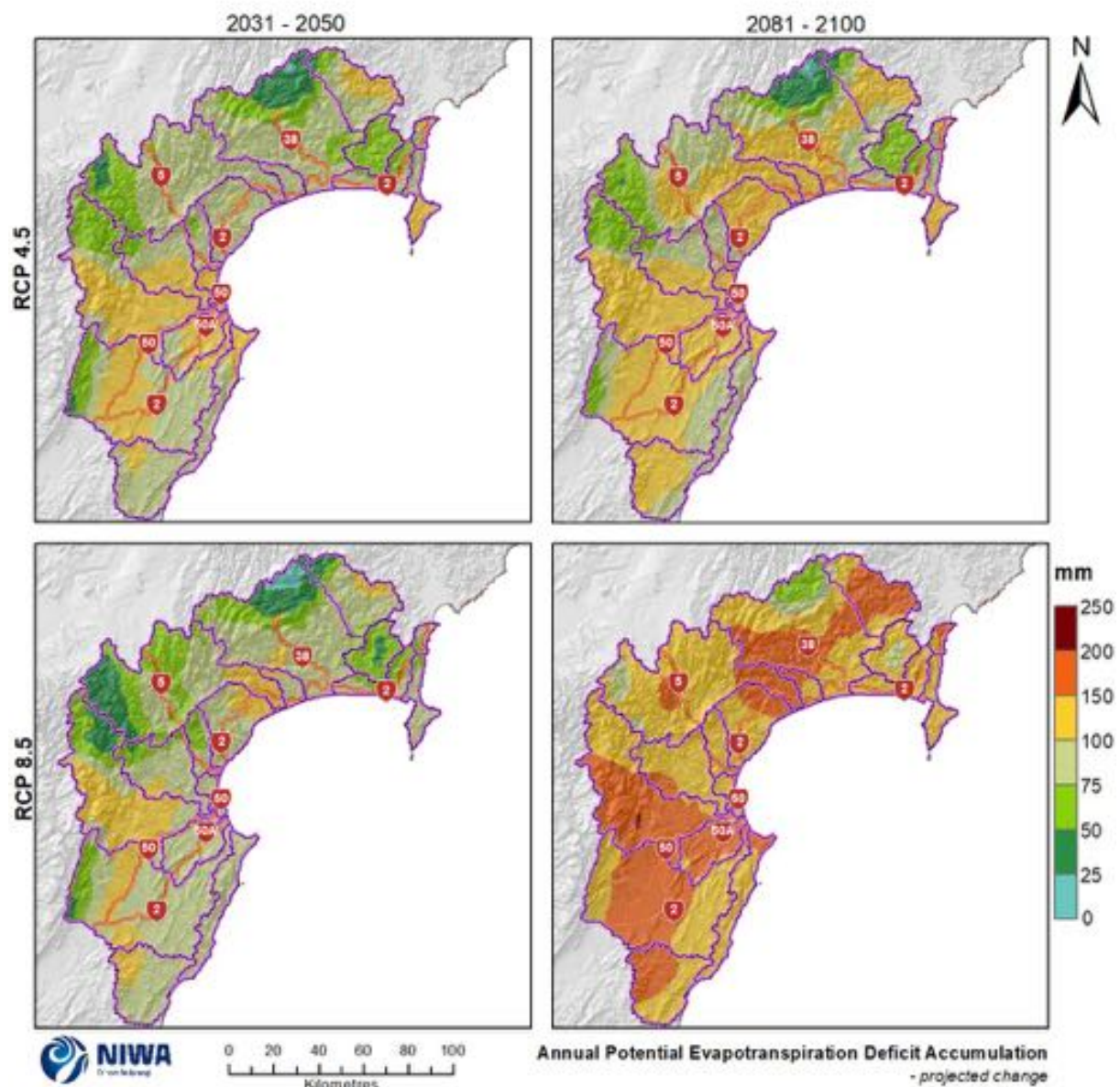


Figure 6-4: Projected annual potential evapotranspiration deficit accumulation (mm) changes for Hawke's Bay by 2040 and 2090 under RCP4.5 and RCP8.5. Relative to 1986-2005 average, based on the average of six global climate models. Results are based on dynamical downscaled projections using NIWA's Regional Climate Model. Resolution of projection is 5km x 5km.

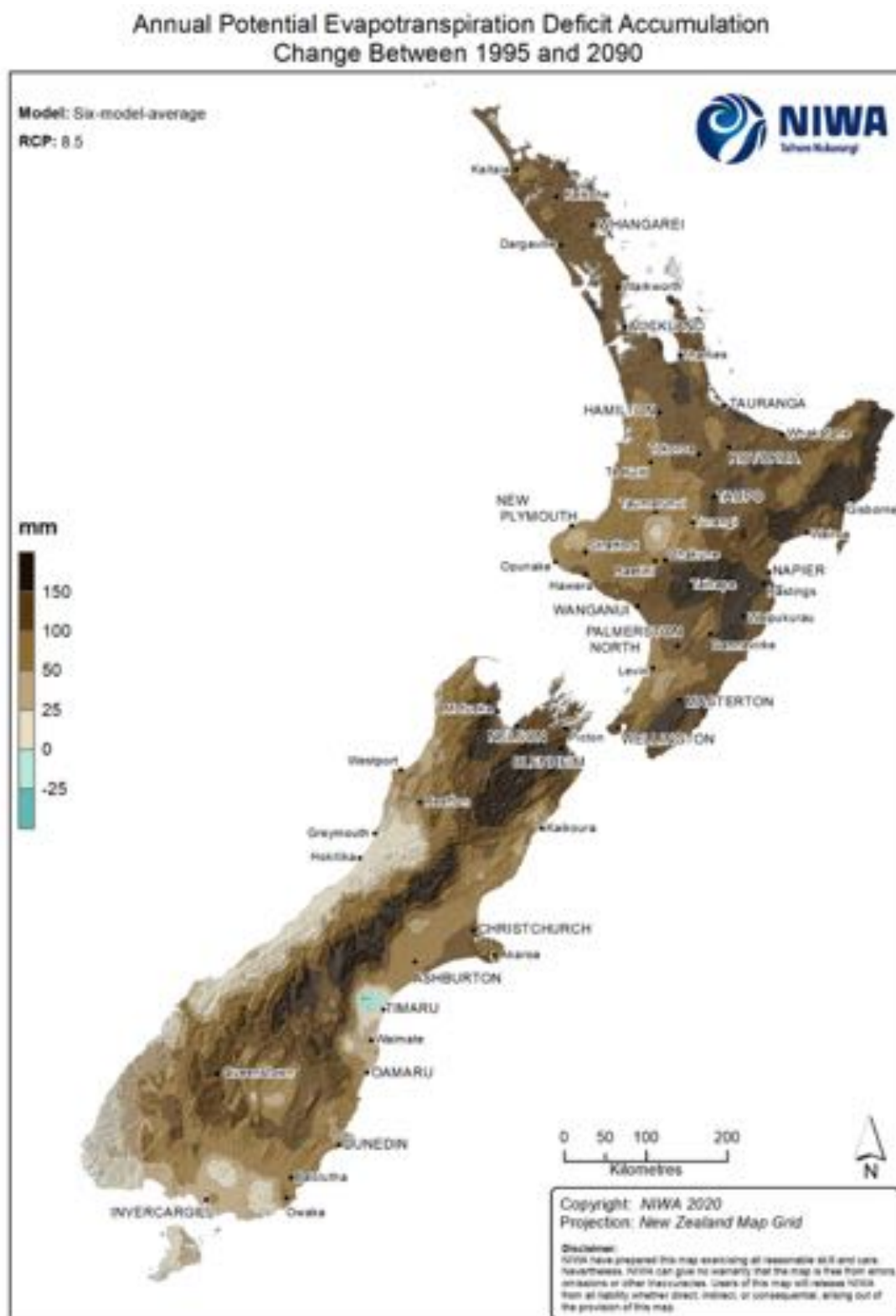


Figure 6-5: Projected annual potential evapotranspiration deficit accumulation (mm) changes for New Zealand by 2090 under RCP8.5. Relative to 1986–2005 average, based on the average of six global climate models. Results are based on dynamical downscaled projections using NIWA's Regional Climate Model. Resolution of projection is 5km x 5km.

6.2 Extreme potential evapotranspiration deficit (>300 mm)

Another way of presenting PED as a drought indicator is to present the probability of PED above a certain threshold in order to evaluate the projected change to PED in terms of extremes. Here, we have chosen 300 mm as the threshold, which represents very dry conditions in the two regions.

Figure 6-6 and Figure 6-7 show the historic (1986-2005 average) probability that PED exceeded 300 mm in any year. The areas around Gisborne City, Hastings and Napier have the highest probability of 300 mm of PED being exceeded (in addition to a few other small coastal locations in Hawke's Bay Region), with the annual probability being 50-80%. The probability of this threshold being exceeded is generally higher for eastern locations and decreases to the west where high elevation locations have probabilities of less than 5%. Similar to the projected pattern for accumulated PED (Section 6.1), an area just inland from Mahia has a lower probability of the threshold being exceeded (0-5%).

Figure 6-8 and Figure 6-9 show the projected future (2031-2050 and 2081-2100) probability of PED exceeding 300 mm during an average year (not the change in probability).

Representative concentration pathway (RCP) 4.5

By 2040, the area with a projected 50-80% probability of PED exceeding 300 mm expands along the eastern coast of both regions as well as over some inland parts of Hawke's Bay, generally at lower elevations. The highest probabilities continue to be located over Gisborne, Hastings and Napier, in addition to several small areas in the Hawke's Bay Region (80-100%). Many high elevation locations however are projected to stay in the 0-5% probability range. By 2090, the spatial pattern is largely the same as for 2040 (Figure 6-8 and Figure 6-9).

Representative concentration pathway (RCP) 8.5

By 2040, the projected pattern is largely the same as for RCP4.5 (at the same time period). By 2090 however, the projected pattern is very different to the other scenarios. Notably, there is greater spatial coverage of locations that have projected probabilities in the 80 to 100% range. As before, this includes Gisborne, Hastings and Napier, although there is greater inland coverage. Similarly, the 50-80% probability category extends further inland at several locations. There are also fewer high elevation locations in the 0-5% probability range (Figure 6-8 and Figure 6-9).

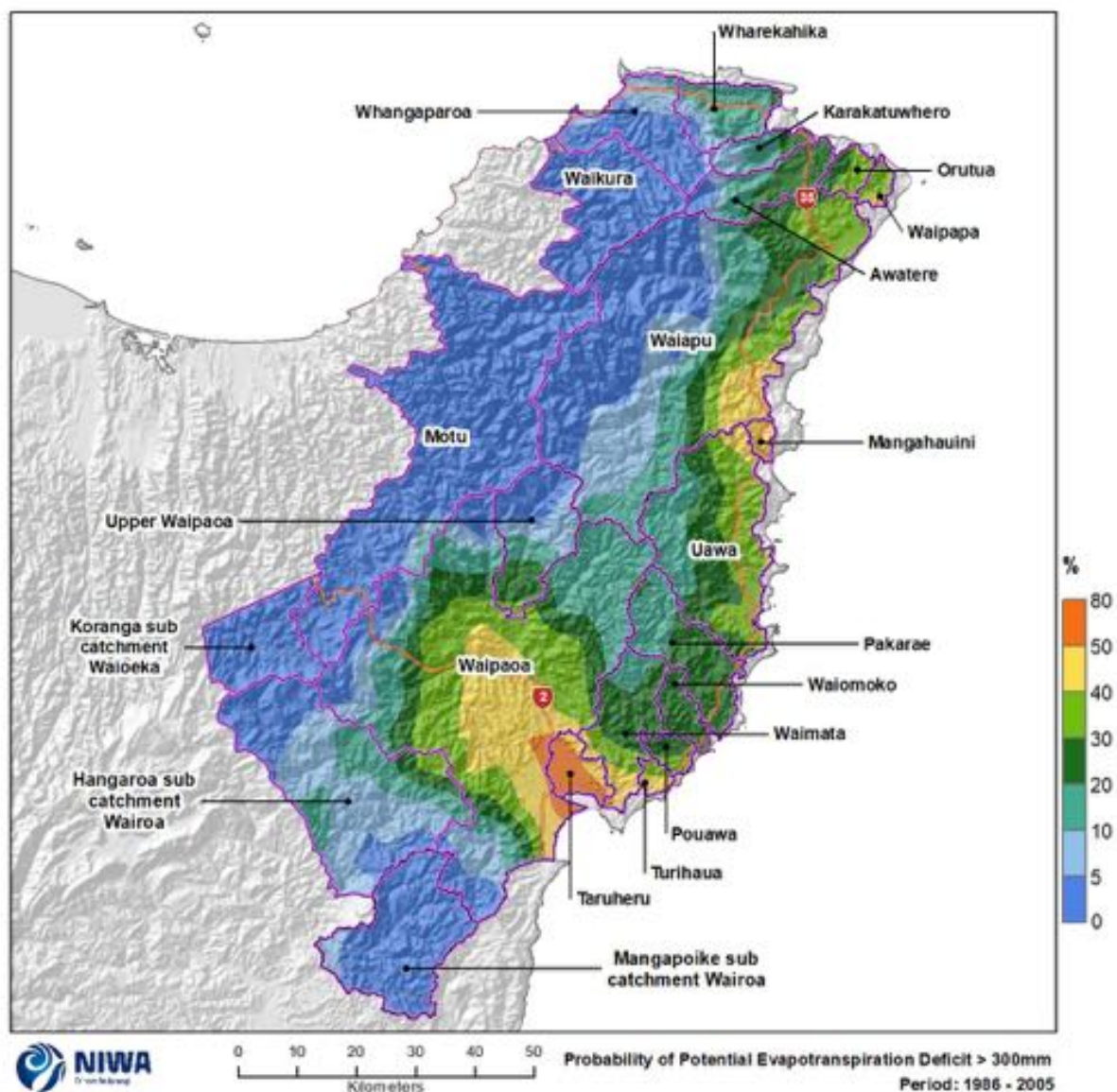


Figure 6-6: Modelled probability of Potential Evapotranspiration Deficit exceeding 300 mm in any year for Tairāwhiti, average over 1986-2005. Results are based on dynamical downscaled projections using NIWA's Regional Climate Model. Resolution of projection is 5km x 5km.

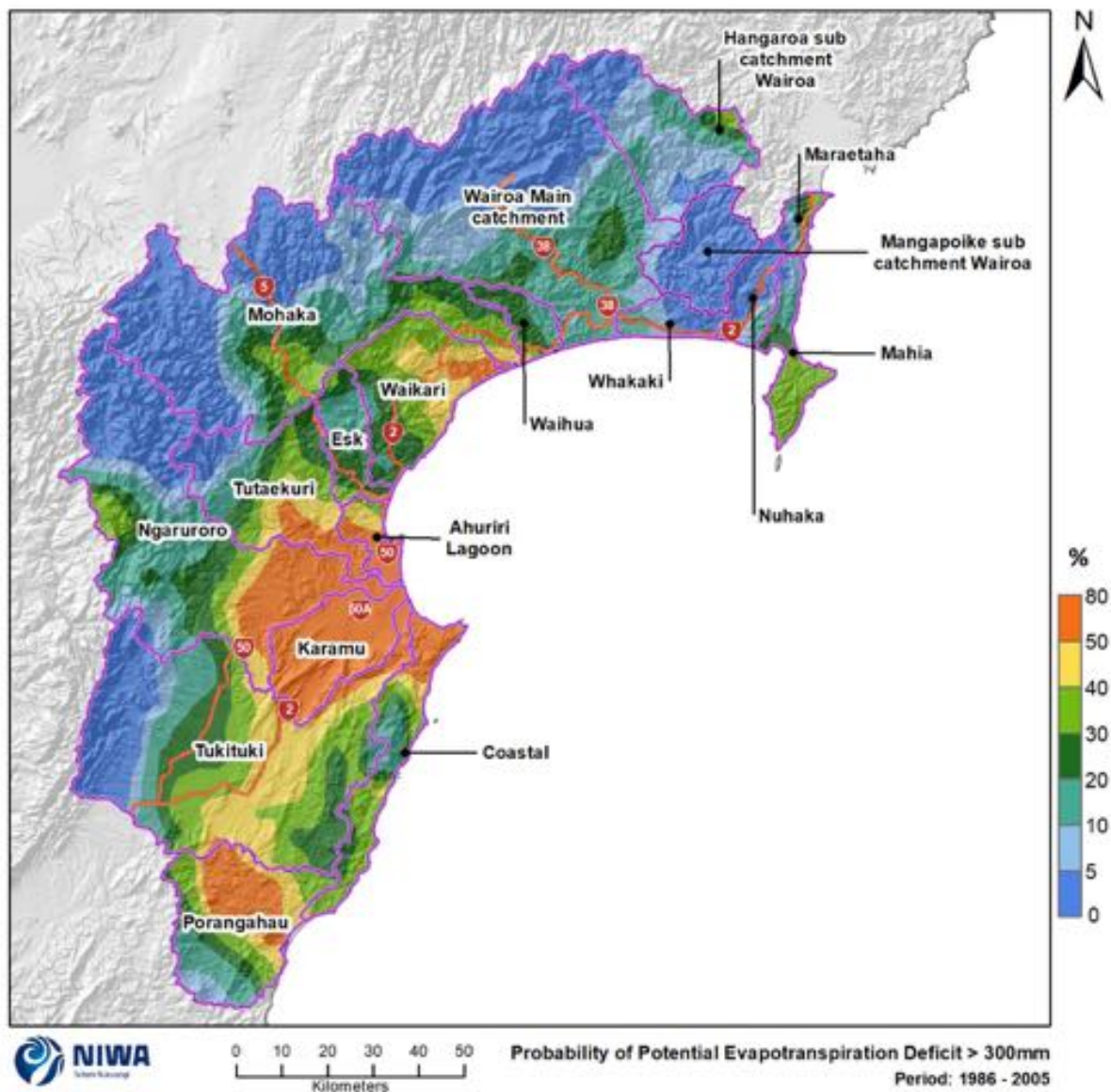


Figure 6-7: Modelled probability of Potential Evapotranspiration Deficit exceeding 300 mm in any year for Hawke's Bay region, average over 1986-2005 . Results are based on dynamical downscaled projections using NIWA's Regional Climate Model. Resolution of projection is 5km x 5km.

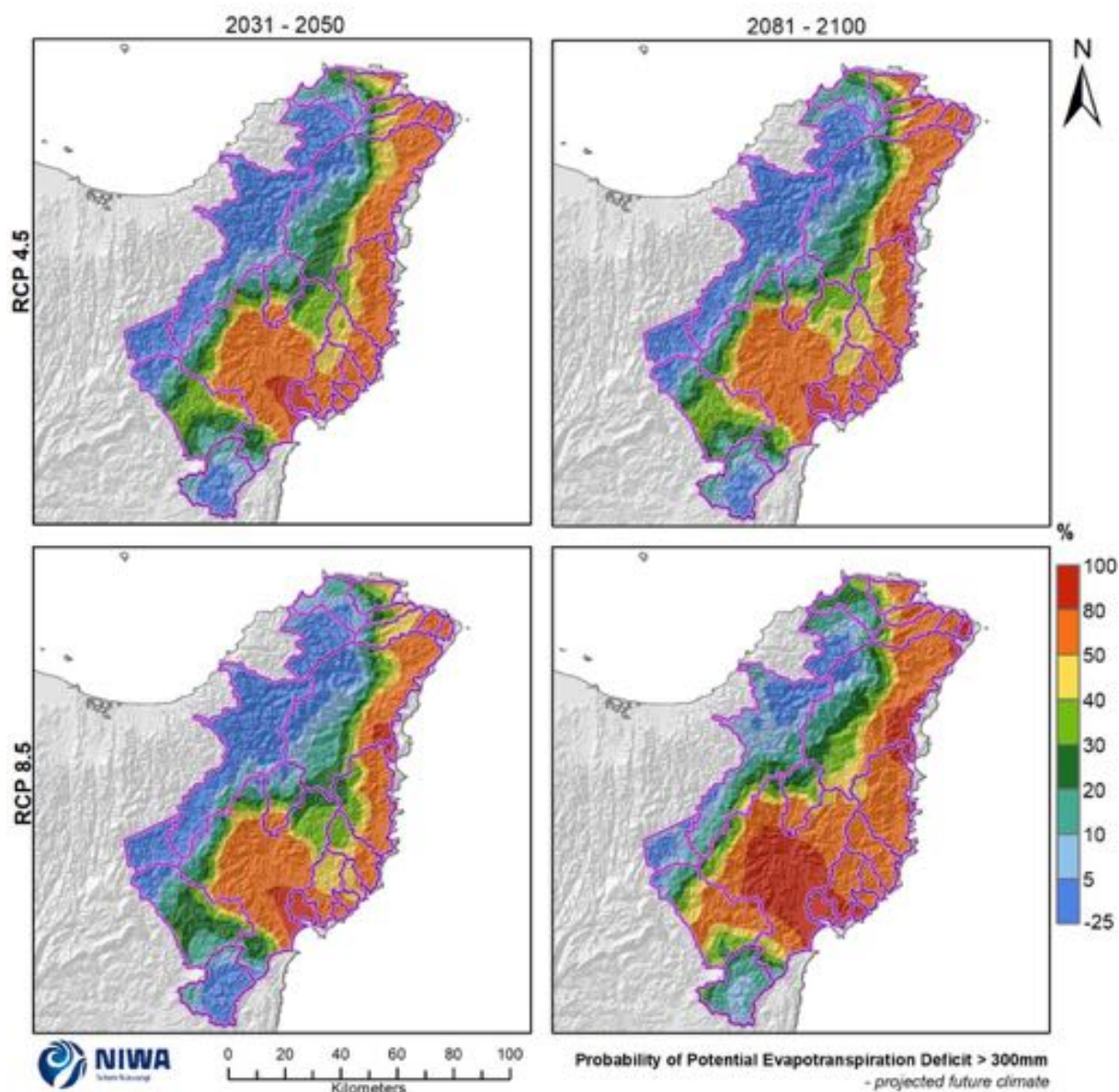


Figure 6-8: Projected probability of annual Potential Evapotranspiration Deficit exceeding 300 mm for Tairāwhiti by 2040 and 2090 under RCP4.5 and RCP8.5. Relative to 1986-2005 average, based on the average of six global climate models. Results are based on dynamical downscaled projections using NIWA's Regional Climate Model. Resolution of projection is 5km x 5km.

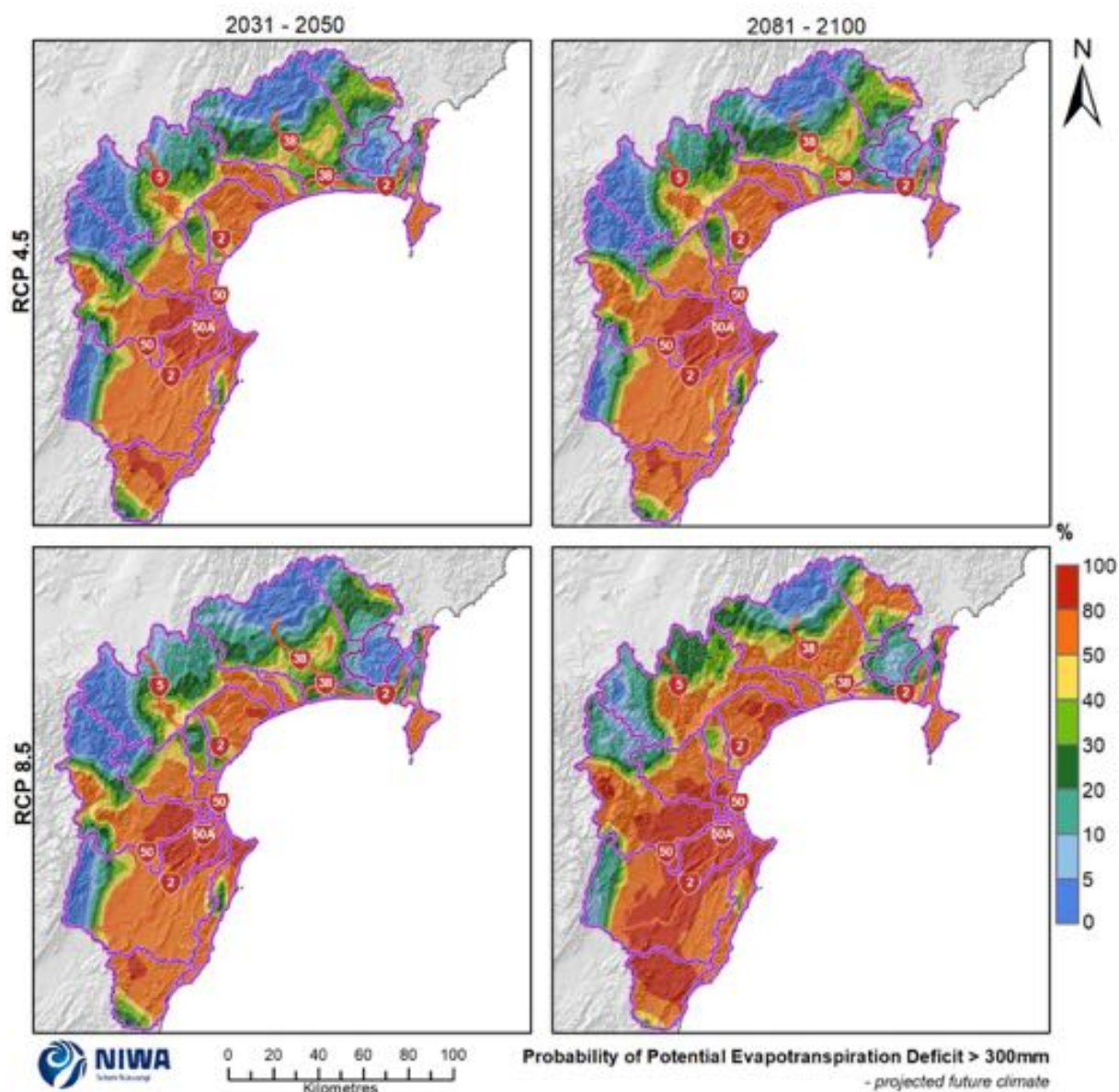


Figure 6-9: Projected annual potential evapotranspiration deficit accumulation (mm) changes for Hawke's Bay by 2040 and 2090 under RCP4.5 and RCP8.5. Relative to 1986-2005 average, based on the average of six global climate models. Results are based on dynamical downscaled projections using NIWA's Regional Climate Model. Resolution of projection is 5km x 5km.

6.3 Soil moisture deficit

Soil moisture deficit (SMD) is calculated based on incoming daily rainfall (mm), outgoing daily potential evapotranspiration (PET), and a fixed available water capacity of 150 mm (the amount of water in the soil 'reservoir' that plants can use). In the calculation, evapotranspiration continues at its potential rate until about half of the water available to plants is used up (75 mm out of the total 150 mm available). Subsequently, the rate of evapotranspiration decreases, in the absence of rain, as further water extraction takes place. Evapotranspiration is assumed to cease if all the available water is used up (i.e. all 150 mm).

A day of SMD is considered in this report to be when soil moisture is below 75 mm of available soil water capacity. The timing of changes in the days of soil moisture deficit projections indicates how droughts may change in timing throughout the year. Soil moisture deficit and PED are similar measures of dryness, but in this report SMD is measured in days and PED is measured in mm of accumulation, so PED is a more sensitive measure of drought intensity than SMD.

Historic (average over 1986-2005) and future (average over 2031-2050 and 2081-2100) maps for days of SMD are shown in this section. The historic maps show the annual and seasonal number of days of SMD and the future projection maps show the change in the number of days of SMD compared with the historic period. Note that the historic maps are on a different colour scale to the future projection maps.

For the modelled historic period, the highest number of SMD days are experienced in the south of the Hawke's Bay Region (250-300 SMD days per year) (Figure 6-10 and Figure 6-11). The area around Gisborne City and the Waipaoa catchment just inland experience 200-250 SMD days per year. Some coastal margins of Tairāwhiti as well as much of eastern Hawke's Bay experience similar values. Many inland locations experience 50-150 SMD days per year. Summer is the season with the highest number of SMD days (70-90 SMD days for the eastern majority of both regions), and winter has the least SMD days (less than 1 SMD day on average at high elevations, and generally less than 40 days for the eastern coast) (Figure 6-12 and Figure 6-13).

Representative concentration pathway (RCP) 4.5

By 2040, the annual number days of soil moisture deficit are projected to increase by 5-15 days for most locations (Figure 6-14 and Figure 6-15). Several isolated areas are projected to experience by as much as 15-20 additional SMD days, and a few coastal locations are projected to increase by only 1-5 days. Winter is projected to experience very little change, particularly at high elevations in the west where the projected number of SMD days remains at zero (Figure 6-16 and Figure 6-17). Summer and spring have slightly larger increases (+5-10 SMD days for most locations).

By 2090, there is a much larger projected increase in the number of annual SMD days with most locations increasing by 10-20 days and even exceeding 20 days in many locations (Figure 6-14 and Figure 6-15). Winter is projected to see some of the largest increases under this scenario (+10-15 at a few locations) (Figure 6-18 and Figure 6-19).

Representative concentration pathway (RCP) 8.5

By 2040, most locations are projected to experience larger increases to the number of annual SMD days than projected for RCP4.5 (+5-20 days under RCP8.5, with very few locations experiencing smaller increases than this) (Figure 6-14 and Figure 6-15). Spring is projected to see slightly more locations with larger magnitude changes (i.e. +10-15 days), although this magnitude of change is

spatially limited in this scenario. Winter is again projected to experience negligible change in the west (Figure 6-20 and Figure 6-21).

By 2090, the increases to the number of soil moisture deficit days are very large, with the majority of both regions projected to experience more than 20 additional days of SMD annually (Figure 6-14 and Figure 6-15). At the seasonal scale, some of the largest increases are projected to occur during winter (15-20 days or more) (Figure 6-22 and Figure 6-23).

It is noted that the increases to SMD days projected for Tairāwhiti and Hawke's Bay are among the largest increases projected for New Zealand (see Figure 6-24 for national scale projections at 2090 under RCP8.5).

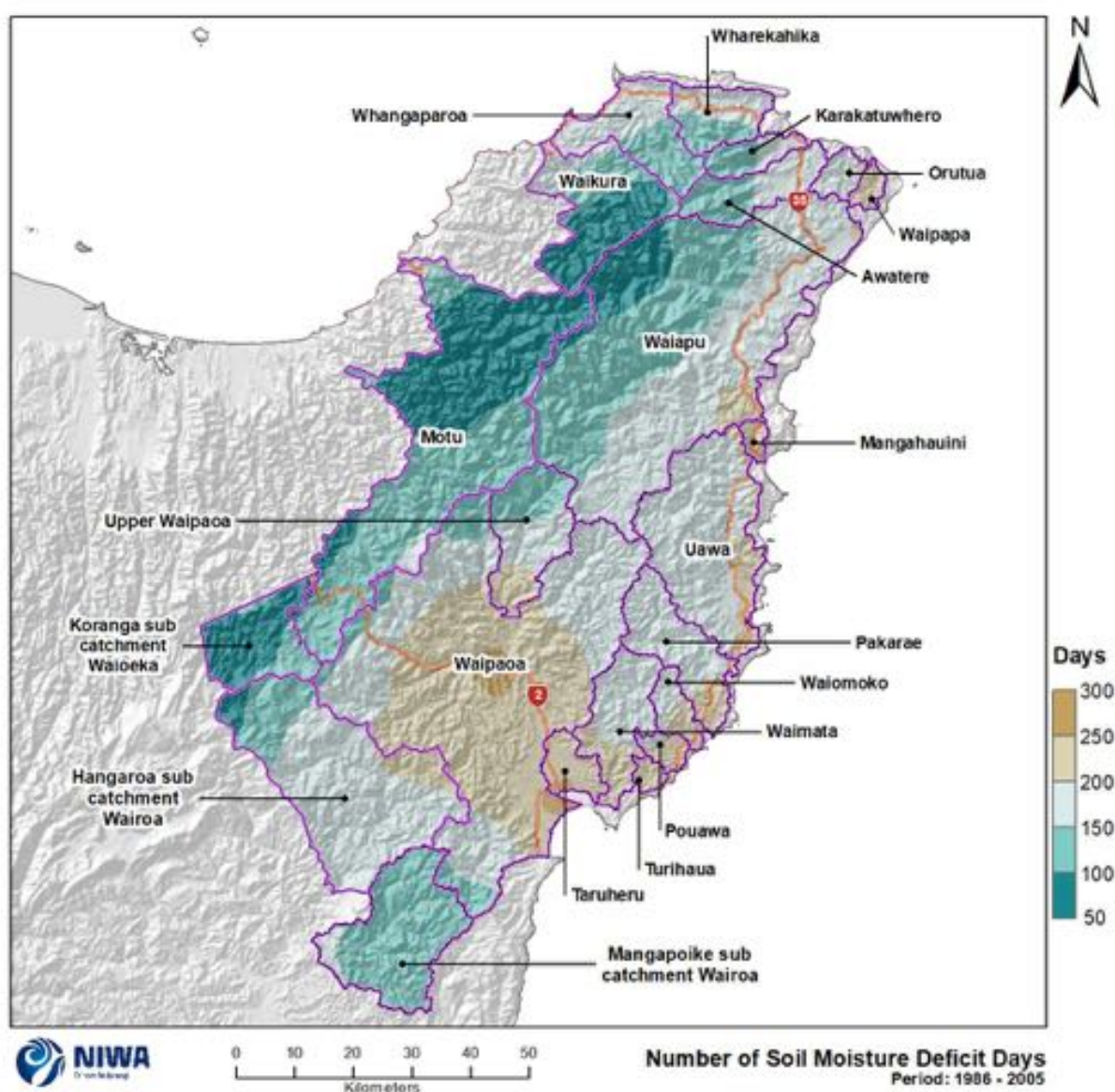


Figure 6-10: Modelled annual number of days of soil moisture deficit for Tairāwhiti, average over 1986-2005. Results are based on dynamical downscaled projections using NIWA's Regional Climate Model. Resolution of projection is 5km x 5km.

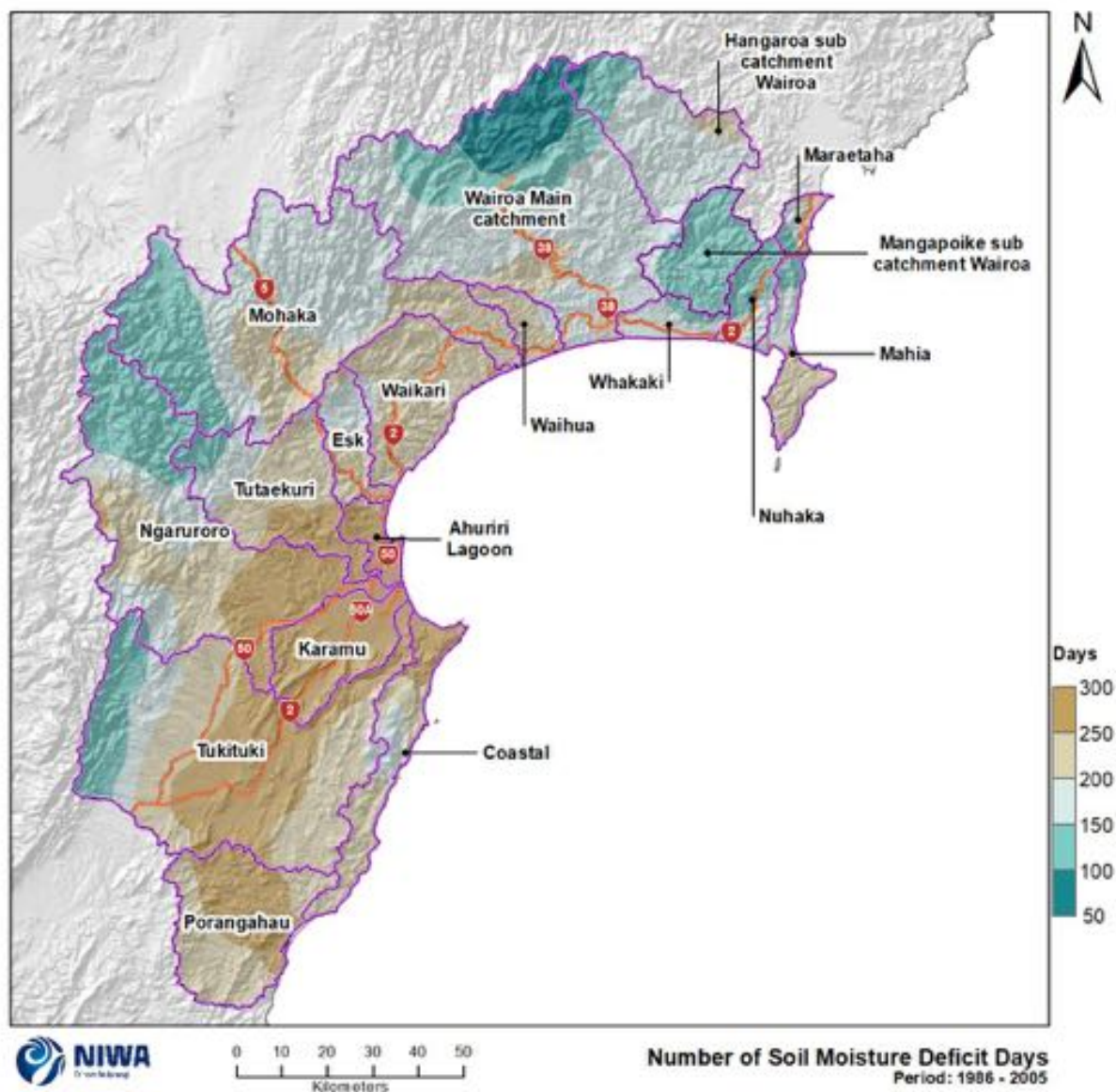


Figure 6-11: Modelled annual number of days of soil moisture deficit for Hawke's Bay region, average over 1986-2005 . Results are based on dynamical downscaled projections using NIWA's Regional Climate Model. Resolution of projection is 5km x 5km.

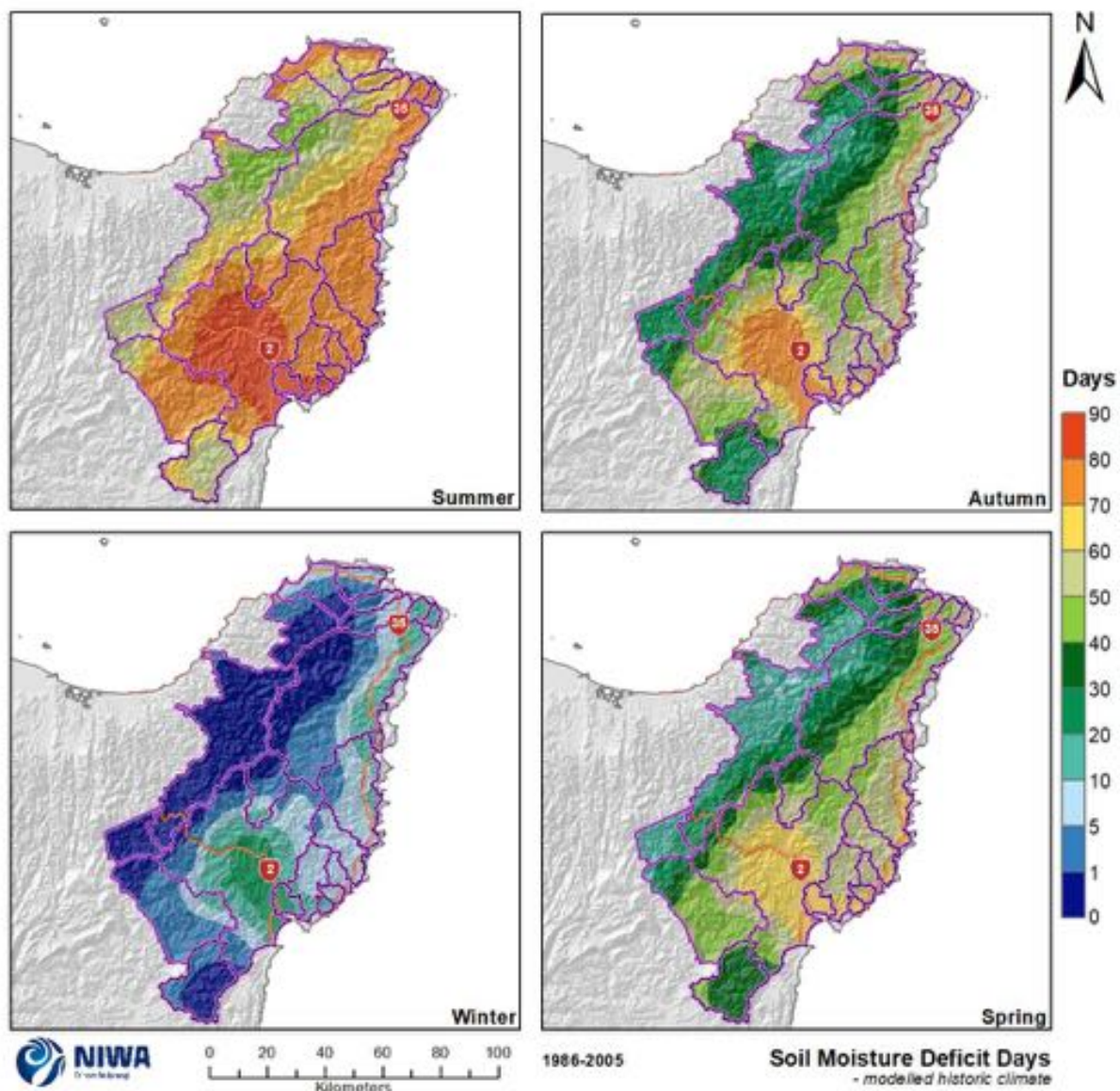


Figure 6-12: Modelled seasonal number of days of soil moisture deficit for Tairāwhiti, average over 1986-2005 . Results are based on dynamical downscaled projections using NIWA's Regional Climate Model. Resolution of projection is 5km x 5km.

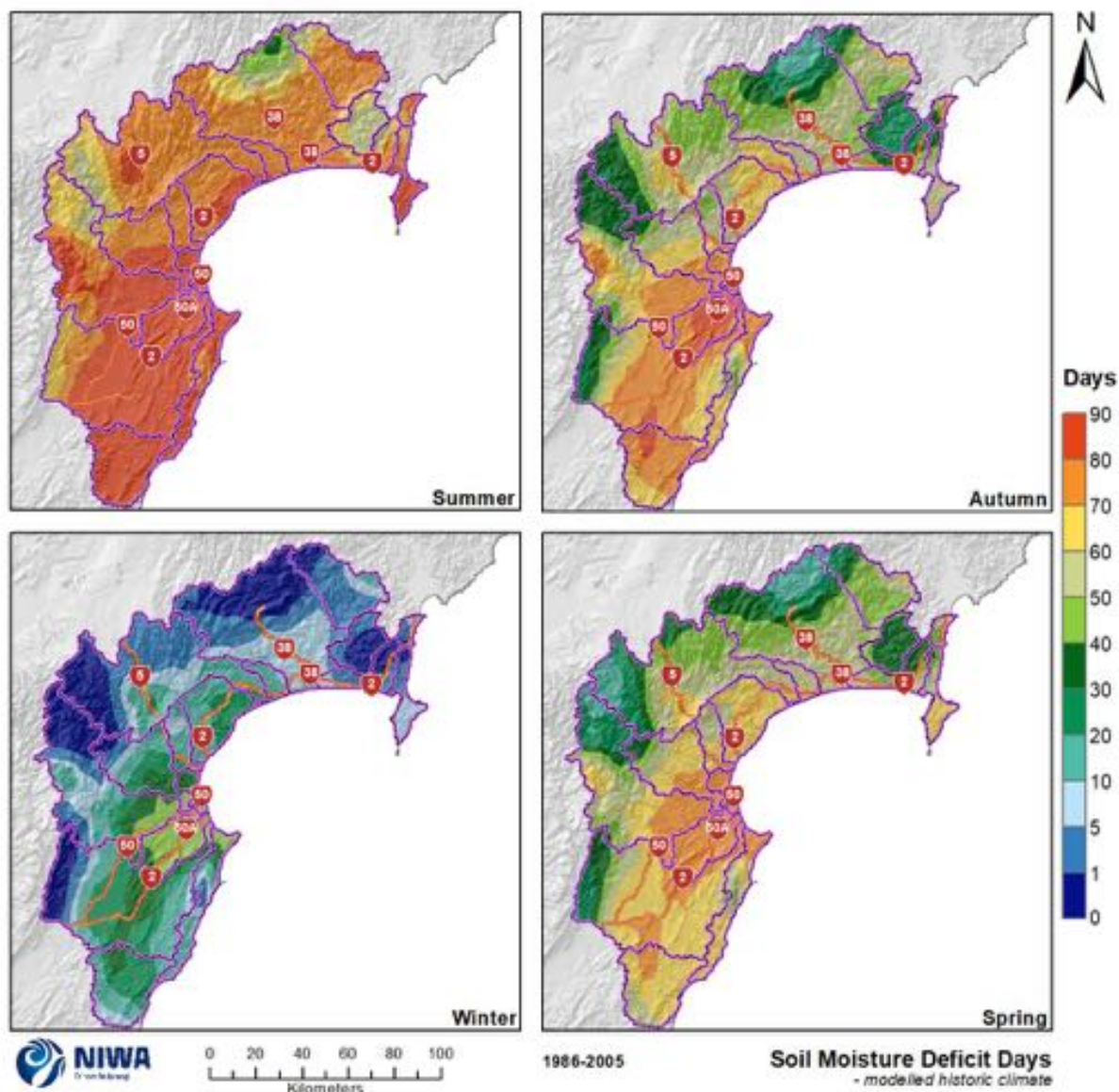


Figure 6-13: Modelled seasonal number of days of soil moisture deficit for Hawke's Bay region, average over 1986-2005 . Results are based on dynamical downscaled projections using NIWA's Regional Climate Model. Resolution of projection is 5km x 5km.

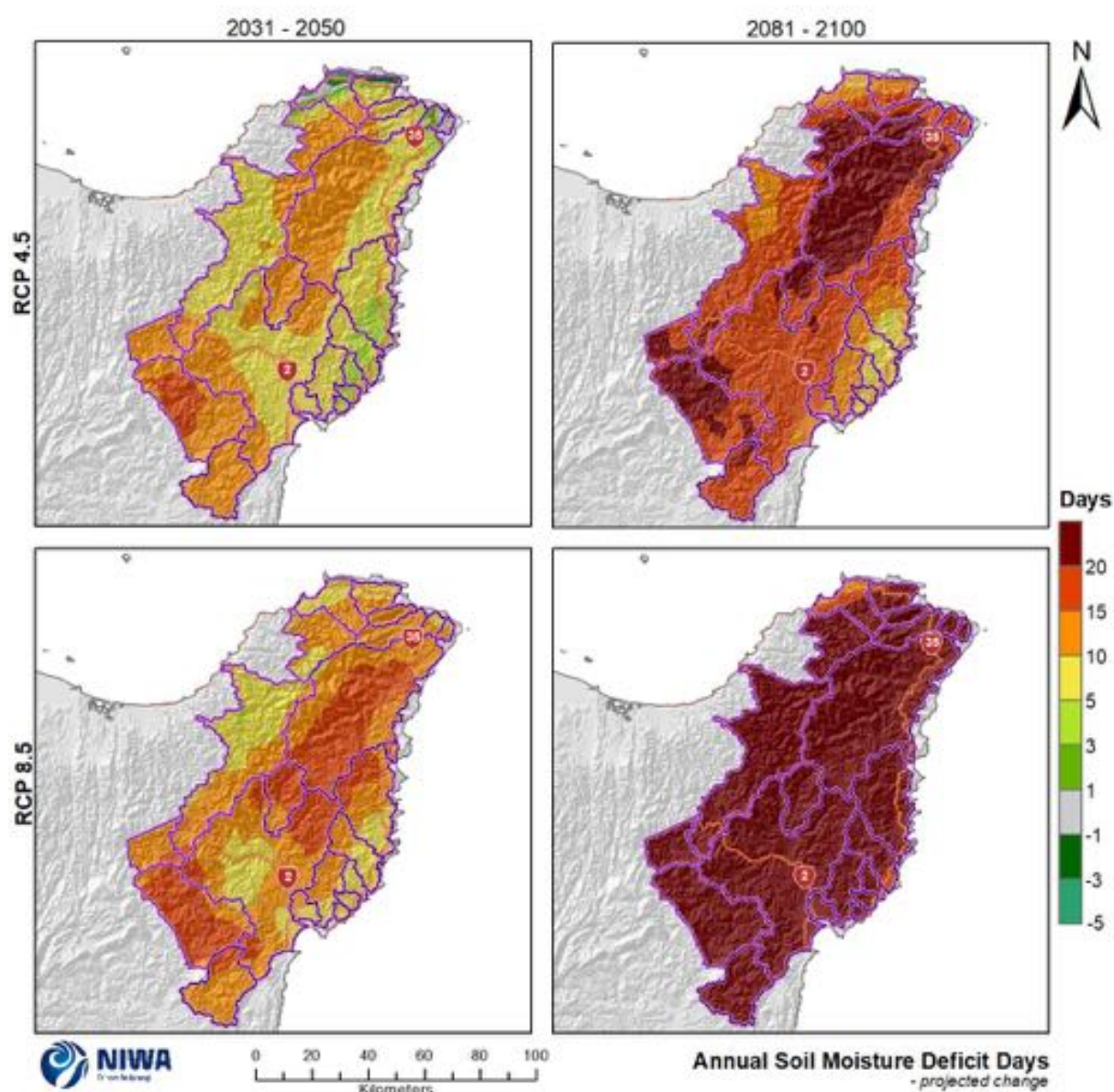


Figure 6-14: Projected change in the number of annual soil moisture deficit days for Tairāwhiti by 2040 and 2090 under RCP4.5 and RCP8.5. Relative to 1986-2005 average, based on the average of six global climate models. Results are based on dynamical downscaled projections using NIWA's Regional Climate Model. Resolution of projection is 5km x 5km.

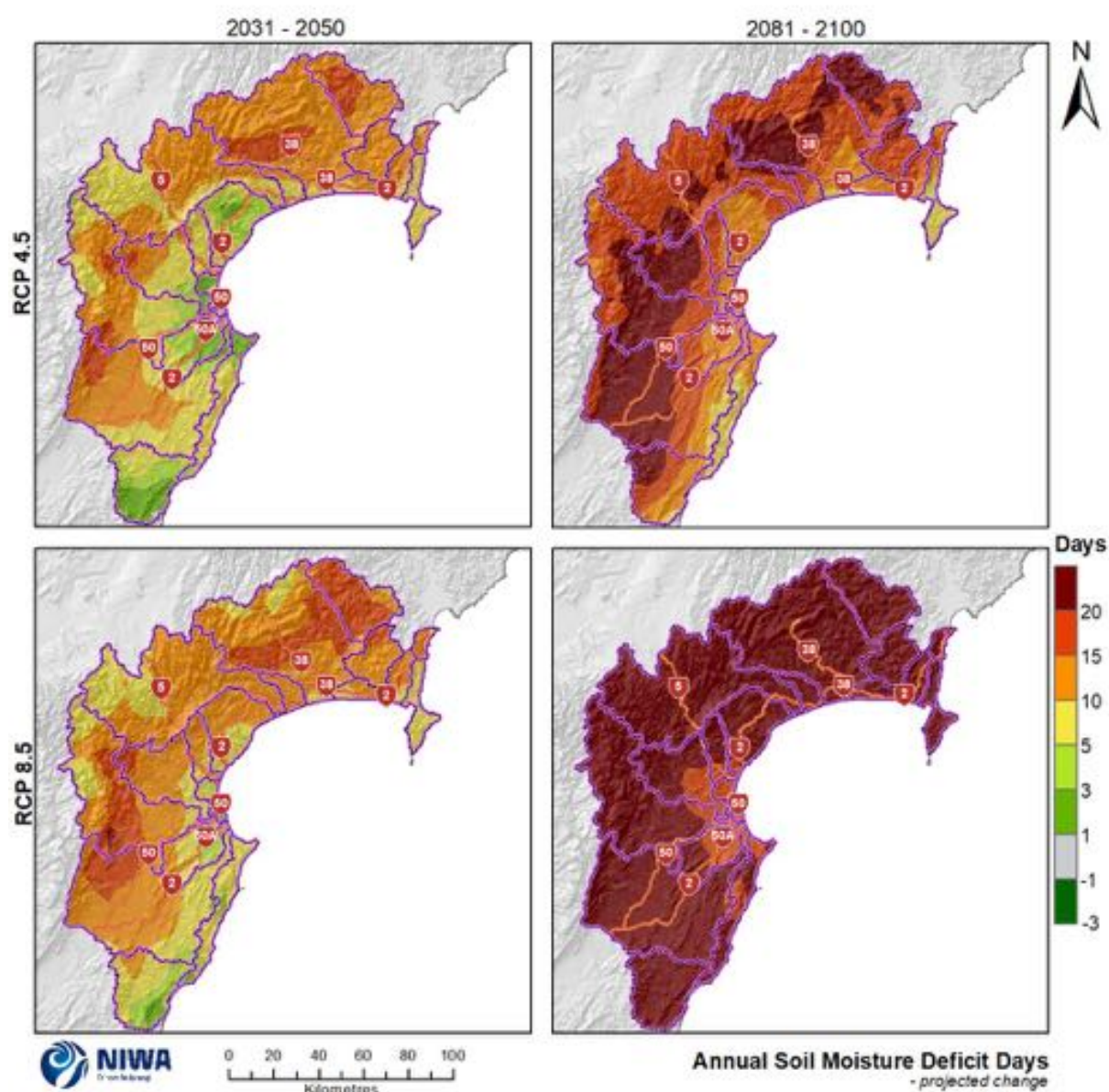


Figure 6-15: Projected change in the number of annual soil moisture deficit days for Hawke's Bay by 2040 and 2090 under RCP4.5 and RCP8.5. Relative to 1986-2005 average, based on the average of six global climate models. Results are based on dynamical downscaled projections using NIWA's Regional Climate Model. Resolution of projection is 5km x 5km.

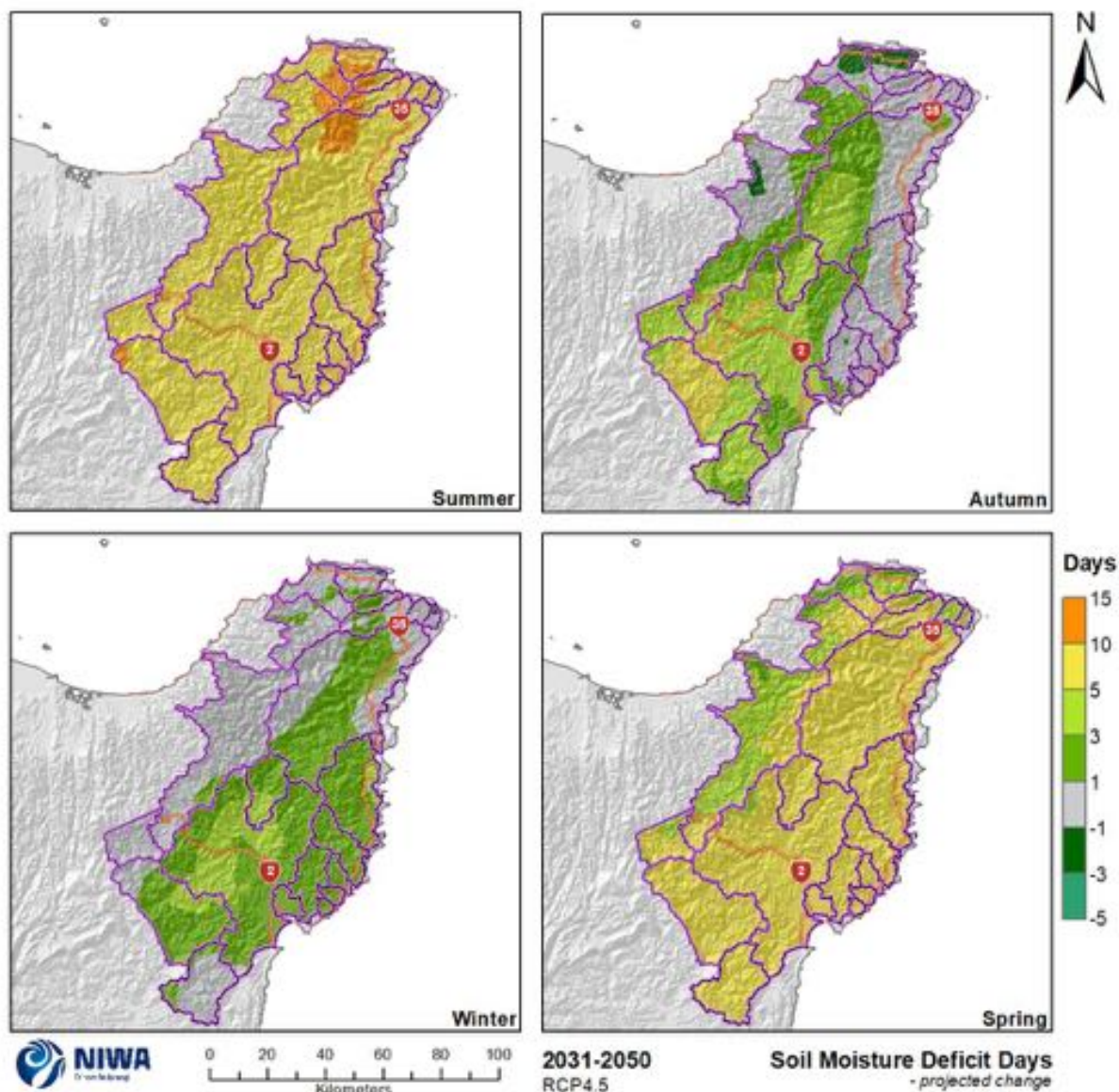


Figure 6-16: Projected change in the number of seasonal soil moisture deficit days for Tairāwhiti by 2040 under RCP4.5. Relative to 1986-2005 average, based on the average of six global climate models. Results are based on dynamical downscaled projections using NIWA's Regional Climate Model. Resolution of projection is 5km x 5km.

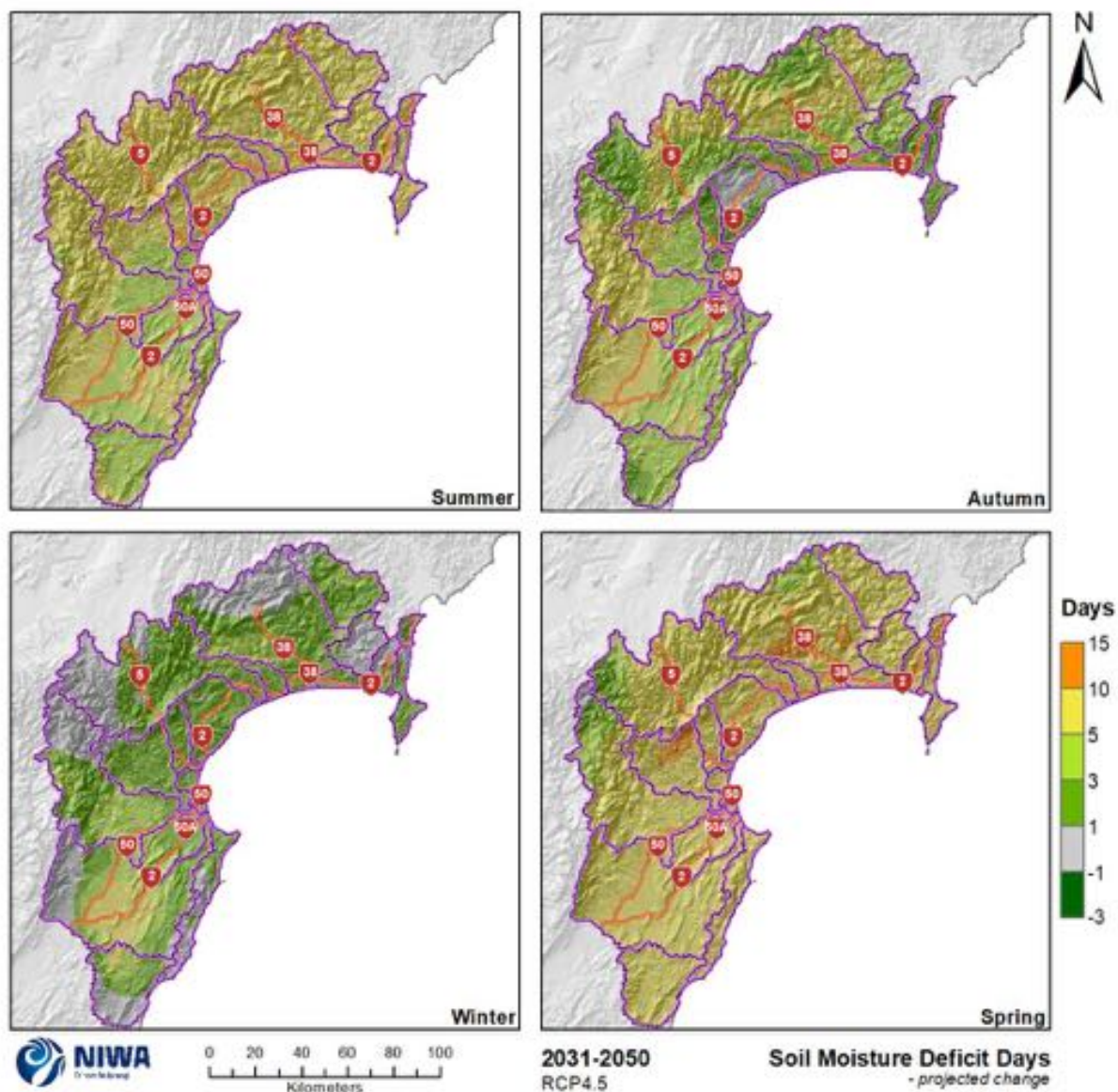


Figure 6-17: Projected change in the number of seasonal soil moisture deficit days for the Hawke's Bay Region by 2040 under RCP4.5. Relative to 1986-2005 average, based on the average of six global climate models. Results are based on dynamical downscaled projections using NIWA's Regional Climate Model. Resolution of projection is 5km x 5km.

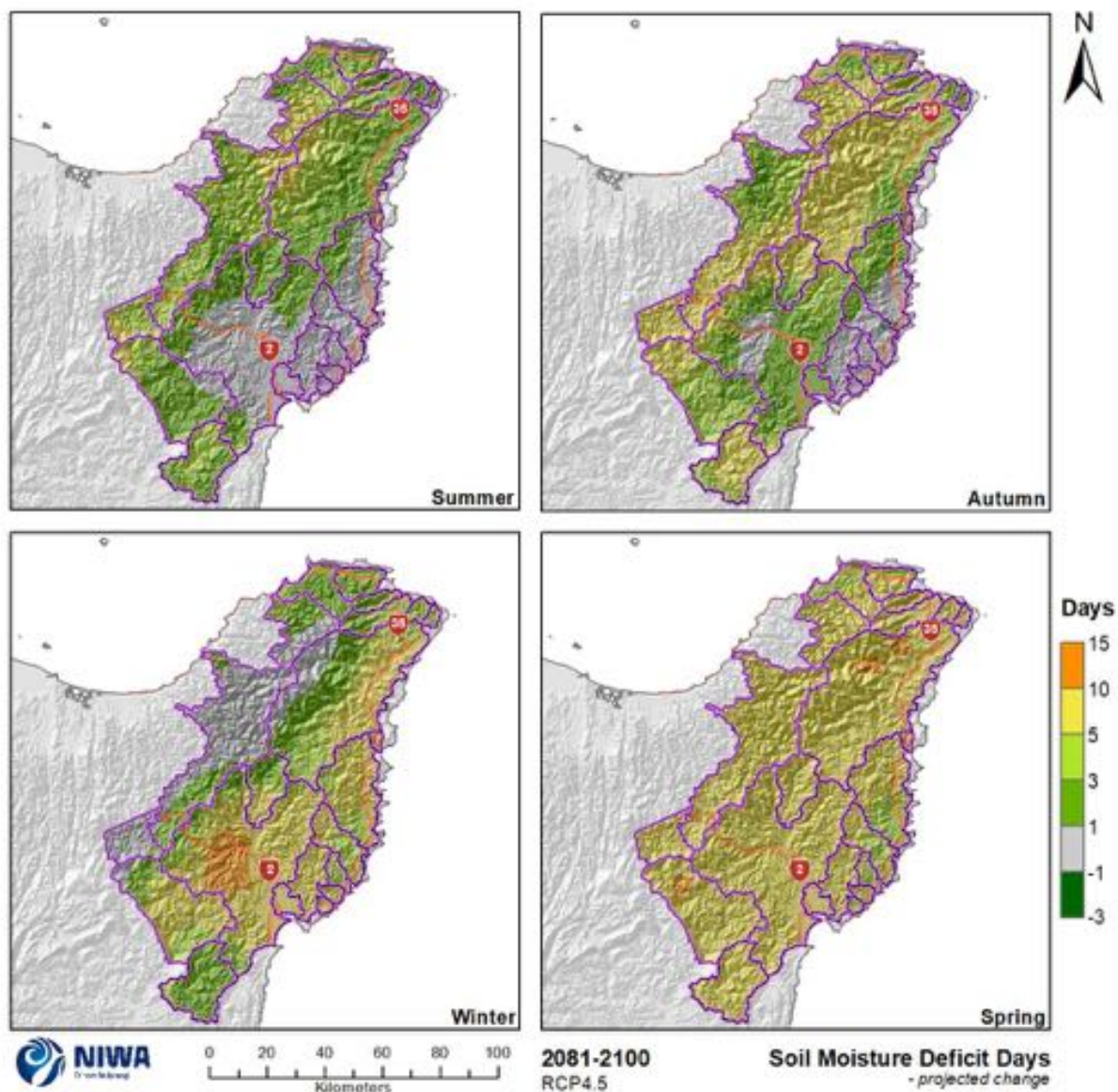


Figure 6-18: Projected change in the number of seasonal soil moisture deficit days for Tairāwhiti by 2090 under RCP4.5. Relative to 1986-2005 average, based on the average of six global climate models. Results are based on dynamical downscaled projections using NIWA's Regional Climate Model. Resolution of projection is 5km x 5km.

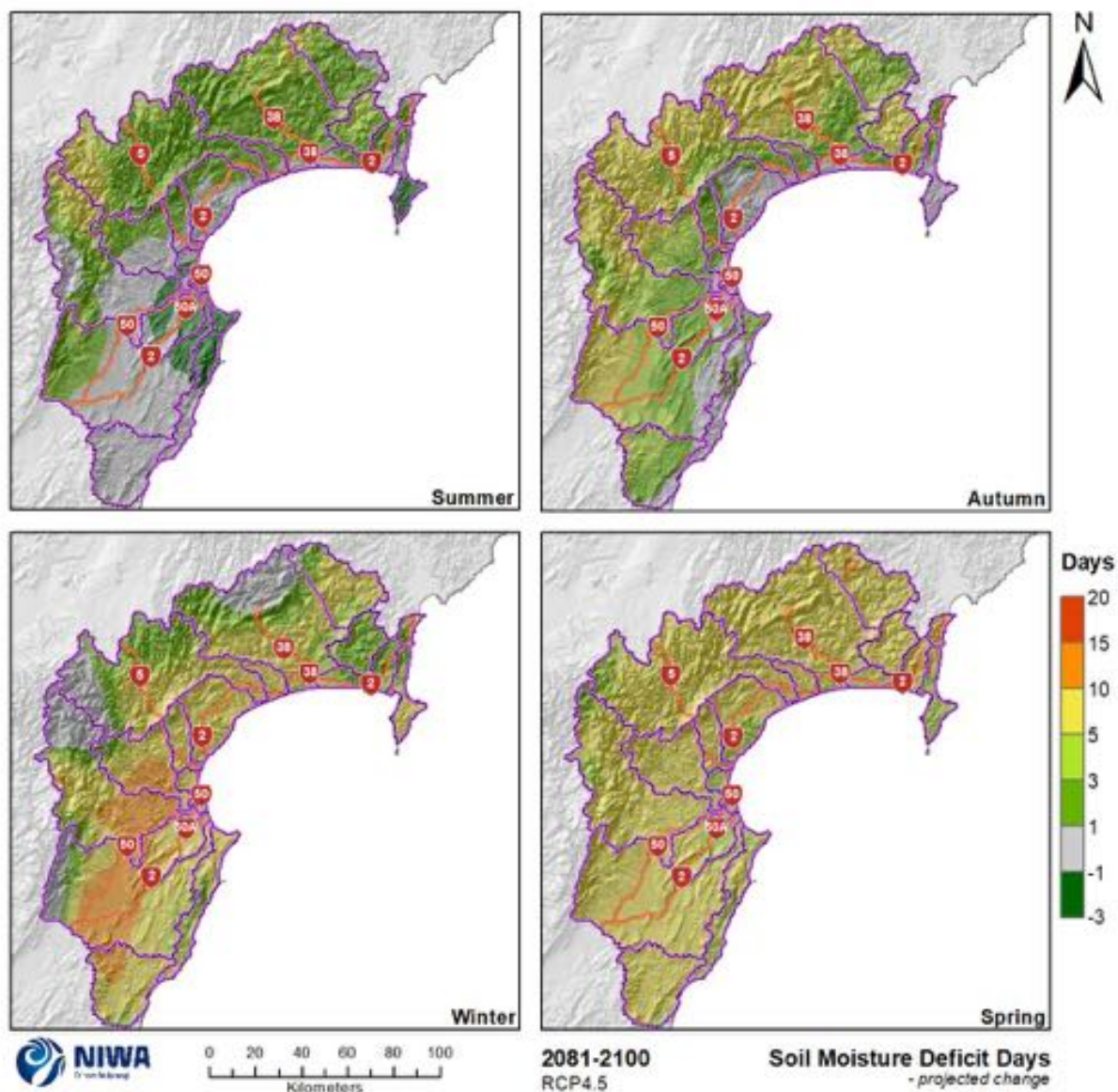


Figure 6-19: Projected change in the number of seasonal soil moisture deficit days for the Hawke's Bay Region by 2090 under RCP4.5. Relative to 1986-2005 average, based on the average of six global climate models. Results are based on dynamical downscaled projections using NIWA's Regional Climate Model. Resolution of projection is 5km x 5km.

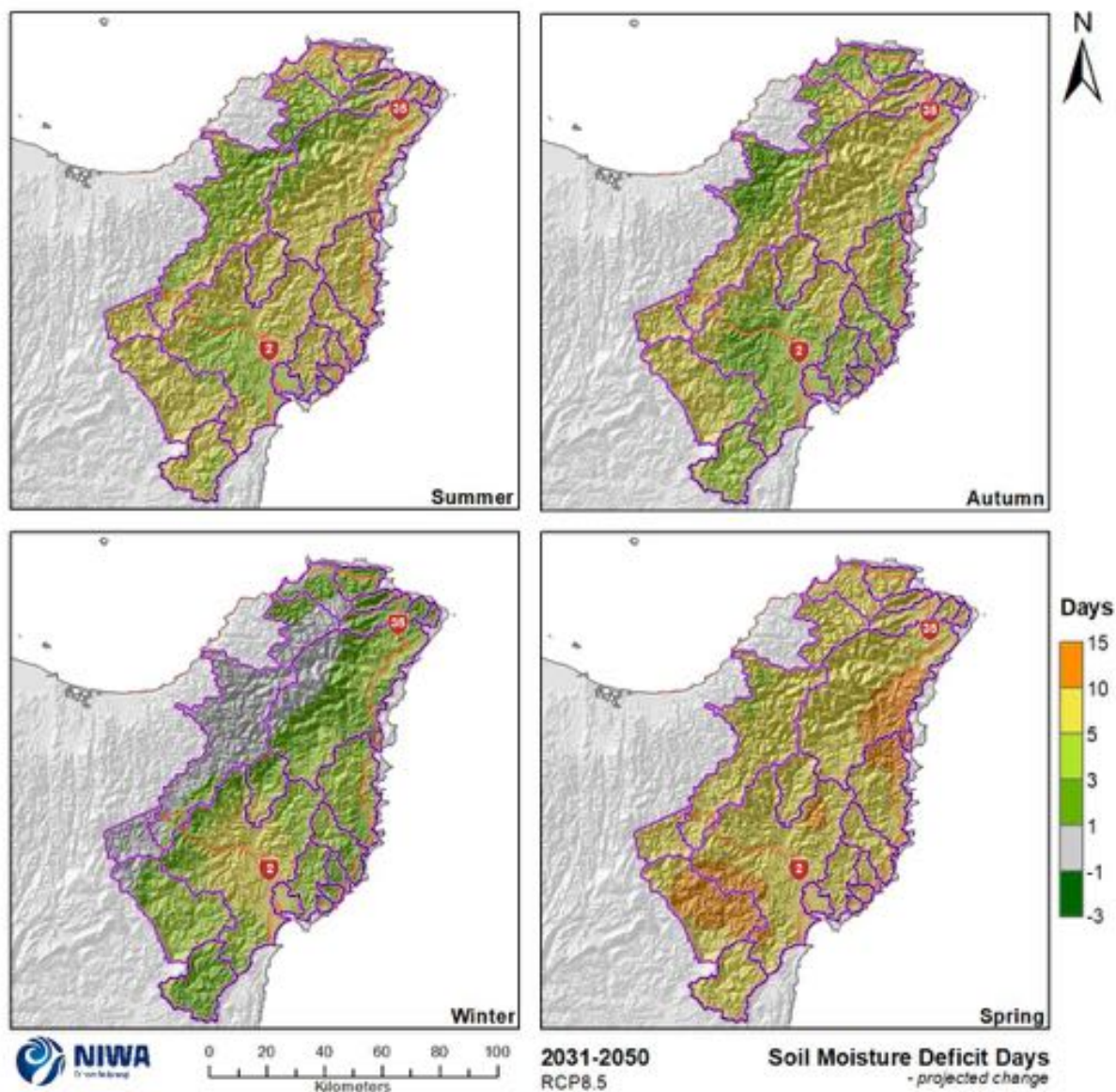


Figure 6-20: Projected change in the number of seasonal soil moisture deficit days for Tairāwhiti by 2040 under RCP8.5. Relative to 1986-2005 average, based on the average of six global climate models. Results are based on dynamical downscaled projections using NIWA's Regional Climate Model. Resolution of projection is 5km x 5km.

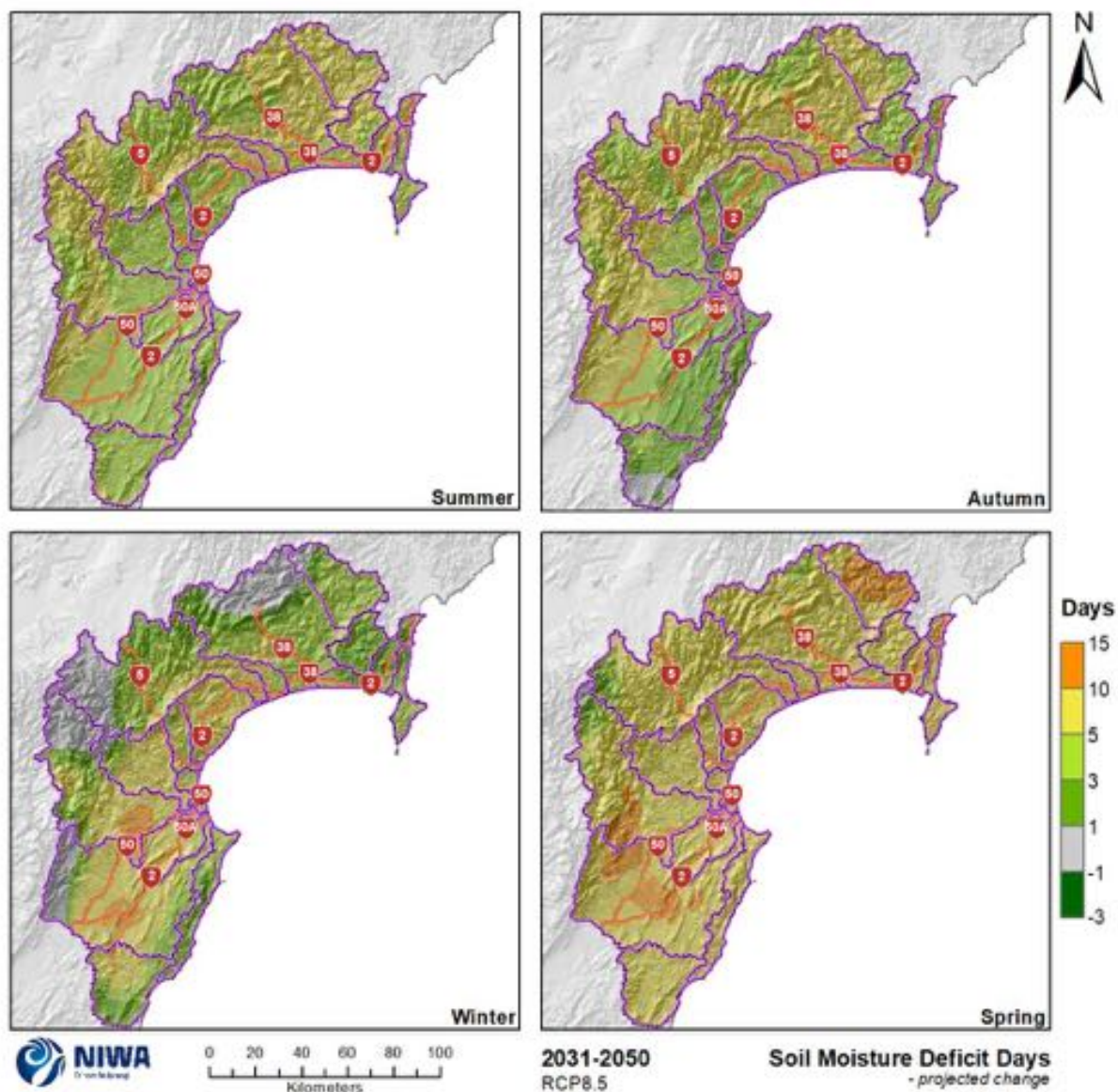


Figure 6-21: Projected change in the number of seasonal soil moisture deficit days for the Hawke's Bay Region by 2040 under RCP8.5. Relative to 1986-2005 average, based on the average of six global climate models. Results are based on dynamical downscaled projections using NIWA's Regional Climate Model. Resolution of projection is 5km x 5km.

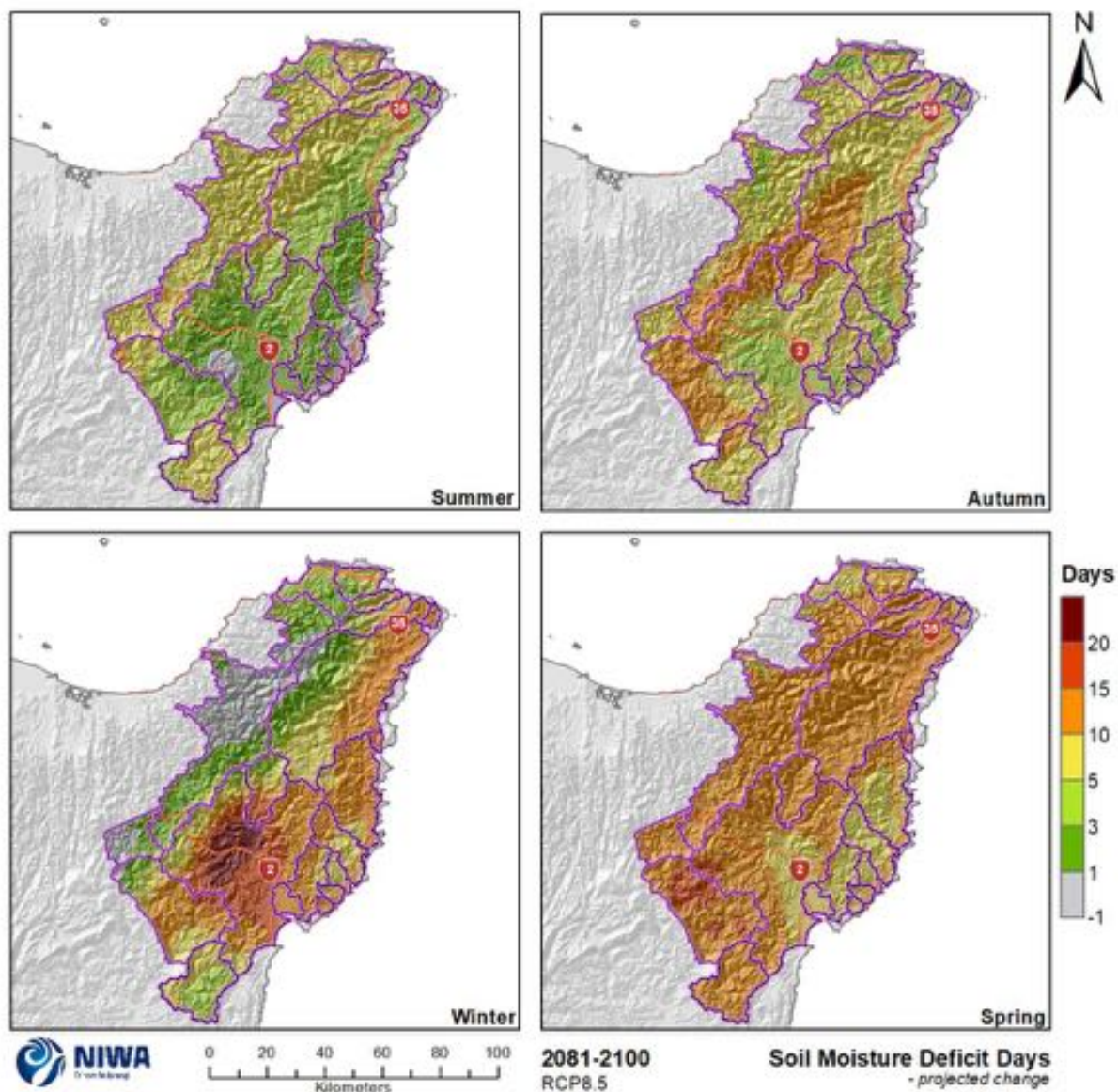


Figure 6-22: Projected change in the number of seasonal soil moisture deficit days for Tairāwhiti by 2090 under RCP8.5. Relative to 1986-2005 average, based on the average of six global climate models. Results are based on dynamical downscaled projections using NIWA's Regional Climate Model. Resolution of projection is 5km x 5km.

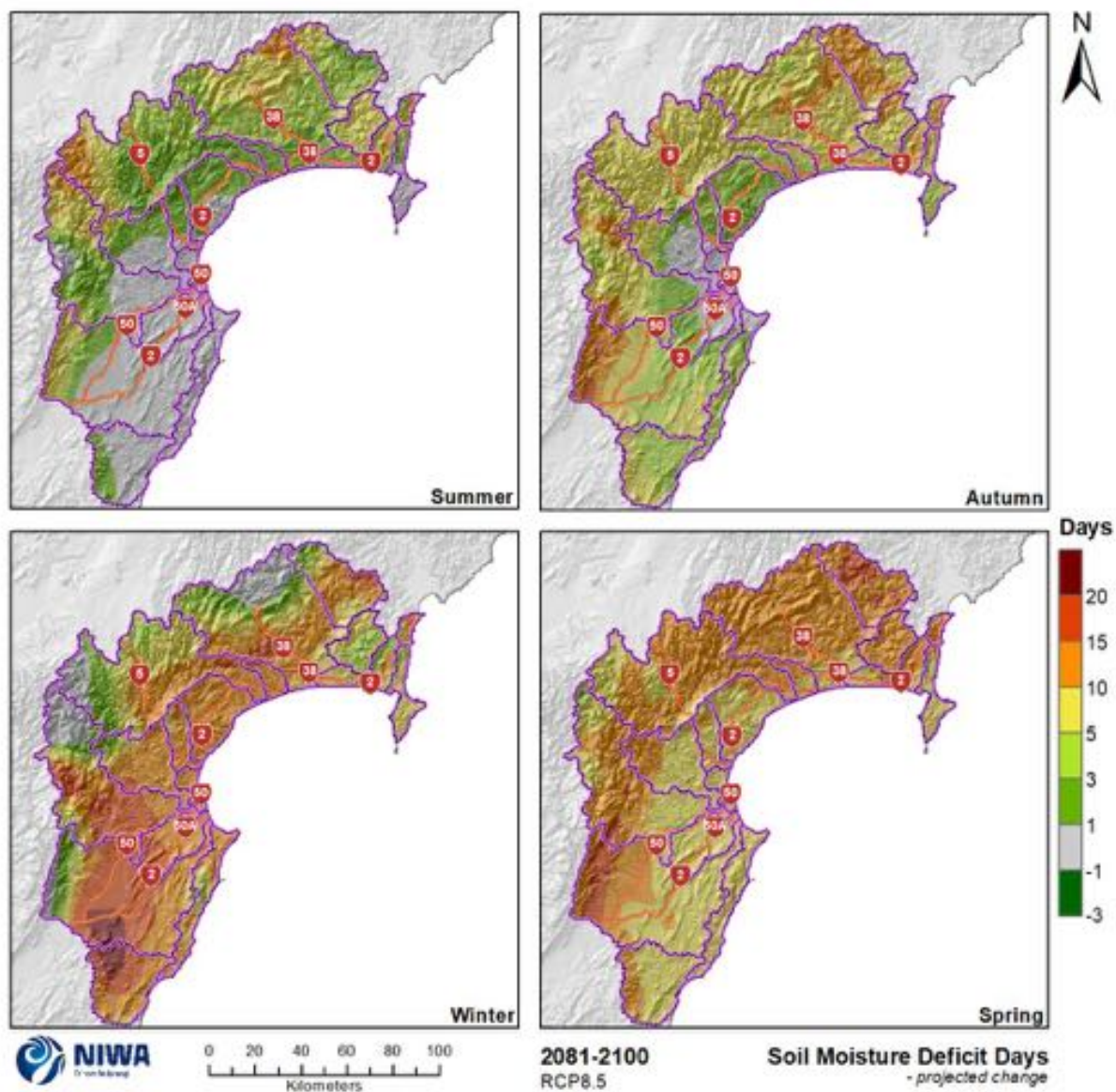


Figure 6-23: Projected change in the number of seasonal soil moisture deficit days for the Hawke's Bay Region by 2090 under RCP8.5. Relative to 1986-2005 average, based on the average of six global climate models. Results are based on dynamical downscaled projections using NIWA's Regional Climate Model. Resolution of projection is 5km x 5km.

Change in Number of Annual Soil Moisture Deficit Days Between 1995 and 2090

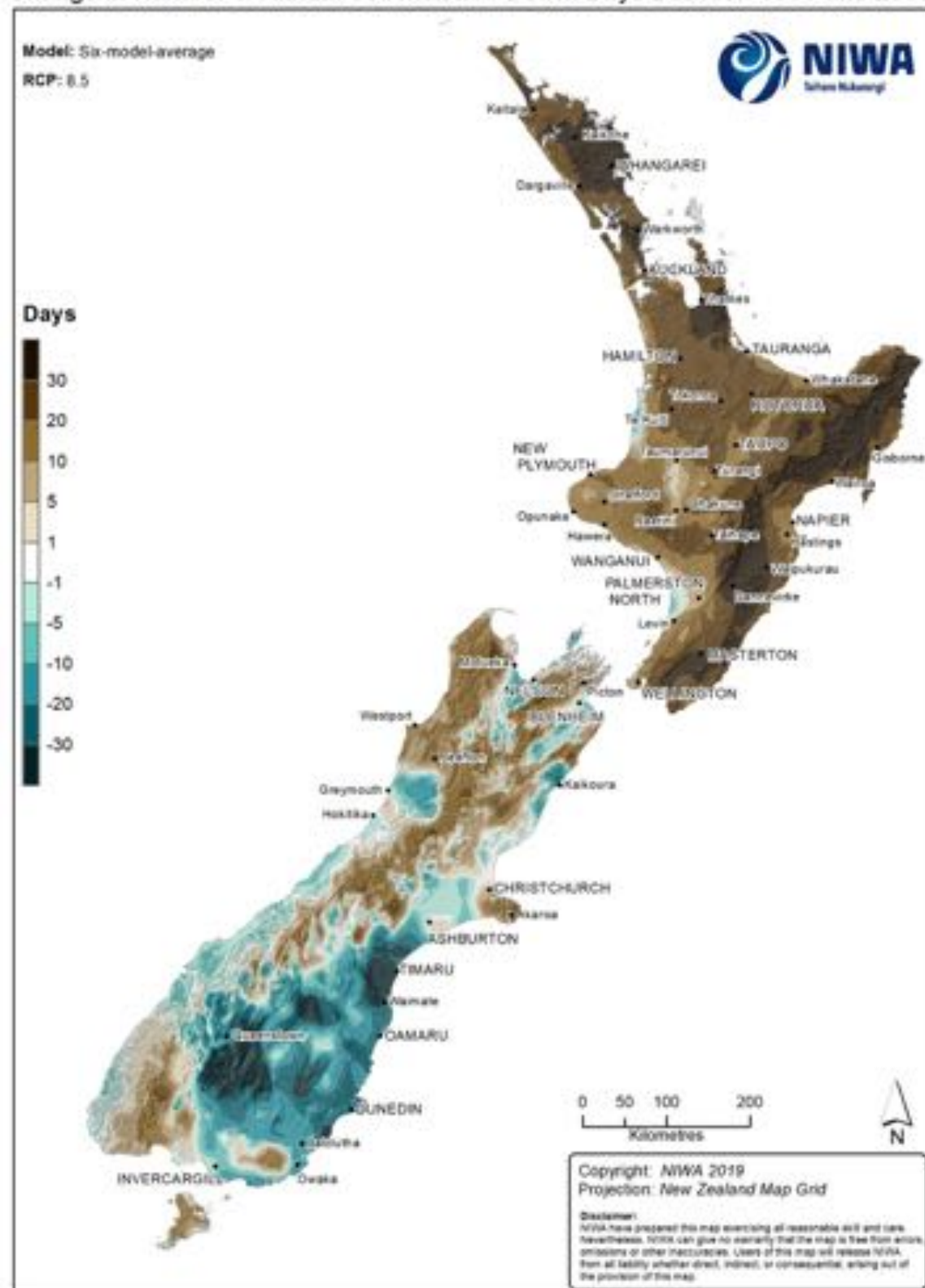


Figure 6-24: Projected change in annual soil moisture deficit days by 2090 under RCP8.5. Relative to 1986-2005 average, based on the average of six global climate models. Results are based on dynamical downscaled projections using NIWA's Regional Climate Model. Resolution of projection is 5km x 5km.

7 Impacts on river flows

7.1 Mean annual discharge

The projected future differences in the annual discharge for RCP4.5 and RCP8.5 at two future time periods are presented in Figure 7-1 for Tairāwhiti and Figure 7-2 for the Hawke's Bay region. At the annual scale, mean discharge across Hawke's Bay region and Tairāwhiti decreases by mid-century across RCPs. By the end of the century, the decrease in mean discharge is accentuated in the north-eastern and south-western area of the Hawke's Bay region and most of Tairāwhiti (above 50% of change) with increasing greenhouse gas concentrations.



Figure 7-1: Percent changes in multi-model median of the mean discharge across Tairāwhiti for mid (top) and late-century (bottom). Climate change scenarios: RCP4.5 (left panels) and RCP8.5 (right panels). Time periods: mid-century (2036-2056) and end-century (2086-2099).



Figure 7-2: Percent changes in multi-model median of the mean discharge across Hawke's Bay region for mid (top) and late-century (bottom). Climate change scenarios: RCP4.5 (left panels) and RCP8.5 (right panels). Time periods: mid-century (2036-2056) and end-century (2086-2099).

7.2 Mean annual low flow

Mean annual low flow (MALF) is defined as the mean of the lowest 7-day average flows in each year of a projection period. Median changes in the MALF are presented for RCP4.5 and RCP8.5 at two time periods in Figure 7-4 for Hawke's bay region and Figure 7-3 for Tairāwhiti. At the annual scale, MALF decreases across RCPs by mid-century across the Hawke's Bay region and Tairāwhiti, with Hawke's Bay's north-eastern area and Tairāwhiti's southern area experiencing large changes. By the end of the century, the decrease in MALF is accentuated, with the decreases exceeding 20%, to nearly all the Hawke's Bay region and Tairāwhiti with increasing greenhouse gas concentrations.

However, under RCP4.5 a number of catchments are expected to see an increase in MALF, as summer rainfall is expected to slightly increase for those catchments.



Figure 7-3: Percent changes in multi-model median of the mean annual low flow (MALF) across Tairāwhiti for mid (top) and late-century (bottom). Climate change scenarios: RCP4.5 (left panels) and RCP8.5 (right panels). Time periods: mid-century (2036-2056) and end-century (2086-2099).

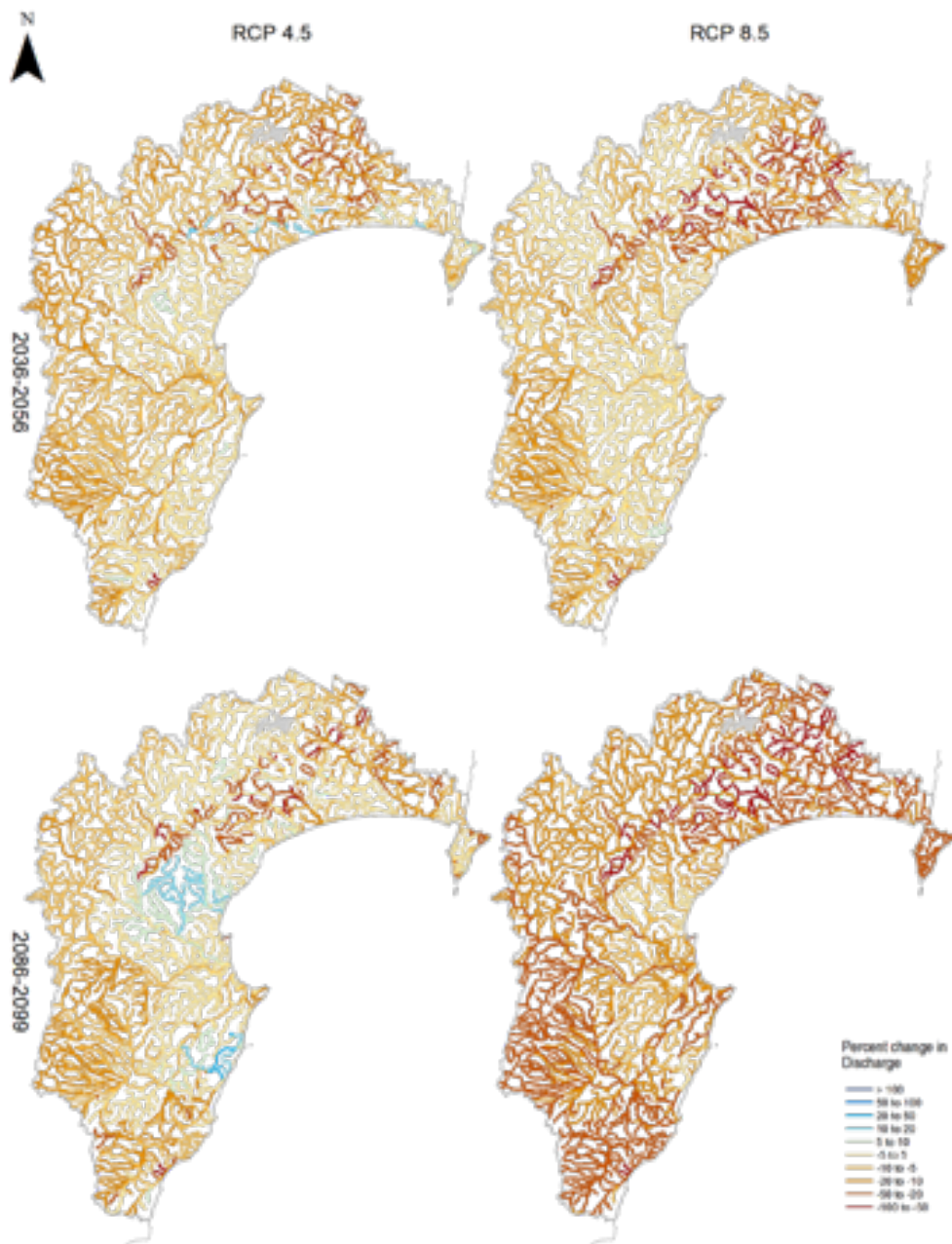


Figure 7-4: Percent changes in multi-model median of the mean annual low flow (MALE) across Hawke's Bay region for mid (top) and late-century (bottom). Climate change scenarios: RCP4.5 (left panels) and RCP8.5 (right panels). Time periods: mid-century (2036-2056) and end-century (2086-2099).

7.3 High flows

The projected future differences in the Q5% flows (flow that is exceeded 5 percent of the time) for RCP4.5 and RCP8.5 at two time periods are presented in Figure 7-5 for Tairāwhiti and Figure 7-6 for Hawke's Bay region.

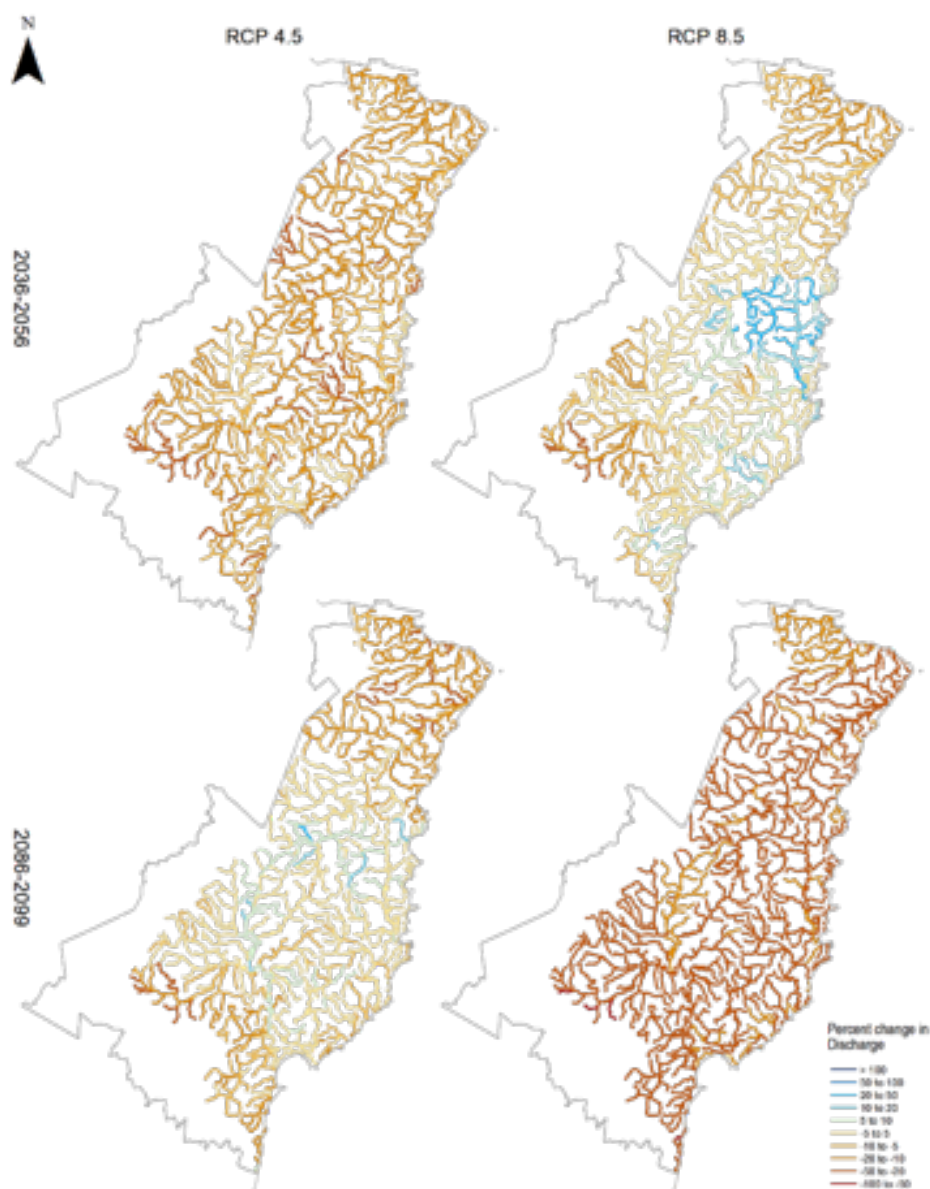


Figure 7-5: Percent changes in multi-model median of the Q5% across Tairāwhiti for mid (top) and late-century (bottom). Climate change scenarios: RCP4.5 (left panels) and RCP8.5 (right panels). Time periods: mid-century (2036-2056) and end-century (2086-2099).

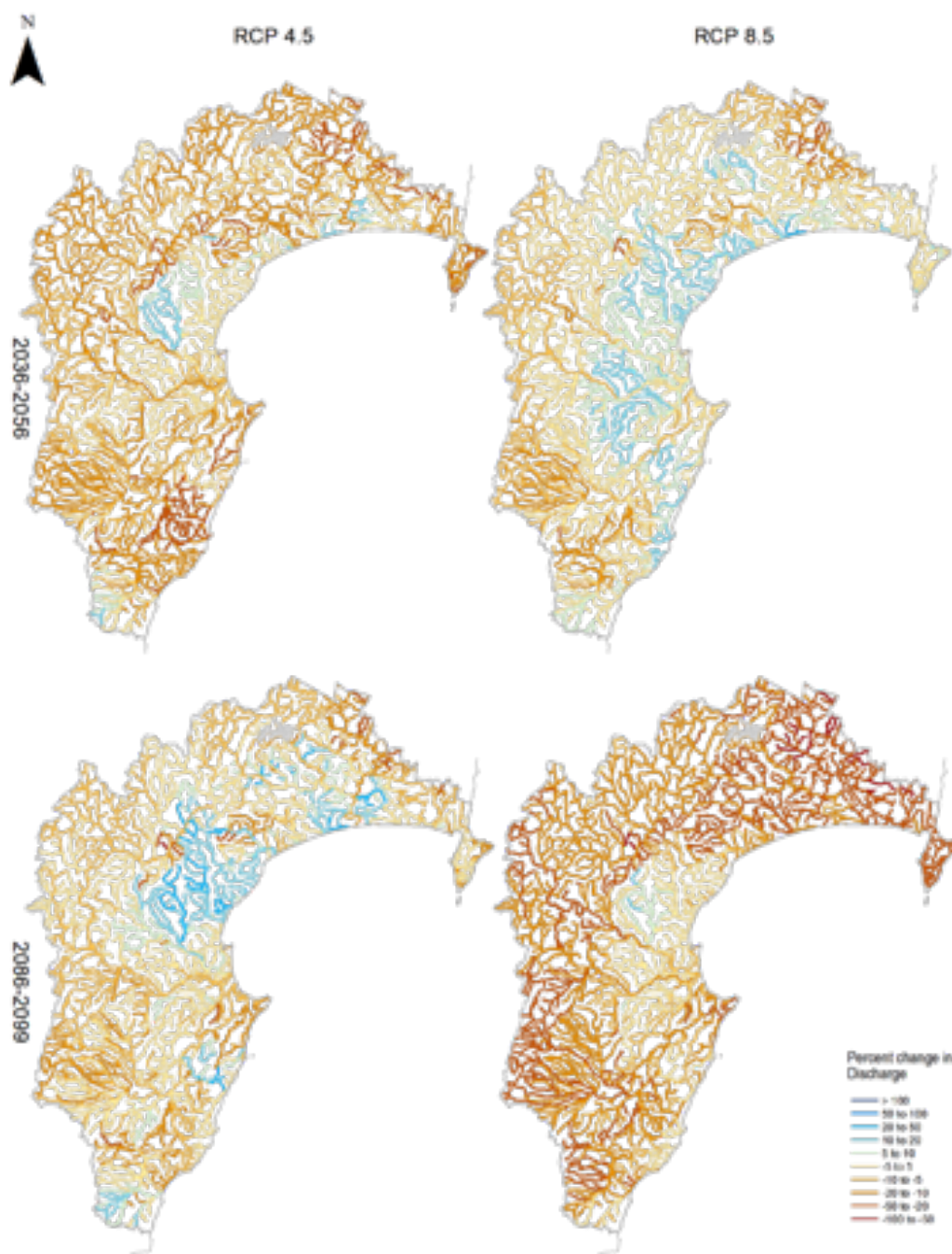


Figure 7-6: Percent changes in multi-model median of the Q5% across Hawke's Bay region for mid (top) and late-century (bottom). Climate change scenarios: RCP4.5 (left panels) and RCP8.5 (right panels). Time periods: mid-century (2036-2056) and end-century (2086-2099).

At the annual time scale, by mid-century larger decreases in high flows (exceeding 20%) are expected under RCP4.5 in the Hawke's Bay region. However, this result cannot be transposed to RCP8.5 as decreases in high flows are smaller and a substantial number of catchments having their headwaters in the mid-range elevations are likely to experience an increase (up to 20%). Similar patterns are

expected in Tairāwhiti, except for the Mangaheia River where an increase in high flows are expected by mid-century under RCP8.5.

By the end of the century the situation is reversed, with more than 75% of the Hawke's Bay region and Tairāwhiti experiencing a decrease in high flows by at least 20% under RCP8.5. These projections of decreasing high flows may seem counterintuitive with rainfall intensities generally projected to increase with more warming. However, the Q5% flow is not considered an 'extreme' flow – it is the flow that is exceeded 5% of the time, i.e. approximately 18 days per year, which is very different to more extreme flows like 1-in-100-year events. Further research and modelling is underway to understand future changes to high flows.

7.4 Mean Annual Flood

The projected future differences in the mean annual flood (MAF; the mean of the series of each year's highest daily mean flow) for RCP4.5 and RCP8.5 at two time periods are presented in Figure 7-7 across Tairāwhiti and Figure 7-8 across the Hawke's Bay region.

At the annual time scale, changes in MAF are spatially diverse with increased greenhouse gas concentrations and time. By mid-century, MAF is expected to increase in a larger number of streams under RCP4.5, than under RCP8.5, with increases located around the central part, the top north-eastern and southern areas of the Hawke's Bay region and headwaters of Tairāwhiti rivers. By the end of the century, MAF is expected to increase with RCP8.5 up to 50% for around half of the Hawke's Bay region's rivers and a smaller proportion of rivers across Tairāwhiti.

A small number of rivers within the Hawke's Bay region will experience an increase in MAF from the headwaters to the outlet at the coast by the end of the century. This does not happen for rivers across Tairāwhiti, except some coastal rivers. For most of the rivers across the Hawke's Bay region and Tairāwhiti, there is no noticeable change in MAF in the river headwaters but large MAF decreases (at least 20%) are expected for the Mangaheia and Pakarae rivers in Tairāwhiti.

The increase in MAF is a change that is largely consistent with the changes to rainfall presented in Ministry for the Environment (2018), especially regarding the 99th percentile of daily rainfall. Analysis of flow records indicates that MAF has a strong correspondence with observed mean annual rainfall (Henderson et al., 2018). It is noteworthy that flood design standards for significant infrastructure are usually made based on events with annual exceedance probabilities much smaller than that represented by MAF. Analysis of RCM rainfall projections undertaken for the High Intensity Rainfall Design project (Carey-Smith et al., 2018), has shown that events with small annual exceedance probability are projected to increase ubiquitously across the country in a way that scales with increasing temperatures. As such, MAF should not be considered a comprehensive metric for the possible impact of climate change on New Zealand flooding.

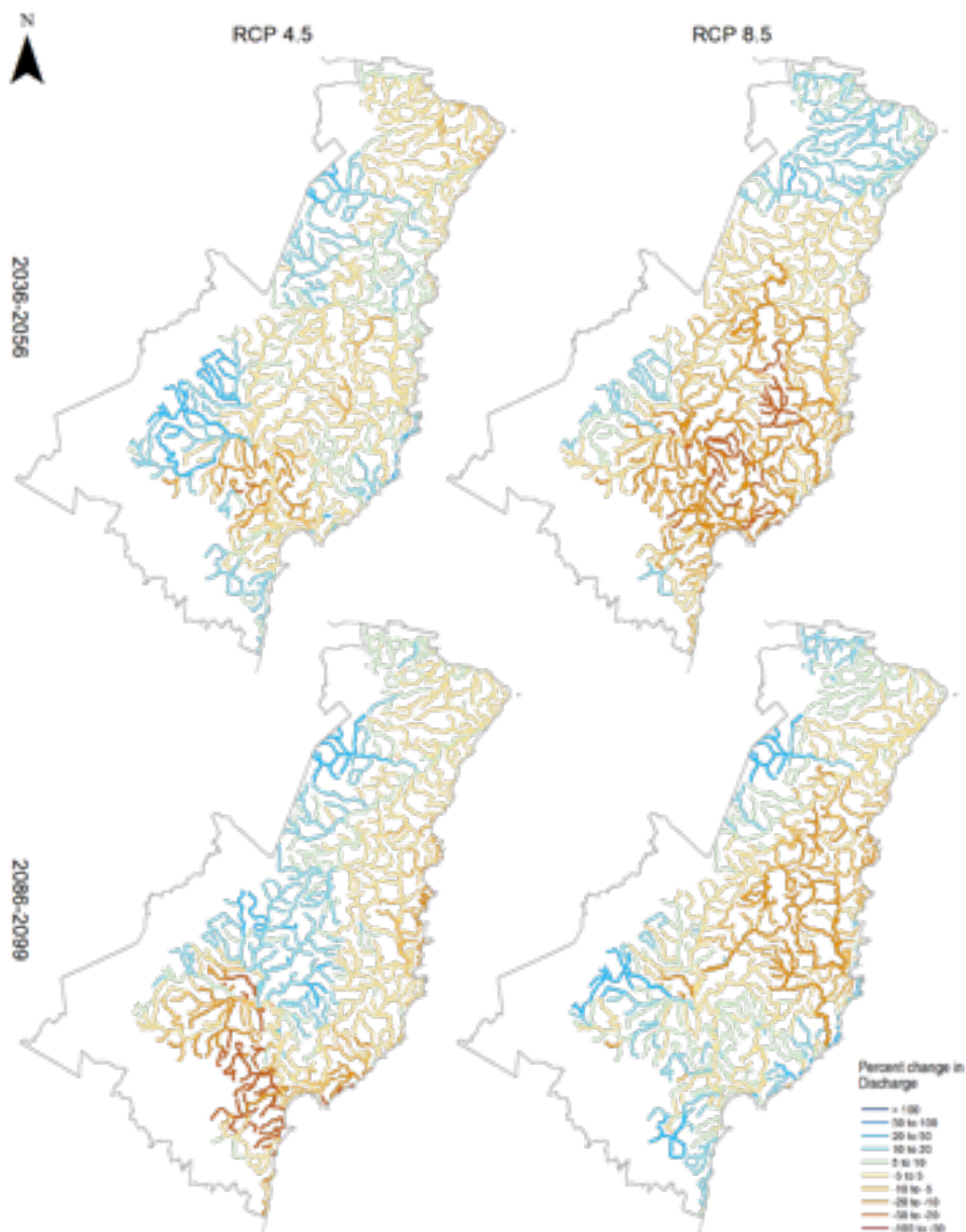


Figure 7-7: Percent changes in multi-model median of the mean annual flood (MAF across Tairāwhiti for mid (top) and late-century (bottom). Climate change scenarios: RCP4.5 (left panels) and RCP8.5 (right panels). Time periods: mid-century (2036-2056) and end-century (2086-2099).

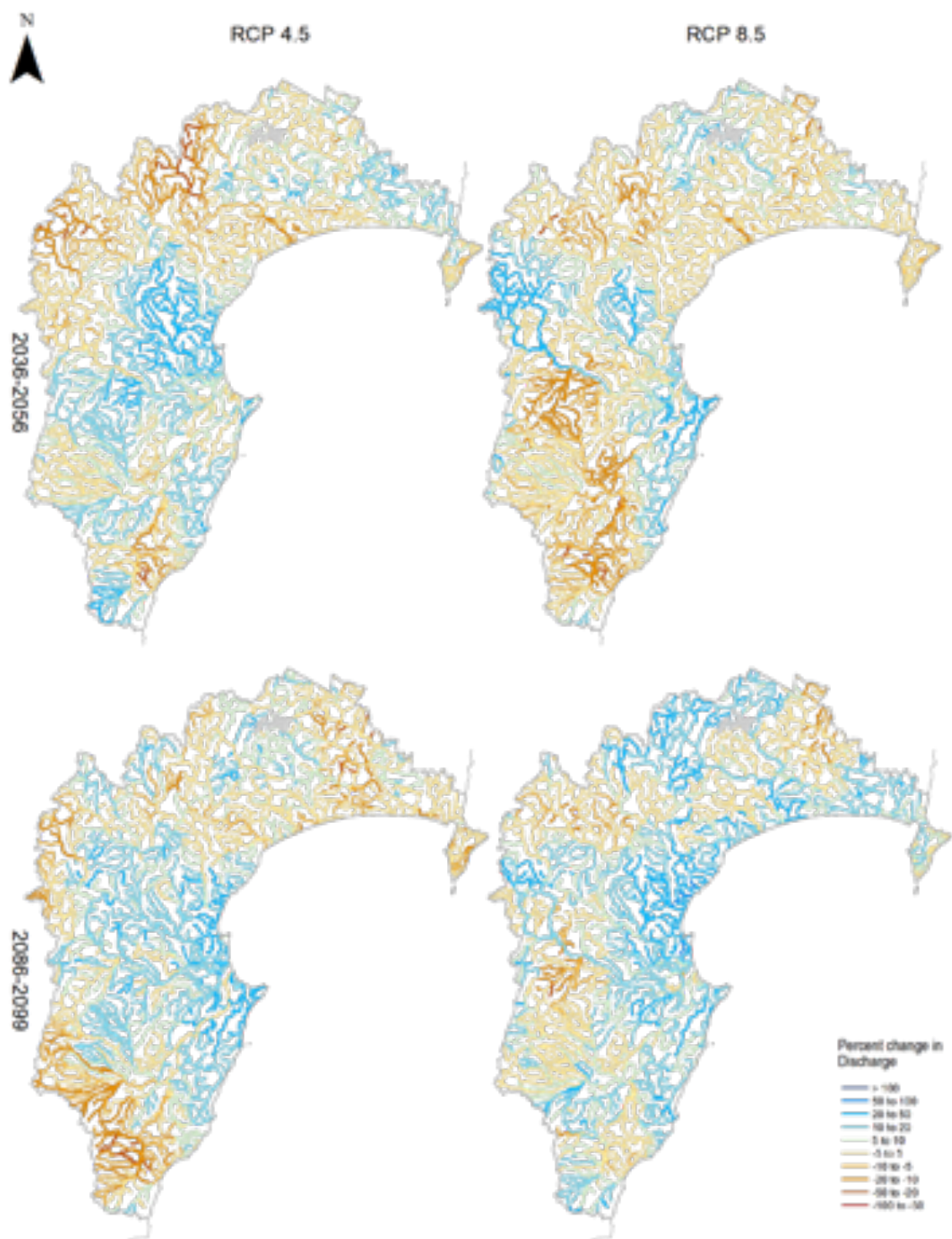


Figure 7-8: Percent changes in multi-model median of the mean annual flood (MAF) across Hawke's Bay region for mid (top) and late-century (bottom). Climate change scenarios: RCP4.5 (left panels) and RCP8.5 (right panels). Time periods: mid-century (2036-2056) and end-century (2086-2099).

8 Sea-level rise and coastal erosion

This section covers variability in seasonal and annual mean sea level (MSL) and historic trends in the Tairāwhiti-Hawke's Bay region alongside future New Zealand projections of sea-level rise (SLR), relative to a baseline period 1986–2005 used by IPCC. Present-day normal high-tide and storm-tide exceedance levels are provided with an indication of the changing frequency of occurrence on the back of rising seas. A general understanding of how storm surge, waves and coastal shoreline position will respond is provided.

A summary of the coastal risk exposure in the Tairāwhiti-Hawke's Bay region is given for areas where LiDAR¹³ surveys have been undertaken.

8.1 Datums and mean sea level

In the Tairāwhiti-Hawke's Bay region several vertical datums are used, with each region using a distinct Local Vertical Datum (LVD) to relate to Chart Datum (CD) allowing the calculation of MSL (Table 8-1; Figure 8-1). In Tairāwhiti, the Gisborne Vertical Datum 1926 (GVD-26) is routinely used for datum offsets and is 1.0546 m above CD. Within the Hawke's Bay Region, the Napier Vertical Datum 1962 (NVD-62) is used for datum offset and is 0.9243 m above CD. The New Zealand Vertical Datum 2016 (NZVD-2016) is now the official vertical datum for New Zealand and its offshore islands, and its relationship to the LVDs is shown in Table 8-1 and Figure 8-1. Annual MSL for the two gauges are shown in Figure 8-2 and Figure 8-3.

Table 8-1: Mean sea level and datum offsets at Gisborne and Napier. Note that for Napier, the average MSL value for the 2011-2019 period is also presented because this value was used for the calculation of relative sea-level rise (RSLR) in Section 8.3, consistent with the averaging period used for Gisborne.

Sea-level gauge location	Local vertical datum	Chart Datum (or gauge zero)	NZVD-2016	Mean sea level	Averaging period
Gisborne	GVD-26	-1.0546 m (GVD-26)	+0.338 m (GVD-26)	+0.20 m (GVD-26)	2011–2019
Napier	NVD-62	-0.9243 m (NVD-62)	+0.193 m (NVD-62)	+0.04 m (NVD-62)	1989–2019
				+0.08 m (NVD-62)	2011-2019 (for RSLR)

¹³ Light Detection and Ranging (LiDAR) is a remote sensing method that measures distances to the Earth using laser light. LiDAR measurements can be used to generate high-resolution digital elevation models (DEMs).

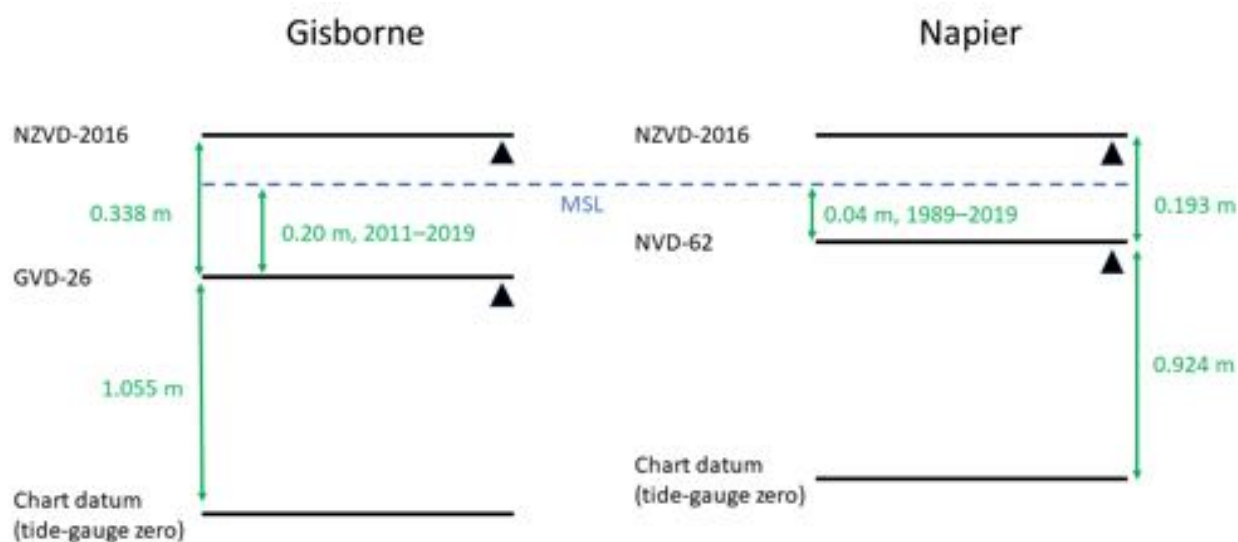


Figure 8-1: Mean sea level and datum offsets at Gisborne and Napier.

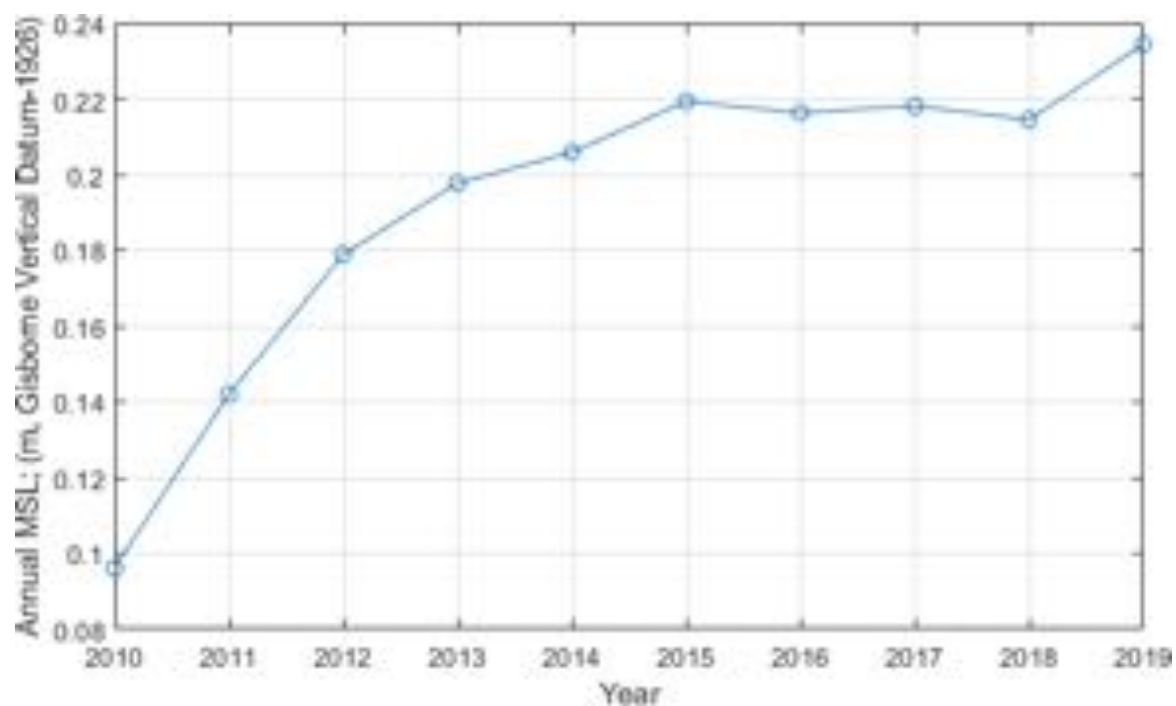


Figure 8-2: Annual MSL at the Port of Gisborne. The digital record covers the period of 2010-2019.

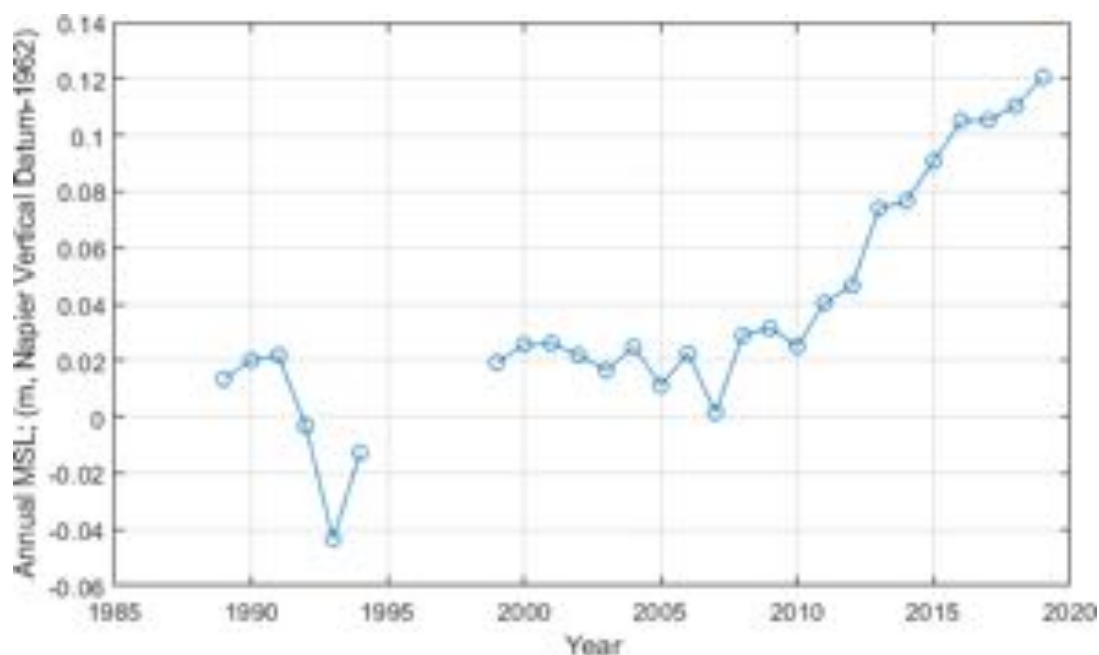


Figure 8-3: Annual MSL at the Port of Napier. The digital record covers the period of 1989-2019.

8.2 Impacts of sea-level rise

One of the major and most certain (and so foreseeable) consequences of increasing concentrations of carbon dioxide¹⁴ and associated warming, is the rising sea level (Parliamentary Commissioner for the Environment, 2015). IPCC (2013) found that warming of the climate system is unequivocal, and many of the changes observed since the 1950s are unprecedented over timescales of decades to millennia. The atmosphere and ocean have warmed, the amounts of snow and ice globally have diminished, causing sea level to rise.

Rising sea level in past decades is already affecting human activities and infrastructure in coastal parts of New Zealand, with a higher base mean sea level contributing to increased vulnerability to storms and tsunamis. Key impacts of an ongoing rise in sea level relative to the land surface are:

- gradual inundation of low-lying marsh and adjoining dry land on spring high tides;
- escalation in the frequency of nuisance and damaging coastal flooding events (which has been evident in several low-lying coastal margins of New Zealand);
- exacerbated erosion of sand/gravel shorelines and unconsolidated cliffs (unless sediment supply increases);
- increased incursion of saltwater in lowland rivers and nearby groundwater aquifers, raising water tables in tidally influenced groundwater systems.

These impacts will have increasing implications for existing development in coastal areas, along with environmental, societal and cultural effects. Infrastructure and its levels of service or performance will be increasingly affected, such as wastewater treatment plants, potable water supplies, and particularly capacity and performance issues with stormwater and overland drainage systems (particularly gravity-driven networks). Transport infrastructure (roads, ports, airports) in the coastal

¹⁴ Global average now above 400 ppm.

margin will also be affected, both by increased nuisance shallow flooding of saltwater (e.g., vehicle corrosion) and more disruptive flooding and damage from elevated storm-tides and wave overtopping.

There are three types of SLR in relation to observations and projections:

- absolute (or eustatic) rise in ocean levels, measured relative to the centre of the Earth, and usually expressed as a global mean (which is used in most sea-level projections e.g., IPCC);
- offsets (or departures) from the global mean absolute SLR for a regional sea, e.g., the sea around New Zealand, which will experience slightly higher rises (5–10%) than the global average rate. There can be significant variation in the response to warming and wind patterns between different regional seas around the Earth;
- relative sea-level rise (RSLR), which is the net rise in sea level experienced on coastal margins from absolute sea-level rise, regional-sea offsets, and local vertical land movement (measured relative to the local landmass). Local or regional adaptation to SLR needs to focus on RSLR, particularly if the coastal margin is subsiding.

The first two types of SLR are measured directly by satellites, using radar altimeters, or by coalescing many tide-gauge records globally (after adjusting for local vertical land movement and ongoing readjustments in the Earth's crust following ice loading during the last Ice Age¹⁵).

RSLR is measured directly by tide gauges. One advantage of knowing the RSLR from gauge measurements is that this directly tracks the SLR that needs to be adapted to locally, or over the wider region represented by the gauge. If, for instance, the local landmass is subsiding, then the RSLR will be larger than the absolute rise in the adjacent ocean level acting alone.

8.3 Historic trend in SLR focused on Gisborne and Hawke's Bay

Hannah and Bell (2012) analysed SLR trends at 10 gauge sites around New Zealand, to extend the picture of local trends at a wider range of locations than just the four main port sites (Auckland, Wellington, Lyttelton, Dunedin), where records exist from 1900 onwards. While the additional 6 sites (Whangarei, Moturiki, New Plymouth, Nelson, Timaru, and Bluff) comprised shorter records, longer term SLR could be inferred by connecting the modern digital records with historic tide measurements (from LINZ archives) used to establish the local vertical datums around New Zealand. At Gisborne and Napier, a digital sea-level record exists from 2004 and 1989, respectively. However, the Gisborne record contains many level shifts before 2011 and so can't be used to establish annual MSL, but we are confident that the data from 2011 onward are reliable. Neither of the records at Napier or Gisborne are long enough for establishing long-term linear RSLR trends without an earlier anchoring point—generally ≥ 50 years is required. However, if we assume a zero MSL at the time the local vertical datums were established in 1926 (Gisborne) and 1962 (Napier), we can form a longer linear trend and provide an anchor point for estimating RSLR. Therefore, using the 2011-2019 average MSL values (Gisborne and Napier) in Table 8-1, divided by the time since LVD inception (93 years for Gisborne, 57 years for Napier) we obtain a RSLR of 2.15 and 1.40 mm/year at Gisborne and Napier respectively.

¹⁵ Scientific term is glacial isostatic adjustment (GIA)

Records from all four main New Zealand port tide gauges (> 110-year records) indicates a doubling in the rate of sea-level rise around the New Zealand coastline over the last five to six decades, from an average of approximately 1 mm/year earlier last century to nearly 2 mm/year from 1961 to 2015 (MfE, 2017). A summary of historic rates of relative SLR across 10 sites in New Zealand is provided in Figure 8-4, with the New Zealand wide average of nearly 1.8 mm/year up to 2015.

Global coverage (between 66°N and 66°S) of satellite altimeters, which measure the ocean surface, commenced in 1993. The global-average rate for absolute SLR from satellite altimetry in the period 1993 to 1 June 2018 is running at ~ 3.2 mm/year, which is about twice the long-term global rate since 1900. In the ocean waters around New Zealand, the trend since 1993 to present has been higher than the global average, with absolute SLR in the Tairāwhiti/Hawke's Bay region trending at around 4 mm/year (Figure 8-5). The NZ-wide average was 4.4 mm/year up to the end of 2015 (see Figure D3, Appendices; MfE, 2017). Some of this increase in the rate of rise is due to the Interdecadal Pacific Oscillation (IPO), a 20–30-year climate cycle, which is in its negative phase at present, leading to increased sea-surface temperature and therefore sea-surface height in the Western Pacific (see darker colours in Figure 8-5), but also is influenced by a warming atmosphere.

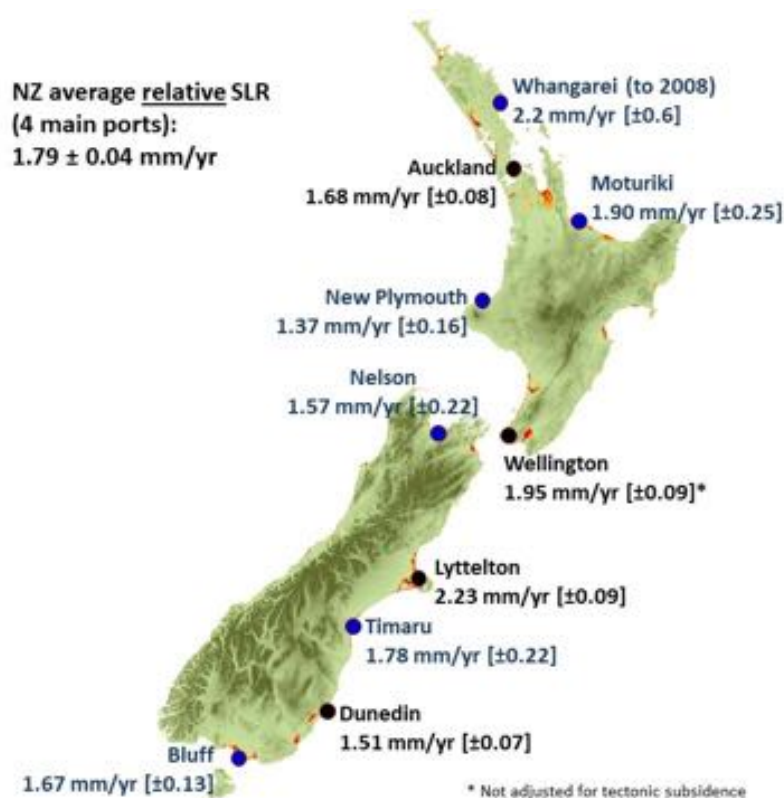


Figure 8-4: Relative SLR rates up to and including 2019 (excluding Whangarei), determined from longer sea-level gauge records at the four main ports (Auckland, Wellington, Lyttelton, Dunedin) and shorter records from the remaining sites. Determined from > 100-year gauge records at the four main ports (black circles) and inferred rates from gauge station records, used in the first half of the 1900s to set the local vertical datums, spliced with modern records (blue circles). Standard deviations of the trend are listed in the brackets. Source: Figure 19; MfE (2017).

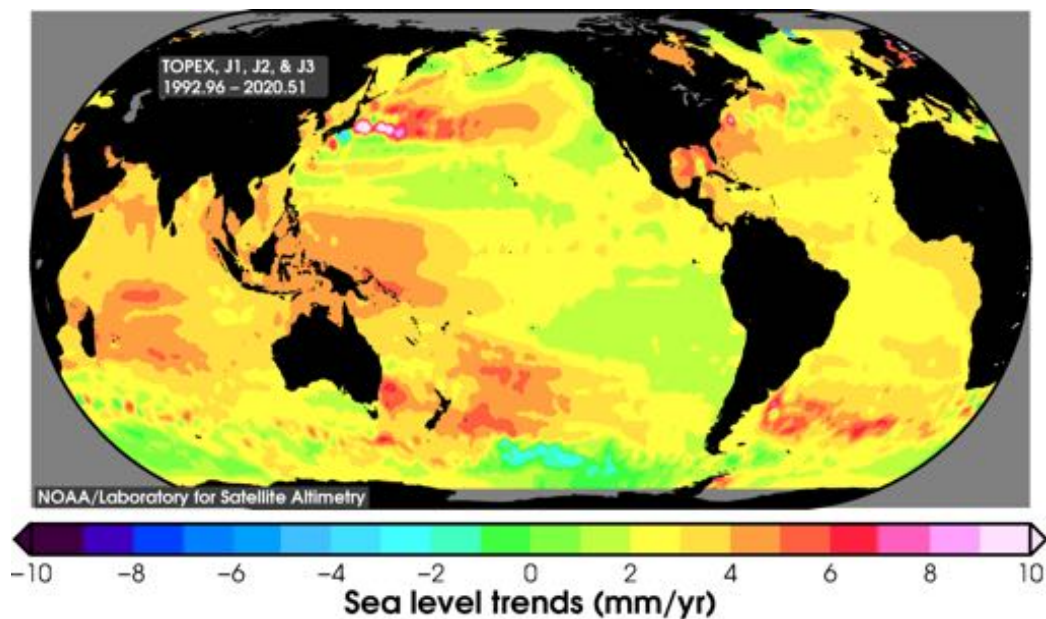


Figure 8-5: Map of regional trend in SLR from 1993 to 1 September 2020 based on satellite altimetry missions. Source: NOAA/NESDIS Center for Satellite Applications and Research.

Relative SLR along the Tairāwhiti-Hawke's Bay region also incorporates a component due to vertical land movement (VLM). Continuous GPS stations have been operated along the coast in the region by GeoNet and LINZ since 2005. Up to 2011, the vertical land movement was a combination of small uplift and subsidence rates of < 0.3 mm/year (Figure 8-6; Beavan and Litchfield, 2012). At certain locations larger rates have been estimated, most notable, MAHI (0.5 mm/yr; Mahia), CKID (1.6 mm/yr; Cape Kidnappers), PUKE (1.6 mm/yr; Waiau Rd). LEYL (-2.3 mm/yr; Leyland Rd), WAHU (-1.1 mm/yr; Mohaka), PARI (-3.4 mm/yr; Paritu Rd).

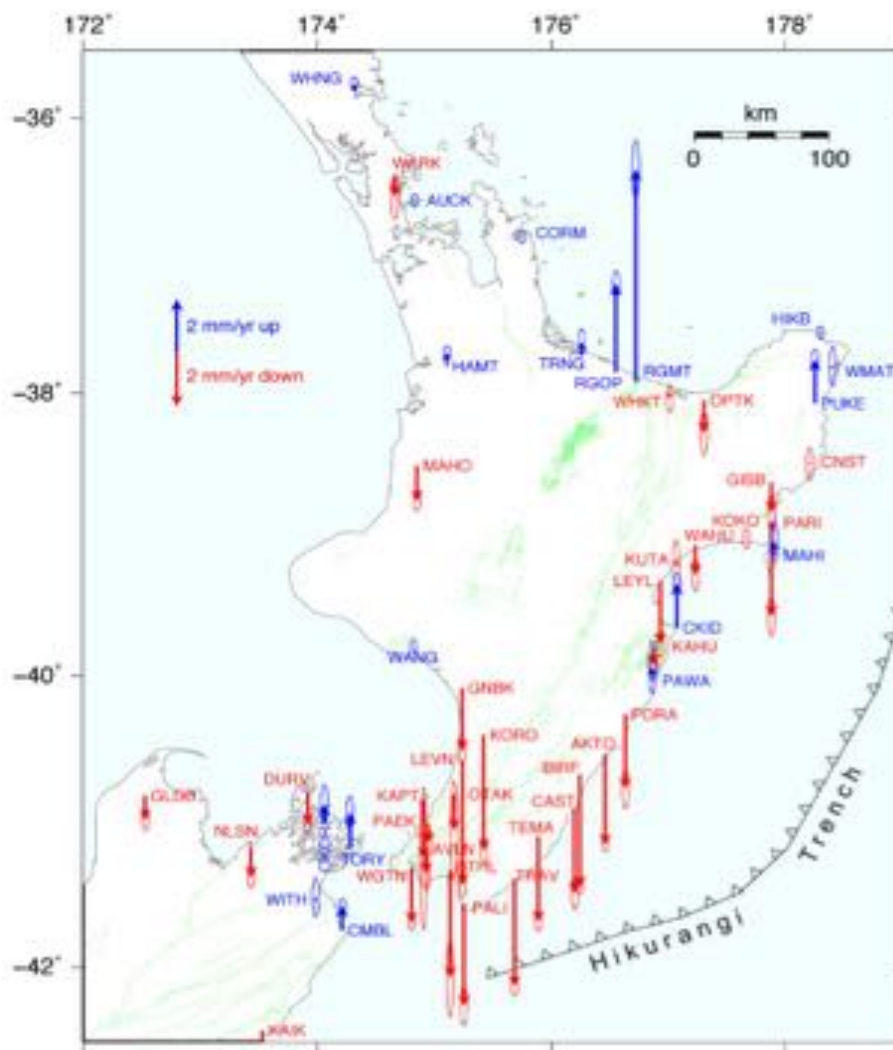


Figure 8-6: Average vertical land movement for near-coastal continuous GPS Sites across the North Island, New Zealand. Blue arrows show average uplift and red arrows average subsidence over around a 10-year period up to 2011. Source: Beavan and Litchfield (2012).

Further updated analysis on vertical land movement around New Zealand, and the implications for long-term sea-level rise, is a component of a new Endeavour Fund research project NZSeaRise, coordinated by Victoria University of Wellington.

In the interim, for the Tairāwhiti-Hawke's Bay region, the above results indicate that mostly in the region only small rates of subsidence and uplift¹⁶ are presently occurring (but uncertain whether they will persist for decades), so the New Zealand-wide SLR scenarios in the Coastal Guidance (Chapter 5; MfE 2017) should be applied directly to the Tairāwhiti-Hawke's Bay coastal margin without any adjustment (as would definitely be required for subsidence) and the historic rate of SLR within the region is close to the New Zealand average.

¹⁶ Uplift means the relative SLR is smaller than the absolute rise in the ocean surface (subsidence means it is larger)

8.4 Projections for New Zealand sea-level rise.

A synthesis of the historic and future projections of SLR, both globally and for New Zealand, is available in the Ministry for the Environment (MfE) guidance for local government: Coastal Hazards and Climate Change (MfE, 2017) and an accompanying Summary¹⁷ and set of Fact Sheets¹⁸.

Chapter 5 of the Coastal Guidance provides four specific New-Zealand based SLR scenarios to use when assessing and planning adaptation to coastal climate change in New Zealand (Figure 8-7). The SLR scenarios in the Coastal Guidance largely follow the synthesis of the IPCC Fifth Assessment Report (IPCC, 2013, Church et al., 2013), but are extended from 2100 to 2150, utilising the longer-range probabilistic projections of Kopp et al. (2014) Further, an adjustment has been made for ocean waters around New Zealand, where climate-ocean models have shown that SLR in our Pacific region will be somewhat higher than the global average rise – with IPCC projections couched in terms of the global average. The adjustment built into the New Zealand scenarios, for the regional ocean around New Zealand, is up to 0.05 m by 2100 for the higher RCP scenarios. A lesser pro-rata increment applies for the lower concentration RCPs.

The Coastal Guidance also listed a table of the time periods for which increments of SLR (relative to the 1986–2005 baseline) could be reached for the four different scenarios (Table 8-2). This information on time brackets can be applied to low-lying coastal areas, once the adaptation threshold SLR is known and agreed on from hazard and risk assessments, beyond which outcomes are not tolerable. All the details on developing firstly, hazard and risk assessments, then adaptation plans using the SLR scenarios, are available in the Coastal Guidance and Appendices (MfE, 2017).

Table E-1, Appendices of MfE (2017) lists local values of sea level to use around New Zealand for the baseline (generally the 1986–2005 average MSL), to which the SLR projections are added—being 0.17 m GVD-26 and 0.02 m NVD-62 respectively for the Tairāwhiti or Hawke's Bay region when adding future SLR projections from Table 8-2 or Figure 8-7.

Figure 8-7 shows the projected SLR for the four scenarios (MfE, 2017). Due to the closeness of trajectories between the high and low projections in the near term, it is not possible to distinguish which path New Zealand SLR measurements will follow and may require another 1–2 decades of monitoring to conclusively determine which RCP trajectory applies. But, SLR trajectories (relative to the RCP scenarios) may change again in the future if polar ice-sheet instabilities emerge later this century and/or global emissions continue to track high or indeed global emissions may be substantially reduced if the 2015 Paris Agreement is adhered to. This future uncertainty is the reason why the Coastal Guidance (MfE 2017) recommends the use of all four SLR scenarios to plan for and test adaptation options in an adaptive planning framework. Thus, considering the IPCC projections with respect to the both Gisborne and Napier, changes in AMSL are compared to RCP projections (Figure 8-8 and Figure 8-9) relative to their respective LVDs. Finally, both Gisborne and Napier (alongside the Moturiki gauge, Bay of Plenty) records are displayed relative to the 1986-2005 IPCC baseline (Figure 8-10).

¹⁷ <http://www.mfe.govt.nz/publications/climate-change/preparing-coastal-change-summary-of-coastal-hazards-and-climate-change>

¹⁸ <http://www.mfe.govt.nz/publications/climate-change/preparing-coastal-change-fact-sheet-series>

Table 8-2: Approximate years, from possible earliest to latest, when specific sea-level rise increments (metres above 1986–2005 baseline) could be reached for various projection scenarios of SLR for the wider New Zealand region. The earliest year listed is based on the RCP8.5 (83rd percentile) or H+ projection and the next three columns are based on the New Zealand median scenarios, with the latest possible year assumed to be from a scenario following RCP2.6 (median), which approximates the fully globally-implemented Paris Agreement. [Source: Table 11 in; MfE 2017]. Note: year for achieving the SLR is listed to the nearest five-year value.

Approximate year for the relevant New Zealand-wide SLR percentile scenario to reach increments of SLR (relative to baseline of 1986–2005)				
SLR (m)	Year achieved for RCP8.5 H+ (83%ile)	Year achieved for RCP8.5 (median)	Year achieved for RCP4.5 (median)	Year achieved for RCP2.6 (median)
0.3	2055	2065	2075	2080
0.4	2060	2075	2090	2105
0.5	2070	2085	2105	2125
0.6	2080	2090	2120	2150
0.7	2085	2100	2135	2175
0.8	2090	2105	2150	2200
0.9	2095	2115	2165	>2200
1.0	2105	2120	2180	>2200
1.2	2115	2140	>2200	>2200
1.5	2135	2165	>2200	>2200
1.8	2150	2190	>2200	>2200
1.9	2155	2200	>2200	>2200

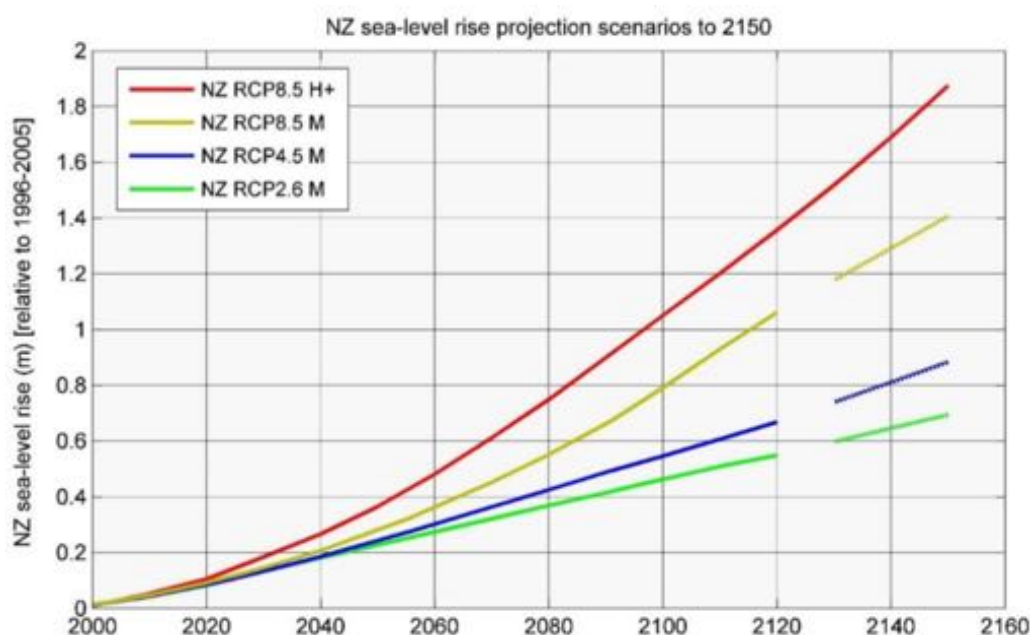


Figure 8-7: Four scenarios of New Zealand-wide regional SLR projections, with extensions to 2150. Based on Kopp et al. (2014)–K14. New Zealand scenario trajectories are out to 2120 (covering a minimum planning timeframe of at least 100 years), and the NZ H+ scenario trajectory is out to 2150 from K14. No further extrapolation of the IPCC-based scenarios beyond 2120 was possible, hence the rate of rise for K14 median projections for RCP2.6, RCP4.5 and RCP8.5 are shown as dashed lines from 2130, to provide an indication of the extension of projections to 2150. Note: All scenarios include a small SLR offset from the global mean SLR for the regional sea around New Zealand. Source: Figure 27, MfE (2017).

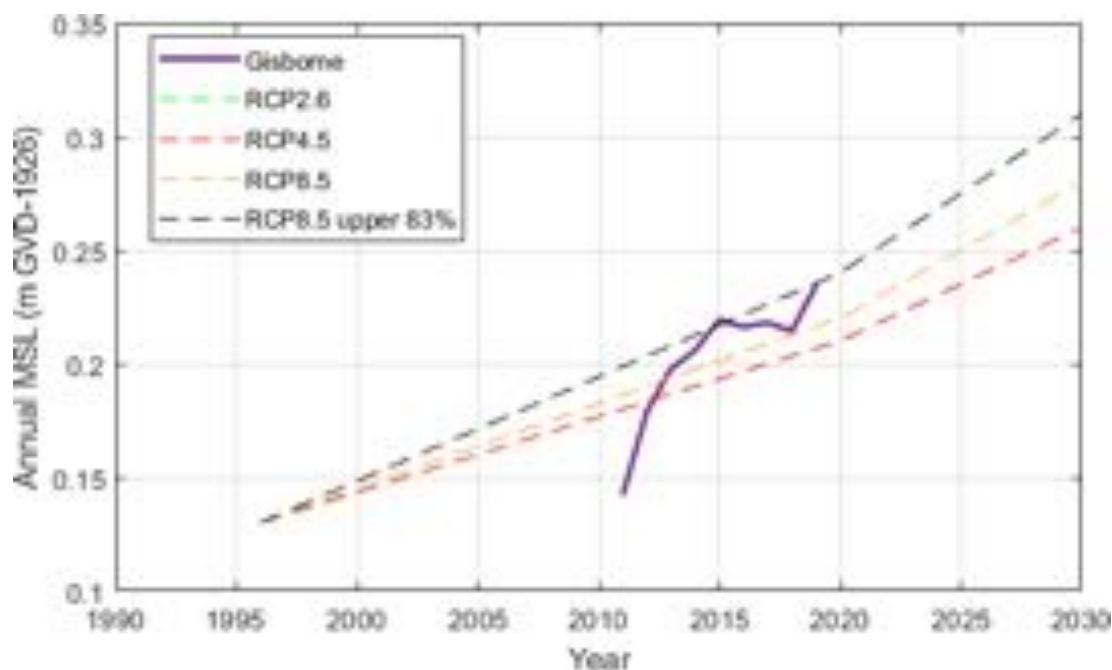


Figure 8-8: Change in annual MSL for Gisborne from 2011–2019. The near-term projections for NZ-based SLR for RCP2.6, RCP4.5 and RCP8.5 are plotted to 2030 (MfE, 2017) and shown relative to GVD-26 (note RCP2.6 and RCP4.5 overlap over this period). The RCP projections were adjusted by 0.13 m manually to match the Gisborne MSL of 0.2 m over the period of 2011–2019.

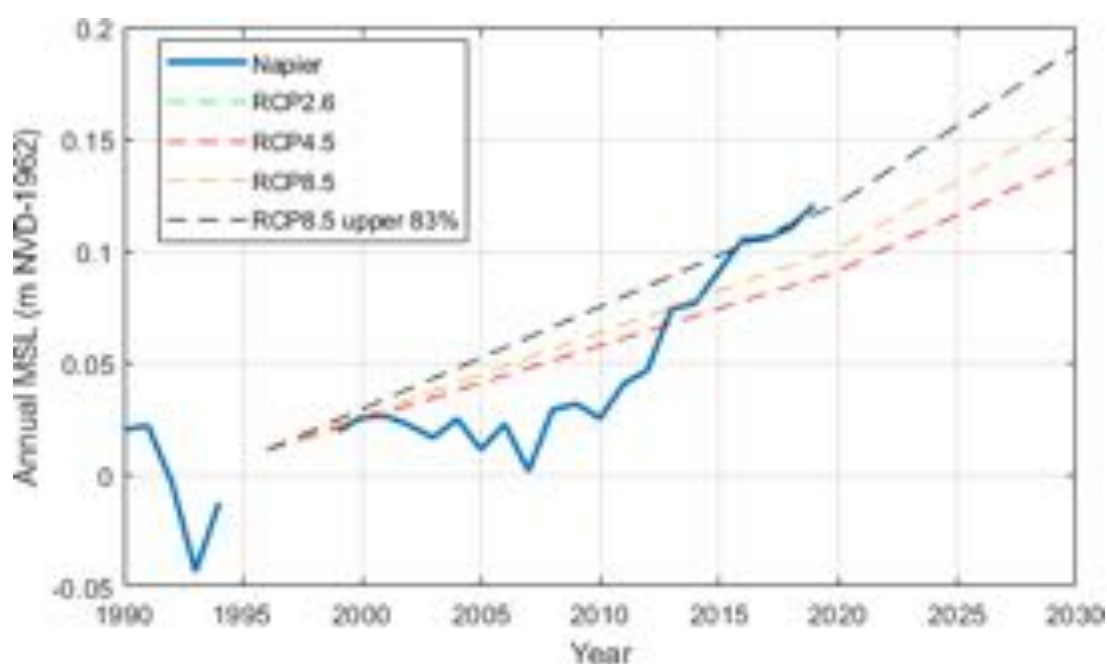


Figure 8-9: Change in annual MSL for Napier from 1990–2019. The near-term projections for NZ-based SLR for RCP2.6, RCP4.5 and RCP8.5 are plotted to 2030 (MfE, 2017) and shown relative to NVD-62. The RCP projections were adjusted by 0.0108 m to match the Napier MSL of 0.97 m over the period 1989–2019.

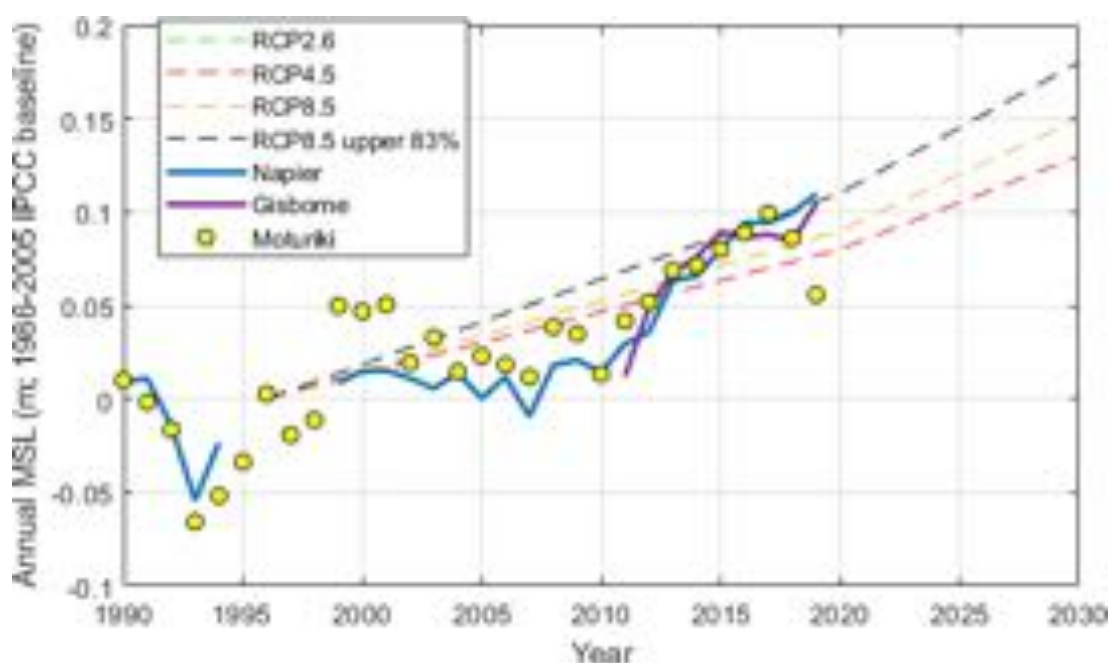


Figure 8-10: Change in annual MSL for Gisborne and Napier from 1990–2019. The near-term projections for NZ-based SLR for RCP2.6, RCP4.5 and RCP8.5 are plotted to 2030 (MfE, 2017). Baseline period is 1986–2005, used in the IPCC AR5 projections. Data from the long-term Moturiki gauge are also shown for reference. Napier record is offset by 0.0108 m based on the 1989–2005 mean. Gisborne record is offset based on a manual offset of 0.13 m relative to the Napier record over the period 2011–2019.

8.5 Tides and the effect of rising sea level

8.5.1 Mean Spring tide levels

The present-day high tide marks are updated regularly by LINZ on their web site¹⁹. The Mean High Water Spring (MHWS) marks are shown in Table 8-3, after converting from chart datum (LINZ) to local vertical datum. The tide marks are based on averages of all spring tides in the 19-year forward period (1 January 2000 - 31 December 2018) using a set of tidal harmonic constituents extracted from the Gisborne and Napier data records.

Table 8-3: Tidal levels at Gisborne and Napier. Metres relative to local vertical datum (GVD-26 and NVD-62). Source: <https://www.linz.govt.nz/sea/tides/tide-predictions/standard-port-tidal-levels>. MHWS = Mean High Water Spring, MHWN = Mean High Water Neap, MLWN = Mean Low Water Neap, MLWS = Mean Low Water Spring.

Standard Port	MHWS	MHWN	MLWN	MLWS	Mean spring range	Mean Sea Level
Gisborne	1.07	0.69	-0.26	-0.65	1.72	0.21
Napier	0.97	0.56	-0.48	-0.84	1.81	0.05

8.5.2 High-tide exceedances and effect of SLR

The full range of possible high tides (excluding weather, climate and SLR influences) was predicted over 100 years, covering all possible tidal combinations, based on tides extracted from both the Gisborne and Napier sea level records. Maximum High Water, Lowest Neap High Tides, and High Tide Range are shown in Table 8-4. The resulting high-tide exceedance curves are shown, as the lower curve in Figure 8-11 and Figure 8-12 for Gisborne and Napier, respectively, in the form of a cumulative frequency of occurrence of high waters and with levels relative to NZVD-2016 (top panel) and local vertical datum (bottom panel).

Table 8-4: High-tide values from 100 year tidal predictions for both Gisborne and Napier.

Standard Port	Maximum High Water	Lowest Neap High Tide	High Tide Range
Gisborne	0.93 m (GVD-26)	0.37 m (GVD-26)	0.57 m
	0.60 m (NZVD-2016)	0.2 m (NZVD-2016)	
Napier	1.06 m (NVD-62)	0.39 m (NVD-62)	0.67 m
	0.87 m (NZVD-2016)	0.2 m (NZVD-2016).	

In Figure 8-11 and Figure 8-12, the other high-tide mark shown is the Mean High Water Spring 10 percentile (MHWS-10), which at 0.77 m (GVD-26) or 0.43 m (NZVD-2016) for Gisborne and 0.86 m (NVD-62) or 0.67 m (NZVD-2016) for Napier, is the high tide above which only 10% of all predicted high tides exceed it for the present-day situation. MHWS-10, which can be consistently defined around the New Zealand coast, was used in the recent national coastal risk exposure study for the Parliamentary Commissioner for the Environment (PCE) in 2015 (Bell et al., 2015, PCE, 2015). As a comparison, the LINZ-defined MHWS level from the previous sub-section (7.5.1) for Gisborne is exceeded by 9.5% of all high tides and for Napier, 14% of all high tides.

¹⁹ <https://www.linz.govt.nz/sea/tides/tide-predictions/standard-port-tidal-levels>

Putting aside storm events, SLR will continually lift the base MSL, on which the tide rides, which will result in an increasing percentage of normal high tides which exceed a given present-day elevation e.g., street level, berm or stopbank crest or present MHWS-10. Figure 8-11 and Figure 8-12 for Gisborne and Napier respectively show the effect of changing high-tide inundation using two example SLR values of 0.4 and 0.8 m SLR (Table 8-2 shows that 0.4 m SLR would arise between 2060–2105, while the latter between 2090–2200). Based on the example of the present-day MHWS-10 level, which is exceeded by only 10% of all high tides (tide only), a 0.4 m SLR will mean that same ground or tidal elevation will be exceeded by 100% of all high tides (up from 10%) These results exclude the influence of weather and storm surges on water level and assume the tidal characteristics for Tairāwhiti/Hawke's bay region don't change substantially – rather they focus just on normal upper tidal inundation levels as seas rise.

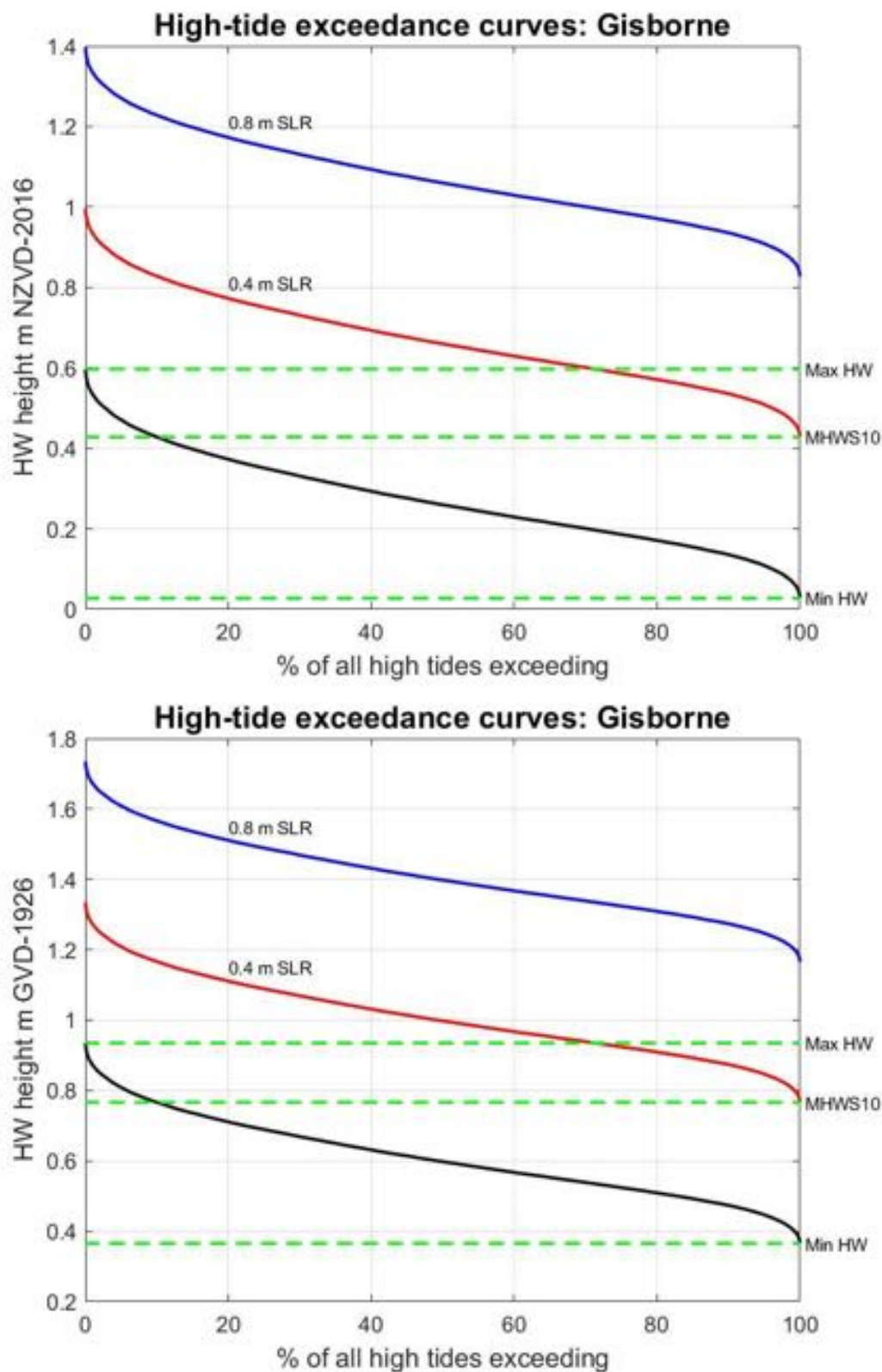


Figure 8-11: High-tide exceedance curve for all predicted high tides at Gisborne (excluding effects of weather, climate and SLR). Datum is: (top), NZ Vertical Datum 2016 - NZVD2016 (using offset of -0.1326 m for present MSL ; and (bottom) GVD-1926 (using offset of 0.2054 m for present MSL). Based on tidal constituents extracted from the Gisborne gauge dataset by LINZ, and processed by NIWA to predict all high tides over a 100-year period (excluding SLR for the heavy black line).

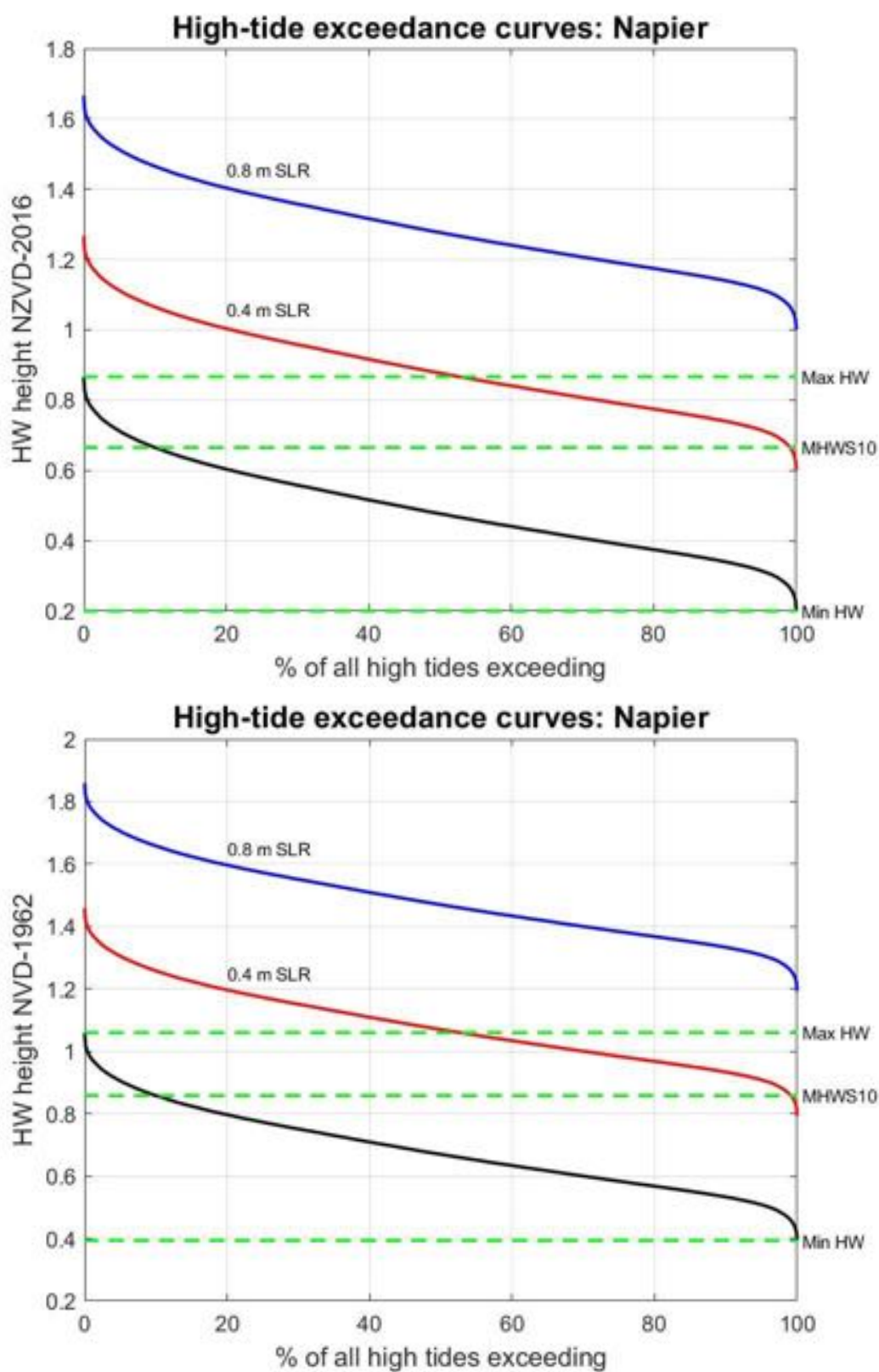


Figure 8-12: High-tide exceedance curve for all predicted high tides at Napier (excluding effects of weather, climate and SLR). Datum is: (top), NZ Vertical Datum 2016 - NZVD2016 (using offset of -0.154 m for present MSL ; and (bottom) NVD-1962 (using offset of 0.0387 m for present MSL). Based on tidal constituents extracted from the Napier gauge dataset by LINZ, and processed by NIWA to predict all high tides over a 100-year period (excluding SLR for the heavy black line).

8.6 Storm-tide elevations and effect of SLR

8.6.1 Components of storm-tide

High storm-tides and waves can cause coastal erosion and coastal/estuarine flooding on both the open-coast and within estuaries.

There are several meteorological and astronomical processes involved in a combined extreme storm-tide and wave event, and these processes can combine in a number of ways to flood low-lying coastal margins, or cause coastal erosion. Storm-tide is defined as the sea-level peak (Figure 8-13) reached during a storm event, from a combination of:

- high tide;
- monthly mean sea-level anomaly (MSLA);
- storm surge – the temporary elevation in sea level above the predicted tide during low-pressure weather systems (through the inverted barometer effect that relaxes the water level as pressure drops) and wind setup.

Future storm-tide levels will be raised directly by SLR. Waves also further raise the effective storm-tide level at the coastline. Wave setup is the increase in the sea level within the surf zone from the release of wave energy as waves break and wave runup is the vertical height reached, usually defined as the level only exceeded by 2% of waves. Freshwater flows, from rivers, streams and stormwater, may also exacerbate coastal flooding when the flood discharge is constrained inside narrower sections of estuaries e.g., within the Waipaoa River at Gisborne.

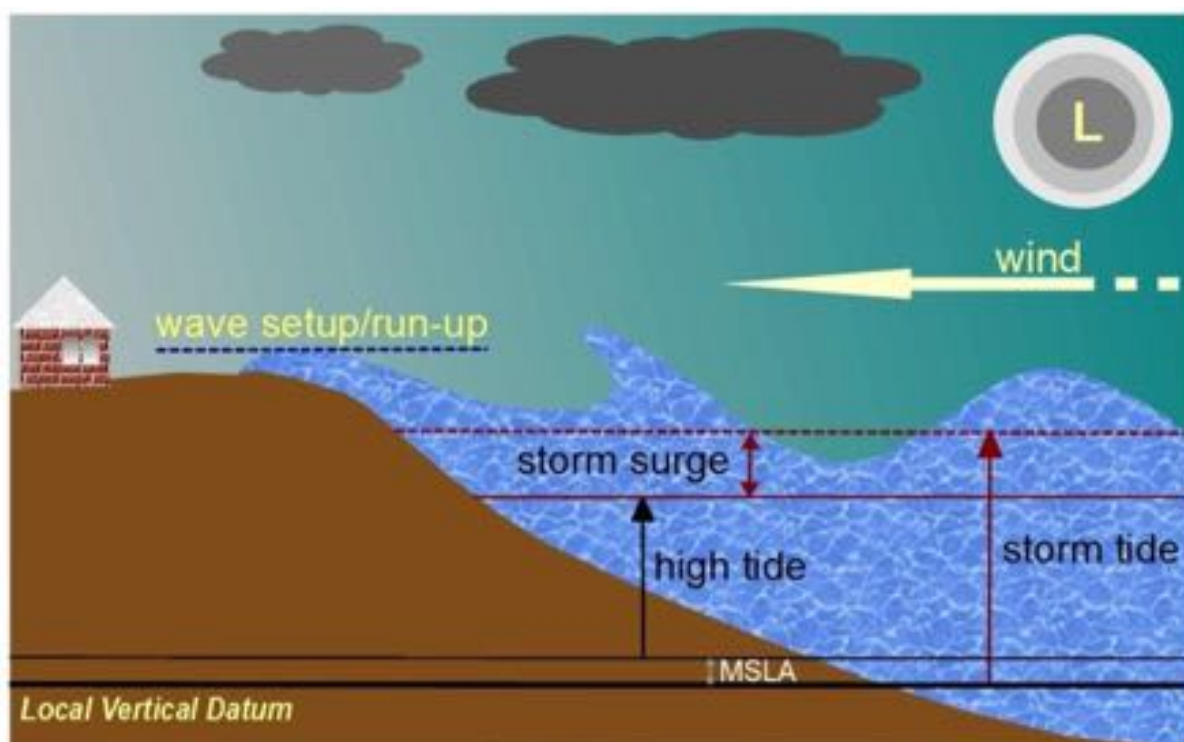


Figure 8-13: Components that contribute to storm-tide and wave overtopping. MSLA = monthly MSL anomaly or monthly variability in MSL, which can vary by around ± 0.2 m. L= low-pressure weather system.

MSLA is the month-to-month variation in MSL from climate and persistent weather patterns, which can vary by around ± 0.2 m, and therefore can be an important contributor to storm-tide levels and wave overtopping. Contributors to this monthly variability are the seasonal cycle in sea-surface height, and the effect of the 2–4 year El Niño-Southern Oscillation (ENSO) and the longer 20–30-year Interdecadal Pacific Oscillation (IPO). La Niña episodes and the negative phase of the IPO usually result in higher-than-normal sea level. The averaged seasonal cycle in monthly sea-surface height from the Port of Gisborne and Napier record is shown in Figure 8-14 and Figure 8-15. The peak sea level is reached in May, which is on average 0.06 m higher than the annual MSL in both locations. This means that storm-tide and wave overtopping events in May coincide with a slightly elevated background MSLA from the seasonal peak.

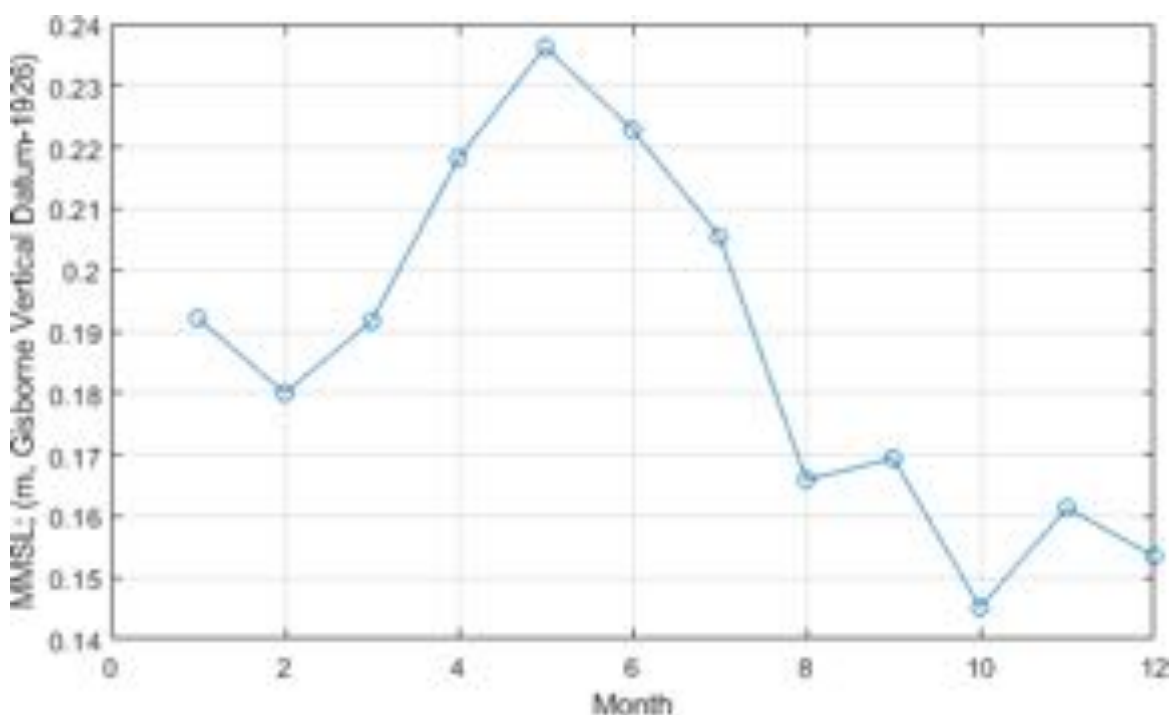


Figure 8-14: Seasonal cycle in monthly sea level at the Port of Gisborne averaged over the period 2009-2019. Month 1 is January to Month 12 (December). Levels are in mm to Gisborne Vertical Datum.

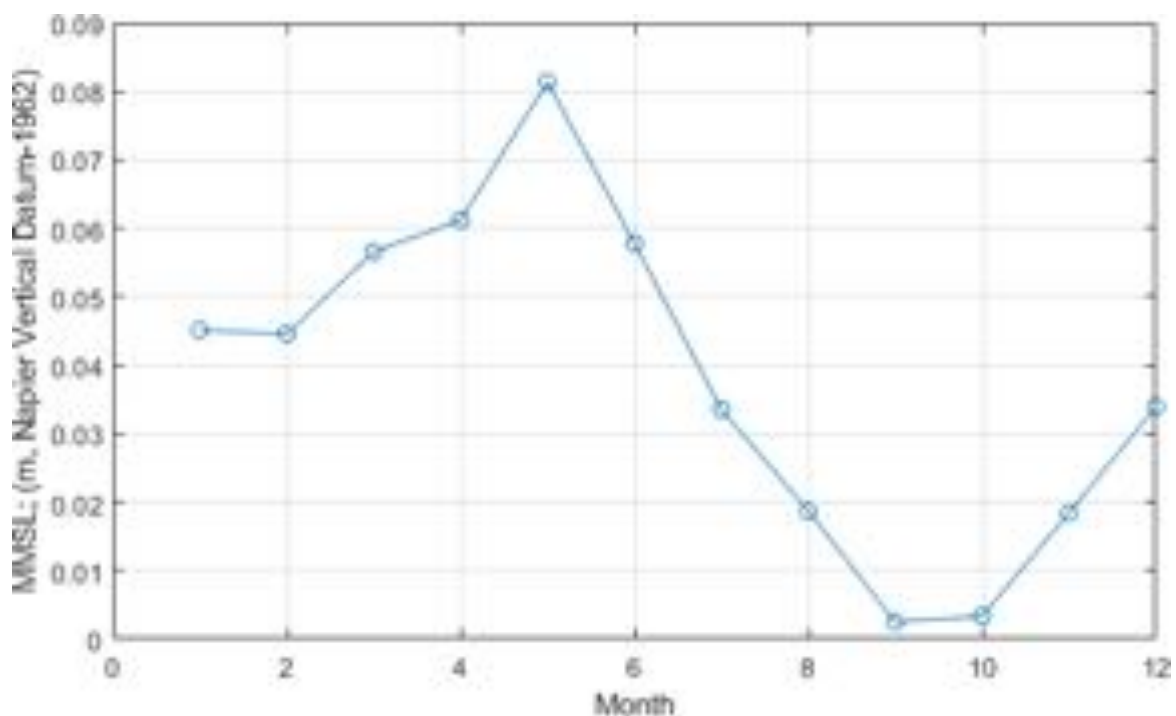


Figure 8-15: Seasonal cycle in monthly sea level at the Port of Napier averaged over the period 1989-2019. Month 1 is January to Month 12 (December). Levels are in mm to Napier Vertical Datum.

8.6.2 Extreme sea-level analyses

Extreme sea-level analyses used the skew-surge²⁰ joint-probability method (SSJPM) (Batstone et al., 2013) to determine extreme storm-tide frequency and magnitude. Joint-probability methods provide more robust low-frequency magnitude estimates for short-duration records than direct maxima methods — because they overcome the main theoretical limitations of extreme value theory application to measured sea-level maxima—splitting the sea level into its deterministic (predictable) tidal and stochastic (e.g., unpredictable, storm-driven) non-tidal components, and analysing the two components separately before recombining. Storm-tide return periods can be estimated from relatively short records because all skew surges are considered, not just those that lead to extreme levels. A limitation of the SSJPM and other joint-probability methods is that it assumes tide and skew surge are independent, which has been shown to be true in the UK (Williams et al., 2016) but has not been fully investigated in NZ, although comparisons with direct maxima methods for > 50-year-long records give similar results for return periods ≥ 10 years and also match observed maxima well, and thus support the validity of the independence assumption for long-return-period events (Stephens et al., 2020). To verify the results we have plotted the SSJPM results against the annual maxima (AM) plotted in their Gringorten (1963) plotting positions, and against a generalised extreme-value distribution fitted to the AM, and against an empirical distribution of the observed peak sea levels at high tide (Figure 8-16 and Figure 8-17). The verification indicates that the SSJPM method is robust.

²⁰ A skew surge is the difference between the maximum observed sea level and the maximum predicted tide regardless of their timing during the tidal cycle

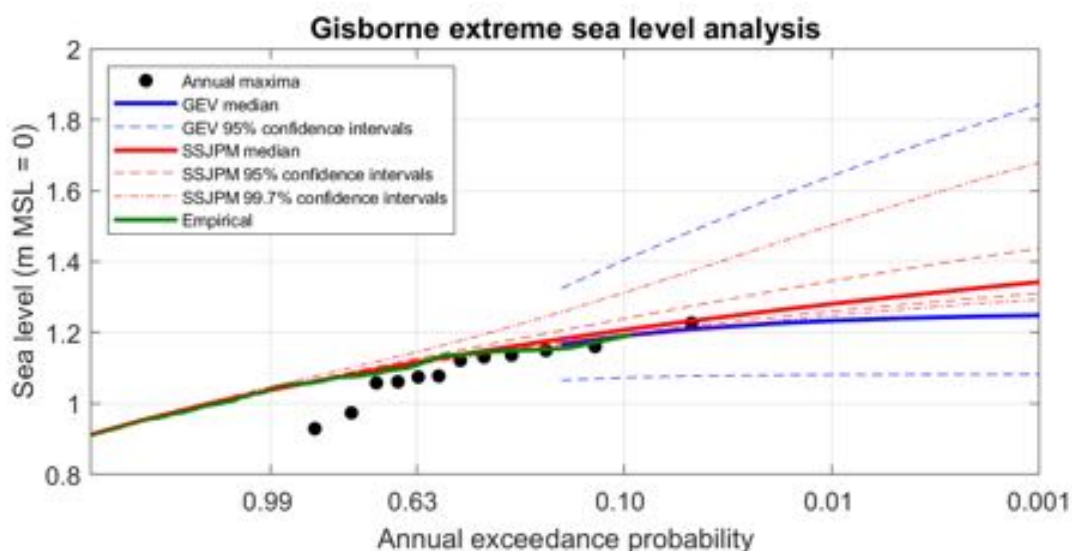


Figure 8-16: Extreme sea level at Gisborne. Elevations are plotted in metres relative to MSL = 0. They require a datum offset to convert them to a known datum. The skew-surge joint-probability method (SSJPM) has been compared to the annual maxima (AM) plotted in their Gringorten (1963) plotting positions, a generalised extreme-value distribution fitted to the AM, and an empirical distribution of the observed peak sea levels at high tide.

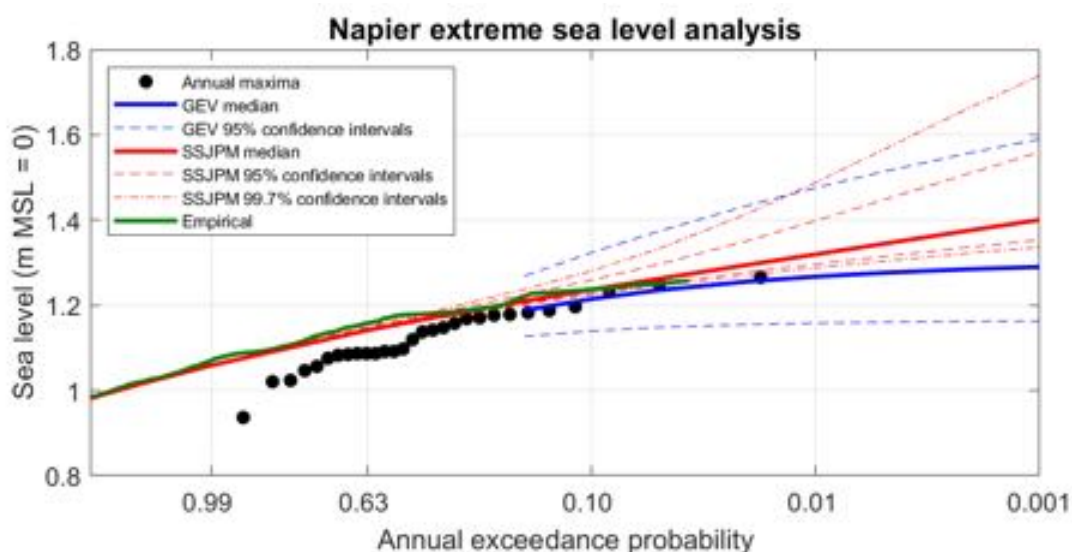


Figure 8-17: Extreme sea level at Napier. Elevations are plotted in metres relative to MSL = 0. They require a datum offset to convert them to a known datum. The skew-surge joint-probability method (SSJPM) has been compared to the annual maxima (AM) plotted in their Gringorten (1963) plotting positions, a generalised extreme-value distribution fitted to the AM, and an empirical distribution of the observed peak sea levels at high tide.

SLR projections from Section 8.4 can be added directly to present-day storm-tide levels in Table 8-5. The key observable indicator of rising seas will come from an increasing frequency of coastal flooding events in low-lying coastal areas (Stephens, 2015, PCE, 2015).

Locally, at the Ports of Gisborne and Napier, a present rare storm-tide event (0.2% annual exceedance probability (AEP) with a 500-year average recurrence interval (ARI)), would become, for

example, a 20% AEP (5-year event) after a RSLR of around 0.16 m, and present-day 100-year ARI event will become a 5-year event after only 0.1 m RSLR (Table 8-5). This ongoing change in frequency as seas rise is likely to apply generally along the Tairāwhiti and Hawke's Bay coastlines. From Table 8-3, the time windows for rare present-day 100-year or 500-year coastal flooding events to become frequent \leq 5-year events is by 2050 or earlier (depending on global greenhouse gas reductions and polar ice-sheet response to warming).

Table 8-5: Extreme sea-level estimates. Elevations are provided relative to MSL = 0. They require a datum offset to convert them to a known datum such as NZVD-2016. Values were calculated using the SSJPM method.

	Average recurrence interval (years)	5	10	20	50	100	200	500
Gisborne	Lower 99.7% confidence interval	1.17	1.19	1.21	1.23	1.25	1.26	1.28
	Lower 95% confidence interval	1.17	1.20	1.22	1.24	1.26	1.27	1.30
	Lower 68% confidence interval	1.18	1.20	1.22	1.25	1.27	1.28	1.31
	Median	1.18	1.21	1.23	1.26	1.28	1.29	1.33
	Upper 68% confidence interval	1.20	1.22	1.25	1.29	1.32	1.33	1.37
	Upper 95% confidence interval	1.21	1.24	1.27	1.31	1.35	1.36	1.41
	Upper 99.7% confidence interval	1.26	1.31	1.37	1.45	1.50	1.53	1.63
Napier	Lower 99.7% confidence interval	1.20	1.22	1.25	1.27	1.29	1.30	1.32
	Lower 95% confidence interval	1.20	1.23	1.25	1.28	1.30	1.31	1.34
	Lower 68% confidence interval	1.21	1.23	1.26	1.29	1.31	1.32	1.36
	Median	1.21	1.24	1.26	1.29	1.32	1.33	1.38
	Upper 68% confidence interval	1.22	1.25	1.28	1.33	1.36	1.38	1.45
	Upper 95% confidence interval	1.22	1.26	1.30	1.35	1.40	1.43	1.51
	Upper 99.7% confidence interval	1.24	1.28	1.33	1.42	1.49	1.53	1.67

Leaving aside SLR, climate change will also have some effect on waves and storm surges, although the projected changes from the present wave and storm surge climatologies are more difficult to discern above natural variability at regional and local scales than is the case for SLR. Small increases are expected in wave heights around New Zealand of the order of 0–5% by 2070–2100. Off the north-east coast of the North Island, the mean annual significant wave height is expected to decrease by a few percentage points (MfE 2017). Anticipated changes in storm surge around New Zealand will be somewhat less, with only South Taranaki Bight and the south Otago coast showing possible increases above 5% (e.g., + 0.03 m). So, while changes to waves/swell and storm surge will be secondary to the direct effect of SLR, the Coastal Guidance (MfE 2017) recommends sensitivity testing for coastal risk assessments of up to 10%, especially for higher risk developments or infrastructure.

Ongoing SLR will also raise groundwater levels in coastal and estuarine fringes, particularly where presently groundwater levels exhibit a tidal influence.

8.7 Generic impacts of climate change on coastal erosion

Coastal erosion generally refers to the migration of the shoreline inland via the movement of beach materials away from the beach/cliff face. Coastal erosion is often split into long- and short-term components; where the long-term refers to a coastal trends which have been observed over years to decades (and may implicitly include a SLR response), and the short-term refers to coastal changes seasons to individual storms.

Generally, SLR will exacerbate situations where erosion has historically been an issue, but as the New Zealand-wide coastal sensitivity index (Figure 8-18) shows for the Tairāwhiti-Hawke's Bay region (Goodhue et al. 2012), the response to climate change will vary from location to location along the coast depending on the local geomorphology, sediment type and wave exposure. The coastal sensitivity index does not include the present state of erosion or accretion – but rather the future net change that could be anticipated from climate change and SLR ranging from low to high sensitivity to erosion. In-depth summaries of the generic effects of climate change on shoreline erosion are given by PCE (2015; Chapter 4) and the Coastal Guidance (MfE 2017; Section 6.4.2 and Appendix J).



Figure 8-18: New Zealand coastal sensitivity index for future coastal erosion from climate change. Source: Figure 3-4, Goodhue et al. (2012).

Because of the complex nature of coastal shoreline change (erosion, accretion or remaining stable), arising from the interactions between sediment budgets (marine and riverine), geomorphology, sequences of storms, waves/swell patterns and variations in MSL, an analysis of present-day and future changes in different localities is beyond the scope of this report. However, a summary from multiple reports commissioned on coastal hazard identification and risk analysis by both the Gisborne District Council and Hawke's Bay Regional Council can be found in the following sections. These reports were prepared for the purpose of controlling the use, subdivision and development of beachfront property, and to advise the public of actual and potential risks to beachfront property from natural hazards at the present day and considering 100-years into the future. The findings and recommendations from these reports were implemented in high level district plans such as Tairāwhiti's Coastal Environmental Plan (Chapter 3.8.4)²¹ and the Combined Regional Land and District Plan (Chapter 5)²² and Hawke's Bay Regional Coastal Environment Plan²³.

8.7.1 Gisborne

Gisborne District Council commissioned Coastal Management Consultancy (CMCL) between 1994–2008 to evaluate areas sensitive to coastal hazards (ASCH), covering the coastline between Tauporo Beach south of Young Nicks Head, and Potikirua Point west of Lottin Point. CMCL reported that the erosion hazard was mostly confined to coastal plains of Holocene unconsolidated sediments and that the types of coastal erosion identified included long-term retreat at rates from 0.02 to –1.24 m/year, short-term shoreline fluctuations ranging from 2 m to greater than 100 m along both advancing and retreating coasts, accounting for river mouth migration and wind erosion of sand dunes. The widths of the ASCH ranged from 75 m for an area of very slow retreat east of Te Araroa, up to 570 m at Hautai Beach for an area of extreme wind erosion further east (Gibb, 1994).

Using the Coastal Hazards Database developed by Gibb et al. (1992) a Coastal Sensitivity Index (CSI) was calculated for the region. The CSI comprises of 8 variables which include elevation, maximum storm wave runup level, inland gradient, maximum tsunami wave runup, lithology, coastal landform type, long-term shoreline trend, and short-term shoreline fluctuations. Out of the 112 CSI sites in the Gisborne region, 84 were given a CSI of *High* with 5 coastal stations given *Very High*. Notable examples being the areas around the river mouths at Tauporo Beach, central Poverty Bay, central Tolaga Bay, Te Araroa and the small barrier beach at Orongo south of Young Nicks Head (Gibb, 1994).

Tonkin & Taylor Ltd (T&T) were commissioned in 2015 (updated in 2016) to review and update the existing ASCH to a specific area susceptible to coastal erosion (ASCE; Tonkin & Taylor, 2015). This was completed for all beaches and cliffed coasts within the Gisborne District not already covered by previous detailed coastal erosion hazard assessments. Yearly increments of 10 years were used in the future analysis over 2015 and 2115, with ASCE maps produced for present day (2015-2016), 2065 and 2115 timeframes. The results indicate ASCE zones for beaches in the 2115 timeframe range from 60 to 180 m inland from the present-day coastline, with the sea-level rise component being the largest contributor to the future erosion potential for sites with flat offshore slopes. ASCE widths in the current timeframe range from 5–105 m or 5–70% (average 30%) of the 2115 timeframe ASCE widths, depending on whether short-term effects dominate erosion or long-term trends and sea-level rise effect dominate.

²¹ <https://www.gdc.govt.nz/coastal-environment-plan/>

²² <https://www.gdc.govt.nz/old-district-plan/>

²³ <https://www.hbrc.govt.nz/environment/coastal-hazards/>

8.7.2 Hawke's Bay

Hawke's Bay Regional Council (HBRC), Hastings District Council (HDC) and Napier City Council (NCC) have similarly commissioned multiple reports looking at coastal erosion. A regional Coastal Hazard Assessment was carried out in 2004 (Tonkin & Taylor, 2004) that identified areas of potential coastal erosion hazards inclusive of sea-level rise to 2100. This was updated by T&T (2016a) and was then used to inform a follow-up Coastal Risk Assessment (Tonkin & Taylor, 2016b). The Coastal Erosion Hazard assessment used a probabilistic approach in determining the potential future shoreline position at 2065 and 2120, considering the following parameters: historic erosion trends, storm effects and backshore slope stability as well as the possible effects of sea-level rise.

Results from the Coastal Hazard Assessment report (Appendix G in T&T, 2016a) showed that Coastal Erosion Hazard Zones (CEHZs) are largest between the Ngaruroro River and Tukituki River for both the 2065 and 2120 timeframes. Slightly smaller CEHZs are evident south of the Tukituki River with the largest maximum CEHZ at Clifton. The large CEHZs, in particular for the 2120 timeframe, south of the Ngaruroro River are potentially a consequence of land subduction following the 1931 earthquake and long-term adjustment to a new post-earthquake equilibrium position. CEHZs north of the Ngaruroro River and south of Napier are significantly smaller and show accretion for the 2120 timeframe, possibly due to the cessation of gravel extraction from the beach face at Awatoto. The CEHZs between Westshore and the Port of Napier have narrow bounds due to reduced wave climate in the lee of the port and construction of revetments along these sections. North of the Port, tectonic uplift during the 1931 earthquake has generally resulted in higher beach crest elevations with respect to dunes south of Napier, except for at the southern end of Westshore. CEHZs to the south of Eskdale are larger compared to zones between Westshore and Bay View, induced by larger negative long-term trends possibly influenced by the Esk River. Further north of Eskdale, CEHZs comprise a maximum width of up to 100 m for the 2120 timeframe.

The Coastal Risk Assessment (Tonkin & Taylor, 2016b) looked to estimate risk to Economics and Social/Culture in the Hawke's Bay region from coastal erosion (storm cut, trends, and effects of sea-level rise) for 66%, 33%, 5% and 1% likelihoods for the present day, 2065 and 2120 timeframes. It reported that the effects from coastal erosion exposure²⁴ are generally low at present, as it only affects properties directly adjacent to the coastal margin. However, the exposure increases progressively with sea-level rise, particularly at the northern and southern ends of the Clifton to Tangoio study area. The main land areas affected are recreation and rural residential land, although there is an increasing exposure to all elements at risk with increased sea-level rise. In the present day, Napier City and Haumoana/Te Awanga are the most exposed to the coastal erosion hazard risk but are generally rated as very low to low. Westshore, East Clive and Haumoana/Te Awanga were noted as being increasingly vulnerable for future scenarios for erosion reaching very high economic losses in 2120. Economically, for the 1% annual exceedance probability (AEP)²⁵ coastal erosion scenario, losses were reported to increase to \$65 million for the Westshore area in the year 2120. With regards to Social/Cultural losses, particularly the potential loss to religious and cultural sites (e.g. Uranga), Westshore, Ahuriri and Pacific Beach shows low to moderate losses for erosion, while Clifton shows moderate to high losses (Tonkin & Taylor, 2016b).

²⁴ The exposure to the hazards is quantified in terms of loss of area and the proportion of the elements at risk affected by the hazard

²⁵ The probability of exceeding a given storm discharge or erosion level within a period of one year

Recommendations made to both Tairāwhiti and Hawke's Bay councils by both CMCL, T&T and other studies are as follows:

- Lines that designate ASCH, ASCE or CEHZs can be superseded by more detailed local or site-specific erosion hazards assessments
- ASCH and CEHZ widths should be reviewed once every 2–5 years based on the results of a coastal monitoring programmes to record the pattern and rate of erosion or accretion, extent of flooding from significant storm events or tsunamis, and significant landslides.
- Councils use the supplied mapping of areas susceptible to coastal erosion to assist it to consider management approaches for coastal erosion
- That lines should be updated as new data (e.g. SLR projections) and methods become available

9 Exposure analysis – coastal and fluvial inundation

A summary of exposure of land, infrastructure and assets in the Tairāwhiti and Hawke's Bay regions to coastal and fluvial inundation is presented in this section. Exposure is summarised for the areas covered by each unitary council or territorial authority – i.e. for Gisborne District Council, Wairoa District Council, Hastings District Council, Napier City Council, and Central Hawke's Bay District Council. Asset and infrastructure datasets were supplied by Gisborne District Council and Hawke's Bay Regional Council. Tables of the coastal and fluvial exposure of land, infrastructure and asset classes are presented in Appendix A and are summarised here.

The coastal inundation data model uses the 1% Annual Exceedance Probability (AEP) or 1-in-100-year storm tide flood levels, plus different increments of sea-level rise. A range of future sea-level elevations (0-1.5 metres in 0.5 m increments) is included in the coastal flooding analysis. This range was used to provide the councils with scenarios of potential exposure under moderate and extreme sea-level rise scenarios. According to Ministry for the Environment (2017) (the Coastal Hazards and Climate Change Guidance Manual for Local Government), sea levels around New Zealand are projected to rise by about 0.2-0.4 m by 2050, and about 0.45-1 m by 2100 depending on the greenhouse gas concentration pathway that is followed globally. The New Zealand Coastal Policy Statement requires quantification of coastal hazards for risk to developments over at least the next 100 years. As shown by the sea-level rise projections in Ministry for the Environment (2017), > 1 m of sea-level rise is possible by 2120 under a high-end representative concentration pathway. Maps showing the areas in the Tairāwhiti and Hawke's Bay regions exposed to a 1% annual exceedance probability (AEP) storm tide event at the present day and with different levels of sea-level rise are presented in Appendix A along with the tabulated exposure data. It is noted that the data coverage of the coastal flooding maps is limited to locations where high resolution digital elevation models (DEMs) were available (Paulik et al., 2020). Refer to Appendix A for additional detail regarding data coverage.

For fluvial exposure, the same asset database of land, assets and infrastructure was intersected with the with the 'flood hazard area'. The national flood hazard area map was created using publicly available flood hazard maps from local government organisations and flood-prone soil maps from Manaaki Whenua Landcare Research (Paulik et al., 2019a). This exercise included all areas inundated by past floods and areas considered to be at risk from flooding. Some flood prone areas may not be

correctly identified and there was no specific return period assigned to this flood hazard area. This exercise did not consider potential changes to flood events with climate change, due to the unavailability of extreme flood projections at present. However, it provides a useful baseline for understanding all areas currently exposed to flood hazards in the Tairāwhiti and Hawke's Bay regions. Note that an Endeavour Research Programme has recently been funded (September 2020) which aims to address some of these research gaps. Maps of the flood hazard area in the Tairāwhiti and Hawke's Bay regions are presented in Appendix A.

See Section 2.5 for additional details on the inundation exposure modelling.

9.1 Coastal inundation exposure

9.1.1 Tairāwhiti

For land cover, the most potentially exposed category to extreme coastal flooding is high producing exotic grassland (1624 ha at 1 m SLR) followed by orchards, vineyards, or another perennial crop (368 ha at 1 m SLR). Some reserves are also exposed to extreme coastal flood levels, with amenity reserves and recreation reserves having the largest areas exposed at higher sea-level increments. Transport infrastructure is potentially exposed to extreme coastal flood levels, with 38 km of roads and 11 km of railway potentially exposed to flooding from a 1% AEP storm tide event and 1 m of SLR. Gisborne Airport is potentially exposed to extreme coastal flooding at all increments of sea-level rise, as well as present-day sea level.

In terms of infrastructure, 2.6 km of stop banks are potentially exposed to extreme coastal flooding with 1 m of SLR, along with 21 floodgates. Over 54 km of three-waters pipelines are potentially exposed to extreme coastal flooding with 1 m of SLR, as well as over 1300 three-waters nodes. Approximately 720 buildings may be exposed to extreme coastal flooding with 1 m of SLR, along with 590 people. The 2016 replacement cost for those buildings exposed is approximately \$209 million.

For more details of potential exposure of land, infrastructure and buildings in Tairāwhiti to extreme coastal flooding with different SLR increments, see Appendix A.

9.1.2 Hawke's Bay

For land cover, like Tairāwhiti, the most potentially exposed category across the whole Hawke's Bay region is high producing exotic grassland (~4000 ha at 1 m of SLR) followed by orchards, vineyards, or other perennial crop (~960 ha at 1 m SLR). About 250 ha of regional parks in Hastings District and 22 ha in Napier City are potentially exposed to extreme coastal flood levels with 1 m SLR. In terms of exposure of the roading network, Napier City has approximately 180 km of roads potentially exposed to extreme coastal flooding with 1 m SLR – the highest rate of the four territorial authorities in Hawke's Bay. About 2 km of railway is potentially exposed at 1 m SLR for each of Wairoa, Hastings, and Napier City council areas. Napier Airport is low-lying and is potentially exposed to extreme coastal flood levels at present-day sea level.

In terms of infrastructure, 18.5 km of stop banks are potentially exposed to extreme coastal flood levels with 1 m SLR in Napier City, along with 2.6 km of stop banks in Hastings District. Over 1000 km of three-waters pipelines and over 37,000 three-waters nodes are potentially exposed to extreme coastal flooding with 1 m SLR in Napier City – this is by far the most exposed territorial authority in Hawke's Bay for these types of infrastructure. Eight pump stations are potentially exposed to extreme coastal flooding with 1 m SLR in Hastings District, and six in Napier City.

Approximately 18,300 buildings in Napier City are potentially exposed to extreme coastal flooding levels with 1 m SLR, and almost 1900 in Hastings District. These buildings have a 2016 replacement cost of \$4.2 billion (Napier City) and \$421 million (Hastings District). 23,410 people are potentially exposed to extreme coastal flooding under the same SLR increment in Napier City, and 2422 in Hastings District.

For more details of potential exposure of land, infrastructure and buildings in Hawke's Bay to extreme coastal flooding with different SLR increments, see Appendix A.

9.2 Fluvial exposure

9.2.1 Tairāwhiti

The flood hazard area intersects with almost 8000 ha of high producing exotic grassland and over 4400 ha of orchard, vineyard, or other perennial crop in Tairāwhiti. 106 ha of exotic forestry are also potentially exposed to fluvial floods. A reasonable amount of reserve area is also potentially exposed, including 172 ha of recreation reserves, 71 ha of amenity reserves, and 12 ha of heritage reserves.

In terms of transport infrastructure, 371 km of roads intersects with the flood hazard area, as well as almost 18 km of railway. Gisborne Airport is located within the flood hazard area. In addition, 29 km of cycleways are potentially exposed to fluvial flooding. Almost 72 km of stop banks intersect the flood hazard area, as well as 157 flood gates and three pump stations. 417 km of three-waters pipelines are potentially exposed to fluvial flooding, as well as 8663 three-waters nodes.

In Tairāwhiti, over 11,800 buildings intersect with the flood hazard area, along with ~15,500 people. Those buildings would cost approximately \$2.2 billion to replace (2016 value).

For more details of potential exposure of land, infrastructure and buildings in Tairāwhiti to fluvial flooding, see Appendix A.

9.2.2 Hawke's Bay

There is considerable existing exposure to fluvial flooding in Hawke's Bay. For the region as a whole, over 10,000 ha of high producing exotic grassland is potentially exposed, as well as over 1500 ha of orchard, vineyard, or perennial crop land. Almost 800 ha of low producing grassland and 240 ha of exotic forestry is also potentially exposed.

In terms of transport infrastructure, about 680 km of roads across the whole region are potentially exposed to fluvial flooding (mostly in Wairoa and Hastings Districts). About 85 km of railway across the region is also potentially exposed. In addition, Napier Airport intersects with the flood hazard area.

There is a large amount of water and flood infrastructure that is potentially exposed to fluvial flooding, a small subset of which is described here. For the full list of potentially exposed infrastructure and assets, refer to Appendix A. For stop banks, almost 35 km intersects with the flood hazard area in Central Hawke's Bay District, and 16.3 km in Hastings District. 203 km of drains are potentially exposed to fluvial flooding in Wairoa District, 58 km in Napier City, and less than 20 km in Wairoa and Central Hawke's Bay Districts. A number of floodgates, culverts and headwalls are also potentially exposed, with the largest number in Hastings District followed by Central Hawke's Bay District. 581 km of three-waters pipelines are potentially exposed to fluvial flooding in Napier City,

115 km in Wairoa District and 100 km in Hastings District. Over 14,500 three-waters nodes are potentially exposed in Napier City, and almost 4000 in both Wairoa and Hastings Districts.

Over 7600 buildings in Napier City are potentially exposed to fluvial flooding, along with over 3800 in Hastings District, 2000 in Wairoa District, and 485 in Central Hawke's Bay District. The total replacement value of these buildings across the region is over \$3.5 billion (2016 value). In addition, almost 18,000 people are potentially exposed to fluvial flooding across Hawke's Bay.

For more details of potential exposure of land, infrastructure and buildings in Hawke's Bay to fluvial flooding, see Appendix A.

10 Impacts of climate change on key sectors

10.1 Forestry

Climate change-induced hazards, such as changes in the temperature, rainfall and CO₂ concentration, could impact natural and modified forests substantially (Kirilenko and Sedjo, 2007, FAO, 2018). The possible impacts of climate change on forests include, but are not limited to, shorter or longer growing seasons, modifications in the forest's biodiversity including its macro and microbiota, changes in the pests and disease factors and their spread pattern, and increase of bushfire frequency (FAO, 2018, Kirilenko and Sedjo, 2007, Whitehead et al., 1992).

New Zealand's forestry, as the nation's third-largest export sector, has been impacted by global and local hazards induced by a changing climate, and the impacts are expected to continue or accelerate under the future scenarios of climate change (MPI, 2018, Watt et al., 2018, Whitehead et al., 1992). Research indicates there are potential impacts of climate change on New Zealand's natural and plantation forests such as: alteration in the forest productivity due to an increase in the growth rate, more wind-related damage, amplified bush fire risk (very high to extreme), and a possible surge in the pest and weed population (Watt et al., 2018). Forestry is an important sector for Tairāwhiti and was seen as a suitable land use for much of the region's steep, highly erodible soil after Cyclone Bola. Recent issues with landslides and mobilisation of harvest residues, i.e. during Cyclone Cook in 2017 and the Queen's Birthday storm of 2018 have highlighted the risks posed by forestry harvest and longer term a move towards permanent indigenous forest cover over the most erodible lands is considered the most sustainable outcome.

Increases to temperature and changing rainfall patterns could negatively influence *P. radiata* productivity, but the effect of increased CO₂ fertilisation is modelled to outweigh these negative impacts, significantly increasing *P. radiata* productivity across New Zealand by 2040 and 2090 of 19% and 37%, respectively (Watt et al., 2018). However, the extra growth caused by CO₂ fertilisation may make trees more susceptible to wind damage.

Extreme rainfall intensity, as discussed earlier in this report, is likely to increase in Tairāwhiti and Hawke's Bay. This may have implications for the forestry sector through exacerbating erosion, landslides, movement of slash, and impacts on access to forests for trucks and machinery. On the flipside, severe droughts are likely to become more frequent for both regions, which may have implications for forestry through reducing water availability for trees and increasing fire risk.

Fire risk is projected to increase in the future in New Zealand, due to the following conditions (Pearce et al., 2011):

- Warmer temperatures, stronger winds, lower rainfall and more drought for some areas will exacerbate fire risk. Note that projected changes to mean wind speed for Tairāwhiti and Hawke's Bay are generally small at the annual scale, with greater change projected at the seasonal scale (e.g. larger increases to mean wind speed during winter). Further work is needed to evaluate changes to wind at the regional scale;
- The fire season will probably be longer - starting earlier and finishing later;
- Potentially more thunderstorms and lightning may increase ignitions;
- Fuel will be easier to ignite (because of increased drying due to increased evapotranspiration/less rainfall); and
- Drier conditions (and possibly windier periods) will result in faster fire spread and greater areas burned.

The East Coast of the North Island, including Tairāwhiti and Hawke's Bay, is currently one of the most at-risk parts of New Zealand to the forest fire. This existing high risk should be kept in mind when interpreting the following potential climatic changes. The following projections for fire risk are based on the IPCC Fourth Assessment Report emission scenarios (Pearce et al., 2011). For Seasonal Severity Rating (SSR)²⁶, the 17-model average projection shows minimal change for Gisborne Airport (the representative climate station for Tairāwhiti and Hawke's Bay regions) by the 2050s (2040-2059) compared to the 1980-1999 historical period. Similar patterns were observed for the 2080s (2070-2089). The average SSR over fire season months (October-April) for Gisborne is projected to increase from 4.41 over the historical period to 5.10 in the 2050s and 5.33 in the 2080s.

The number of days of Very High and Extreme (VH+E) forest fire danger is projected to increase for Gisborne by the 2050s and the 2080s compared to 1980-1999. The historical number of VH+E forest fire danger days for Gisborne is 34.1 days, and this is projected to increase to 41.1 days in the 2050s and 43.7 days in the 2080s.

Note that some individual models project a higher increase in Very High and Extreme forest fire danger days, as noted by Reisinger et al. (2014). The reader is directed to Pearce et al. (2011) for more information on the projections of Seasonal Severity Rating and Very High and Extreme forest fire danger days in New Zealand. Although SSR and days of VH&E fire danger are not projected to change as much as some other parts of New Zealand, the East Coast region still remains one of the regions most at risk to forest fire in the country.

Pest species are likely to shift to new habitat areas due to climate change. Existing tree pathogens causing dothistroma needle blight and cyclaneusma needle cast are likely to decline in severity throughout the 21st century in North Island plantations (Watt et al., 2018). However, increasing average temperatures and changing rainfall patterns across the country may make conditions more suitable for climate-limited tree pathogens such as pitch canker (currently present in northern coastal areas). Insect pests may become more of an issue for forestry plantations with climate

²⁶ Seasonal Severity Rating (SSR) is a seasonal average of the Daily Severity Rating (DSR), which captures the effects of both wind and fuel dryness on potential fire intensity, and therefore control difficulty and the amount of work required to suppress a fire. It allows for comparison of the severity of fire weather from one year to another. Source: http://www.nrfa.org.nz/OperationalFireManagement/ResourceLibraries/AlertsAndNotices/Documents/Seasonal%20Fire%20Danger%20Outlook_North%20Island.pdf

change, as the major limiting factor for most insect pests is cold stress. Therefore, subtropical insect pests may be able to establish in a warmer New Zealand in the future, and existing insect pests may increase their distribution within New Zealand. Climate change may also affect the severity of damage from existing insect pests because warmer temperatures can be expected to accelerate insect development and therefore lead to an increase in population levels, especially in species that can complete more than one generation per year (e.g. the Monterey pine aphid *Essigella californica*).

Increasing competition with weeds is also a concern for the forestry industry. New Zealand's future climate may become more suitable for some weeds which are already established in some parts of New Zealand but have not spread, so-called "sleeper weeds" (Kean et al., 2015). An example of this is *Melaleuca quinquenervia*, an exotic tree that is currently established in Auckland and Northland. If the species' thermal requirement for reproduction is reached with a warming climate, this could become quite invasive and difficult to control. Also, woody tree species that are native to Australia (e.g. *Acacia spp.*) have very high growth rates and vigorously compete with *P. radiata* seedlings. As tree species, they can compete further into the plantation rotation than other weed species which are predominantly shrubs.

Overall, there are potential positive and negative impacts on the forestry sector from climate change. Tree growth may be more vigorous due to increasing concentrations of CO₂ in the atmosphere and warmer temperatures, but these benefits may be counteracted by reduced water availability and risk of fire. Forestry operations may be negatively affected by increasing rainfall intensity causing more erosion, flooding, and site access issues, as well as more frequent and prolonged droughts as well as fire risk which may affect safety of workers.

10.2 Horticulture

The horticulture industry is likely to be subject to increasing impacts of climate change over time (MPI, 2014). The production of horticultural crops (such as apples, kiwifruit and grapes) is projected to be influenced by changes in precipitation patterns, temperature variability, and greenhouse gas concentrations (MPI, 2014). For example, temperature rise, either annual or seasonal, alters the evaporation rate, hydrological cycles of the catchment, and water availability; therefore, influencing the quality and quantity of horticultural products (Rehman et al., 2015). Table 10-1 shows a snapshot of the potential impacts of climate change on some horticultural products.

Table 10-1: Overall impacts of climate change on the main horticultural crops in NZ. Source: Clothier et al. (2012).

	Apples	Grapes	Kiwifruit
Temperature			
Temperature means ↑	Yield ↑ Quality ↑ Disease risk ↑ Sunburn ↑	Yield ↑ Quality ↑ Disease risk ↑	Yield ↓ Quality ↑ (and ↓) Disease risk ↑
Temperature extremes Frost ↓ Heatwaves ↑	Frost damage ↓	Frost damage ↓	Frost damage ↓
CO ₂ ↑	Biomass ↑	Biomass ↑	Biomass ↑
Rainfall variability ↑↓	Irrigation ↑	Irrigation ↑ Drought risk ↑	Irrigation ↑
Water quality	Leachate load ↓	Leachate load ↓	Leachate load ↓
Extreme events Hail – Wind –	Damage to fruit – Damage to trees –	Damage to fruit – Damage to vines –	Damage to fruit – Damage to vines –
Combined impacts –	↑ unless pest & disease impacts override	↑ unless pest & disease impacts override	↑↓

In Tairāwhiti, the top five horticultural crops by area are maize/sweetcorn, squash, wine grapes, citrus, and kiwifruit (Gisborne District Council, 2020). In Hawke's Bay, the top five horticultural crops by area are apples, wine grapes, squash, peas and beans, and onions (New Zealand Horticulture, 2018). Increasing temperatures will impact all types of crops, as plant phenological development may occur at a faster rate. Different stages of plant growth (e.g. bud burst, flowering, and fruit development) may happen at different times, which may affect the harvested crop. For example, the hottest summer on record for New Zealand in 2017/18 saw wine grapes in multiple New Zealand regions ripen faster than usual (Salinger et al., 2019). In Central Otago, this resulted in the earliest start to harvest of Pinot Noir grapes on record (almost a month earlier than usual). In Wairarapa, the period from flowering to harvest for wine grapes was about 10 days shorter than usual²⁷.

Extreme heat affects the rate of evapotranspiration, or the uptake of water by plants. Therefore, increases to extreme heat may affect water availability, as under hot conditions, plants use more water. Extreme heat may also result in current varieties of crops and pasture becoming unsustainable if they are not suited to growing in hot conditions. Extreme heat may also affect fruit quality, such as sunburn on apples and kiwifruit, and 'shrivelling' of grapes (Clothier et al., 2012).

Reductions in cold conditions may have positive impacts for diversification of new crop varieties that are not able to currently be grown in Tairāwhiti and Hawke's Bay. For example, certain crops (e.g. kumara) are currently grown in warmer parts of New Zealand such as Northland, and other crop species are currently not grown in New Zealand at all. In the future, with a warmer climate, there may be opportunities for growers in Tairāwhiti and Hawke's Bay to take advantage of the overall warmer climate to diversify their crops. However, future warmer temperatures may create issues for horticulture in both areas. The increasing risk from pests (plants and animals) and diseases is a concern. Currently, many pests are limited by cold conditions, so that they cannot survive low winter

²⁷ <https://michaelcooper.co.nz/2018-regional-vintage-overview-report/>

temperatures, and therefore their spread is limited (Kean et al., 2015). Under a warmer climate, these pests may not be limited by cold conditions and therefore cause a larger problem for farmers and growers in Tairāwhiti and Hawke's Bay. The risk of the disease apple black spot is projected to increase with temperature, but decrease with rainfall reductions (Beresford and McKay, 2012). However, the risk of kiwifruit disease Psa may decrease with increased temperature and reduced rainfall totals. In addition, crops that require a certain amount of winter chilling to break winter dormancy (e.g. kiwifruit, deciduous fruit trees) may be negatively affected by overall warmer conditions in winter (Tait et al., 2017, Clothier et al., 2012).

Increased prevalence of drought and longer dry spells in Tairāwhiti and Hawke's Bay will likely have impacts on water availability for irrigation and other horticultural uses. The amount of irrigation may need to be expanded to maintain productivity, however this may be limited by future water availability. Average and low river flows are likely to decline in these areas, with reduced flow reliability (the time period where river water abstraction is unconstrained) (Collins and Zammit, 2016). Groundwater recharge is also likely to be affected by reductions in average river flows and rainfall, which in turn may affect the amount of water available for irrigation and other horticultural uses. More frequent and severe droughts may negatively affect horticultural productivity, particularly for crops that require larger quantities of water. Soils may be more exposed to wind erosion with increasing drought severity. With ongoing risk of wildfire, smoke taint may be an issue for crops such as wine grapes (Mira de Orduña, 2010).

Increases in extreme rainfall event magnitude and frequency may impact horticulture in several different ways. Slips on hill country land may become more prevalent during these events (Basher et al., 2012), and soils may become waterlogged more often. This has impacts on the quality of soil for horticulture, the area of land available for production, and other impacts such as sedimentation of waterways (which can impact flooding and water quality). Slips may also impact transport infrastructure (e.g. roads, farm tracks) which may, in turn, affect the connectivity of farms and orchards to markets. High rainfall will impact soil moisture, and saturated soils may be detrimental for horticulture. Wet soils may cause issues for vegetable growers in particular, as crops may get washed away or the lack of oxygen around the plants may reduce their growth rate. Heavy rain at harvest times for fruit may cause a decline in fruit quality, with skins splitting and increased prevalence of diseases.

Many horticultural areas are located on low-lying land in Tairāwhiti and Hawke's Bay. This means they may be more exposed to extreme coastal flooding exacerbated by sea-level rise as well as fluvial flooding. For example, the alluvial soils of the Poverty Bay Flats in Tairāwhiti are among the most productive soils in New Zealand (Gisborne District Council, 2020), but they are also potentially exposed to flooding. There are 174 ha of orchard, vineyard, or other perennial crop land cover type potentially exposed to extreme coastal flooding at current sea levels in Tairāwhiti, which rises to 368 ha with 1 m of SLR (Table A-1). In Hawke's Bay, the current area of the same land cover type potentially exposed to extreme coastal flooding is 257 ha which rises to 962 ha with 1 m of SLR (Table A-4). However, the exposure of this land cover type to fluvial flooding is potentially much higher: 4431 ha are in the flood hazard area in Tairāwhiti (Table A-7), and 1524 ha in Hawke's Bay (Table A-10). See Appendix A for more details on exposure of land cover types to extreme coastal flooding under different increments of sea-level rise.

Overall, climate change impacts on horticulture in Tairāwhiti and Hawke's Bay are likely to be significant. Increasing temperatures may provide opportunities for new crop types to be grown in the area but this may also cause issues for some existing crop types and encourage the spread of new

pests. Droughts are likely to cause significant issues for the sector in terms of water availability for irrigation and resulting productivity. However, increasing rainfall intensity is likely to have impacts on soil erosion, sedimentation, and saturation of soils.

10.3 Agriculture

The influence of climate change on the agricultural industry and agricultural diversity is an increasing concern, both globally and New Zealand-wide. According to global modelling, more uncertain and severe impacts on the agricultural industry are predicted by the end of the century (FAO, 2019). A survey of farmers suggests that, in their opinion, about 65% of New Zealand's agriculture will be moderately or severely impacted by climate change in the next 30 years (MPI, 2019). Climate change affects New Zealand's agriculture directly and indirectly. Direct impacts include, for example, the role of increasing temperature on modifying the growing season and crop and pasture productivity, and the role of changes to rainfall on water availability. Further, the availability of agricultural land due to sea-level rise, and damage to farm infrastructure due to increased flooding events are examples of indirect climate change impacts.

From a regional perspective, climate change is projected to have significant impacts on the agriculture industry in Tairāwhiti and Hawke's Bay areas (Savage, 2006). Climate change impacts may include reduced water availability from decreasing low river flows, a surge in water demand (for irrigation purposes) due to reducing rainfall, high risk of wildfire, more soil erosion due to both droughts and extreme rainfall events, and increased biosecurity problems for the region by the end of the century (MfE, 2020, Savage, 2006). Reductions in rainfall and increased temperatures are expected to increase the incidence of drought over time. This may directly impact pasture growth, the health of livestock, and overall agricultural productivity. At the same time, an increased intensity in severe rainfall events and high storm surge/ coastal inundation events can be expected to affect water quality, reduce the quality of grazing areas and risk the safety of farm buildings, machinery, staff and livestock. At current sea levels, 965 ha and 2385 ha of high producing exotic grassland (i.e. pastoral farms) are potentially exposed to extreme coastal flooding events in Tairāwhiti (Table A-1) and Hawke's Bay (Table A-4), respectively. This increases to 1624 ha and 3598 ha with 1 m of SLR for Tairāwhiti and Hawke's Bay, respectively. In addition, 7993 ha and 10,704 ha of high producing exotic grassland are potentially exposed to fluvial flooding in Tairāwhiti (Table A-7) and Hawke's Bay (Table A-10), respectively.

Animal heat stress may be a future consideration for areas with land suitable for pastoral farming in Tairāwhiti and Hawke's Bay. The whole region is projected to experience increased heatwave conditions compared to the historical period, but the eastern lowland areas of both Tairāwhiti and Hawke's Bay will likely see the largest increases in heatwave days. Cattle experience heat stress in hot and humid conditions. Generally, the threshold for heat stress for cows is 25°C (Lee et al., 2012). Heat stress results in reduced feed intake, which in turn, results in lower milk production (Bryant et al., 2007). Heat can also affect milk composition in terms of proportions of fats and proteins. As cattle release heat during the night to cool down, increased daily minimum temperatures may have a detrimental impact on their ability to do so. While a prolonged growing season, due to warmer temperatures year-round, may increase the pasture productivity in the short term, productivity could be negatively influenced by the extended risk of drought, flooding and heavy rainfall events in the Tairāwhiti and Hawke's Bay regions (Savage, 2006, MfE, 2020)

The risks of severe events or pest outbreaks notwithstanding, climate change can be reasonably expected to have some positive impacts. For example, the increase in temperatures over time is

expected to favour wheat yields (Reisinger et al., 2014, MBIE, Undated) and pasture production is likely to increase unless limited by water availability (Lee et al., 2012). However, there is also likely to be an increased risk of pests and diseases with increased temperature, humidity and pest generation times owing to prolonged seasons (Clothier et al., 2012). Drought is likely to be a limiting factor for agricultural productivity in Tairāwhiti-Hawke's Bay, as it is well-known to cause a decline in crop and pasture yield (Teixeira et al., 2012). It is important to recognise that for all types of agriculture the reliance on an effective transportation system is critical for operations. As addressed in Sections 9 and 10.7 transportation infrastructure can be negatively impacted by climate change impacts, for example because of increased risk of inundation from coastal flooding. The need to maintain the connectivity of the region to maintain or resume commercial operations following extreme events applies for all sectors.

To summarise, the agriculture sector in Tairāwhiti and Hawke's Bay is likely to feel some impacts related to climate change. Productivity may be affected by changes to rainfall patterns and drought, and resulting impacts on water availability. Increases in temperature may encourage more pests and diseases to establish, as well as causing increased heat stress to livestock. Coastal and fluvial flooding may cause transport infrastructure connectivity issues, particularly as sea levels continue to rise.

10.4 Tourism

The tourism industry is one of the major contributors to New Zealand's GDP and the main provider of job opportunities nationwide, with a turnover of \$40.9 billion in 2019 (Tourism New Zealand, 2020). Climate change-related issues may increasingly influence the tourism industry from three different aspects. The first aspect refers to ethical concerns regarding ecological/carbon footprint of tourism activities, and their impacts on the Earth's systems, which in turn could lead to a lower number of (international) tourists in the long-term. The second aspect addresses the economic pressures that climate change impacts load on the profitability of other sectors and thereby lower people's affordability to go on holidays. The third aspect relates to the direct impacts of climate change hazards, such as rising temperature, changes in the precipitation patterns (e.g. extreme rainfall), sea-level rise and coastal flooding on tourism hotspots and infrastructure such as roads, airports, coastal premises (Munshi et al., 2020).

The impacts of climate change on tourism activities are not unified and they vary from one sector to another. For example, while warmer temperatures may increase some seasonal tourist activities, particularly nature and water-based activities, increased temperatures in winter may negatively affect other activities (e.g. skiing). In general, warmer and drier conditions mostly benefit most tourism activities, but wetter conditions and extreme climate events undermine tourism.

Much of the tourism in the Tairāwhiti and Hawke's Bay regions is reliant upon the natural environment which requires attractive environments for tramping, camping, cycling, and sightseeing. There are many unknowns about how climate change may affect the natural environment, but increased prevalence of drought and warmer temperatures may have negative impacts on ecosystems (Section 10.5). Many tourists come to the Tairāwhiti and Hawke's Bay regions for their offerings in wine tourism – so if the grape-growing industry is affected by climate change then this could have negative consequences for wine tourism as well.

Some potential consequences of climate change on Tairāwhiti and Hawke's Bay area's tourism sectors include:

- Potential difficulties in accessing Napier Airport during coastal flooding events, due to its close proximity to the shoreline. As discussed in Section 9.1.2 Napier Airport is already exposed to extreme coastal flooding, and this may exacerbate over time with ongoing sea-level rise. This airport is a major gateway to the east coast regions. Gisborne Airport is also potentially exposed to extreme coastal flooding at present and under future SLR increments.
- Significant numbers of roads and buildings are potentially exposed to extreme coastal flooding at present and with future increments of SLR, as well as fluvial flooding, which impacts tourists' accessibility to recreation hotspots. For example, 38 km of roads are potentially exposed to extreme coastal flooding under 1 m of SLR in Tairāwhiti, and 217 km in Hawke's Bay is potentially exposed at that same level (with the largest amount in Napier City with 182 km of roads potentially exposed). A much larger amount of roading is potentially exposed to river flooding: 371 km in Tairāwhiti and 681 km in Hawke's Bay.
- Flooding impacts for tourist hotspots due to extreme rainfall or SLR and extreme storm tides. For example, as shown in Table A-1, 127 hectares of reserves in Tairāwhiti (all categories of reserves combined as an example of tourism recreational areas) may potentially be exposed to extreme coastal flooding under 1 m of SLR.
- Increased likelihood of drought events in Tairāwhiti and the Hawke's Bay regions, with more chance of water shortages and high risk of wildfires which may affect tourism activities.
- Sea-level rise will likely affect the natural character of sandy beaches by causing erosion over time. Coastal inundation and erosion may also affect holiday homes and resorts that are located close to the coastline. In the Hawke's Bay Region, 20,400 buildings are potentially exposed to extreme coastal flooding under 1 m of SLR.

10.5 Ecosystem health

The impact of climate change on terrestrial, aquatic and marine ecosystems has been the subject of much research in the past couple of decades (Brodie and Pearson, 2016, Rapport et al., 1998, Wang and Cao, 2011, Malhi et al., 2020). Climate change is expected to be a stressor on terrestrial, freshwater, coastal and marine ecosystems, particularly under high-warming scenarios. For example, wetlands are highly sensitive areas and are amongst the most threatened ecosystems in New Zealand. In the future, wetlands will be threatened by changes to rainfall patterns, drought and surface and groundwater hydrology. Wetlands close to the coast will also be at risk from sea-level rise (inundation and erosion) and changes to the salinity of groundwater which may impact the distribution and assemblage of species. Although many of New Zealand's ecosystems are being degraded due to climate change-oriented hazards, some of them, such as alpine, freshwater and coastal ecosystems, are more vulnerable than others (DOC, 2020). For example, rising sea level, coastal inundation and flooding may lead to the loss of habitat for coastal and estuary species, which could cause an interruption in the food chain for a wider range of biodiversity (DOC, 2020).

Climate change hazards could impact the ecosystem's health from two different, but interrelated aspects including: biodiversity and habitat loss, and pests and biosecurity issues.

10.5.1 Native biodiversity (terrestrial, aquatic and marine biodiversity)

Climate change is continuously impacting all aspects of biodiversity on the planet, from terrestrial to marine ecosystems and biodiversity. Anthropogenic climate change is already impacting 19% of threatened species recorded in the IUCN Red List, and pushing them toward extinction (IUCN, 2019). Climate change-induced hazards, such as temperature rise, have significant impacts on native biodiversity, including their abundance, behaviour and genetic properties (IUCN, 2019). Changing the features of the food chain, increasing invasive species, habitat loss, and ocean acidification are only a few examples of climate change impacts that threaten native biodiversity, both globally and in New Zealand (Christie, 2014). For example, changes in temperature and rainfall, and sea-level rise, are expected to lead to secondary effects, including erosion, landslips, and flooding, affecting coastal habitats and their dependent species, for example, loss of habitat for nesting birds.

Almost 60% of New Zealand's unique ecosystems, including its native biodiversity, are under threat (Hawke's Bay Regional Council, 2020). Further, about 4000 of New Zealand's threatened species are pushed towards the brink of extinction, partly due to climate change (MfE, 2019). Many indigenous New Zealand species are already and will be at further risk from climate-related impacts such as river water abstraction for irrigation (in response to reductions in rainfall and higher drought incidence), hydroelectric power schemes (a potential mitigation response to greenhouse gas emissions), and non-climate-related impacts such as predation, habitat loss and fragmentation from land use change, urban area and infrastructure expansion, and pollution (McGlone and Walker, 2011). Many species will be at risk from new and existing pests that are able to colonise and spread further in New Zealand because of climate change (Kean et al., 2015).

The direct responses of terrestrial biodiversity to future climate changes will be challenging to predict, due to uncertainty about climate projections, species' responses to climate change and the ability of species to adapt (McGlone and Walker, 2011, Christie, 2014). This is particularly because of the existing pressures of invasive species and human-related habitat loss on native biodiversity. The capacity of native species and ecosystems to adapt to a changing climate is unknown, especially given New Zealand's oceanic setting and existing highly variable climate regime. However, the indirect responses of terrestrial biodiversity to climate change can be predicted with more certainty. Indirect impacts involve the exacerbation of existing invasive species problems and human-related threats, such as habitat loss (Christie, 2014). Land use and land management practice change in anticipation of climate change may result in further restrictions of native species abundance and distribution.

The New Zealand National Climate Change Risk Assessment (AECOM et al., 2020) highlights the ten most significant climate change risks to New Zealand, based on urgency. Two of the top ten are in the 'natural environment' domain, with 'major' consequence ratings and urgency scores greater than 70. They are:

- Risks to coastal ecosystems, including the intertidal zone, estuaries, dunes, coastal lakes and wetlands, due to ongoing sea-level rise and extreme weather events; and
- Risks to indigenous ecosystems and species from the enhanced spread, survival and establishment of invasive species due to climate change.

Ten other risks in the natural environment domain were identified which incorporate most ecosystem types in New Zealand and a range of climate-related impacts.

Some mitigation aspects of climate change might have negative impacts on terrestrial biodiversity. Afforestation with exotic tree species (e.g. *Pinus radiata*) may lead to reductions in catchment water yield, with negative impacts on streamflow and freshwater biodiversity, stabilisation of previously dynamic systems (e.g. pines on coastal dunes) with consequent loss of indigenous flora, invading areas where the native forest was either absent or limited and creating flammable forest communities (McGlone and Walker, 2011). The conversion of native scrub and shrubland to forestry may also cause the direct loss of native ecosystems.

Changes to rainfall patterns and river flows, as well as the human impact of greater abstraction of freshwater for irrigation and increasing storage (in the form of reservoirs) for hydroelectricity and urban water supply, will lead to impacts on freshwater ecosystems (Parliamentary Commissioner for the Environment, 2012). The role of floods in New Zealand rivers is extremely important for maintaining ecological integrity, so changes to the hydrological regime may have dramatic impacts on biological communities (Death et al., 2016, Crow et al., 2013). Altered natural flow patterns may result in invasive predators gaining increased access to habitats crucial for sensitive life cycle stages (e.g. islands in river channels used by nesting birds) and changes in habitat type, and some aquatic species (e.g. invertebrates) are likely to be impacted more than others, depending on their life cycles (McGlone and Walker, 2011). Habitat size, availability and quality may be reduced for some species, and drought may threaten already isolated fish and invertebrate populations.

Egan et al. (2020) carried out a climate change vulnerability assessment for freshwater taonga species in New Zealand. Increasing risk of drought is likely to have negative impacts on several taonga species found in Tairāwhiti and Hawke's Bay, for example tuna (longfin eel), due to changes in habitat availability. The timing of seasonal rainfall and changes to river levels may affect īnanga (whitebait) reproduction cycles. Increasing water temperature may be beneficial in the cooler part of the year for tuna (shortfin eel), because feeding activity increases when temperatures exceed 12°C. However, changes to temperature regimes throughout the year may impact environmental cues for spawning for a number of species including giant kōkopu (whitebait) and kākahi (mussels).

Sea-level rise may increase salinity at river mouths and further upstream than at present, thereby reducing freshwater habitats, particularly in short catchments. Increases in extreme rainfall intensity may lead to more sedimentation and turbidity in waterways, with consequent habitat loss. Banded kōkopu (*Galaxias fasciatus*) have been found to have reduced abundance in turbid streams, so increasing runoff and sediment flowing into streams could limit their distribution (Rowe et al., 2000). Other oceanic changes (e.g. changes to salinity, sea temperatures, and pH (Law et al., 2018) may also have an impact on diadromous fish species and their migration patterns.

Whakakī Lake is an example of a sensitive coastal ecosystem in the northern part of Hawke's Bay region (Hawke's Bay Regional Council, 2018). The largest coastal lake on the east coast of the North Island, Whakakī provides a diversity of natural and ecological services, as well as social-economic values for the region. The lake is significant to the iwi and hapū of Te Rohe o Te Wairoa, Ngāti Kahukura, Ngāti Kirituna and Te Whakakī Nui-a-Rua. Whakakī Lake provides a safe habitat for native fauna and flora, including 46 species of waterbirds, six native fish species, several native aquatic and dune plant species, and a variety of invertebrate species. However, due to significant historical modifications, only 10% of the original wetland area remains. The remaining wetland area is in a degraded state with frequent algal blooms.

Coastal lakes like Whakakā are sensitive to potential climate change impacts resulting from sea-level rise, changes to lake inflows, rainfall and air and water temperature (Tait and Pearce, 2019). Based on the projections discussed earlier in this report and findings by Tait and Pearce (2019) for a similar type of coastal lagoon in Southland, potential climate change-related impacts for Whakakā may include:

- Increased sedimentation from extreme rainfall, runoff, and higher flood flows into the lake;
- Reductions in inflows and lower lake water levels due to reduced rainfall and increased drought conditions;
- The boundary of the lake and wetland area may shift landward and the lake may become more brackish due to sea-level rise;
- Increased water temperature may increase the abundance of algae and algal blooms and cause heat stress for aquatic species;
- Habitat may become less suitable for aquatic and terrestrial species due to the above physical changes to the lake.

A study similar to Tait and Pearce (2019) could be carried out for Whakakā Lake to understand potential climate change-related impacts in more detail.

Coastal systems are particularly sensitive to three key drivers related to climate change: sea level, ocean temperature, and ocean acidity (Wong et al., 2014). Soft shorelines (beaches and estuaries) are likely to be more severely affected by sea-level rise than hard (rocky and consolidated cliffs) shores. Due to the extensive development near beaches, estuaries and marshes, it is unlikely that natural adjustment of the coast will be readily allowed in the future (i.e. coastal retreat and reconfiguration as sea level rises). A potential human response to sea-level rise will be by building hard barriers, protecting sand dunes, replenishing beaches, and infilling estuaries to prevent erosion and to protect property and infrastructure.

The lack of space for natural coastal adjustment is often termed *coastal squeeze*. Coastal squeeze has varying definitions, but a narrower focus is the definition by Pontee (2013): “Coastal squeeze is one form of coastal habitat loss, where intertidal habitat is lost due to the high water mark being fixed by a defence or structure (i.e. the high water mark residing against a hard structure such as a sea wall) and the low water mark migrating landwards in response to SLR”.

Consequently, running in parallel with the impacts of climate-change and SLR on coastal and estuarine/marsh systems will be the ongoing direct and indirect pressures of society’s responses to climate-change adaptation (Swales et al., submitted). If cascading climate-change effects are not thoroughly explored and evaluated in a holistic manner, attempts to counteract the SLR impacts on the built environment and existing land-use rights (e.g. shoreline protection works, reclamations to reinstate shoreline buffers, stopbanks and alteration to drainage schemes), will invariably lead to coastal squeeze and loss of intertidal habitats and beaches (Kettles and Bell, 2015).

There are numerous examples of coastal squeeze around New Zealand as coastal erosion affects the areas around hard defences. In one such example, Figure 10-1 shows erosion next to a sea wall in Whitianga, Coromandel.



Figure 10-1: Erosion beside a sea wall in Whitianga. Photo: R. Bell, NIWA.

Loss of productive estuarine habitats and biota is likely to accelerate with sea-level rise and other climate-related impacts discussed above, with the more visible ecological effects being reduced populations and altered migratory patterns of coastal birds, and declines in certain commercially-important marine fishes that use estuaries for part of their life cycle (e.g. snapper, *Pagrus auratus*) (McGlone and Walker, 2011). The effects of changes in waves and freshwater inputs will also have significant adverse impacts on coastal ecosystems (Hewitt et al., 2016).

Warming has been observed in coastal and oceanic waters around New Zealand over the past few decades, with the strongest warming happening off the coast of Wairarapa and the weakest warming signal between East Cape and North Cape (Sutton and Bowen, 2019). Projections for the Southwest Pacific show an increase in SST by mid- and end-century, regardless of RCP and climate model (Law et al., 2016). The mean increase is $\sim 1^{\circ}\text{C}$ by mid-century, and $\sim 2.5^{\circ}\text{C}$ by end-century for RCP8.5. Figure 10-2 shows the spatial variation of change in SST for end-century under RCP8.5, with surface warming across the entire Southwest Pacific. The most striking feature is the strong warming of $+4^{\circ}\text{C}$ in the western Tasman Sea (in region 2 on Figure 10-2) associated with the southerly penetration of the East Australian Current off southeast Australia in region 2 (Ridgway, 2007). The western Tasman Sea region is warming at a rate four times that of the global average as a result of the climate-driven spin-up of the South Pacific gyre (Roemmich et al., 2016). This warming propagates across the northern Tasman Sea (region 3) along 35°S in association with the Tasman Front, causing the most significant regional SST increase in the New Zealand Exclusive Economic Zone. Warming oceans are likely to have impacts on the distribution of marine species as well as pests from warmer areas. For example, distribution shifts and changes in abundance of numerous fish species have been observed in the southeast Australia region due to substantial ocean warming that has already occurred there

(Last et al., 2011). Similar effects may occur in New Zealand waters as the oceans warm in the future but there is no published evidence of this happening to date.

Marine species are likely to be affected by ocean acidification. Growth rates and shell development of species with carbonate shells, such as oyster, paua, and some phytoplankton are reduced in more acidic waters (Cummings et al., 2013). The behaviour of Australian reef fish is affected by ocean acidification, with olfaction, hearing, visual risk assessment and activity altered due to the impact on neurotransmitter function (Munday et al., 2014). An investigation into the effects of ocean acidification and heatwave conditions on juvenile snapper (*Pagrus auratus*) was undertaken in New Zealand by McMahon et al. (2019). They found that critical swimming speed and maximum metabolic rates increased with higher temperatures but decreased with higher CO₂ (i.e. higher acidity), which means ocean acidification could have negative effects on snapper population recruitment. However, it is uncertain at this stage whether the same behaviours will be affected in a wider range of New Zealand temperate and subantarctic fish species (Law et al., 2018).

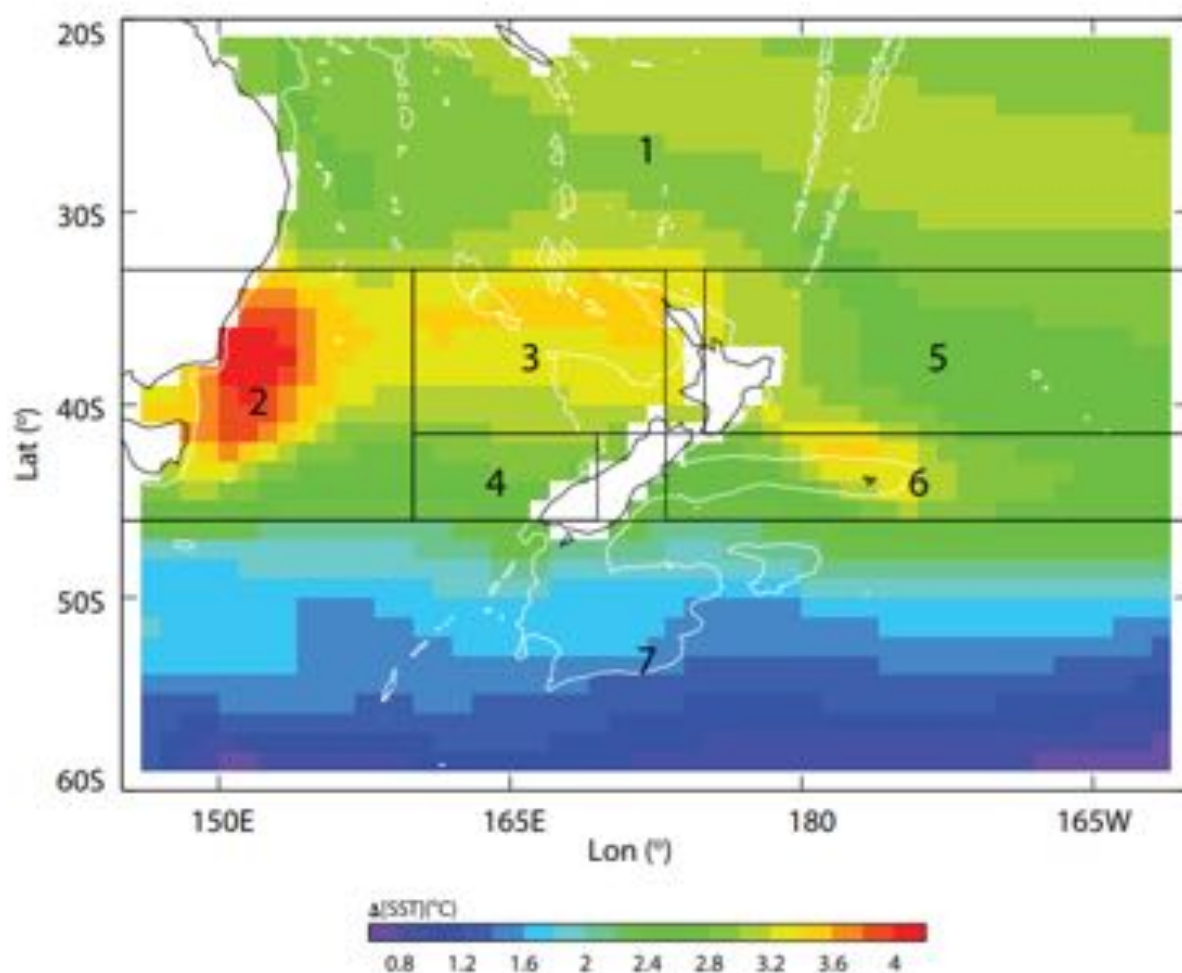


Figure 10-2: Regional variation of the projected change in SST for the End-Century (2081-2100) compared with present-day (1976-2005) under RCP8.5 (Law et al., 2016).

10.5.2 Pests and biosecurity

Climate change hazards such as rising temperatures, heatwaves, and changes in precipitation patterns are likely to increase biosecurity issues including rising numbers of invasive species, pests and pathogens (Luck et al., 2014).

Terrestrial biosecurity

Climate change is widely regarded as one of the greatest challenges facing indigenous ecosystems in the coming century. As New Zealand (and much of the Tairāwhiti and Hawke's Bay regions) has an economy based on very efficient primary production systems, the risk of exotic pests and diseases affecting the primary industries also needs to be minimised. Climate change will create new biosecurity challenges by allowing the establishment of new exotic pest animals, weeds and diseases which are currently prevented by New Zealand's climate. The potential establishment of subtropical pests and current seasonal immigrants are of greatest concern, along with species that are already recognised as high risk (Kean et al., 2015).

Although climate change may affect organisms and ecosystems in a range of ways, the most important driver of pest invasion is likely to be temperature, modified by rainfall, humidity and carbon dioxide (Kean et al., 2015). In addition, changes in large-scale weather patterns will influence the frequency and intensity of extreme weather events (e.g. flooding, drought, damaging wind). Regional winds and currents may affect the ability of potential invaders to reach New Zealand and establish. Myrtle rust (*Austropuccinia psidii*) is a fungus that has been recently (in 2017) found in northern New Zealand. It attacks plants belonging to the Myrtaceae family, including pōhutukawa, mānuka, rātā, and feijoa. There is concern that myrtle rust may spread further in New Zealand as the climate warms and other fungi that are spread by wind may become established in the country in the future with changes to atmospheric circulation, temperature, wind patterns, and storminess.

Big headed (*Pheidole megacephala*) and Argentine (*Linepithema humile*) ants are some of the worst invasive pest species in the world, as they can wreak havoc on the native arthropod fauna, and they are already present in New Zealand. Continued warming and drying of eastern climates such as in Tairāwhiti and Hawke's Bay are likely to encourage their spread. Wasps are highly responsive to climate conditions; wet winters with flooding do not favour nest survival and can lower populations, while warm, dry conditions are ideal for explosive population growth (McGlone and Walker, 2011). Subtropical fruit flies are already considered major threats to the New Zealand horticulture industry. A modelling exercise done for the Queensland fruitfly (Figure 10-3) shows that in the historic period, only the northern parts of New Zealand are suitable for population establishment. However, the envelope of suitability (indicated by red and orange shades) spreads further south during the future periods of 2030-2049 and 2080-2099. Tairāwhiti and Hawke's Bay generally have low suitability under the historic climate (except for a few small coastal areas), but suitability considerably increases over time to cover a large portion of both regions (Kean et al., 2015).

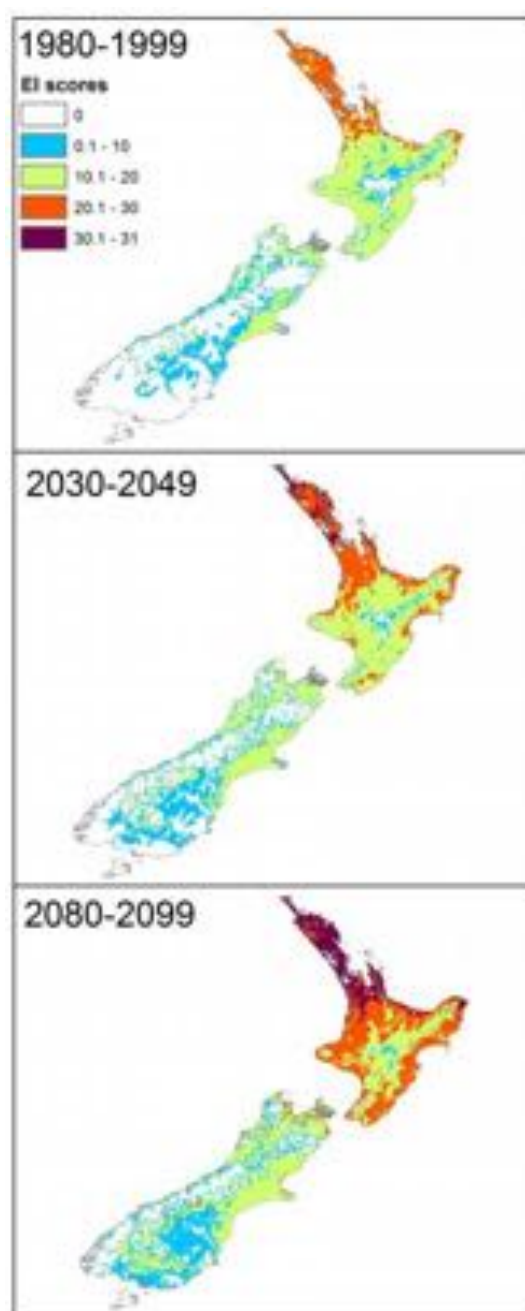


Figure 10-3: Ecoclimatic Index scores for the Queensland fruitfly, *Bactrocera tryoni*, for three periods 1980-1999, 2030-2049, and 2080-2099. EI scores >19 indicate a high probability that the site is suitable for long-term population persistence (e.g. red and orange shades). The climate data are for the A1B scenario (equivalent to RCP6.0) and the CM2.1-GFDL general circulation model. Source: Kean et al. (2015).

The arrival of new pest plants and the increased invasiveness of existing weeds is one of the most significant likely consequences of climate change. More plant species are present in warmer regions, so as frost declines in frequency, winters warm, and more insect pollinator species are able to survive in warmer temperatures, a much larger range of weed species will be able to compete with local species (McGlone and Walker, 2011). It is expected that farmers and growers in the Tairāwhiti and Hawke's Bay regions will increase their usage and dependence on existing subtropical plant species

and introduce new commercial species. This increased use of subtropical plants may make the regions more susceptible to invasion by subtropical pests and diseases and new host-pest associations (Kean et al., 2015). Ornamental plants may escape cultivation when climatic constraints (such as frosts) are reduced and subsequently may naturalise and become invasive (Sheppard et al., 2016). Sheppard (2013) modelled the potential distribution of recently naturalised plant species in New Zealand with future climate change (*Archontophoenix cunninghamiana* (bungalow palm), *Psidium guajava* (common guava), and *Schefflera actinophylla* (Queensland umbrella tree)). All three species, which are currently only present in northern New Zealand (Northland and Auckland), have the potential to significantly increase their range further southward in the future, particularly into coastal areas around the country.

The shift towards reliance on drought and heat tolerant plants (in particular, pasture grasses) may cause new pest species to spread and for new host/pest associations to develop (Kean et al., 2015). The 2014 emergence of two native moths (*Epyaxa rosearia* and *Scopula rubraria*) as major plantain (a variety of pasture grass) pests demonstrates how a large increase in usage elevated these previously harmless species to pest status. In addition, as kikuyu grass (*Cenchrus clandestinus*) is likely to become the most prevalent forage grass with increasing temperatures, pests that affect kikuyu grass are likely to be important. Some pest species from Australia (e.g. the *Sphenophorus venatus vestitus* weevil) have already been recorded on kikuyu in Northland and pests such as this are likely to spread further in New Zealand as the climate warms. However, the projected reduction in rainfall and humidity in some areas may actually reduce certain fungal disease pressures that require a wetter environment (Coakley et al., 1999).

It is important to note that although much of the biosecurity risk with climate change will come from beyond New Zealand's borders, many of the future's pest, disease and weed problems are currently dormant in New Zealand, awaiting some perturbation, such as climate change, to allow them to spread and flourish. These types of pests are often weeds but may also be invertebrates. A few examples of sleeper invertebrate pests that are affected by temperature include (after Kean et al. (2015)):

- Migratory locust *Locusta migratoria*, found in grassland from Christchurch northwards. Because existing temperatures are not usually high enough to trigger swarming behaviour, the insect currently is not regarded as a pest. However, the locusts have retained the capacity to swarm with a small swarm observed near Ahipara, Northland in the 1980s.
- Tropical armyworm *Spodoptera litura*. While this pest can be found through many lowland North Island districts, epidemic outbreak populations, when caterpillars move 'like an army' through crops and pastures, are rare. However, the combination of events that cause outbreaks will be more common under projected climate change scenarios and include above-average summer and autumn temperatures, allowing for additional generations to develop.

The reader is directed to Kean et al. (2015) for more detailed information about the potential effects of climate change on current and potential terrestrial biosecurity pests and diseases in New Zealand.

Aquatic biosecurity

The primary source of entry for aquatic biosecurity risk organisms into New Zealand is and will continue to be through international shipping. These risk organisms are contained within ballast water or attached to the hulls of ships. However, changes in water temperature and ocean currents into the future, because of climate change, may result in species (including pests and pathogens) not usually seen in New Zealand waters to arrive and establish. Sea temperatures are projected to increase around New Zealand, particularly to the west of the country, and seawater is likely to decrease in pH (i.e. become more acidic) (Law et al., 2018).

Long-term changes in marine environmental variables, such as seawater temperature, may lead to new ecological compatibilities and may alter existing host-pathogen interactions. It is commonly accepted that warmer sea and freshwater temperatures modify host-pathogen interactions by increasing host susceptibility to disease. Such changes could contribute to the emergence of aquatic diseases in new regions (Castinel et al., 2014). Of concern for Tairāwhiti and Hawke's Bay is a strengthening East Auckland Current off the east coast of the northern North Island, which connects with the East Cape Current which flows past Tairāwhiti and Hawke's Bay. This strengthening current is expected to promote the establishment of tropical or subtropical species that currently occur as vagrants in warm La Niña years (Willis et al., 2007). The establishment of these species may have negative impacts on wild fisheries and aquaculture operations.

In terms of freshwater biosecurity, increased water temperatures are likely to favour the expansion of warm water species such as koi carp, goldfish, tench, rudd, and catfish (Office of the Prime Minister's Chief Science Advisor, 2017). These fish can cause water quality degradation and reduced indigenous biodiversity. Increased water temperatures may also facilitate the establishment of tropical fish that are sold in the New Zealand aquarium trade and intentionally or accidentally released. Increasing water temperatures will also favour warm-climate invasive aquatic plant species such as water hyacinth (*Eichhornia crassipes*) and water fern (*Salvinia molesta*).

As discussed above for terrestrial biosecurity, aquatic organisms already established within the New Zealand region that are not currently pests may become problematic under changed environmental conditions with climate change – these are called “sleepers pests”.

10.6 Human health

Most of the information in this section is summarised from Royal Society of New Zealand (2017) – a report titled *Human health impacts of climate change for New Zealand*.

Around the world, climate change has already contributed to increased levels of ill health, particularly in connection with summer heatwaves. Climate change affects human health in a number of ways. The ideal healthy human has complete physical, mental and social wellbeing, and not merely the absence of disease or infirmity. Changes to the climate can impact on these:

- Directly via air and sea temperature, flooding or storms;
- Indirectly due to changes to the environment and ecosystems; and
- Indirectly due to social and economic changes, such as migration stresses, health inequality and socioeconomic deprivation.

In New Zealand, children, the elderly, people with disabilities and chronic disease, and low-income groups are particularly vulnerable to climate change-related health impacts. Maori are also particularly vulnerable due to existing health inequalities, having an economic base invested in primary industries, housing and economic inequalities, and a greater likelihood of having low-income housing in areas vulnerable to flooding and sea-level rise.

10.6.1 Direct health impacts

Increased flooding, fires and infrastructure damage

Increased frequency and magnitude of fires, floods, storm tides and extreme rainfall events will affect public health directly through injury (e.g. being burnt by fire or swept away by floods or landslides). These extreme events may also have negative effects on wellbeing through disease outbreaks, toxic contamination, effects of damp buildings, mental health issues, disruption to healthcare access and damage to homes (lasting from weeks to months after the initial event).

Displacement

Sea-level rise and coastal erosion, as well as river flooding, may require people to leave their homes. This can cause uncertainty and lead to mental health issues from the trauma of leaving familiar surroundings, the breaking of social ties, and the difficulty of resettlement.

Extreme heat

Hot days have well-established negative impacts on the levels of illness and death, and diabetes and cardiovascular disease increase sensitivity to heat stress. Heat stress is particularly significant when hot spells occur at the beginning of the hot season before people have become acclimatised to hotter weather. The increasing numbers of heatwave days in Tairāwhiti and Hawke's Bay will likely cause detrimental impacts on health.

Heat also poses health risks for people who work outdoors, including heatstroke and renal (kidney) impairment. The increased heat is also associated with increased incidences of aggressive behaviour, violence, and suicide. Individuals with mental health conditions are especially vulnerable to high temperatures or heat waves, primarily due to not drinking enough fluids, getting access to cool places, or recognising symptoms of heat exposure.

10.6.2 Indirect health impacts

Harmful algal blooms

Increasing temperatures will increase the likelihood of blooms of harmful algae, including blue-green algae (cyanobacteria). These algae produce toxins that can, by either contact or ingestion, cause liver damage, skin disorders, and gastrointestinal, respiratory and neurological symptoms. These blooms can be widespread and long-lasting and can have impacts on commercial seafood harvesting and people reliant on non-commercial harvesting (particularly Maori and Pasifika people), as well as drinking water supplies and recreational water use.

Microbial contamination

Changing weather patterns, including more extreme rainfall events, flooding, and higher temperatures, are likely to interact with agricultural runoff and affect the incidence of diseases transmitted through contaminated drinking and recreational water. Conditions may also be more suitable for bacterial growth – extreme rainfall may be a key climatic factor influencing the incidence

of waterborne diseases like *Norovirus*. *Vibrio* marine bacteria are highly responsive to rising sea temperatures and may cause infected wounds, diarrhoea and septicaemia.

Food availability, quality and safety

Climate change-induced changes to weather patterns and sea-level rise have direct effects on food production, which can affect food affordability and availability, locally and globally. Changes in air and water temperatures, rainfall patterns and extreme events can also shift the seasonal and geographic occurrence of bacteria, viruses, parasites, fungi and other pests and chemical contaminants. This can lead to reduced food safety prior to, during and after harvest, and during transport, storage, preparation and consumption. For example, higher temperatures can increase the number of microorganisms already present on fruit and vegetables, and flooding is a factor in the contamination of irrigation water and farm produce and the *E. coli* contamination of shellfish.

Mental health and wellbeing

Increased temperatures, extreme weather events, and the displacement of people from homes and communities will have significant mental health and wellbeing consequences. These range from minimal stress and distress symptoms to clinical disorders such as anxiety, depression, post-traumatic stress and suicidal thoughts. For New Zealanders, the natural environment is at the heart of the nation's identity. Disruption of bonds with the natural environment (e.g. through relocation of communities) can cause grief, loss and anxiety.

Outdoor air quality

Changes in temperature, rainfall, and air stagnation can affect air pollution levels and human health. Chronic health conditions such as asthma and chronic obstructive pulmonary disease are particularly affected by outdoor air quality. Climate change is expected to increase the risk of fire, which may cause more particulate emissions (PM10 and PM2.5) as well as ozone. Particulate matter smaller than 2.5 µm in diameter (PM2.5) is associated with severe chronic and acute health effects, including lung cancer, chronic obstructive pulmonary disease, cardiovascular disease, and asthma development and exacerbation. The amount of soil-derived PM10 dust in the air may also increase in areas more frequently affected by drought. Due to extended growing seasons with climate change (due to higher CO₂ and higher temperatures), allergenic pollen may become more abundant in the atmosphere (seasonally, spatially and at higher volumes).

However, improvements in outdoor and indoor air quality may be realised with ongoing warming and consequent reductions in wintertime domestic fire use, as well as a move towards an electrified vehicle fleet.

Carriers of new diseases

There are a number of organisms, including mosquitoes, ticks, and fleas that can transmit infectious diseases between humans or from animals to humans. The seasonality, distribution and common occurrence of diseases spread by these carriers are largely influenced by climatic factors, particularly high and low-temperature extremes and rainfall patterns. Therefore, climate change may create favourable conditions and increase the risk of infectious disease transmission in some areas.

Increased temperature, in particular, heightens the risk for mosquito-borne diseases which are currently absent from New Zealand because the mosquitoes that carry these diseases (*Aedes aegypti* and *Aedes albopictus*) are not established in our current climate (it is too cold) (Derraik and Slaney, 2015). These diseases include West Nile virus, dengue fever, Murray Valley encephalitis, Japanese

encephalitis, Ross River virus, and Barmah Forest virus (most of these are present in Australia). Mosquito-borne diseases like Zika and chikungunya that are already present in the Pacific Islands could become more of a risk for New Zealand if climate change allows important disease-transmitting mosquitoes to become established here. Disease-carrying mosquitoes are often intercepted in New Zealand, particularly at seaports.

Summary

Overall, climate change-induced hazards are likely to expose Tairāwhiti and Hawke's Bay to a variety of direct and indirect health impacts. Both types of impacts could threaten residents' life (existential threats) or degrade their health and wellbeing. Increased flooding and bushfire events and extreme heat are examples of direct drivers of potential health issues in these regions. The indirect impacts include the drivers that cause some secondary health issues over time. These impacts include harmful algal blooms and microbial contamination which release toxic substances to drinking water resources, reduced rainfall or flooding that impact food production and distribution system, or increased abundance and distribution pattern of pathogens and disease due to rising temperature. Mental health and wellbeing is another aspect of human health issues that could be impacted by climate change-oriented hazards such as heat stress, flooding and fire events.

10.7 Infrastructure and the built environment

Impacts of climate-related hazards on the built environment and infrastructure are evident in New Zealand, and these are projected to increase in the future with ongoing climate change. Around 75% of the insurance claims in New Zealand are linked to climate-related hazards (NIWA, 2012). Like the rest of New Zealand, infrastructure and the built environment in Tairāwhiti and Hawke's Bay are being affected by climate change-induced hazards, which consequently creates social and economic issues for these regions (MfE, 2020, NIWA, 2012, Savage, 2006). For example, Savage (2006) indicates the vulnerability of Tairāwhiti to severe cyclonic and cell-type storms which increases the risk of soil erosion and damage to flood protection infrastructure. These types of storms may also impact urban, farming, water and transport-related infrastructure.

The New Zealand National Climate Change Risk Assessment (AECOM et al., 2020) highlights the ten most significant climate change risks to New Zealand, based on urgency. Two of the top ten are in the 'built environment' domain, with 'extreme' consequence ratings and urgency scores greater than 90. They are:

- Risk to potable water supplies (availability and quality) due to changes in rainfall, temperature, drought, extreme weather events and ongoing sea-level rise; and
- Risks to buildings due to extreme weather events, drought, increased fire weather and ongoing sea-level rise.

Six other risks in the built environment domain were identified, including risks to landfills and contaminated sites, wastewater and stormwater systems, ports, airports, linear transport networks, and electricity infrastructure.

As discussed above for agriculture and horticulture, increasing risk of drought in Tairāwhiti and Hawke's Bay could impact water availability in the regions, for supply to the primary sector, industry and residents. In addition to reducing water availability, drought and high temperatures can result in higher water demand levels which can exacerbate supply issues. In addition, sea-level rise may lead to salinity stress of potable water supplies and increases in heavy rainfall may affect water supply

through contamination and sedimentation (the impact of sedimentation on water supply reservoirs was seen in Auckland following a large rainfall event in 2017).

As discussed in Section 9.1, extreme storm tides combined with sea-level rise are a significant hazard affecting coastal environments and infrastructure. Levels of potential exposure of different types of infrastructure are presented in Section 9 and Appendix A. Impacts associated with extreme storm tide events could include temporary flooding and damage to roads, buildings, bridges, port facilities, and increased maintenance costs due to damage or increased wear and tear from more frequent flooding, and service disruption.

Transport infrastructure is also particularly at risk from slips and landslides associated with heavy rainfall. Although there is no quantitative data to draw upon regarding exposure to slips in Tairāwhiti and Hawke's Bay, Tairāwhiti in particular has some of the most erodible soils in New Zealand (Gisborne District Council, 2020). Heavy rainfall events are likely to increase in intensity as the climate continues to warm (Section 5.2). Therefore, it is likely that the parts of the region which already have geology susceptible to slips and landslides may be more at risk in the future.

Reliable transportation infrastructure is critical for functioning social and economic systems from local to international scales. Distribution of goods and services, access to healthcare systems, schools and markets, and delivering emergency responses in catastrophic situations rely on functioning transportation infrastructure. Therefore, the impacts of climate change-induced hazards on transport infrastructure are highly likely to affect other sectors such as agriculture, tourism, forestry, human safety and well-being. For example, climate change impacts on transportation infrastructure could have vast consequences on development programmes (such as building houses, infrastructure, etc.), especially those that rely on transportation to gain access to the target audience they serve. Impacts on airport, railways and roads could interrupt the supply and distribution chains of agricultural and horticultural products, thus creating food security problems. Also, by limiting access to the regions (due to non-functioning airports and roads), their tourist hotspots (due to flooding), and safe accommodation, the tourism industry may suffer.

11 Summary and conclusions

This report presents climate change projections for the Tairāwhiti and Hawke's Bay regions. Historic climatic conditions are presented to provide a context for future changes. The future changes discussed in this report consider differences between the historical period 1986-2005 and two future time-slices, 2031-2050, "2040", and 2081-2100, "2090". Note, the modelled differences between two time periods should not be attributed solely to climate change, as natural climate variability is also present and may add to or subtract from the climate change effect. The effect of natural variability has been reduced in the projections by averaging results from six GCM simulations, but it will still be present.

It is internationally accepted that further climate changes will result from increasing amounts of anthropogenically produced greenhouse gases in the atmosphere. The influence from anthropogenic greenhouse gas contributions to the global atmosphere is the dominant driver of climate change conditions, and it will continue to become more dominant if there is no slowdown in emissions, according to the IPCC. In addition, the climate will vary from year to year and decade to decade owing to natural variability.

Notably, future climate changes depend on the pathway taken by the global community (i.e. through mitigation of greenhouse gas emissions or a 'business as usual' approach). The global climate system

will respond differently to future pathways of greenhouse gas concentrations. The representative concentration pathway approach taken here reflects this variability through the consideration of multiple scenarios (i.e. RCP4.5, the mid-range scenario, and RCP8.5, the high-end scenario). The six climate models used to project New Zealand's future climate were chosen by NIWA because they produced the most accurate results when compared to historical climate and circulation patterns in the New Zealand and southwest Pacific region. They were as varied as possible to span the likely range of model sensitivity. The average of outputs from downscaling simulations derived from all six models (known as the 'ensemble average'), is presented in the climate change projection maps in this report. The ensemble-average was presented as taking averages over a number of simulations reduces the effect of 'noise' from natural climate variability, while usage of multiple models provides a consensus projection.

Changes to the future climate of Tairāwhiti and Hawke's Bay are likely to be significant. An increase in extreme hot days, a reduction in frost days, and a shift to larger extreme rainfall events are some of the main impacts. The following list summarises the projections of different climate variables in Tairāwhiti and Hawke's Bay:

- The projected temperature changes for the two regions increase with time and greenhouse gas concentration scenario. Future annual average warming spans a wide range: 0.5-1.0°C by 2040, and 1.0-1.5°C (RCP4.5) or 2.0-3.0°C (RCP8.5) by 2090. Similarly, annual average minimum temperatures are expected to warm for most locations in both regions by 0.5-1.0°C by 2040. By 2090, minimum temperatures at most locations are projected to warm by 0.5-1.0°C (RCP4.5) or 1.5-2.5°C (RCP8.5). For both mean temperature and minimum temperature, warming is generally greatest to the west.
- The average number of frost days is expected to decrease with time and scenario. The largest decreases are projected for high elevation locations in the west, where 5-20 fewer frost days are projected by 2040, and 10-30 fewer days by 2090 (10-50 days under RCP8.5). Smaller decreases are generally projected for coastal locations because fewer frosts historically occur in these locations.
- The average number of heatwave days per year is projected to increase with time and scenario. By 2090, and under RCP8.5, the majority of both regions is projected to receive 20-60 additional heatwave days per year. Increases are generally not as large for higher elevation locations further inland. Eastern and coastal parts of both regions historically experience the largest number of hot days, and these locations are expected to see the greatest increases to the future number of hot days
- Projected changes in rainfall show variability across the two regions. By 2040 under both scenarios, annual rainfall is expected to decrease by a small amount for the majority of both regions, generally in the 0-5% range. By 2090, larger and more extensive decreases to annual rainfall are projected, decreasing by up to 10% under RCP4.5, and up to 15% under RCP8.5. Spring is generally projected to experience the greatest and most extensive drying, while winter rainfall is generally projected to increase on the western side of the mountain ranges (despite a drying signal for the eastern majority of both regions under most winter scenarios).

- Extreme, rare rainfall events are projected to become more severe in the future. Short duration rainfall events have the largest relative increases compared with longer duration rainfall events. For the selected locations analysed in this report, rainfall depths for 1-in-50-year and 1-in-100-year events are projected to increase across the radiative forcing scenarios and future time periods.
- The annual maximum 1-day and 5-day rainfall amount is generally projected to increase by large amounts over and west of the Raukumara Range (more than 15 mm for many parts), except for the 2040 period under RCP4.5 where there is less of a clear signal. The annual maximum 5-day value is also projected to decrease for eastern parts of Tairāwhiti and is one of the few locations in New Zealand projected to see decreases by 2090 under RCP8.5.
- Drought potential is projected to increase across both regions, with annual accumulated Potential Evapotranspiration Deficit (PED) totals increasing with time and increasing greenhouse gas concentrations. Areas east of the mountain ranges are projected to observe the largest increases to PED accumulation, and eastern Tairāwhiti is projected to experience some of the largest increases in the country by 2090. The probability of PED exceeding 300 mm in a given year is also projected to increase significantly for most eastern and coastal locations in both regions. Additionally, large portions of both regions are projected to experience some of the largest decreases to the annual number of days of soil moisture deficit compared to other parts of the country.

The effects of climate change on hydrological characteristics were examined by driving NIWA's national hydrological model with downscaled Global Climate Model (GCM) outputs from 1971-2099 under different global warming scenarios. Using a combination of six GCMs and four warming scenarios allows us to consider a plausible range of future trajectories of greenhouse gas concentrations and climatic responses. The changing climate over this century is projected to lead to the following hydrological effects:

- Annual average discharge is expected to decrease across RCPs and future time periods.
- Mean annual low flow (MALF) changes are also expected to decrease across RCPs and future periods for most catchments. However, under RCP4.5 a number of catchments are expected to see an increase in MALF, as summer rainfall is expected to slightly increase for those catchments.
- High flows (expressed as Q5% flow) are generally expected to see larger decreases by mid-century (2036-2056) under RCP4.5 when compared to the RCP8.5 scenario. Increases to high flows are also expected for some catchments by the mid-century time period, with larger increases expected under RCP8.5 (particularly in Hawke's Bay). The largest decreases to high flows are modelled for RCP8.5 by the end of the century (2086-2099). However, the climate models underpinning this analysis are not able to correctly reproduce ex-tropical cyclone tracks and other intense storms. Further research and modelling is therefore required to understand future changes to high flows.
- Changes in the Mean Annual Flood (MAF) are expected to be spatially diverse across time and RCP scenarios. By the end of the century, under RCP8.5, MAF is expected to

increase by up to 50% for around half of the Hawke's Bay region's rivers and a smaller proportion of rivers across Tairāwhiti.

One of the major and most certain (and so foreseeable) consequences of increasing concentrations of carbon dioxide and associated warming, is the rising sea level. Rising sea level in past decades have already affected human activities and infrastructure in coastal areas in New Zealand, with a higher base mean sea level contributing to increased vulnerability to storms and tsunamis.

- Absolute sea-level rise (SLR), calculated from satellite altimetry, in the Gisborne/Hawke's Bay region is trending at around 4 mm/year (trend for 1993-present) close to the New Zealand-wide average of 4.4 mm/year (calculated up to the end of 2015). Digital records for both the Ports of Gisborne and Napier show increasing trends in annual mean sea level.
- Relative sea-level rise (RSLR) calculated from the sea-level gauges is estimated as 2.15 and 1.40 mm/year at Gisborne and Napier since the establishment of the local vertical datums in 1926 and 1962, respectively.
- Based on the example of the present-day mean high water spring (MHWS-10 level), which is exceeded by only 10% of all high tides (tide only), a 0.4 m increase in sea-level (above 1986–2005 baseline) is estimated to be reached in New Zealand by 2090 under RCP4.5, and 2060 under RCP8.5. A 0.4 m SLR will mean that same ground or tidal elevation will be exceeded by 100% of all high tides (up from 10%; this excludes the influence of weather and storm surges on water level).
- Extreme sea-level analysis shows that a present rare storm-tide event (0.2% annual exceedance probability (AEP) with a 500-year average recurrence interval (ARI)), would become, for example, a 20% AEP (5-year event) after a relative sea-level rise (RSLR) of around 0.16 m, and present-day 100-year ARI event will become a 5-year event after only 0.1 m RSLR.
- The coastal sensitivity index for coastal erosion from climate change in the Gisborne/Hawke's Bay region varies from location to location along the coast and is rated from *Moderate* to *Very High*. Within the Gisborne region, the widths of specific area susceptible to coastal erosion have been calculated to be 5–105 m inland from the present-day coastline, this is estimated to increase to 60 to 180 m by 2115.
- Areas susceptible to coastal erosion have been identified for both the Gisborne and Hawke's Bay coastlines. Estimates of long-term retreat rates range from 0.02 to -1.24 m/year, with short-term shoreline fluctuations ranging from 2 m to greater than 100 m along both advancing and retreating coasts. Areas susceptible to coastal erosion have been mapped and inform Regional Coastal Environment Plans. The widths of the areas susceptible to coastal erosion (from the present-day coastline inland) are shown to generally be increasing.
- There is an increasing exposure of economic and social/culture elements at risk with increased sea-level rise. In the present day the coastal erosion hazard risk is generally *very low* to *low*, but recreation and rural residential land will become increasingly vulnerable for future scenarios for erosion, reaching *very high* economic losses and *low* to *very high* (extremely case dependant) social/cultural losses by 2120.

Exposure of land, infrastructure and assets in the Tairāwhiti and Hawke's Bay regions to coastal and fluvial inundation was analysed. The coastal inundation data model used the 1% Annual Exceedance Probability (AEP) or 1-in-100-year storm tide flood levels, plus different increments of sea-level rise. The fluvial inundation data model was used publicly available flood hazard maps from local government organisations and flood-prone soil maps from Manaaki Whenua Landcare Research, to create a national flood hazard area map.

- For both Tairāwhiti and Hawke's Bay, the most potentially exposed land cover type to extreme coastal flooding and sea-level rise, as well as fluvial flooding, is high producing exotic grassland, followed by orchards, vineyards, or other perennial crop.
- A varying amount of roads and railways are potentially exposed to extreme coastal flooding and sea-level rise, as well as fluvial flooding, in both regions. Napier City has the highest road exposure to coastal flooding out of all territorial authorities (also including Gisborne District), and Hawke's Bay region has approximately twice the road exposure to fluvial flooding than Gisborne District does. Both Napier and Gisborne airports are potentially exposed to extreme coastal flooding under current and future sea levels, as well as fluvial flooding.
- In terms of the potential exposure of buildings to extreme coastal flooding, Napier City has the highest exposure rate of the territorial authorities and Gisborne District (approx. 18,300 buildings potentially exposed to extreme coastal flooding with 1 m of sea-level rise). The potential exposure of buildings to fluvial flooding is less than for coastal flooding in Napier City, but higher in Gisborne District.
- Detailed information about exposure of a range of flood protection infrastructure and three-waters infrastructure types is provided. Again, Napier City is the most exposed territorial authority to extreme coastal flooding and sea-level rise in terms of infrastructure. There is a large range of flood protection and three-waters infrastructure exposed to fluvial flooding across the Gisborne District and Hawke's Bay Region.

A changing climate will have impacts on different sectors and environments in Tairāwhiti and Hawke's Bay, which are summarised in the table below:

Sector	Climate change impact/opportunity
Exotic forestry	<ul style="list-style-type: none"> • Increased productivity due to increased temperatures and CO₂ • Increased severity of droughts and fire risk • Increased rainfall intensity – impacts on erosion, landslides, movement of slash, access to forests for trucks and machinery • Increased incidence of pests and diseases as temperatures increase (e.g. pitch canker, subtropical insect pests)
Horticulture	<ul style="list-style-type: none"> • Increased temperature causing changes to plant development stages and evaporation rates, affecting the quality and quantity of the harvested crop • Extreme heat may result in the regions becoming unsuitable for some crop types

	<ul style="list-style-type: none"> • Reduced frost damage, new opportunities for crop diversification • Increased biomass with increased CO₂ • Rainfall reductions and more severe droughts mean more irrigation may be needed, but there may be water availability issues with projected reductions in river flows • Increased rainfall intensity – impacts on erosion, sedimentation, quality of fruit and vegetables, access to market • Increased incidence of pests and diseases as temperatures increase (e.g. apple black spot) • Exposure to extreme coastal flooding with sea-level rise and fluvial flooding
Agriculture	<ul style="list-style-type: none"> • Increased pasture productivity and yields of some crops (e.g. wheat) (when not limited by rainfall reductions/drought) • Reduced water availability for irrigation with rainfall and river flow reductions • Increased erosion due to more severe droughts and intense rainfall events • Exposure to extreme coastal flooding with sea-level rise and fluvial flooding • Animal heat stress during heatwaves, which affects milk composition and production rate
Tourism	<ul style="list-style-type: none"> • Warmer temperatures may increase some activities (e.g. water-based activities) • Increased tourism season with warmer conditions stretching further into spring and autumn • Many unknowns how climate change will affect the natural environment, but increased prevalence of drought, fire, and warmer temperatures may have negative impacts on native ecosystems • If the wine industry is affected by climate change then this could have flow-on impacts for the tourism sector • Exposure of Napier and Gisborne airports and roads around the regions to coastal and fluvial flooding – likely to affect accessibility by tourists • More intense rainfall events may impact tourism in the region • Sea-level rise will likely affect the natural character of sandy beaches

Ecosystems	<ul style="list-style-type: none"> • Loss of habitat due to sea-level rise and coastal erosion (coastal squeeze) – this could be made worse by human responses to climate impacts e.g. sea walls • Risks to indigenous ecosystems and species due to the increased spread of invasive species • Impacts on freshwater and terrestrial ecosystems from changes to water temperature, rainfall patterns, drought, and river flows, as well as greater abstraction for irrigation • Warming oceans may impact the distribution of marine species (native and invasive) • Ocean acidification may affect marine species with carbonate shells (e.g. paua, oysters, some phytoplankton) and fish behaviour
Human health	<ul style="list-style-type: none"> • Direct impacts on health via increased flooding, fires, and infrastructure damage, displacement of people, extreme heat • Indirect impacts on health via things such as harmful algal blooms, microbial contamination, food availability and quality, mental health and wellbeing, outdoor air quality, and carriers of new diseases
Infrastructure and the built environment	<ul style="list-style-type: none"> • Increasing intensity of storms and rainfall rates may impact infrastructure including buildings, roads, etc. through floods, slips and erosion • Risk to potable water supplies due to changes to rainfall, temperature, drought, extreme weather events and sea-level rise • Increasing infrastructure exposure over time to coastal flooding with ongoing sea-level rise

Increasing temperatures and changing rainfall patterns are likely to result in higher biosecurity risks in Tairāwhiti and Hawke's Bay, through pest incursions (both animal and plant pests). This may have implications for the primary sector and the natural environment.

11.1 Recommendations for future work

This report provides the most comprehensive and up-to-date climate change projections for New Zealand currently available. However, there are areas that were out of scope for this report, or where there is currently no New Zealand-specific information available, which may be considerations for future work. Some of these are indicated below:

- Projections of changes to large floods (magnitude and frequency) are not currently available, but investigations into how large floods may change in the future are ongoing at NIWA. It is anticipated that data will likely become available for use by councils in due course.

- Analysis of future changes to wind was out of scope for this report, but these data exist and could be mapped and analysed for Tairāwhiti and Hawke's Bay. Broadly speaking, projected changes to mean daily wind speed at the annual scale are relatively small under the climate change scenarios presented in this report, with mean wind speeds increasing or decreasing by about 0-3% under RCP8.5 by 2090 (i.e. the extreme end of the scenarios evaluated here). At the seasonal scale however, there is more significant change in both directions (i.e. larger increases and decreases), with the largest increases to mean wind speed projected for winter. In most scenarios, increases are typically projected for locations just east of the mountain ranges, with decreases typically projected for most other locations in both regions. Regional scale mapping and analysis however is required to better highlight the spatial distribution of these projections.
- A detailed analysis of wildfire risk in the context of projected climate change was beyond the scope of this report and there is much potential for future research on this front. One possibility for such work could be to analyse and map future areas of high fire risk by combining projected climate data such as temperature, precipitation, and wind with relevant fire risk factors such as vegetation type and flammability. Such work would likely require a collaborative research effort between NIWA and an institute specialised in wildfire research such as Scion.
- Potential changes to crop suitability with climate change – modelling specific to Tairāwhiti and Hawke's Bay could be carried out as this has been done for other parts of New Zealand for a range of crop types (e.g. Ausseil. et al., 2019, Teixeira et al., 2020)²⁸.

²⁸ For additional information about this work, refer to the "Climate change & its effect on our agricultural land" project at: <https://www.deepsouthchallenge.co.nz/projects/climate-change-its-effect-our-agricultural-land>

12 Acknowledgements

Dr Kathleen Kozyniak (Hawke's Bay Regional Council), Dr Murry Cave (Gisborne District Council), and additional staff members from both councils are thanked for their feedback on this report in its draft form. Thank you also to Rob Bell, Michael Allis and Scott Stephens from NIWA for their guidance and feedback on the sea-level rise and coastal erosion chapter, with an additional thanks to Scott Stephens for undertaking the review of this chapter.

13 Glossary of abbreviations and terms

Term	Definition
Anthropogenic	Human-induced; man-made. Resulting from or produced by human activities.
Bias correction	Procedures designed to remove systematic climate model errors.
Clausius-Clapyeron relationship	The thermodynamic relationship between small changes in temperature and vapour pressure in an equilibrium system with condensed phases present. For trace gases such as water vapour, this relation gives the increase in equilibrium (or saturation) water vapour pressure per unit change in air temperature.
Climate model	A numerical representation of the climate system based on the physical, chemical and biological properties of its components, their interactions and feedback processes, and accounting for some of its known properties. The climate system can be represented by models of varying complexity, that is, for any one component or combination of components a spectrum or hierarchy of models can be identified, differing in such aspects as the number of spatial dimensions, the extent to which physical, chemical or biological processes are explicitly represented or the level at which empirical parametrizations are involved. Coupled Atmosphere–Ocean General Circulation Models (AOGCMs) provide a representation of the climate system that is near or at the most comprehensive end of the spectrum currently available. There is an evolution towards more complex models with interactive chemistry and biology. Climate models are applied as a research tool to study and simulate the climate, and for operational purposes, including monthly, seasonal and inter-annual climate predictions.
Downscaling	Deriving local climate information (at the 5-kilometre grid-scale in this report) from larger-scale model or observational data. Two main methods exist – statistical and dynamical. Statistical methods develop statistical relationships between large-scale atmospheric variables (e.g., circulation and moisture variations) and local climate variables (e.g., rainfall variations). Dynamical methods use the output of a regional climate/weather model driven by a larger-scale global model.
Emission scenario	A plausible representation of the future development of emissions of substances that act as radiative forcing factors (e.g., greenhouse gases, aerosols) based on a coherent and internally consistent set of assumptions about driving forces (such as demographic and socioeconomic development, technological change) and their key relationships.
Ensemble	A collection of model simulations characterizing a climate prediction or projection. Differences in initial conditions and model formulation result in different evolutions of the modelled system and may give information on uncertainty associated with model error and error in initial conditions in the case of climate forecasts and on uncertainty associated with model error and

	with internally generated climate variability in the case of climate projections.
Greenhouse gas	Greenhouse gases are those gaseous constituents of the atmosphere, both natural and anthropogenic, that absorb and emit radiation at specific wavelengths within the spectrum of terrestrial radiation emitted by the Earth's surface, the atmosphere itself, and by clouds. This property causes the greenhouse effect. Water vapour (H ₂ O), carbon dioxide (CO ₂), nitrous oxide (N ₂ O), methane (CH ₄) and ozone (O ₃) are the primary greenhouse gases in the Earth's atmosphere. Moreover, there are many entirely human-made greenhouse gases in the atmosphere, such as the halocarbons and other chlorine- and bromine-containing substances, dealt with under the Montreal Protocol. Beside CO ₂ , N ₂ O and CH ₄ , the Kyoto Protocol deals with the greenhouse gases sulphur hexafluoride (SF ₆), hydrofluorocarbons (HFCs) and perfluorocarbons (PFCs).
Heatwave days	A period of three or more consecutive days where the maximum daily temperature (T _{max}) exceeds a given threshold, either 25°C or 30°C.
High Intensity Rainfall Design System (HIRDS)	High Intensity Rainfall Design System (http://hirds.niwa.co.nz). HIRDS uses a regionalized index-frequency method to predict rainfall intensities at ungauged locations and returns depth-duration-frequency tables for rainfall at any location in New Zealand. Temperature increases can be inserted and corresponding increases in rainfall for each duration and frequency are calculated
Mean annual flood (MAF)	The mean of the series of each year's highest daily mean flow.
Mean annual low flow (MALF)	The mean of the lowest 7-day average flows in each year of a projection period.
Mean discharge	The average annual streamflow or discharge of a river.
Mitigation	A human intervention to reduce the sources or enhance the sinks of greenhouse gases.
Paris climate change agreement	The Paris Agreement aims to respond to the global climate change threat by keeping a global temperature rise this century well below 2°C above pre-industrial levels and to pursue efforts to limit the temperature increase even further to 1.5°C.
Potential evapotranspiration deficit	PED can be thought of as the amount of water needed to be added as irrigation, or replenished by rainfall, to keep pastures growing at levels that are not constrained by a shortage of water. The unit of PED is millimetres.
Projections	A numerical simulation (representation) of future conditions. Differs from a forecast; whereas a forecast aims to predict the exact time-dependent conditions in the immediate future, such as a weather forecast a future cast aims to simulate a time-series of conditions that would be typical of the future (from which statistical properties can be calculated) but does not predict future individual events.
Radiative forcing	A measure of the energy absorbed and retained in the lower atmosphere. More technically, radiative forcing is the change in the net (downward minus upward) irradiance (expressed in W/m ² , and including both short-wave energy from the sun, and long-wave energy from greenhouse gases) at the tropopause, due to a change in an external driver of climate change, such as, for example, a change in the concentration of carbon dioxide or the output of the sun

Regional climate model	A numerical climate prediction model run over a limited geographic domain (here around New Zealand), and driven along its lateral atmospheric boundary and oceanic boundary with conditions simulated by a global climate model (GCM). The RCM thus downscales the coarse resolution GCM, accounting for higher resolution topographical data, land-sea contrasts, and surface characteristics. RCMs can cater for relatively small-scale features such as New Zealand's Southern Alps
Representative Concentration Pathway	They describe four possible climate futures, all of which are considered possible depending on how much greenhouse gases are emitted in the years to come. The four RCPs, RCP2.6, RCP4.5, RCP6, and RCP8.5, are named after a possible range of radiative forcing values in the year 2100 relative to pre-industrial values (+2.6, +4.5, +6.0, and +8.5 W/m ² , respectively)
Sea-level rise	Sea level can change, both globally and locally due to (1) changes in the shape of the ocean basins, (2) a change in ocean volume as a result of a change in the mass of water in the ocean, and (3) changes in ocean volume as a result of changes in ocean water density.
Soil Moisture Deficit (SMD)	A day of soil moisture deficit is considered in this report to be when soil moisture is below 75 mm of available soil water capacity. SMD is calculated based on incoming daily rainfall (mm), outgoing daily potential evapotranspiration (PET, mm), and a fixed available water capacity (the amount of water in the soil 'reservoir' that plants can use) of 150 mm. Evapotranspiration (ET) is assumed to continue at its potential rate until about half of the water available to plants is used up, whereupon it decreases, in the absence of rain, as further water extraction takes place. ET is assumed to cease if all the available water is used up
Storm tide	Storm tide refers to the total observed sea level during a storm, which is the combination of storm surge (caused by low atmospheric pressure and by high winds pushing water onshore) and normal high tide
TopNet	A semi-distributed hydrological model for simulating catchment water balance and river flow, developed by NIWA.
Uncertainty	A state of incomplete knowledge that can result from a lack of information or from disagreement about what is known or even knowable. It may have many types of sources, from imprecision in the data to ambiguously defined concepts or terminology, or uncertain projections of human behaviour. Uncertainty can therefore be represented by quantitative measures (e.g., a probability density function) or by qualitative statements (e.g., reflecting the judgment of a team of experts).
Virtual climate station network (VCSN)	Made up of observational datasets of a range of climate variables: maximum and minimum temperature, rainfall, relative humidity, solar radiation, and wind. Daily data are interpolated onto a 0.05° longitude by 0.05° latitude grid (approximately 4 kilometres longitude by 5 kilometres latitude), covering all New Zealand (11,491 points). Primary reference to the spline interpolation methodology is Tait et al (2006).

Appendix A Coastal and fluvial inundation exposure

This information is additional to that presented in Sections 9 and 10.

Figure A-1 shows the extent to which available high-resolution Digital Elevation Models (DEMs) derived from airborne LiDAR²⁹ covered the coastline of New Zealand when the coastal flood exposure mapping exercise was undertaken (Paulik et al., 2020). Locations with available LiDAR coverage were sufficient for mapping the exposure to a 1% annual exceedance probability (AEP) storm tide event with 0.1 m SLR increments (selected increments of 0.5m, 1m and 1.5m of SLR are considered here). Remaining locations could only be mapped using coarser resolution satellite-derived DEMs for a single SLR increment of 3 m and are therefore not part of the exposure analysis presented in this report. Additional information about the coastal flood mapping methodology can be found in Paulik et al. (2020).

Maps of areas in the Tairāwhiti and Hawke's Bay regions exposed to a 1% annual exceedance probability (AEP) storm tide event at the present day and with different levels of sea-level rise are presented in Figure A-2 through to Figure A-8. Tables of the coastal exposure of land, infrastructure and asset classes are presented in Table A-1 to Table A-6.

Maps of the flood hazard area in the Tairāwhiti and Hawke's Bay regions are presented in Figure A-9 and Figure A-10, and tables of the fluvial exposure of land, infrastructure and asset classes are presented in Table A-7 to Table A-12. The flood hazard area map has been described in Section 2.5 and Section 9, and further information can be found in Paulik et al. (2019a).

²⁹ Light Detection and Ranging (LiDAR) is a remote sensing method that measures distances to the Earth using laser light. LiDAR measurements can be used to generate high-resolution digital elevation models (DEMs) suitable for flood exposure assessments for smaller SLR increments resolvable over decades (Paulik et al., 2020).

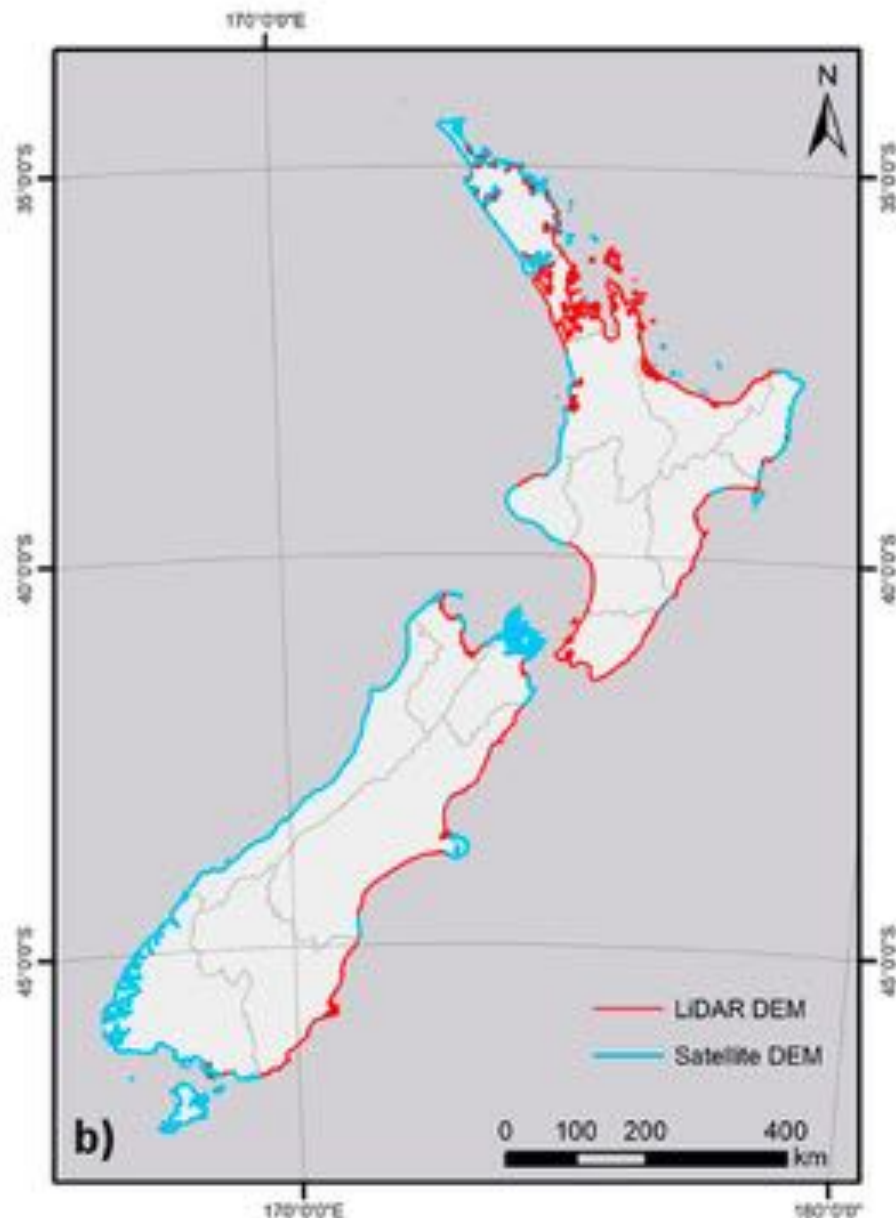


Figure A-1: Map of New Zealand showing regional boundaries and coastline coverage represented by LiDAR and satellite Digital Elevation Models (DEMs). Locations with LiDAR coverage were used for the 1% AEP storm tide exposure analysis with 0.5 m SLR increments. Remaining locations with satellite-derived DEMs were not suitable for coastal flood mapping at 0.5 m SLR increments and are therefore not part of the exposure analysis presented in this report. Source: Paulik et al. (2020).

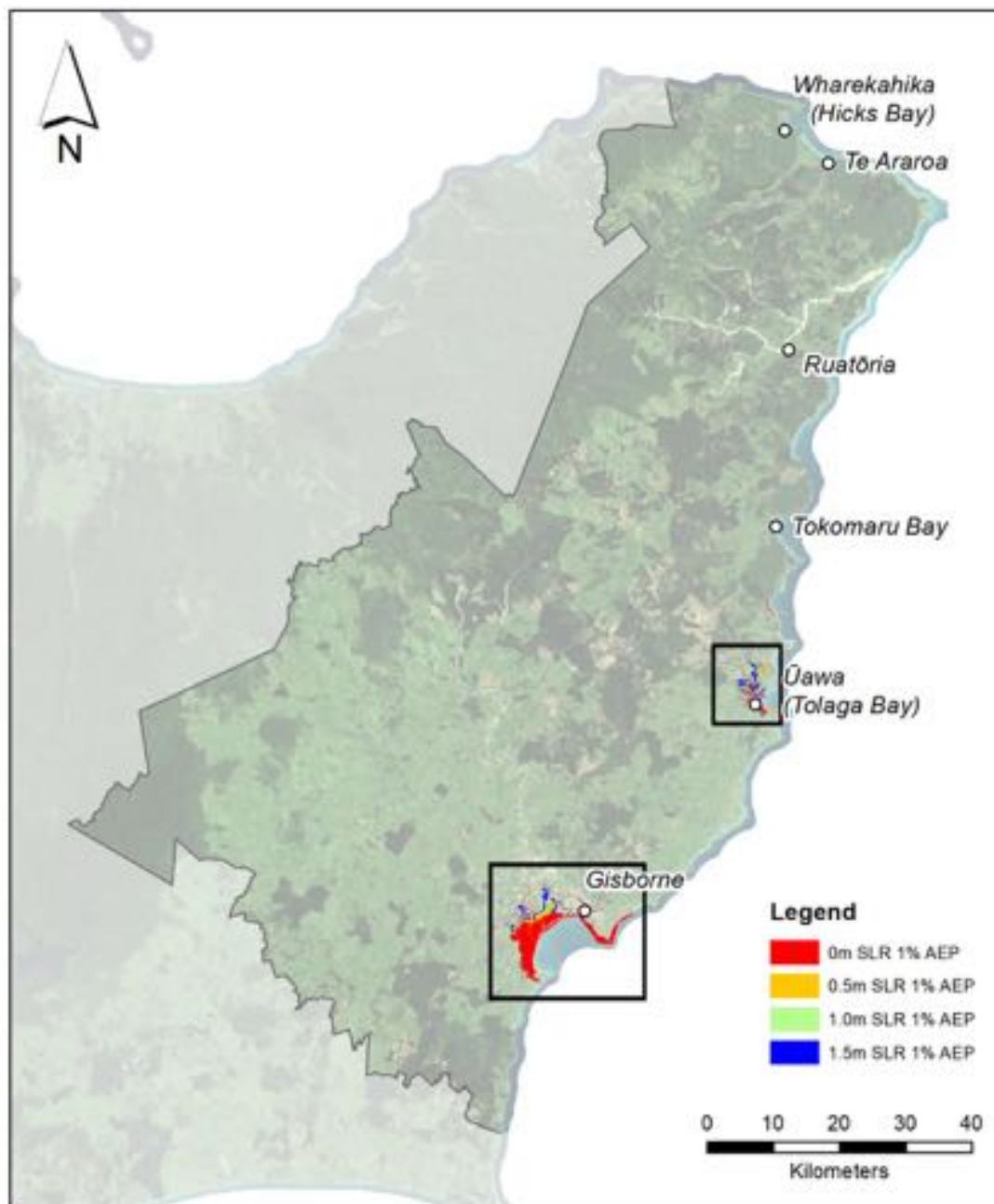


Figure A-2: 1% AEP storm tide + sea-level rise elevations exposure for Tairāwhiti. The top boxed area is Tolaga Bay, see Figure A-3 for more detail. The bottom boxed area is that surrounding Poverty Bay and Gisborne Town, see Figure A-4 for detail. Note that due to the lack of high-resolution elevation data in this part of the country (Figure A-1), much of the coastline could not be analysed using SLR increments of 0.5 m. Source: Paulik et al. (2019b).

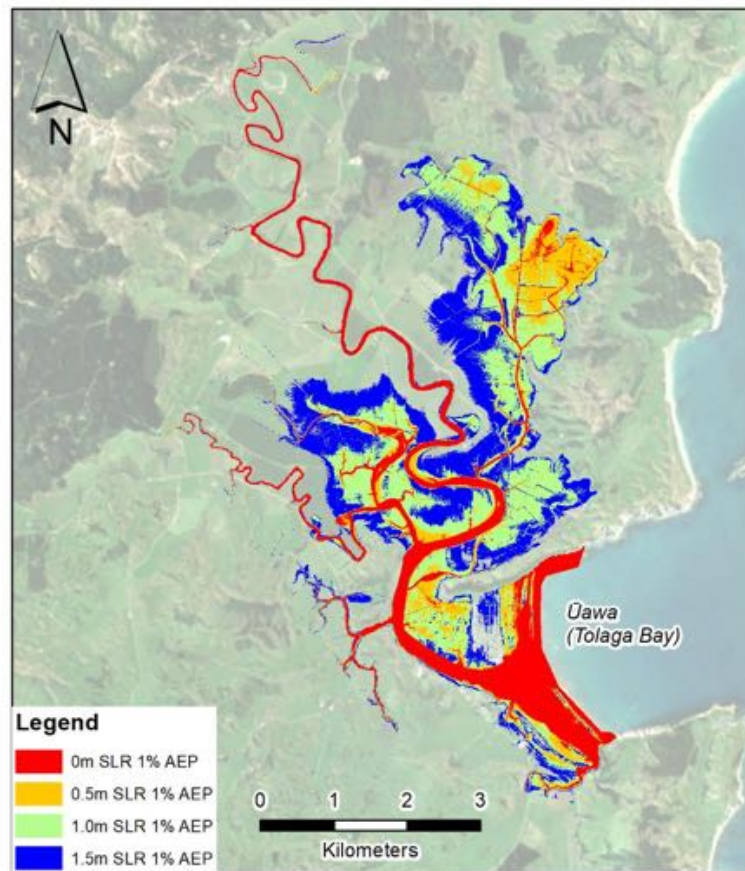


Figure A-3: 1% AEP storm tide + sea-level rise elevations exposure near Tolaga Bay, Tairāwhiti. Source: Paulik et al. (2019b).

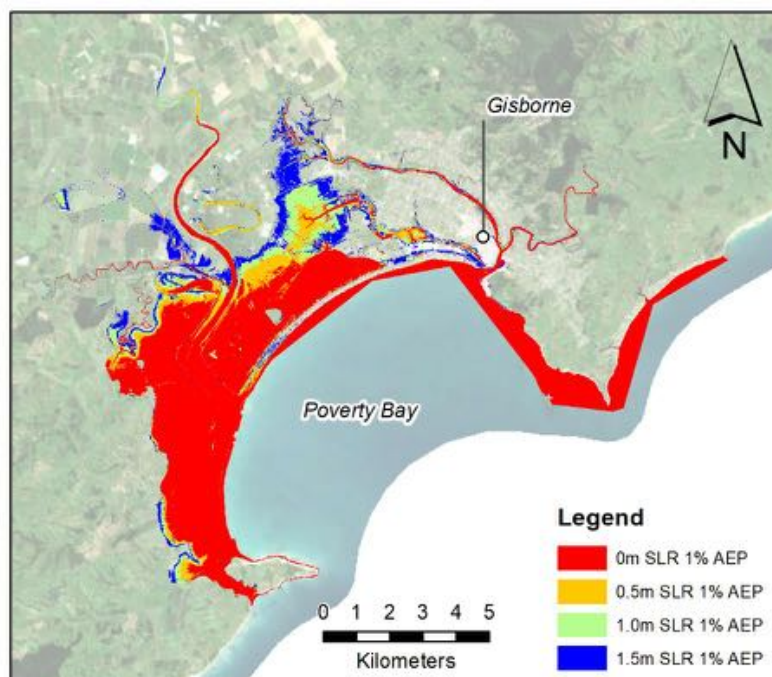


Figure A-4: 1% AEP storm tide + sea-level rise elevations exposure near Poverty Bay, Tairāwhiti. Source: Paulik et al. (2019b).

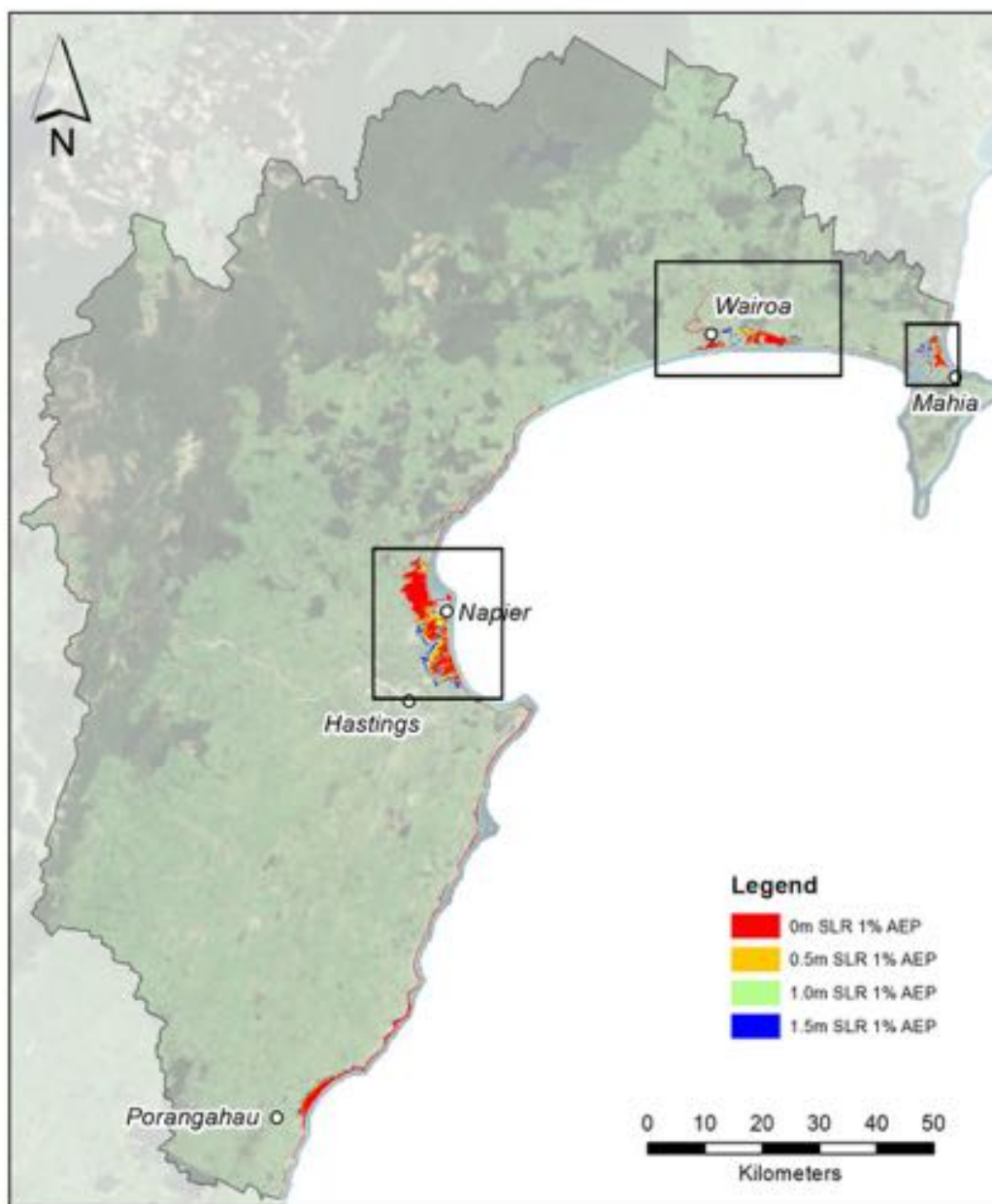


Figure A-5: 1% AEP storm tide + sea-level rise elevations exposure for Hawke's Bay Region. The boxed areas from left to right are shown in more detail in Figure A-6 (area near Napier) Figure A-7 (near Wairoa) and Figure A-8 (near Mahia). Note that as shown in Figure A-1, several parts of the coastline lack elevation data of sufficient resolution for analysis using SLR increments of 0.5 m.

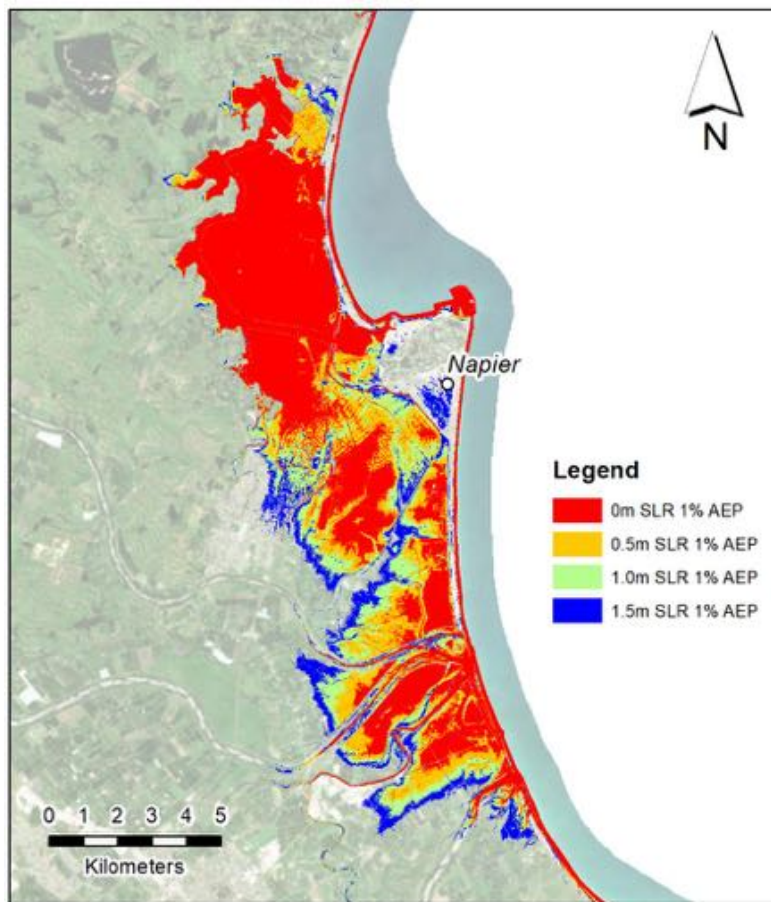


Figure A-6: 1% AEP storm tide + sea-level rise elevations exposure near Napier, Hawke's Bay Region.
Source: Paulik et al. (2019b).

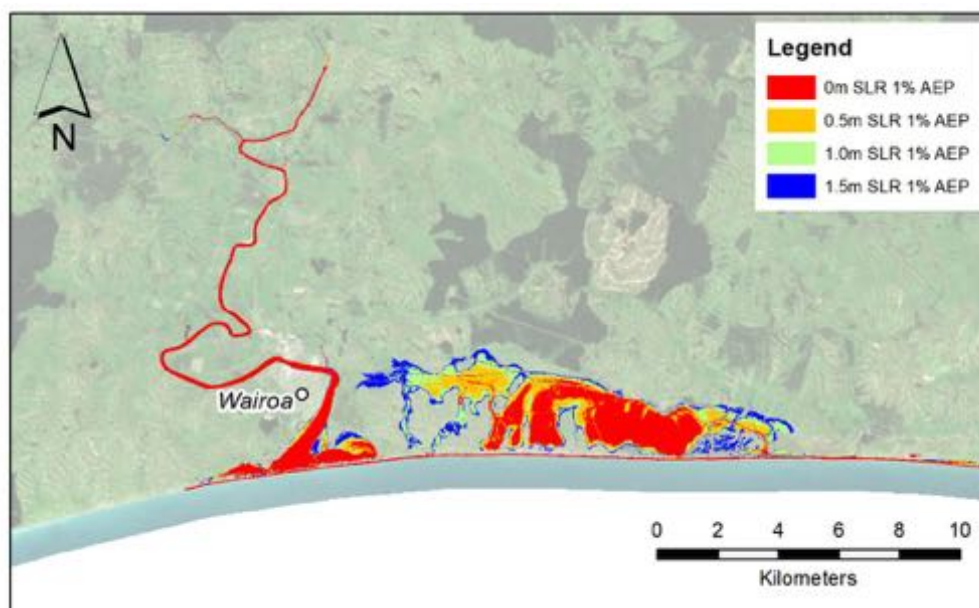


Figure A-7: 1% AEP storm tide + sea-level rise elevations exposure near Wairoa, Hawke's Bay Region.
Source: Paulik et al. (2019b).

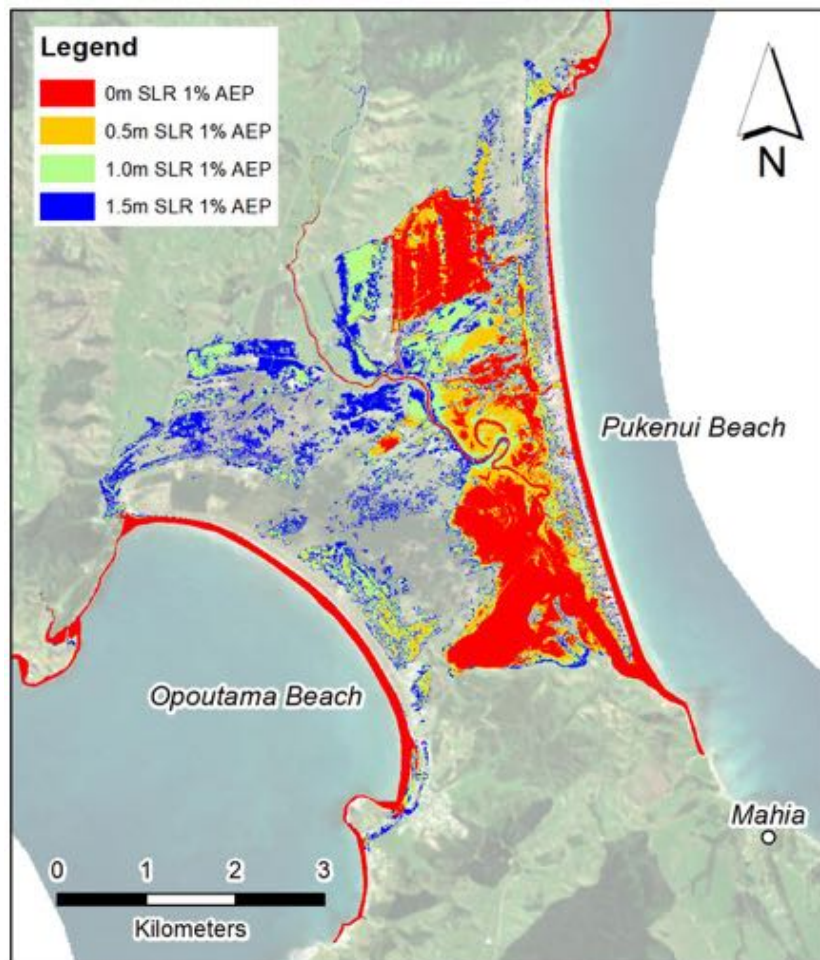


Figure A-8: 1% AEP storm tide + sea-level rise elevations exposure just northwest of Mahia (township), Hawke's Bay Region. Source: Paulik et al. (2019b).

Table A-1: Exposure of land and reserves in Gisborne District to a 1% annual exceedance probability (AEP) storm tide event and different increments of sea-level rise.

	Exposure to 1% AEP storm tide + SLR			
Sea-level rise increment	0 m SLR	0.5 m SLR	1.0 m SLR	1.5 m SLR
Land cover (hectares)				
Exotic Forest	9.6	10.4	12.0	14.1
Forest - Harvested	0.0	0.0	0.0	0.0
High Producing Exotic Grassland	964.6	1172.3	1623.7	2038.5
Low Producing Grassland	14.5	21.3	28.9	36.9
Orchard, Vineyard or Other Perennial Crop	173.8	245.1	367.6	533.0
Reserves (hectares)				
Amenity Reserve	47.2	59.9	75.9	85.5
Heritage Reserve	7.1	8.9	10.6	12.4
Neighbourhood Reserve	0.3	0.8	1.8	2.2
Recreation Reserve	6.1	13.0	38.2	78.9

Table A-2: Exposure of transport infrastructure in Gisborne District to a 1% annual exceedance probability (AEP) storm tide event and different increments of sea-level rise.

	Exposure to 1% AEP storm tide + SLR			
Sea-level rise increment	0 m SLR	0.5 m SLR	1.0 m SLR	1.5 m SLR
<i>Transport infrastructure</i>				
Roads (km)	13.8	23.6	38.1	55.3
Railway (km)	9.2	10.3	11.2	13.5
Airports (#) – Gisborne Airport	1	1	1	1
Cycle lanes (km)	0.6	2.6	4.4	6.3
<i>Water infrastructure</i>				
Stopbanks (km)	1.2	1.7	2.6	3.4
Floodgates (#)	15	18	21	24
Pump stations (#)	2	2	2	2
Three waters pipelines (km)	19.7	36.7	54.8	87.6
Three waters nodes (#)	457	888	1304	2019
<i>Other infrastructure</i>				
Transmission lines (km)	0	0	0	0

Table A-3: Exposure of buildings and population in Gisborne District to a 1% annual exceedance probability (AEP) storm tide event and different increments of sea-level rise.

	Exposure to 1% AEP storm tide + SLR			
Sea-level rise increment	0 m SLR	0.5 m SLR	1.0 m SLR	1.5 m SLR
<i>Buildings and population</i>				
Buildings (#)	159	367	729	1251
Buildings (\$ million replacement value)	34.0	107.8	209.2	313.6
Population (#)	92	247	590	1110

Table A-4: Exposure of land and regional parks in Hawke's Bay Region to a 1% annual exceedance probability (AEP) storm tide event and different increments of sea-level rise.

	Exposure to 1% AEP storm tide + SLR			
Sea-level rise increment	0 m SLR	0.5 m SLR	1.0 m SLR	1.5 m SLR
<i>Land cover (hectares)</i>				
Exotic Forest	16.0	21.4	36.3	60.4
Forest - Harvested	0.4	1.0	2.7	6.3
High Producing Exotic Grassland	2395.1	3228.8	3957.9	4559.6
Low Producing Grassland	101.1	177.9	292.1	412.4
Orchard, Vineyard or Other Perennial Crop	257.0	619.6	962.1	1313.5
Regional Parks – Hastings District	177.0	216.0	248.0	266.0
Regional Parks – Napier City	10.4	16.0	22.0	25.0

Table A-5: Exposure of transport infrastructure in Hawke's Bay Region (ordered by territorial authority) to a 1% annual exceedance probability (AEP) storm tide event and different increments of sea-level rise.

	Exposure to 1% AEP storm tide + SLR			
Sea-level rise increment	0 m SLR	0.5 m SLR	1.0 m SLR	1.5 m SLR
Transport infrastructure				
Roads (km) – Wairoa District	1.4	3.8	5.9	9.2
Railway (km) – Wairoa District	0.3	0.6	2	4.2
Roads (km) – Hastings District	6.9	17.7	25.9	33.5
Railway (km) – Hastings District	0.4	1	2	3.9
Cycle lanes (km) – Hastings District	0.1	0.8	1.8	2.0
Quiet street (km)	0.8	1.2	1.3	1.6
Roads (km) – Napier City	78.4	141.1	181.7	220.7
Railway (km) – Napier City	0.2	0.7	2.4	5.7
Airports (#) – Napier Airport	1	1	1	1
Cycle lanes (km) – Napier City	0.2	0.5	1.0	1.2
Roads (km) – Central Hawke's Bay District	0.4	1.9	3.1	3.9
Railway (km) – Central Hawke's Bay District	0	0	0	0
Water infrastructure				
Stopbanks (km) – Wairoa District	0.0	0.1	0.2	0.4
Drains (km) – Wairoa District	17.9	25.3	29.4	33.0
Culverts (#) – Wairoa District	1	2	2	3
Floodgates (#) – Wairoa District	0	1	1	1
Headwalls (#) – Wairoa District	4	4	7	7
Pump stations (#) – Wairoa District	0	1	1	1
Three waters nodes (#) – Wairoa District	94	246	609	1146
Three waters pipelines (km) – Wairoa District	1.2	1.9	3.2	5.4
Stopbanks (km) – Hastings District	0.9	1.9	2.6	4.1
Drains (km) – Hastings District	48.6	56.8	65.8	75.1
Drain access (km) – Hastings District	19.9	32.6	41.3	49.6
Groyne (km) – Hastings District	0.3	0.3	0.3	0.3
Pipelines (km) – Hastings District	0.9	1.3	1.7	2.2
Rope Rail L (km) – Hastings District	0.5	1.0	1.6	2.1
Rope Rail M (km) – Hastings District	0.3	0.3	0.4	1.0
Vehicle track (km) – Hastings District	2.4	5.3	7.2	8.1
Culverts (#) – Hastings District	1	5	9	10
Floodgates (#) – Hastings District	16	19	25	31
Headwalls (#) – Hastings District	25	28	33	35
Pump stations (#) – Hastings District	5	7	8	8
Three waters nodes (#) – Hastings District	1268	1959	2381	2889
Three waters pipelines (km) – Hastings District	24.3	47.8	63.5	78.6

Stopbanks (km) – Napier City	3.9	12.4	18.5	18.8
Drains (km) – Napier City	50.7	55.6	59.1	60.8
Drain access (km) – Napier City	40.9	61.8	73.4	79.3
Drain NCC (km) – Napier City	25.0	28.7	30.8	32.5
Pipelines (km) – Napier City	0.5	0.7	1.2	1.4
Gas lines (km) – Napier City	0.0	0.1	1.0	1.2
Vehicle track (km) – Napier City	0.3	0.6	0.8	1.7
Culverts (#) – Napier City	0	1	1	1
Floodgates (#) – Napier City	2	3	5	5
Headwalls (#) – Napier City	3	2	2	2
Pump stations (#) – Napier City	4	5	6	6
Three waters nodes (#) – Napier City	19349	29544	37069	44879
Three waters pipelines (km) – Napier City	459.3	790.5	1031	1254
Three waters nodes (#) – Central HB	0	0	0	0
Three waters pipelines (km) – Central HB	0	0	0	0
Other infrastructure				
Transmission lines (km) – Wairoa District	0	0	0	0
Transmission lines (km) – Hastings District	0.8	0.9	1.5	2.2
Transmission lines (km) – Napier City	0	0	0	0
Transmission lines (km) – Central HB	0	0	0	0

Table A-6: Exposure of buildings and population in Hawke’s Bay Region (ordered by territorial authority) to a 1% annual exceedance probability (AEP) storm tide event and different increments of sea-level rise.

Sea-level rise increment	Exposure to 1% AEP storm tide + SLR			
	0 m SLR	0.5 m SLR	1.0 m SLR	1.5 m SLR
Buildings and population				
Buildings (#) – Wairoa District	3	10	36	122
Buildings (\$ million replacement value) – Wairoa District	0.5	1.1	10.3	27.1
Population (#) – Wairoa District	2	5	18	66
Buildings (#) – Hastings District	476	1316	1895	2490
Buildings (\$ million replacement value) – Hastings District	110.4	282.2	421.4	530.1
Population (#) – Hastings District	643	1738	2422	3118
Buildings (#) – Napier City	4082	11321	18362	23037
Buildings (\$ million replacement value) – Napier City	911.3	2526	4224	5604
Population (#) – Napier City	5497	14266	23410	29984
Buildings (#) – Central Hawke’s Bay District	13	34	61	87
Buildings (\$ million replacement value) – Central HB	2.3	5.8	10.4	18.3
Population (#) – Central Hawke’s Bay District	11	22	39	61

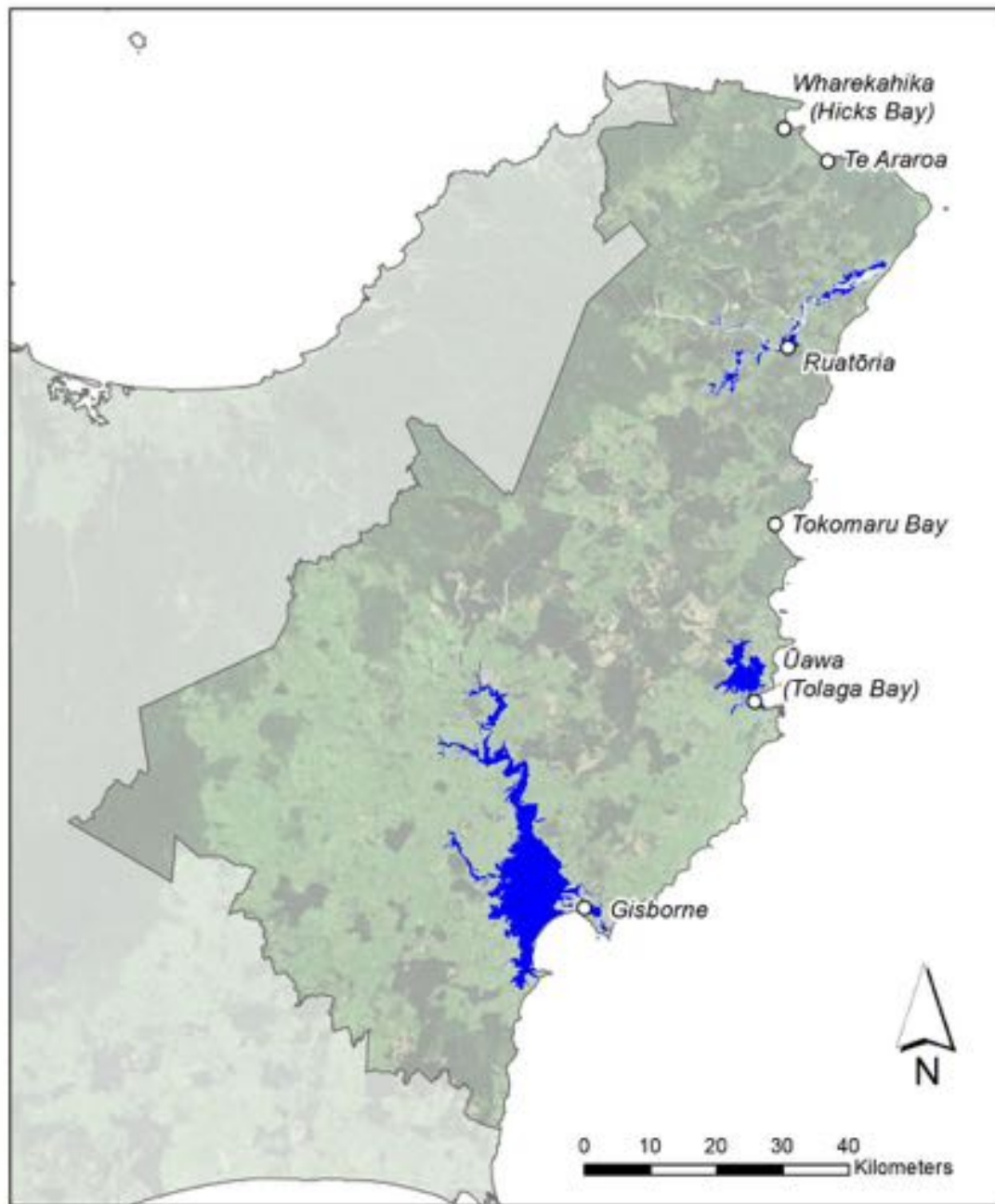


Figure A-9: Flood Hazard Area for Tairāwhiti. Blue shading indicates areas currently identified as exposed to flooding. Source: Paulik et al. (2019a).

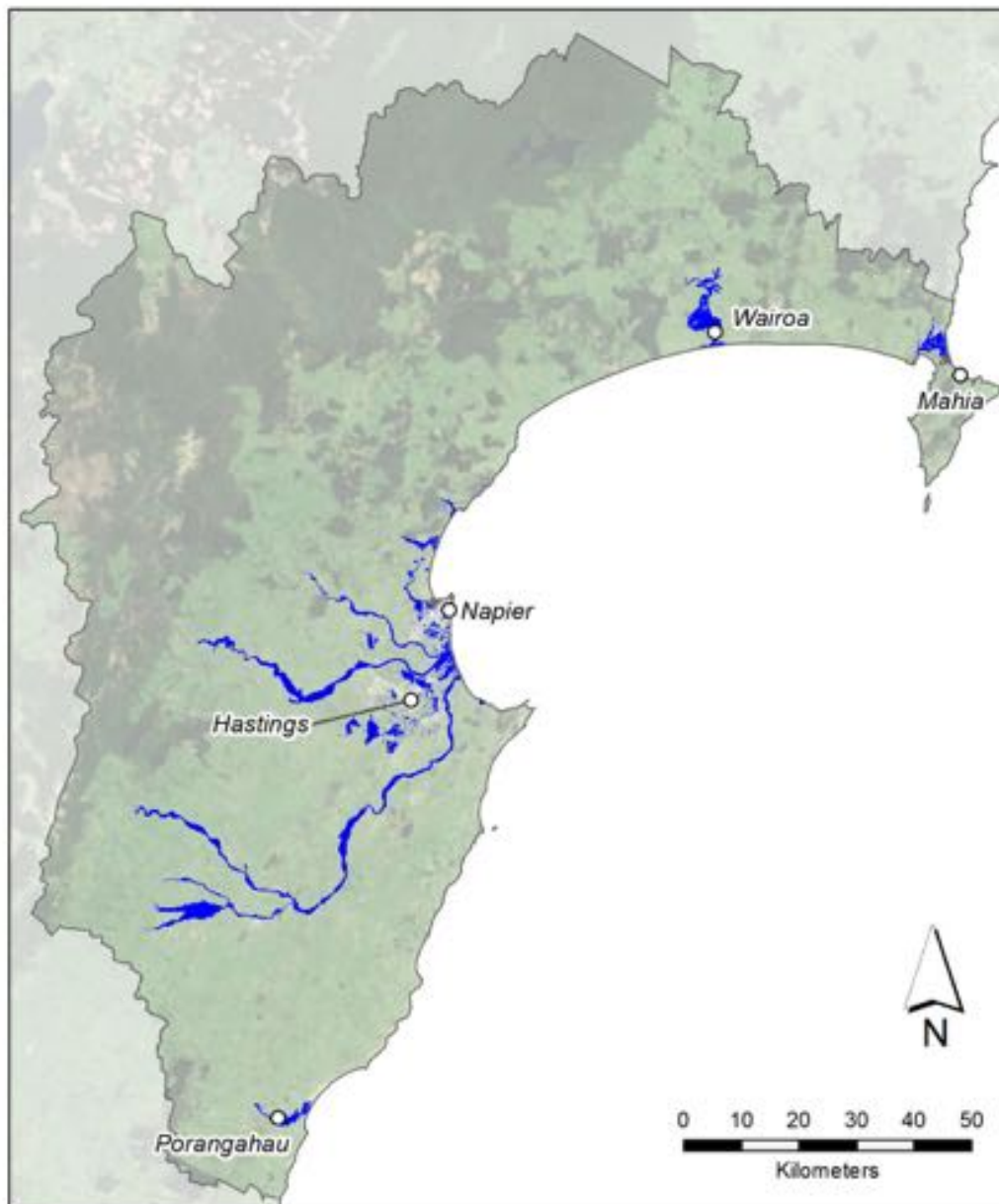


Figure A-10: Flood Hazard Area for the Hawke's Bay Region. Blue shading indicates areas currently identified as exposed to flooding. Source: Paulik et al. (2019a).

Table A-7: Exposure of land and reserves in Gisborne District to the flood hazard area.

	Exposure to fluvial hazard
<i>Land cover (hectares)</i>	
Exotic Forest	106.8
Forest - Harvested	9.5
High Producing Exotic Grassland	7993.2
Low Producing Grassland	83.1
Orchard, Vineyard or Other Perennial Crop	4430.7
<i>Reserves (hectares)</i>	
Amenity Reserve	70.8
Heritage Reserve	12.3
Neighbourhood Reserve	7.7
Recreation Reserve	172.6

Table A-8: Exposure of transport infrastructure in Gisborne District to the flood hazard area.

	Exposure to fluvial hazard
<i>Transport infrastructure</i>	
Roads (km)	370.8
Railway (km)	17.6
Airports (#) – Gisborne Airport	1
Cycle lanes (km)	29.2
<i>Water and other infrastructure</i>	
Stopbanks (km)	71.7
Floodgates (#)	157
Pump stations (#)	3
Three waters pipelines (km)	416.8
Three waters nodes (#)	8663
Transmission lines (km)	0

Table A-9: Exposure of buildings and population in Gisborne District to the flood hazard area.

	Exposure to fluvial hazard
<i>Buildings and population</i>	
Buildings (#)	11804
Buildings (\$ million replacement value)	2231
Population (#)	15455

Table A-10: Exposure of land and regional parks in Hawke's Bay Region to the flood hazard area.

	Exposure to fluvial hazard
<i>Land cover (hectares)</i>	
Exotic Forest	238.8
Forest - Harvested	50.5
High Producing Exotic Grassland	10703.6
Low Producing Grassland	786.9
Orchard, Vineyard or Other Perennial Crop	1524.2
Regional Parks – Hastings District	2.5
Regional Parks – Napier City	0.2

Table A-11: Exposure of transport infrastructure in Hawke's Bay Region (ordered by territorial authority) to the flood hazard area.

	Exposure to fluvial hazard
<i>Transport infrastructure</i>	
Roads (km) – Wairoa District	230.3
Railway (km) – Wairoa District	55.6
Roads (km) – Hastings District	200.2
Railway (km) – Hastings District	15.9
Cycle lanes (km) – Hastings District	3.4
Shared path (km) – Hastings District	13.5
Roads (km) – Napier City	125.2
Railway (km) – Napier City	13.5
Airports (#) – Napier Airport	1
Cycle lanes (km) – Napier City	0.8
Shared path (km) – Napier City	7.8
Roads (km) – Central Hawke's Bay District	125.7
Railway (km) – Central Hawke's Bay District	1
<i>Water infrastructure</i>	
Stopbanks (km) – Wairoa District	2.6
Drains (km) – Wairoa District	17.5
Culverts (#) – Wairoa District	4
Floodgates (#) – Wairoa District	3
Headwalls (#) – Wairoa District	6
Three waters nodes (#) – Wairoa District	3918
Three waters pipelines (km) – Wairoa District	115.2
Stopbanks (km) – Hastings District	16.3
Drains (km) – Hastings District	203.4
Pipelines (km) – Hastings District	3.2
Drain access (km) – Hastings District	110.9
Groyne (km) – Hastings District	10.9
Rope Rail L (km) – Hastings District	66.3
Rope Rail M (km) – Hastings District	23.8
Bridges (#) – Hastings District	2
Control gates (#) – Hastings District	2
Culverts (#) – Hastings District	33
Floodgates (#) – Hastings District	82
Headwalls (#) – Hastings District	74

Pump stations (#) – Hastings District	6
Deflection bank (#) – Hastings District	43
Groyne (#) – Hastings District	225
Dam (#) – Hastings District	2
Screen (#) – Hastings District	8
Three waters nodes (#) – Hastings District	3994
Three waters pipelines (km) – Hastings District	99.6
Stopbanks (km) – Napier City	0.0
Drains (km) – Napier City	57.8
Pipelines (km) – Napier City	0.8
Drain access (km) – Napier City	34.4
Drain NCC (km) – Napier City	14.0
Rope Rail L (km) – Napier City	2.8
Vehicle track (km) – Napier City	8.5
Control gate (#) – Napier City	3
Culverts (#) – Napier City	1
Floodgates (#) – Napier City	6
Headwalls (#) – Napier City	3
Pump stations (#) – Napier City	2
Dam (#) – Napier City	2
Screen (#) – Napier City	5
Three waters nodes (#) – Napier City	14577
Three waters pipelines (km) – Napier City	581.2
Stopbanks (km) – Central HB District	34.7
Drains (km) – Central HB District	14.3
Rock edge protection (km) – Central HB	0.1
Rope Rail M (km) – Central HB	0.5
Vehicle Track (km) – Central HB	11.2
Willow edge protection (km) – Central HB	1.2
Culverts (#) – Central HB District	13
Floodgates (#) – Central HB District	32
Headwalls (#) – Central HB District	14
Deflection bank (#) – Central HB District	106
Weir (#) – Central HB District	1
Other infrastructure	
Transmission lines (km) – Wairoa District	208.5
Transmission lines (km) – Hastings District	50.1
Transmission lines (km) – Napier City	4.0
Transmission lines (km) – Central HB	7.9

Table A-12: Exposure of buildings and population in Hawke's Bay Region (ordered by territorial authority) to the flood hazard area.

	Exposure to fluvial hazard
<i>Buildings and population</i>	
Buildings (#) – Wairoa District	1999
Buildings (\$ million replacement value) – Wairoa District	480.4
Population (#) – Wairoa District	3038
Buildings (#) – Hastings District	3844
Buildings (\$ million replacement value) – Hastings District	819.3
Population (#) – Hastings District	4793
Buildings (#) – Napier City	7614
Buildings (\$ million replacement value) – Napier City	2138.8
Population (#) – Napier City	9356
Buildings (#) – Central Hawke's Bay District	485
Buildings (\$ million replacement value) – Central HB	96.3
Population (#) – Central Hawke's Bay District	601

14 References

- AECOM, TAYLOR, T., NIWA & LATITUDE 2020. Assessment Report: National Climate Change Risk Assessment for Aotearoa New Zealand, report prepared for Ministry for the Environment, 117pp.
- AUSSEIL, A.-G., VAN DER WEERDEN, T., BEARE, M., TEIXEIRA, E., BAISDEN, T., LIEFFERING, M., GUO, J., KELLER, L., LAW, R. & NOBLE, A. 2019. Climate change impacts on land use suitability. Prepared for the Deep South and Our Land and Water National Science Challenges. Manaaki Whenua Contract Report: LC3573. Lincoln, New Zealand: Manaaki Whenua.
- BANDARAGODA, C., TARBOTON, D. G. & WOODS, R. 2004. Application of TOPNET in the distributed model intercomparison project. *Journal of Hydrology*, 298, 178-201.
- BASHER, L., ELLIOTT, S., HUGHES, A., TAIT, A., PAGE, M., ROSSER, B., MCIVOR, I., DOUGLAS, G. & JONES, H. 2012. Impacts of climate change on erosion and erosion control methods - A critical review. MPI Technical Paper No: 2012/45, 216pp.
- BATSTONE, C., LAWLESS, M., TAWN, J., HORSBURGH, K., BLACKMAN, D., MCMILLAN, A., WORTH, D., LAEGER, S. & HUNT, T. 2013. A UK best-practice approach for extreme sea-level analysis along complex topographic coastlines. *Ocean Engineering*, 71, 28-39.
- BEAVAN, R. & LITCHFIELD, N. J. 2012. *Vertical land movement around the New Zealand coastline: implications for sea-level rise*, GNS Science.
- BELL, R. G., R. PAULIK & WADHWA, S. 2015. National and regional risk exposure in low-lying coastal areas. Areal extent, population, buildings and infrastructure. NIWA Client Report, HAM2015-006, prepared for the Parliamentary Commissioner for the Environment.
- BERESFORD, R. M. & MCKAY, A. H. 2012. Climate change impacts on plant diseases impacting New Zealand horticulture, Plant and Food Research report for MPI and MSI, report number C11X1102, 65pp.
- BEVEN, K., LAMB, R., QUINN, P., ROMANOWICZ, R. & FREER, J. 1995. TOPMODEL. Computer models of watershed hydrology. *VP Singh*, 627-668.
- BRODIE, J. & PEARSON, R. G. 2016. Ecosystem health of the Great Barrier Reef: time for effective management action based on evidence. *Estuarine, Coastal and Shelf Science*, 183, 438-451.
- CAREY-SMITH, T., HENDERSON, R. & SINGH, S. 2018. High Intensity Rainfall Design System Version 4, NIWA Client Report 2018022CH.
- CASTINEL, A., FORREST, B. & HOPKINS, G. 2014. Review of disease risks for New Zealand shellfish aquaculture: perspectives for management. Prepared for Ministry of Business, Innovation and Employment. Cawthron Institute Report No. 2297, 31p.
- CHAPPELL, P. R. 2013. The climate and weather of Hawke's Bay. *NIWA Science and Technology Series*, 58, 44.
- CHAPPELL, P. R. 2016. The climate and weather of Gisborne. *NIWA Science and Technology Series*, 70, 40.
- CHRISTIE, J. E. 2014. Adapting to a changing climate: a proposed framework for the conservation of terrestrial native biodiversity in New Zealand. Department of Conservation, Wellington, 23 p.
- CHURCH, J. A., P. U. CLARK, A. CAZENAVE, J. M. GREGORY, S. JEVREJEVA, A. LEVERMANN, M. A. MERRIFIELD, G. A. MILNE, R. S. NEREM, P. D. NUNN, A. J. PAYNE, W. T. PFEFFER, D. STAMMER & UNNIKRISHNAN, A. S. 2013. Sea level change. In: STOCKER, T. F., D. QIN, G.-K. P., M. TIGNOR, S. K. ALLEN, J. BOSCHUNG, A. NAUELS, Y. XIA, V. BEX & MIDGLEY, P. M. (eds.) *Climate change 2013: The physical science basis*. Cambridge, United Kingdom and New York, NY, USA: Cambridge University Press.
- CLARK, M. P., RUPP, D. E., WOODS, R. A., ZHENG, X., IBBITT, R. P., SLATER, A. G., SCHMIDT, J. & UDDSTROM, M. J. 2008. Hydrological data assimilation with the ensemble Kalman filter: Use of streamflow observations to update states in a distributed hydrological model. *Advances in water resources*, 31, 1309-1324.

- CLOTHIER, B., HALL, A. & GREEN, S. 2012. Chapter 6 - Horticulture: Adapting the horticulture and vegetable industries to climate change. In: CLARK, A. & NOTTAGE, R. (eds.) *Impacts of climate change on land-based sectors and adaptation options. Technical Report to the Sustainable Land Management and Climate Change Adaptation Technical Working Group, Ministry for Primary Industries*, 408 p.
- COAKLEY, S. M., SCHERM, H. & CHAKRABORTY, S. 1999. Climate change and plant disease management. *Annual Review of Phytopathology*, 37, 399-426.
- COLLINS, D. & ZAMMIT, C. 2016. Climate change impacts on agricultural water resources and flooding. NIWA Client Report for the Ministry of Primary Industries, 2016144CH, 70p.
- CROW, S. K., BOOKER, D. J. & SNELDER, T. H. 2013. Contrasting influence of flow regime on freshwater fishes displaying diadromous and nondiadromous life histories. *Ecology of Freshwater Fish*, 22, 82-94.
- CUMMINGS, V., HEWITT, J., ALLEN, S., MARRIOTT, P., BARR, N. & HEATH, P. 2013. Ocean acidification: impacts on key NZ molluscs, with a focus on flat oysters (*Ostrea chilensis*). Final Research Report for the NZ Ministry of Primary Industries on project ZBD200913. 18 p.
- DEAN, S., ROSIER, S., CAREY-SMITH, T. & STOTT, P. A. 2013. The role of climate change in the two-day extreme rainfall in Golden Bay, New Zealand, December 2011. *Bulletin of the American Meteorological Society*, 94, 561-563.
- DEATH, R., BOWIE, S. & O'DONNELL, C. 2016. Vulnerability of freshwater ecosystems due to climate change. In: ROBERTSON, H., BOWIE, S., DEATH, R. & COLLINS, D. (eds.) *Freshwater conservation under a changing climate. Proceedings of a workshop hosted by the Department of Conservation, 10-11 December 2013, Wellington*. Christchurch: Department of Conservation.
- DERRAIK, J. G. & SLANEY, D. 2015. Notes on Zika virus – an emerging pathogen now present in the South Pacific. *Australian and New Zealand Journal of Public Health*, 39, 5-7.
- DOC. 2020. *Climate change risks to conservation* [Online]. [Accessed 14/07/2020].
- EGAN, E., WOOLLEY, J. M. & WILLIAMS, E. 2020. Climate change vulnerability assessment of selected taonga freshwater species: Technical report. NIWA Client Report 2020073CH, April 2020, 85p.
- FAO 2018. Climate change for forest policy-makers – An approach for integrating climate change into national forest policy in support of sustainable forest management– Version 2.0. *FAO Forestry Paper no.181*. Rome: FAO.
- FAO 2019. Agriculture and climate change – Challenges and opportunities at the global and local Level – Collaboration on Climate-Smart Agriculture. Rome: Food and Agricultural Organisation.
- FOREMAN, M. G. G., CHERNIAWSKY, J. Y. & BALLANTYNE, V. A. 2009. Versatile Harmonic Tidal Analysis: Improvements and Applications. *Journal of Atmospheric and Oceanic Technology*, 26, 806-817.
- GIBB, J. 1994. Initial assessment of Areas Sensitive to Coastal Hazards for selected parts of the Gisborne District Coast. Consultancy Report C.R. 1994/18 prepared for Gisborne District Council.
- GIBB, J. G., SHEFFIELD, A. T. & FOSTER, G. A. 1992. A standardised coastal sensitivity index based on an initial framework for physical coastal hazards information. Department of Conservation Science and Research Series. No.55. 101p
- GISBORNE DISTRICT COUNCIL 2020. State of our Environment, Accessed from: <https://www.gdc.govt.nz/state-of-our-environment/>.
- GORING, D. G. Kinematic shocks and monoclinal waves in the Waimakariri, a steep, braided, gravel-bed river. Proceedings of the International Symposium on waves: Physical and numerical modelling, University of British Columbia, Vancouver, Canada, 1994.
- GRINGORTEN, I. I. 1963. A plotting rule for extreme probability paper. *Journal of Geophysical Research*, 68, 813-814.

- HANNAH, J. & BELL, R. G. 2012. Regional sea level trends in New Zealand. *Journal of Geophysical Research: Oceans*, 117.
- HAWKE'S BAY REGIONAL COUNCIL 2018. Whakakī Lake, Accessed from: <https://www.hbrc.govt.nz/assets/Document-Library/Projects/Outstanding-Water-Body/Lake-Whakaki-candidate-OWB-report-201807111.pdf>, 1 July 2020.
- HAWKE'S BAY REGIONAL COUNCIL. 2020. *Biodiversity* [Online]. Hawke's Bay Regional Council Available: <https://www.hbrc.govt.nz/environment/biodiversity/> [Accessed 14/07/2020].
- HENDERSON, R. D., COLLINS, D. B. G., DOYLE, M. & WATSON, J. 2018. Regional Flood Estimation Tool for New Zealand Final Report Part 2. NIWA Client Report, 2018177CH, Prepared for EnviroLink Tools (MBIE):44. .
- HEWITT, J., ELLIS, J. I. & THRUSH, S. F. 2016. Multiple stressors, nonlinear effects and the implications of climate change impacts on marine coastal ecosystems. *Global Change Biology*, 22, 2665-2675.
- IBBITT, R. & WOODS, R. 2002. Towards rainfall-runoff models that do not need calibration to flow data. *International Association of Hydrological Sciences, Publication*, 189-196.
- IPCC (ed.) 2013. *Climate Change 2013: The Physical Science Basis. Contribution of Working Group I to the Fifth Assessment Report of the Intergovernmental Panel on Climate Change*, Cambridge, United Kingdom and New York, NY, USA: Cambridge University Press.
- IPCC (ed.) 2014a. *Climate Change 2014: Impacts, Adaptation, and Vulnerability. Part A: Global and Sectoral Aspects. Contribution of Working Group II to the Fifth Assessment Report of the Intergovernmental Panel on Climate Change*, Cambridge, United Kingdom and New York, USA: Cambridge University Press.
- IPCC (ed.) 2014b. *Climate Change 2014: Impacts, Adaptation, and Vulnerability. Part B: Regional Aspects. Contribution of Working Group II to the Fifth Assessment Report of the Intergovernmental Panel on Climate Change*, Cambridge, United Kingdom and New York, USA: Cambridge University Press.
- IPCC 2014c. Climate change 2014: Mitigation of climate change. Contribution of Working Group III to the Fifth Assessment Report of the Intergovernmental Panel on Climate Change. In: EDENHOFER, O., PICHES-MADRUGA, R., SOKONA, Y., FARAHANI, E., KADNER, S., SEYBOTH, K., ADLER, A., BAUM, I., BRUNNER, S., EICKEMEIER, P., KRIEMANN, B., SAVOLAINEN, J., SCHLÖMER, S., VON STECHOW, C., ZWICKEL, T. & MINX, J. C. (eds.). Cambridge University Press.
- IPCC 2018. Global warming of 1.5C: An IPCC Special Report on the impacts of global warming of 1.5C above pre-industrial levels and related global greenhouse gas emission pathways, in the context of strengthening the global response to the threat of climate change, sustainable development, and efforts to eradicate poverty, Accessed on 8/10/2018 from <http://ipcc.ch>.
- IUCN. 2019. Species and Climate Change [Accessed 14/07/2020].
- KEAN, J. M., BROCKERHOFF, E. G., FOWLER, S. V., GERARD, P. J., LOGAN, D. P., MULLAN, A. B., SOOD, A., TOMPKINS, D. M. & WARD, D. F. 2015. Effects of climate change on current and potential biosecurity pests and diseases in New Zealand. Prepared for Ministry for Primary Industries, MPI Technical Paper No: 2015/25. 100p.
- KETTLES, H. & BELL, R. G. 2015. Estuarine ecosystems. In: ROBERTSON, H., BOWIE, S., WHITE, R., DEATH, R. & COLLINS, D. (eds.) 2015: *Freshwater conservation under a changing climate. Proceedings of a workshop hosted by the Department of Conservation, 10-11 December 2013, Wellington*. Christchurch: Dept of Conservation publication.
- KIRILENKO, A. P. & SEDJO, R. A. 2007. Climate change impacts on forestry. *Proceedings of the National Academy of Sciences*, 104, 19697-19702.
- KOPP, R. E., HORTON, R. M., LITTLE, C. M., MITROVICA, J. X., OPPENHEIMER, M., RASMUSSEN, D., STRAUSS, B. H. & TEBALDI, C. 2014. Probabilistic 21st and 22nd century sea-level projections at a global network of tide-gauge sites. *Earth's future*, 2, 383-406.

- LAST, P. R., WHITE, W. T., GLEDHILL, D. C., HOBDDAY, A. J., BROWN, R., EDGAR, G. J. & PECL, G. 2011. Long-term shifts in abundance and distribution of a temperate fish fauna: a response to climate change and fishing practices. *Global Ecology and Biogeography*, 20, 58-72.
- LAW, C. S., RICKARD, G. J., MIKALOFF-FLETCHER, S. E., PINKERTON, M., GORMAN, R. G., BEHRENS, E., CHISWELL, S. M., BOSTOCK, H. C., ANDERSON, O. & CURRIE, K. 2016. The New Zealand EEZ and the South West Pacific. Synthesis Report RA2, Marine Case Study. Climate Changes, Impacts and Implications (CCII) for New Zealand to 2100. MBIE Contract C01X1225. 41pp.
- LAW, C. S., RICKARD, G. J., MIKALOFF-FLETCHER, S. E., PINKERTON, M. H., BEHRENS, E., CHISWELL, S. M. & CURRIE, K. 2018. Climate change projections for the surface ocean around New Zealand. *New Zealand Journal of Marine and Freshwater Research*, 52, 309-335.
- LEE, J., BURKE, C., KALAUGHER, E., ROCHE, J., BEUKES, P. & CLARK, A. 2012. Chapter 3 - Dairy: Adapting dairy farming systems in a changing climatic environment. In: CLARK, A. & NOTTAGE, R. (eds.) *Impacts of climate change on land-based sectors and adaptation options. Technical Report to the Sustainable Land Management and Climate Change Adaptation Technical Working Group, Ministry for Primary Industries*, 408 p.
- LUCK, J., CAMPBELL, I. D., MAGAREY, R., ISARD, S., AURAMBOUT, J.-P. & FINLAY, K. 2014. Climate Change and Plant Biosecurity: Implications for Policy. In: GORDH, G. & MCKIRDY, S. (eds.) *The Handbook of Plant Biosecurity: Principles and Practices for the Identification, Containment and Control of Organisms that Threaten Agriculture and the Environment Globally*. Dordrecht: Springer Netherlands.
- MALHI, Y., FRANKLIN, J., SEDDON, N., SOLAN, M., TURNER, M. G., FIELD, C. B. & KNOWLTON, N. 2020. Climate change and ecosystems: threats, opportunities and solutions. The Royal Society.
- MBIE Undated. About CCII (Climate Changes, Impacts and Implications for New Zealand). Available online at: <https://ccii.org.nz/climate-changes-impacts-and-implications-nz/>.
- MCGLONE, M. & WALKER, S. 2011. Potential effects of climate change on New Zealand's terrestrial biodiversity and policy recommendations for mitigation, adaptation and research. *Science for Conservation*, 312, 1-80.
- MCMAHON, S. J., PARSONS, D. M., DONELSON, J. M., PETHER, S. M. J. & MUNDAY, P. L. 2019. Elevated CO₂ and heatwave conditions affect the aerobic and swimming performance of juvenile Australasian snapper. *Marine Biology*, 167, 6.
- MFE. 2019. *Why biodiversity matters* [Online]. Ministry for the Environment [Accessed 2020].
- MFE. 2020. *Climate change projections for the Gisborne and Hawke's Bay region* [Online]. Ministry for the Environment Available: <https://www.mfe.govt.nz/climate-change/likely-impacts-of-climate-change/how-could-climate-change-affect-my-region/gisborne> [Accessed 30/04/2020].
- MINISTRY FOR THE ENVIRONMENT 2008. Climate Change Effects and Impacts Assessment. A Guidance Manual for Local Government in New Zealand. In: MULLAN, B., WRATT, D., DEAN, S., HOLLIS, M., ALLAN, S., WILLIAMS, T., KENNY, G. & MFE (eds.). Wellington: Ministry for the Environment.
- MINISTRY FOR THE ENVIRONMENT 2017. Coastal hazards and climate change: Guidance for local government. Lead authors: Bell, R.; Lawrence, J.; Allan, S.; Blackett, P.; Stephens, S. Ministry for the Environment Publication ME-1292. Accessed at: <http://www.mfe.govt.nz/publications/climate-change/preparing-coastal-change-summary-of-coastal-hazards-and-climate-change>.
- MINISTRY FOR THE ENVIRONMENT 2018. Climate change projections for New Zealand: atmospheric projections based on simulations undertaken for the IPCC 5th Assessment, 2nd edition. Accessed at: <https://www.mfe.govt.nz/node/21990>.
- MIRA DE ORDUÑA, R. 2010. Climate change associated effects on grape and wine quality and production. *Food Research International*, 43, 1844-1855.

- MPI 2018. A review of climate change research in New Zealand focusing on forestry. In: ANDREW DUNNINGHAM, ANDREA GRANT, WREFORD, A. & KIRK, N. (eds.). New Zealand: Ministry for Primary Industries.
- MPI 2019. Climate Issues Facing Farmers Sustainable Land Management and Climate Change Research Programme. the Ministry for Primary Industries.
- MULLAN, A. B., PORTEOUS, A., WRATT, D. & HOLLIS, M. 2005. Changes in drought risk with climate change. NIWA report WLG2005-23 for Ministry for the Environment and Ministry of Agriculture and Fisheries, Wellington.
- MUNDAY, P. L., CHEAL, A. J. & DIXSON, D. L., ET AL. 2014. Behavioural impairment in reef fishes caused by ocean acidification at CO₂ seeps. *Nature Climate Change* 4, 487-492.
- MUNSHI, D., KURIAN, P., MORRISON, S., KATHLENE, L. & CRETNEY, R. 2020. Centring Culture in Public Engagement on Climate Change Adaptation: Re-shaping the Future of the NZ Tourism Sector. A report to the Deep South National Science Challenge. New Zealand: University of Waikato and Wellington.
- NEW ZEALAND HORTICULTURE 2018. FreshFacts, Accessed from: <https://www.freshfacts.co.nz/files/freshfacts-2018.pdf>.
- NEWSOME, P. F. J., WILDE, R. H. & WILLOUGHBY, E. J. 2012. *Land Resource Information System Spatial Data*, Palmerston North, Landcare Research New Zealand Ltd.
- NIWA, M., GNS AND BRANZ 2012. Impacts of Climate Change on Urban Infrastructure and the Built Environment: Toolbox Handbook.
- OFFICE OF THE PRIME MINISTER'S CHIEF SCIENCE ADVISOR 2017. New Zealand's fresh waters: Values, state, trends and human impacts. Wellington: Office of the Prime Minister's Chief Science Advisor. Retrieved from: <http://www.pmcsa.org.nz/wp-content/uploads/PMCSA-Freshwater-Report.pdf>.
- PARLIAMENTARY COMMISSIONER FOR THE ENVIRONMENT 2012. Hydroelectricity or wild rivers? Climate change versus natural heritage. Wellington: Parliamentary Commissioner for the Environment. Retrieved from: <http://www.pce.parliament.nz/media/1277/wild-riversweb.pdf>.
- PARLIAMENTARY COMMISSIONER FOR THE ENVIRONMENT 2015. Preparing New Zealand for rising seas: certainty and uncertainty. Wellington: Parliamentary Commissioner for the Environment. Retrieved from: <https://www.pce.parliament.nz/publications/preparing-new-zealand-for-rising-seas-certainty-and-uncertainty>.
- PAULIK, R., CRAIG, H. & COLLINS, D. 2019a. New Zealand fluvial and pluvial flood exposure. Prepared for the Deep South National Science Challenge, NIWA Client Report Number 2019118WN, 58pp.
- PAULIK, R., STEPHENS, S., BELL, R. G., WADHWA, S. & POPOVICH, B. 2020. National-scale built environment exposure to 100-year extreme sea levels and sea-level rise. *Sustainability*, 12.
- PAULIK, R., STEPHENS, S., WADHWA, S., BELL, R. G., POPOVICH, B. & ROBINSON, B. 2019b. Coastal flooding exposure under future sea-level rise for New Zealand. Prepared for the Deep South National Science Challenge, NIWA Client Report Number 2019119WN, 76pp.
- PAWLOWICZ, R., BEARDSLEY, B. & LENTZ, S. 2002. Classical tidal harmonic analysis including error estimates in MATLAB using T_TIDE. *Computers & Geosciences*, 28, 929-937.
- PEARCE, H. G., KERR, J., CLARK, A., MULLAN, A. B., ACKERLEY, D., CAREY-SMITH, T. & YANG, E. 2011. Improved estimates of the effect of climate change on NZ fire danger, Prepared for Ministry of Agriculture and Fisheries by Scion and NIWA, Scion Report No. 18087. 83p.
- PEARCE, P., BELL, R., BOSTOCK, H., CAREY-SMITH, T., COLLINS, D., FEDAEFF, N., KACHHARA, A., MACARA, G., MULLAN, B., SOMERVILL, E., PAULIK, R., SOOD, A., TAIT, A., WADHWA, S. & WOOLLEY, J.-M. 2018. Auckland Region climate change projections and impacts. Revised January 2018. Prepared by the National Institute of Water and Atmospheric Research, NIWA, for Auckland Council. Auckland Council Technical Report, TR2017/030-2.

- PEARCE, P., FEDAEFF, N., MULLAN, B., SOOD, A., BELL, R., TAIT, A., COLLINS, D. & ZAMMIT, C. 2017. Climate change and variability - Wellington Region. Prepared by the National Institute of Water and Atmospheric Research, NIWA, for Greater Wellington Regional council, NIWA Client Report 2017066AK.
- PONTEE, N. 2013. Defining coastal squeeze: A discussion. *Ocean and Coastal Management*, 84, 204-207. <http://dx.doi.org/10.1016/j.ocecoaman.2013.07.010>
- RAPPORT, D. J., COSTANZA, R. & MCMICHAEL, A. 1998. Assessing ecosystem health. *Trends in ecology & evolution*, 13, 397-402.
- REHMAN, M. U., RATHER, G. H., GULL, Y., MIR, M. R., MIR, M. M., WAIDA, U. I. & HAKEEM, K. R. 2015. Effect of Climate Change on Horticultural Crops. In: HAKEEM, K. R. (ed.) *Crop Production and Global Environmental Issues*. Cham: Springer International Publishing.
- REISINGER, A., KITCHING, R. L., CHIEW, F., HUGHES, L., NEWTON, P. C. D., SCHUSTER, S. S., TAIT, A. & WHETTON, P. 2014. Australasia. In: BARROS, V. R., FIELD, C. B., DOKKEN, D. J., MASTRANDREA, M. D., MACH, K. J., BILIR, T. E., CHATTERJEE, M., EBI, K. L., ESTRADA, Y. O., GENOVA, R. C., GIRMA, B., KISSEL, E. S., LEVY, A. N., MACCRACKEN, S., MASTRANDREA, P. R. & WHITE, L. L. (eds.) *Climate Change 2014: Impacts, Adaptation, and Vulnerability. Part B: Regional Aspects. Contribution of Working Group II to the Fifth Assessment Report of the Intergovernmental Panel on Climate Change*. Cambridge, UK, and New York, NY, USA: Cambridge University Press.
- RENWICK, J. A. & THOMPSON, D. 2006. The Southern Annular Mode and New Zealand climate. *Water & Atmosphere*, 14, 24-25.
- RIDGWAY, K. R. 2007. Long term trend and decadal variability of the southward penetration of the East Australian Current. *Geophysical Research Letters*, 34.
- ROEMMICH, D., GILSON, J., SUTTON, P. J. H. & ZILBERMAN, N. 2016. Multidecadal change of the South Pacific Gyre circulation. *Journal of Physical Oceanography*, 46, 1871-1883.
- ROWE, D. K., HICKS, M. & RICHARDSON, J. 2000. Reduced abundance of banded kokopu (*Galaxias fasciatus*) and other native fish in turbid rivers of the North Island of New Zealand. *New Zealand Journal of Marine and Freshwater Research*, 34, 545-556.
- ROYAL SOCIETY OF NEW ZEALAND 2016. Climate change implications for New Zealand, 72 pp. Available from: <http://www.royalsociety.org.nz/expert-advice/papers/yr2016/climate-change-implications-for-new-zealand/>.
- ROYAL SOCIETY OF NEW ZEALAND 2017. Human health impacts of climate change for New Zealand: Evidence summary. 18 pp. Available from: <https://royalsociety.org.nz/assets/documents/Report-Human-Health-Impacts-of-Climate-Change-for-New-Zealand-Oct-2017.pdf>.
- SALINGER, M. J. & MULLAN, A. B. 1999. New Zealand climate: temperature and precipitation variations and their links with atmospheric circulation 1930–1994. *International Journal of Climatology*, 19, 1049-1071.
- SALINGER, M. J., RENWICK, J., BEHRENS, E., MULLAN, A. B., DIAMOND, H. J., SIRGUEY, P., SMITH, R. O., TROUGHT, M. C. T., ALEXANDER, L., CULLEN, N., FITZHARRIS, B. B., HEPBURN, C. D., PARKER, A. K. & SUTTON, P. J. H. 2019. The unprecedented coupled ocean-atmosphere summer heatwave in the New Zealand region 2017/18: drivers, mechanisms and impacts. *Environmental Research Letters*, 14.
- SALINGER, M. J., RENWICK, J. A. & MULLAN, A. B. 2001. Interdecadal Pacific oscillation and south Pacific climate. *International Journal of Climatology*, 21, 1705-1721.
- SAVAGE, L. 2006. An overview of climate change and possible consequences for Gisborne District. Gisborne: Gisborne Civil Defence and Emergency Management Group.
- SHEPPARD, C. S. 2013. Potential spread of recently naturalised plants in New Zealand under climate change. *Climatic Change*, 117, 919-931.

- SHEPPARD, C. S., BURNS, B. R. & STANLEY, M. C. 2016. Future-proofing weed management for the effects of climate change: is New Zealand underestimating the risk of increased plant invasions? *New Zealand Journal of Ecology*, 40, 398-405.
- SNELDER, T. H. & BIGGS, B. J. 2002. Multiscale River Environment Classification for water resources management. *J. Am. Water Resour. Assoc.*, 38, 1225-1239.
- SOOD, A. 2015. Improved bias corrected and downscaled regional climate model data for climate impact studies: Validation and assessment for New Zealand, submitted.
- STEPHENS, S. 2015. The effect of sea-level rise on the frequency of extreme sea levels in New Zealand. Prepared by NIWA for the Parliamentary Commissioner for the Environment. Wellington: Parliamentary Commissioner for the Environment. Retrieved from <https://www.pce.parliament.nz/media/1382/the-effect-of-sea-level-rise-on-the-frequency-of-extreme-sea-levels-in-new-zealand-niwa-2015.pdf>.
- STEPHENS, S. A., BELL, R. G. & HAIGH, I. D. 2020. Spatial and temporal analysis of extreme storm-tide and skew-surge events around the coastline of New Zealand. *Nat. Hazards Earth Syst. Sci.*, 20, 783-796.
- SUTTON, P. J. H. & BOWEN, M. 2019. Ocean temperature change around New Zealand over the last 36 years. *New Zealand Journal of Marine and Freshwater Research*, 53, 305-326.
- SWALES, A., BELL, R. G. & LOHRER, A. submitted. Estuaries and lowland brackish habitats. In: AL., M. E. (ed.) *Coastal systems and sea-level rise*. NZ Coastal Society Special Publication.
- TAIT, A., PAUL, V., SOOD, A. & MOWAT, A. 2017. Potential impact of climate change on Hayward kiwifruit production viability in New Zealand. *New Zealand Journal of Crop and Horticultural Science*, <https://doi.org/10.1080/01140671.2017.1368672>.
- TAIT, A. & PEARCE, P. R. 2019. Impacts and implications of climate change on Waituna Lagoon, Southland. *Science for Conservation*, 335, 30.
- TAYLOR, K. E., STOUFFER, R. J. & MEEHL, G. A. 2012. An Overview of CMIP5 and the Experiment Design. *Bulletin of the American Meteorological Society*, 93, 485-498.
- TEIXEIRA, E., AUSSEIL, A.-G., BURGUEÑO, E., BROWN, H., CICHOTA, R., DAVY, M., EWERT, F., GUO, J., HOLMES, A., HOLZWORTH, D., HU, W., RUITER, J. D., HUME, E., JESSON, L., JOHNSTONE, P., POWELL, J., KERSEBAUM, K. C., KONG, H., LIU, J., LILBURNE, L., MEIYALAGHAN, S., STOREY, R., RICHARDS, K., TAIT, A. & VAN DER WEERDEN, T. 2020. A Spatial Analysis Framework to Assess Responses of Agricultural Landscapes to Climates and Soils at Regional Scale. *Landscape Modelling and Decision Support*. Springer.
- TEIXEIRA, E. I., BROWN, H. E., FLETCHER, A. L., HERNANDEZ-RAMIREZ, G., SOLTANI, A., VILJANEN-ROLLINSON, S., HORROCKS, A. & JOHNSTONE, P. 2012. Chapter 5 - Broad acre cropping: Adapting broad acre farming to climate change. In: CLARK, A. & NOTTAGE, R. (eds.) *Impacts of climate change on land-based sectors and adaptation options. Technical Report to the Sustainable Land Management and Climate Change Adaptation Technical Working Group, Ministry for Primary Industries*, 408 p.
- TONKIN & TAYLOR 2004. Hawke's Bay Regional Council. Regional Coastal Hazard Assessment: Volume I Assessment. Tonkin & Taylor Client Report No. 20514 Prepared for Hawke's Bay Regional Council. <https://www.hbrc.govt.nz/assets/Document-Library/Reports/Coastal-Hazards/Coastal-Hazard-Assessment-Vol-1-web.pdf>.
- TONKIN & TAYLOR 2015. Update of Areas Susceptible to Coastal Erosion Hazard. Tonkin & Taylor Client Report Job No. 30548 prepared for Gisborne District Council. <http://www.gdc.govt.nz/assets/Files/Planning-Policy/Areas-Susceptible-to-Coastal-Erosion-Hazard-ASCE-Tonkin-and-Taylor-July-2015.pdf>.
- TONKIN & TAYLOR 2016a. Clifton to Tangoio Coastal Hazards Strategy 2120. Coastal Hazard Assessment. Tonkin & Taylor Client Report Job No. 20514.005.CHA.v8 Prepared for Hawke's Bay Councils (HBRC, NCC, and HDC). <https://www.hbrc.govt.nz/assets/Document-Library/Reports/Coastal-Hazards/Coastal-Hazard-Assessment.pdf>.

- TONKIN & TAYLOR 2016b. Hawke Bay Coastal Strategy. Coastal Risk Assessment. Tonkin & Taylor Client Report Job No. 20514.006.v5 prepared for Hawke's Bay Regional Council.
<https://www.hbcoast.co.nz/assets/Document-Library/Technical-Documents/2015.SHAF.Risk-Assessment-Report.R5-print-version.pdf>.
- TOURISM NEW ZEALAND. 2020. *About the tourism industry* [Online]. Tourism New Zealand,. [Accessed 21072020].
- WANG, Y. & CAO, S. 2011. Carbon sequestration may have negative impacts on ecosystem health. ACS Publications.
- WATT, M. S., KIRSCHBAUM, M. U. F., MOORE, J. R., PEARCE, H. G., BULMAN, L. S., BROCKERHOFF, E. G. & MELIA, N. 2018. Assessment of multiple climate change effects on plantation forests in New Zealand. *Forestry: An International Journal of Forest Research*, 92, 1-15.
- WHITEHEAD, D., LEATHWICK, J. R. & HOBBS, J. F. 1992. How will New Zealand's forests respond to climate change? Potential changes in response to increasing temperature. *New Zealand Journal of Forestry Science*, 22, 39-53.
- WILLEIT, M., GANOPOLSKI, A., CALOV, R. & BROVKIN, V. 2019. Mid-Pleistocene transition in glacial cycles explained by declining CO² and regolith removal. *Science Advances*, 5, eaav7337.
- WILLIAMS, J., HORSBURGH, K. J., WILLIAMS, J. A. & PROCTOR, R. N. F. 2016. Tide and skew surge independence: New insights for flood risk. *Geophysical Research Letters*, 43, 6410-6417.
- WILLIS, T. J., HANDLEY, S. J., CHANG, F. H., LAW, C. S., MORRISEY, D. J., MULLAN, A. B., PINKERTON, M., RODGERS, K. L., SUTTON, P. J. H. & TAIT, A. 2007. Climate change and the New Zealand Marine Environment. NIWA Client Report NEL2007-025 for the Department of Conservation. 76 pp.
- WONG, P. P., LOSADA, I. J., GATTUSO, J.-P., HINKEL, J., KHATTABI, A., MCINNIS, K. L., SAITO, Y. & SALLENGER, A. 2014. Coastal systems and low-lying areas. In: BARROS, V. R., FIELD, C. B., DOKKEN, D. J., MASTRANDREA, M. D., MACH, K. J., BILIR, T. E., CHATTERJEE, M., EBI, K. L., ESTRADA, Y. O., GENOVA, R. C., GIRMA, B., KISSEL, E. S., LEVY, A. N., MACCRACKEN, S., MASTRANDREA, P. R. & WHITE, L. L. (eds.) *Climate Change 2014: Impacts, Adaptation, and Vulnerability. Part A: Global and Sectoral Aspects. Contribution of Working Group II to the Fifth Assessment Report of the Intergovernmental Panel on Climate Change*. Cambridge, UK and New York, NY, USA: Cambridge University Press.